NASA Contractor Report 178292

# Development of Response Models for the Earth Radiation Budget Experiment (ERBE) Sensors:

# Part I – Dynamic Models and Computer Simulations for the ERBE Nonscanner, Scanner and Solar Monitor Sensors



Nesim Halyo, Sang H. Choi, Dan A. Chrisman, Jr. and Richard W. Samms

Information & Control Systems, Incorporated
Hampton, Virginia 23666

Contract NAS1-16130

March 20, 1987

National Aeronautics and Space Administration

Langley Research Center
Hampton, Virginia 23665-5225

# FOREWORD

This report entitled "Development of Response Models for the Earth Radiation Budget Experiment (ERBE) Sensors" consists of the following four parts.

This is Part I, NASA CR-178292, entitled "Dynamic Models and Computer Simulations for the ERBE Nonscanner, Scanner and Solar Monitor Sensors".

Part II, NASA CR-178293, is entitled "Analysis of the ERBE Integrating Sphere Ground Calibration".

Part III, NASA CR-178294, is entitled "ERBE Scanner Measurement Accuracy Analysis Due to Reduced Housekeeping Data".

Part IV, NASA CR-178295, is entitled "Preliminary Nonscanner Models and Count Conversion Algorithms".

TABLE OF CONTENTS

TABLE OF CONTENTS (CONCLUDED)

LIST OF FIGURES

LIST OF FIGURES (CONCLUDED)

## LIST OF SYMBOLS

| Symbol | Definition |
|---|---|
| $A_c$ | Area of conductive transfer in an element |
| $A_r$ | Area of radiative transfer in an element |
| $A_{k-i}$ | Contacting area between elements k and i |
| a | Radius of a contacting point, e.g. Fig. 7 |
| $A_i$ | Inside surface area for $i^{th}$ surface |
| $\bar{A}$ | Constant defined in Eq. 14 |
| $A_r$ | Area of radiative interaction |
| $A_c$ | Area of nodes covered by a heater |
| a | Thermal wave velocity, e.g. Eq. 58 |
| b | Bias term, e.g. Eq. 25 |
| B | Vector of coefficients for irradiance from the source |
| $B_Q$ | Coefficient which describes heating contributions from the control systems |
| $b_E$ | Electronic bias |
| $B_k$ | Constants related with the irradiance at a FOV limiter |
| $C_k$ | Specific heat capacity of element k |
| $\bar{C}$ | Constant defined in Eq. 15 |
| C | Number of counts |
| $\Delta C_B$ | Baseband signal |
| D | Enclosure coupling factor through the interactive boundaries |

LIST OF SYMBOLS (CONTINUED)

| Symbol | Definition |
|---|---|
| $e_k$ | Energy in element k |
| $E_n^m$ | Rate of incoming radiant energy to surface n in enclosure m |
| $\tilde{E}_n^m$ | Rate of incoming radiant energy to non-opaque boundary surface n in enclosure m from a neighboring surface |
| e | Noise term, Eq. 25 |
| $\hat{E}$ | Total incident radiation esitmate |
| $\Delta E_{os}$ | Baseband signal |
| $E_\lambda(t)$ | Spectral irradiance at the instrument due to radiation from the footprint at time t |
| $e_i(t)$ | Combined error of the measurement and count conversion accuracy |
| $E_{Bi}(T_B)$ | Output of count conversion when viewing the blackbody at temperature $T_B$ |
| $E_{B\lambda}(T_B)$ | Spectral irradiance from the blackbody at $T_B$ |
| $F_{k-i}$ | Configuration factor between elements k and i |
| $\bar{F}_{k-i}$ | Exchange factor between elements k and i |
| F | System boundary conditions imposed by surroundings |
| $F_E(s)$ | Control electronics transfer function. |
| $h_{k-i}$ | Thermal conductance of the contact between elements k and i |
| $H_z$ | Hertz |

| Symbol | Definition |
|---|---|
| I | Identity Matrix |
| i | Calibration sequence |
| J | Number of measurements in the scanner mode. |
| $k_k$ | Thermal conductivity of element k |
| $K_i$ | Electronic gain for component i |
| $k_{fo}$ | Post amplification gain |
| l | Longwave |
| $L_{k-i}$ | Shortest distance between the center of mass of element k and the contacting point of element k to its neighboring element i |
| L | Length of a solar monitor shutter |
| l | Exposure length to solar radiation |
| $M_i^*$ | Opaque radiosity - the rate of outgoing radiant energy from surface i from diffuse and specular reflectance |
| $M_i$ | Total radiosity - opaque radiosity plus energy flux transmitted through surface i |
| ms | Milliseconds |
| m | Meter |
| n | Number of contacts per unit area |
| $n_i$ | Noise from source i |

| Symbol | Definition |
|---|---|
| $\dot{Q}_k$ | Dynamic heat transfer due to behavior of element k as a heat source or sink |
| $\dot{q}''_c$ | Heat flux by conduction through the contacting area between two elements |
| $R_{k-i}$ | Thermal resistance through the contacting area between elements k and i |
| $R_i$ | Inside radius of solar monitor barrel |
| $R_o$ | Outside radius of solar monitor barrel |
| $S_n^m$ | Heat flux arriving at the system boundary at surface n in enclosure m |
| s | Shortwave |
| T | Total radiation channel |
| $T_k$ | Temperature (vector) of element k |
| $\dot{T}_k$ | Governing equation for a radiometer with a dynamic response to an incoming radiance at element k |
| T(i) | Temperature change for thermal node i or voltage change for electronic node i |
| $T_\infty$ | Ambient temperature |
| $T_b$ | Current shutter temperature in solar monitor |
| $\Delta t$ | Total scan period |
| $t_k$ | Time at end of space-look |
| t | Sampling instant |

LIST OF SYMBOLS (CONTINUED)

| Symbol | Definition |
|---|---|
| $T_B$ | Temperature of a blackbody |
| $u(x)$ | Unit step function |
| $V_k$ | Volume of element k |
| $V(t)$, $v(t)$ | Instrument output (in volts) at time t |
| $\bar{v}(t_k)$ | Space clamp value at time $t_k$, i.e. at the end of space look |
| $v(t_{ki})$ | Instrument output (in volts) when viewing space at time $t_k$ |
| $V_B(t)$ | Detector bridge bias voltage at time t or most recent value (v) |
| $V_d(t_k)$ | Drift balance DAC voltage measurement at time t or most recent value (v) |
| $v_{Bi}(T_B)$ | Steady-state output of the $i^{th}$ channel when viewing blackbody temperature $T_B$ |
| W | Watts |
| x | Distance from end of barrel in a solar monitor |
| $\mathbf{x}$ | Vector consisting of electrical signal processing variables, e.g. Eq. 73 |
| $\mathbf{x}$ | Vector consisting of the offset temperature and radiative constant, e.g. Eq. 109 |
| $\Delta\bar{x}_i$ | Lower frequency signal portion of $\Delta x$ for component i, e.g. Eq. 79 |
| $\Delta\tilde{x}_i$ | Noise and irradiance portion of $\Delta x$ for component i, e.g. Eq. 79 |

| Greek Symbol | Definition |
|---|---|
| $\gamma_k$ | Density of element k |
| $\delta_1$ | Surface roughness of surface 1 |
| $\delta$ | Thickness of solar monitor shutter |
| $\delta_k$ | Estimate of unaccounted drift during $k^{th}$ scan period (v) |
| $\varepsilon_k$ | Emissivity of element k |
| $\varepsilon_{k-i}$ | Exchange factors between specular surfaces k and i |
| $\eta_k$ | Attenuation factor for element k |
| $\lambda_k$ | Wavelength k |
| $\rho_k$ | Reflectivity of surface k |
| $\rho$ | Density of solar monitor shutter |
| $\sigma$ | Stefan-Boltzmann constant |
| $\sigma_k^2$ | Noise variance estimate during space look |
| $\tau_k$ | Transmissivity of surface k |
| $\tau_i$ | Time constant for electronic element i |
| $\tau$ | Average time lag (in seconds) |
| $\tau_i(k)$ | Transmittance of $i^{th}$ channel |
| $\phi_k$ | Radiative energy supplied to surface k |

| Superscript | |
|---|---|
| d | Diffuse |
| s | Specular |
| m | Number of an enclosure in a system |

| Superscript | Definition |
|---|---|
| M | Medium field-of-view |
| W | Wide field-of-view |
| P | Photo-diode |

| Subscript | |
|---|---|
| s | Shortwave band |
| l | Longwave band |
| s | Surface, Eq. 6 |
| k-i | between k and i elements |
| n | Number of an enclosure's surface in a system |
| H | Heater, Eq. 35 |
| A | Precision aperture |
| F | Field-of-view limiter |
| B | Bridge |
| A | Amplifier |
| E | Electronic |
| v | Volatage |
| B | Blackbody |
| o | Initial |
| s | Solar, Eq. 58 |
| H | Heat sink, Eq. 99 |

# LIST OF ACRONYMS

| Acronym | Definition |
|---|---|
| ACR | Active Cavity Radiometer |
| Al Heat Sink | Aluminum Heat Sink |
| A/D | Analog-to-Digital (conversion) |
| B.C. | Boundary Conditions |
| CCA | Count Conversion Algorithm |
| Cu Heat Sink | Copper Heat Sink |
| DAC | Digital-to-Analog Conversion |
| ERBE | Earth Radiation Budget Experiment |
| EXP | Exponential |
| FOV | Field-of-view |
| FOVL | Field-of-view limter |
| G.E. | Governing Equations |
| HK | Housekeeping |
| HKD | Housekeeping data |
| IBB | Internal blackbody |
| I/O | Input/Output (data processing) |
| I.C. | Initial Conditions |
| LW | Longwave |
| MFOV | Medium Field-of-View |
| MFVOT | Medium Field-of-View Total |
| MFOVSW | Medium Field-of-View Shortwave |
| MAM | Mirror Attenuator Mosaic |
| MRBB | Master Reference Blackbody |

## LIST OF ACRONYMS (CONCLUDED)

| Acronym | Definition |
|---|---|
| ms | Millisecond |
| NS | Nonscanner |
| NFOV | Narrow Field-of-View |
| RHS | Right hand side |
| RMS | Root mean square |
| SW | Shortwave |
| SWICS | Shortwave Internal Calibration Source |
| SiPD | Silicon Photo-Diode |
| T | Total radiation channel |
| WFOV | Wide Field-of-View |
| WFOVT | Wide Field-of-View Total |
| WFOVSW | Wide Field-of-View Shortwave |
| WRT | With respect to |

## 1. INTRODUCTION

The radiometric measurement system for the Earth Radiation Budget Experiment (ERBE) is designed to measure the earth's radiation fluxes which result from the earth and its atmosphere's emmitted energy as well as from reflected energy, i.e., the earth's albedo. A general overview of the concept behind the three-satellite ERBE radiometric system and its instruments has been described in many internal NASA documents, such as the Science Team Minutes and Contractor Status Reports, as well as in journal publications, (e.g., Ref. 1).

The radiometer package on each ERBE satellite consists of eight instruments distinguished by their mode of operation, field-of-view and spectral response. Four of the eight instruments are nonscanner (NS) type radiometers, two with a Medium Field-of-View (MFOV) and two a Wide Field-of-View (WFOV). Two of the nonscanner radiometers, one MFOV and one WFOV, have a suprasil filter which eliminates the instrument's response to longwave radiative effects so that they only remain sensitive to shortwave radiative effects. Shortwave (SW) radiative effects are defined here as having wavelengths between 0.2 and 5 μm and longwave radiative effects as having wavelengths between 5 and 50 μm. Since radiometers without filters measure total radiation, they are designated "Total" (T). The four nonscanner radiometers are therefore the Medium Field-of-View Total (MFOVT), Medium Field-of-View Shortwave (MFOVSW), Wide Field-of-View Total (WFOVT) and Wide Field-of-View Shortwave (WFOVSW). Three of the remaining instruments or "channels" are Narrow Field-of-View (NFOV) scanning radiometers, two of which have filters. One scanner radiometer has a filter which eliminates longwave radiative effects and another has a filter which eliminates shortwave radiative effects. Hence the three scanner radiometers are the Narrow Field-of-View Shortwave (NFOVSW), the Narrow Field-of-View Longwave (NFOVLW) and the

Narrow Field-of-View Total (NFOVT). The eighth instrument in the ERBE radiometric package is the solar monitor radiometer.

After the ERBE radiometers perform their earth, space and/or sun view and calibration measurements, the measurement results undergo an analog-to-digital (A/D) conversion and the data now in counts is transmitted to the earth through the spacecraft telemetry system. Counts for the nonscanners are measured every 0.8 seconds. Heat sink temperatures are read every 8 seconds and other housekeeping (HK) temperatures every 16 seconds. Therefore, in 16 seconds the data record for one nonscanner consists of 20 radiometric count readings, 2 heat sink temperature readings and 1 reading for each of the other HK temperatures.

The scanners perform a measurement cycle once every 4 seconds. During a normal, earth-viewing scan each scanner performs 8 space-look measurements, 62 earth-view measurements and 4 calibration measurements. The Longwave and Total NFOV scanners utilize the Internal Blackbody (IBB) for calibration measurements, whereas the Shortwave NFOV scanner utilizes the Shortwave Internal Calibration Source (SWICS). During a Mirror Attenuator Mosaic (MAM) scan cycle, the NFOVT and NFOVSW scanners measure solar flux performing 8 space-look measurements, 46 MAM measurements and 4 calibration measurements. Housekeeping (HK) data is sampled once per scan.

The solar monitor uses the same type of Active Cavity Radiometer (ACR) that is used by the nonscanners. The three major differences between these ACR's are as follows:

a) the solar monitor has a shutter to cut off the solar flux every 32 seconds,

b) the configuration of the solar monitor housing is totally different and

c) the solar monitor has no heat sink heater.

Solar Monitor count measurements are made every 0.033 seconds and HK measurements are made every 4 seconds.

The radiometric instruments described above will have inherently different behavior and responses to arbitrary input signals since no instrument can be exactly duplicated or subjected to exactly the same calibration or operating environment. Even when viewing the problems of sensor performance from this macroscopic point of view, there are many things that have to be dealt with and accounted for. For example, environmental contamination and aging effects influence the material degradation of the sensors. Sensor behavior may also be questioned when the thermal load and leakage exceed the design level. One example of abnormal thermal load is in the sun-blip case, where the sensor is subjected to a sunrise and sunset during its orbit.

In attempting to account for such problems found in the sensor's radiometric performance and capability, it is therefore necessary to develop a radiometer sensor model. A sensor model should describe both a transient and steady-state sensor response for a given radiative input. It must provide sufficiently simple analytical expressions for parameters of particular interest and describe the model's behavior, e.g., the model's sensitivity to changes in the modeling assumptions. The model must also be able to incorporate changes resulting from instrument design requirements during its construction as well as instrument aging, i.e., sensor material degradation and unexpected thermal load and leakage during its long-term orbital operation. The products obtained from the sensor model and simulation must be in a form that is useful to the users. The sensors' response must therefore be validated by updating model parameters and converted into data with useful engineering units.

This report entitled "Development of Response Models for the Earth Radiation Budget Experiment (ERBE) Sensors" consists of the following four parts.

Part I, NASA CR-178292, is entitled "Dynamic Models and Computer Simulations for the ERBE Nonscanner, Scanner and Solar Monitor Sensors".

Part II, NASA CR-178293, is entitled "Analysis of the ERBE Integrating Sphere Ground Calibration".

Part III, NASA CR-178294, is entitled "ERBE Scanner Measurement Accuracy Analysis Due to Reduced Housekeeping Data".

Part IV, NASA CR-178295, is entitled "Preliminary Nonscanner Models and Count Conversion Algorithms".

## 2. SENSOR MODELING

The following ERBE radiometer sensor models were developed by Information & Control Systems, Incorporated (ICS) to consider thermal and radiative exchange effects. These models consider the surface specularity and spectral dependence of a filter as well as the thermal conductive and radiative interactions among the nodes in an enclosure of a radiometer. An enclosure is a domain in which an instrument's geometry is divided into appropriate elements. These enclosures in an instrument's model are set up using real or fictitious boundaries to effectively alleviate the computational load for defining configuration factors. The instrument's model also includes the electronic thermal control sytems which are coupled with the energy equations. A general form of the energy equations can be used for all the sensors, despite differences in the mode of operation, field-of-view and spectral response, as long as the radiative enclosures and thermal nodes in the sytem's sensor configuration comply with the first law of thermodynamics.

A sensor model can be tested and evaluated by comparing its behavior with the actual results obtained from the sensor's ground and inflight calibrations. The sensor model includes additional uncertainty since it incorporates outputs from the calibration source models. Once the sensor and calibration source models produce sufficiently accurate results, they can be used to define the parameters for the count conversion procedure.

The characteristics of a sensor's simulation model are such that it has a dynamic response to the time dependence of an arbitrary input signal. The model also has a spectral response which is due to the spectral dependence of a sensor's filter and its exposed surfaces. Thermal effects for the model can be determined from the conductive and radiative properties of the sensor. The

model's measurement error can therefore be determined after its time response, spectral response and thermal effects have been obtained. The model can simulate the sensor's response to the temporal incident radiation received through the field-of-view limiter in both the transient and steady-states.

The purpose of modeling and simulating is therefore 1) to understand sensor performance, 2) to improve measurement accuracy by updating the model parameters and 3) to provide appropriate constants necessary for the count conversion algorithms.

## 2.1 General Description of the ERBE Sensor Models

### 2.1.1 Models

A sensor's geometry can be appropriately divided by considering its thermal and radiative interactions as a consequence of its design. Figures 1 through 6 provide diagrams of how sensor elements have been geometrically partitioned for the nonscanner, scanner and solar monitor. Each element has a time resonse to the energy flowing to and from its neighboring elements.

One might assume that maximizing the number of sensor nodes would maximize the accuracy of the model's prediction of energy from a target source. However, increasing the number of nodes would introduce additional sources of error since the large set of equations required would incorporate additional parameter approximations. Such equation approximations would need to be made to calculate constants such as thermal resistance, exchange factors and surface spectral and specular characteristics. There is an accuracy tradeoff between increasing the number of nodes and approximating the sensor's size, material properties, geometry, enclosure surface characteristics, temporal incident

# NONSCANNER MEDIUM FIELD-OF-VIEW TOTAL (MFOVT)

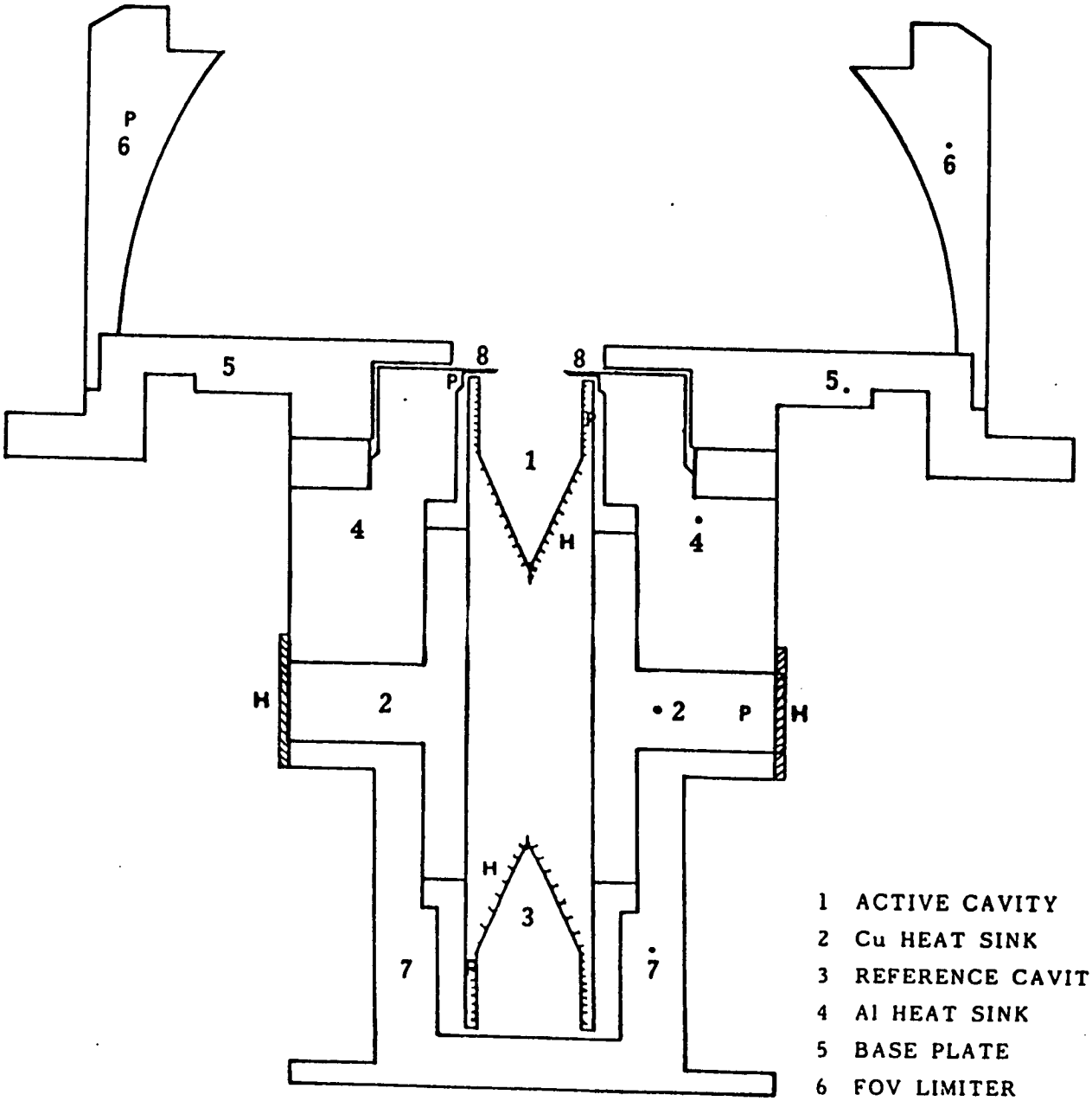


1 ACTIVE CAVITY
2 Cu HEAT SINK
3 REFERENCE CAVITY
4 Al HEAT SINK
5 BASE PLATE
6 FOV LIMITER
7 Al HEAT SINK
8 APERTURE

H HEATER
P TEMPERATURE PROBE

FIGURE 1.

# NONSCANNER MEDIUM FIELD-OF-VIEW SHORTWAVE (MFOVSW)

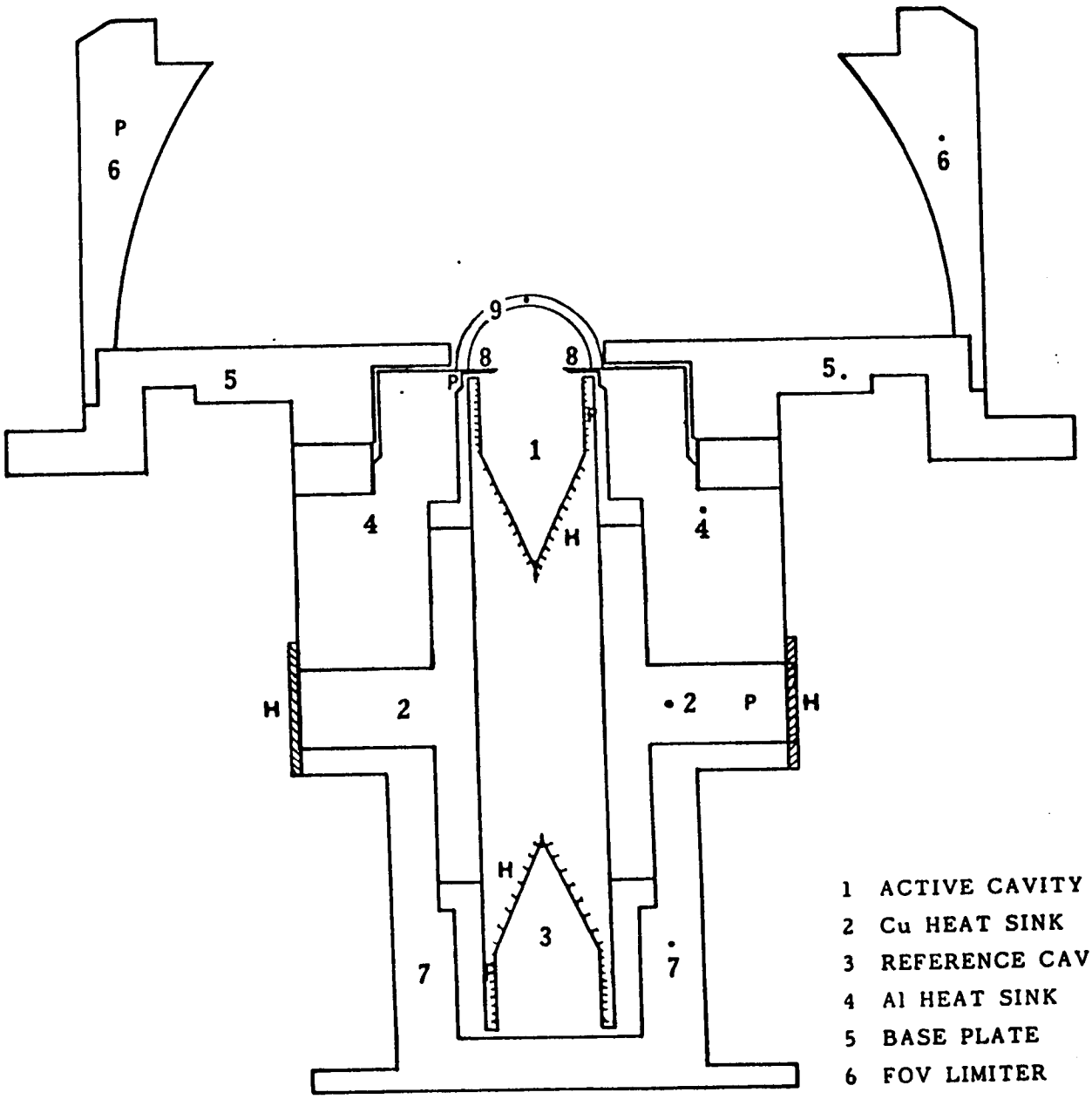


1 ACTIVE CAVITY
2 Cu HEAT SINK
3 REFERENCE CAVITY
4 Al HEAT SINK
5 BASE PLATE
6 FOV LIMITER
7 Al HEAT SINK
8 APERTURE
9 SW FILTER DOME
H HEATER
P TEMPERATURE PROBE

FIGURE 2.

# NONSCANNER WIDE FIELD-OF-VIEW TOTAL (WFOVT)

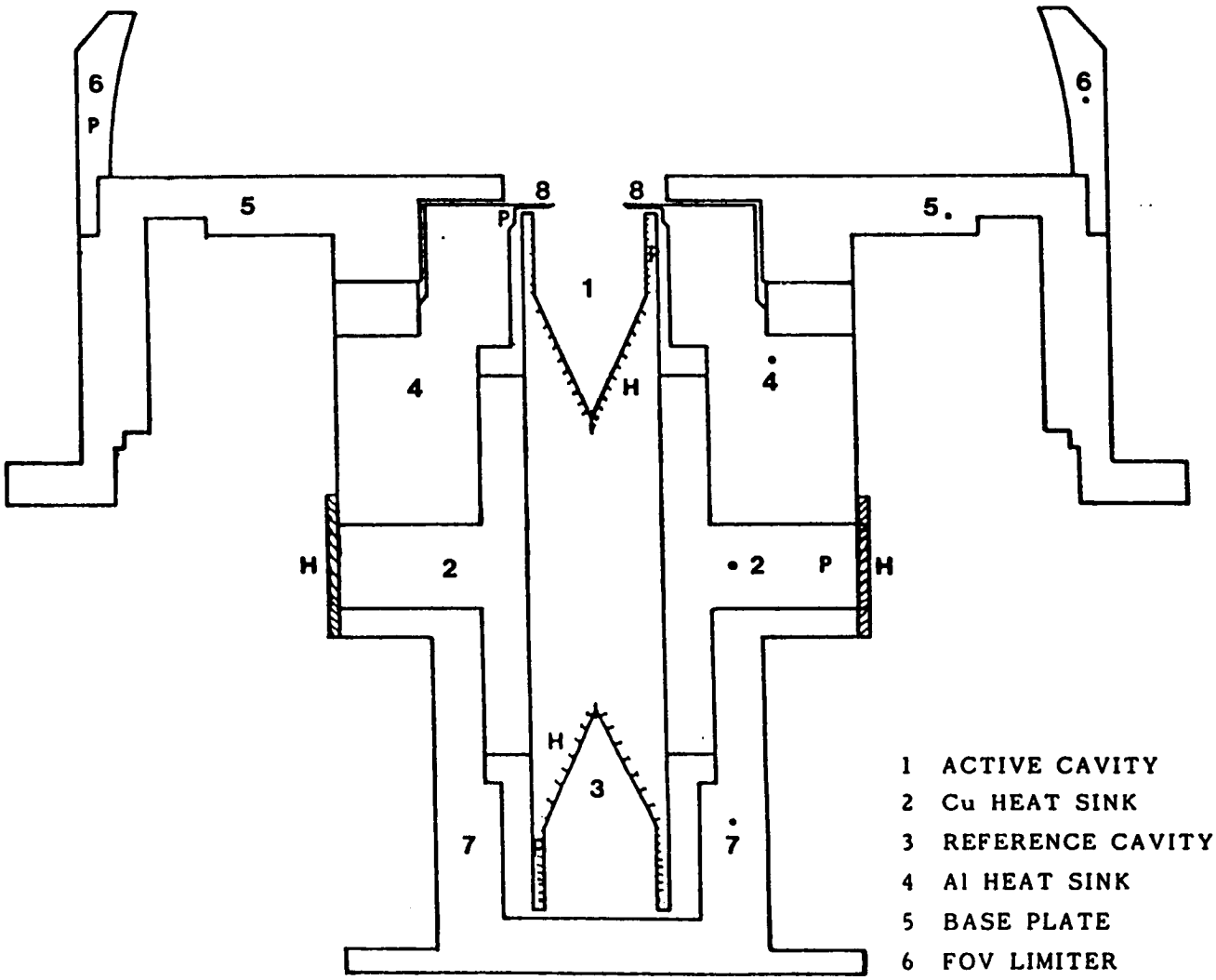


1 ACTIVE CAVITY
2 Cu HEAT SINK
3 REFERENCE CAVITY
4 Al HEAT SINK
5 BASE PLATE
6 FOV LIMITER
7 Al HEAT SINK
8 APERTURE

H HEATER
P TEMPERATURE PROBE

FIGURE 3.

## NONSCANNER WIDE FIELD-OF-VIEW SHORTWAVE (WFOVSW)

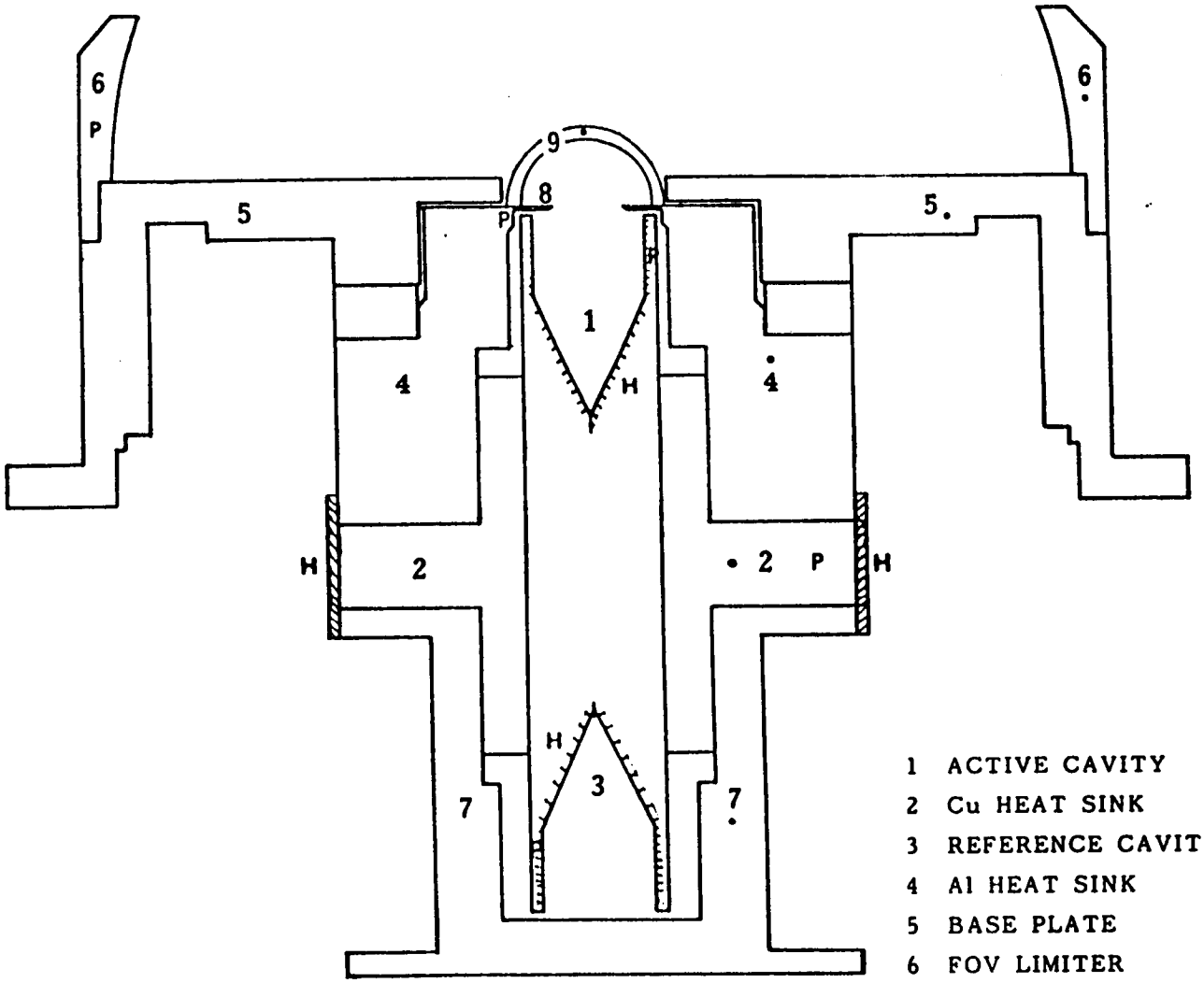


1 ACTIVE CAVITY
2 Cu HEAT SINK
3 REFERENCE CAVITY
4 Al HEAT SINK
5 BASE PLATE
6 FOV LIMITER
7 Al HEAT SINK
8 APERTURE
9 SW FILTER DOME
H HEATER
P TEMPERATURE PROBE

FIGURE 4.

## SCANNER NARROW FIELD-OF-VIEW TOTAL (NFOVT)

1. ACTIVE FLAKE
2. HEAT SINK & DETECTOR ASSY.
3. COMPENSATING FLAKE
4. PRECISION APERTURE
5. INSERT, PRIMARY
6. PRIMARY MIRROR
7. CAP ASSEMBLY
8. HOUSING & HEATER
9. SECONDARY MIRROR
10. FOV LIMITER
11. MOUNT, SECONDARY(A)
12. MOUNT, SECONDARY(B)
13. LW OR SW FILTER
14. SW FILTER
15. FICTITIOUS SURFACE AT FOV
16. FICTITIOUS SURFACE AT SECONDARY
17. FICTITIOUS SURFACE AT APERTURE

p. TEMPERATURE PROBE

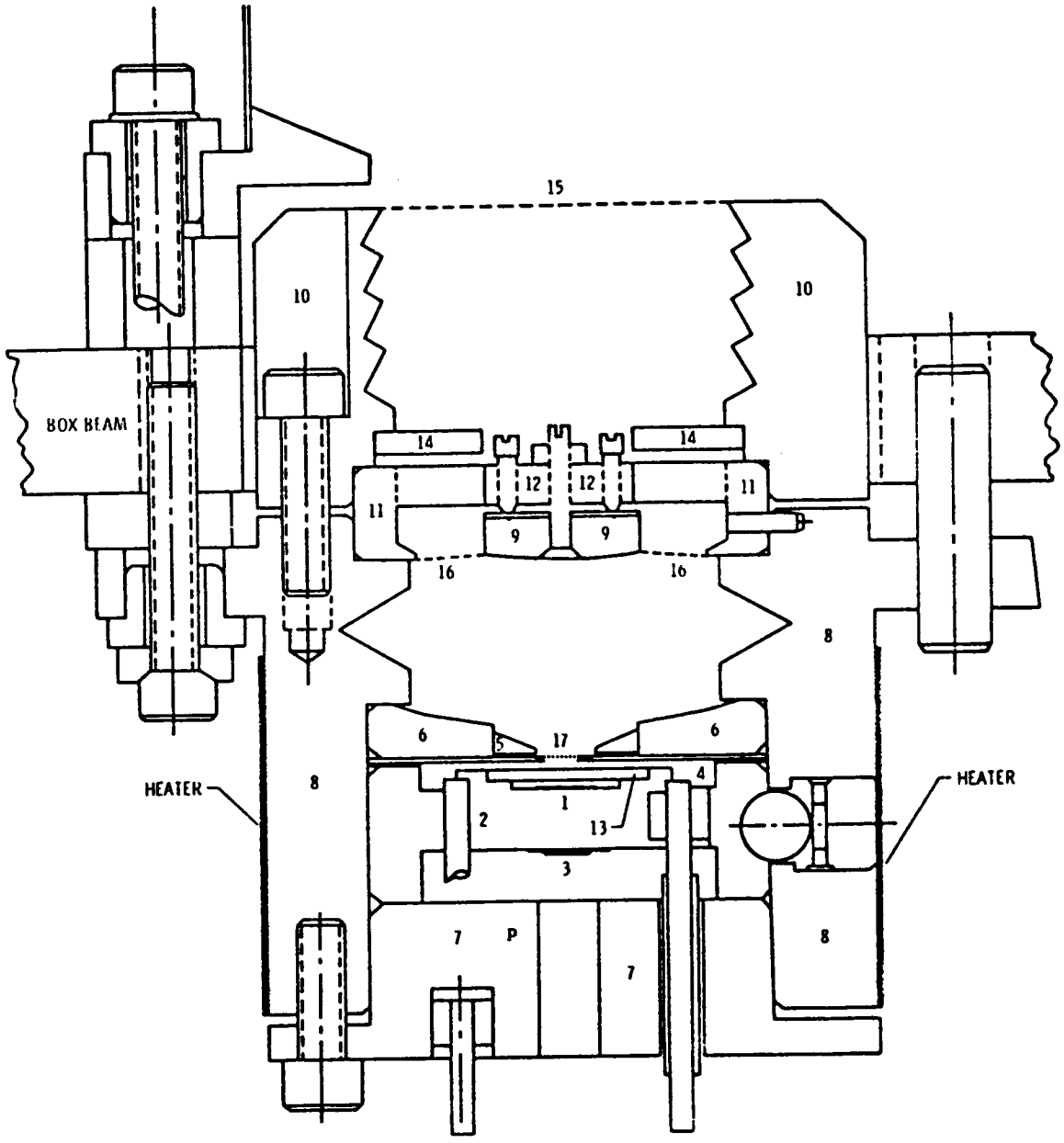


FIGURE 5.

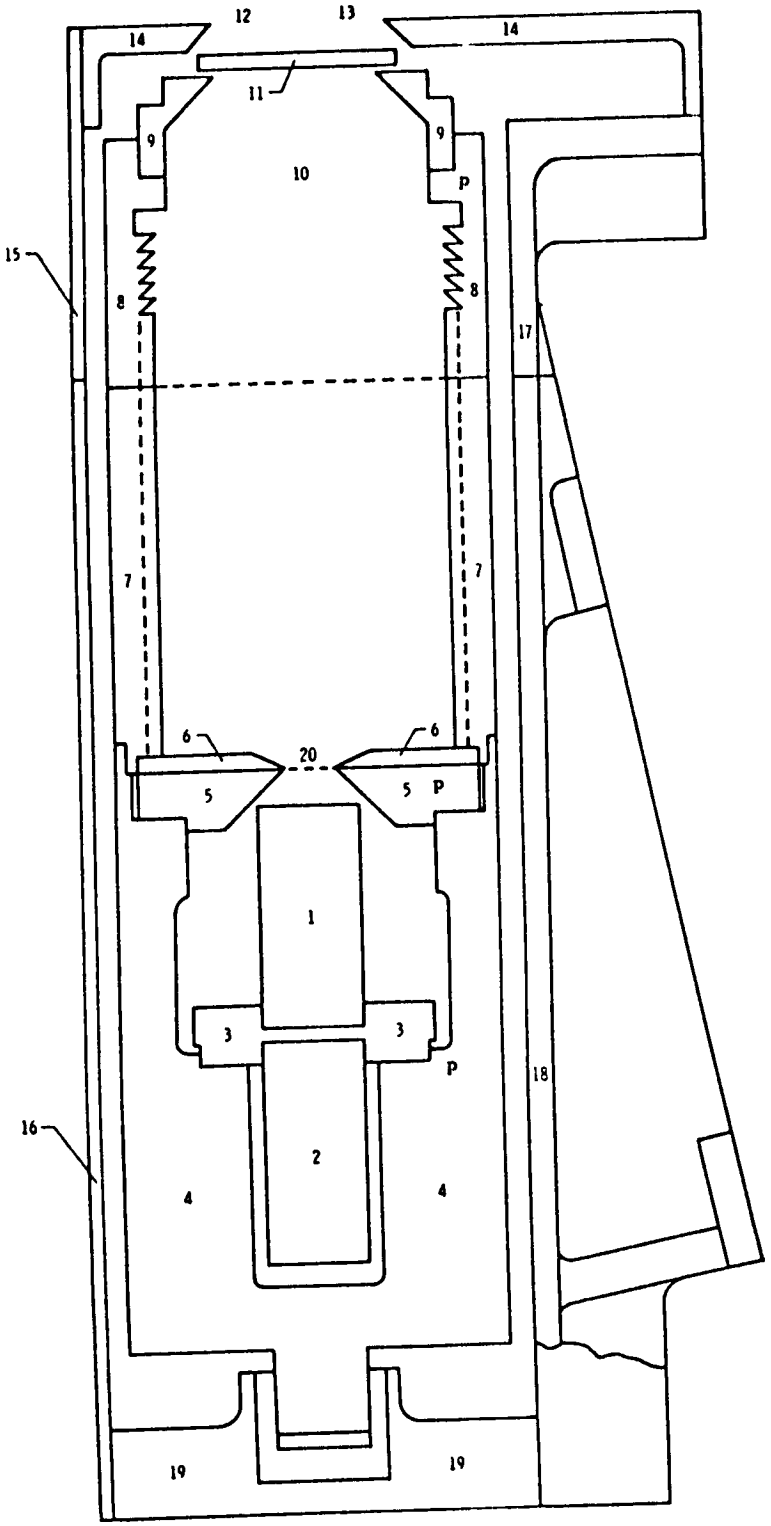


1. ACTIVE CAVITY
2. REFERENCE CAVITY
3. BUTTON, DUPLEX CONE CAVITIES
4. HEAT SINK
5. APERTURE, PRIMARY
6. SHIELD, APERTURE
7. BODY (REAR BARREL)
8. BODY (FRONT BARREL)
9. APERTURE, SECONDARY (OR FOV LIMITER)
10. MOTOR HOUSING
11. CHOPPER BLADE
12. CHOPPER PENDLUM
13. MOTOR, CHOPPER
14. FOV LIMITER
15. FRONT TOP HOUSING COVER
16. REAR TOP HOUSING COVER
17. FRONT HOUSING
18. REAR HOUSING
19. HOLDER, HEAT SINK
20. FICTITIOUS SURFACE

p. TEMPERATURE PROBES

FIGURE 6.

energy flux intensity and electronic control system. If the temperature gradients within a node and between nodes are small enough, a model approximation with only a few nodes would not jeopardize the accuracy required to perform the parameter estimates and error analysis. Factors which would decrease these temperature gradients within a sensor include uniform thermal properties, simple and symmetrical geometry, uniformity in directional and spectral properties of an enclosure surface and small temporal change in incident energy flux.

A nonscanner sensor has 9 nodes if it has a suprasil filter dome (Figures 2 and 4) and 8 nodes if it does not (Figures 1 and 3). The sensor's geometry is divided into nodes based on material homogeneity, overall sensor size, thermal conductivity of materials, thermal resistance between materials and surface radiative properties. The 9 nodes of the MFOVSW model (Figure 2) are therefore, as numbered: 1) the active cavity with a heating and sensor coil 2) the copper heat sink with a heater, 3) the reference cavity with a sensor coil, 4) the aluminum heat sink, which is partly covered by a heater, 5) the base plate or substrate, 6) the field-of-view limiter, 7) the aluminum heat sink which houses the reference cabity, which is partly covered by a heater, 8) the precision aperture and 9) the filter dome for shortwave channels.

Similarly, the scanner model (Figure 5) is divided into 12 nodes for the total channel, 13 nodes for the longwave channel and 14 nodes for the shortwave channel. The solar monitor is divided into 19 nodes (Figure 6).

In addition to their nodes, these sensor models incorporate fictitious surfaces to define and simplify enclosure geometries. Since the specular property of each surface in an enclosure is taken into consideration, the simple geometry facilitates the exchange factor calculation, alleviating the computational work load for determining the exchange factors. A net radiation

analysis is performed for each enclosure which has surfaces with specular and spectral characteristics. This analysis appropriately deals with any partial specular and diffuse characteristics of an enclosure surface (Ref. 2). The model can also easily include transient response and thermal conduction. This net radiation method utilizes the waveband approximation to an enclosure's surface which has a specific spectral dependence.

### 2.1.2 Thermal Conductive and Radiative Interactions

A volumetrically defined node, or control volume, complies with the first law of thermodynamics as in the following equation

$$\frac{de}{dt} = A_c \dot{q}_c'' + A_r \phi \tag{1}$$

The first and second terms of the right hand side of Equation 1 represent the conductive transfer through contacting surfaces and radiative transfer from surrounding elements of an enclosure, respectively. The rate of energy change in a single node, therefore, depends on the difference between the ingoing and outgoing energy fluxes through a control surface or "boundary". This rate of energy gain or loss is composed of the rate of energy stored in a node as well as the rate of energy source or sink as indicated in the following equation

$$\frac{de}{dt} = V\gamma C \frac{dT}{dt} - \dot{Q} \tag{2}$$

where V is the volume of a node, $\gamma$ the density of a node, C the specific heat, T the temperature and $\dot{Q}$ the rate of energy, or heat, at a source or sink.

Combining Equations 1 and 2 yields

$$V\gamma C \frac{dT}{dt} = A_c \dot{q}_c'' + A_r \phi + \dot{Q} \tag{3}$$

Equation 3 represents an energy balance in a single node. In the geometrically partitioned model, the conduction term can be written in the following form

$$\left(A_c \dot{q}''_c\right)_{i-j} = \frac{T_j - T_i}{R_{i-j}} \tag{4}$$

where $A_{i-j}$ is the contacting area of i element to j element, $\dot{q}''_c$ the heat flux by conduction through the contacting area between i and j elements. $R_{i-j}$ is the thermal resistance between i and j elements. The thermal resistance between nodes is defined by the following realationship

$$R_{i-j} = \frac{L_{i-j}}{k_i A_{i-j}} + \frac{1}{h_{i-j} A_{i-j}} + \frac{L_{j-i}}{k_j A_{j-i}} \tag{5}$$

where $L_{i-j}$ is the distance from the thermal center of a node to the center of the contacting surface, k the thermal conductivity and h the thermal conductance of the contact between i and j elements. The thermal center is normally coincident with the geometrical center if a node material has homogeneous and isotropic thermal properties. The contact resistance (1/hA) is mainly dependent on the surface roughness and the contacting pressure. The well-machined surface has a regular and uniform roughness. In such a case, the contact resistance can be determined by the following empirical relations (Ref. 3) as functions of the surface roughness and the thermal conductivities of two contacting materials.

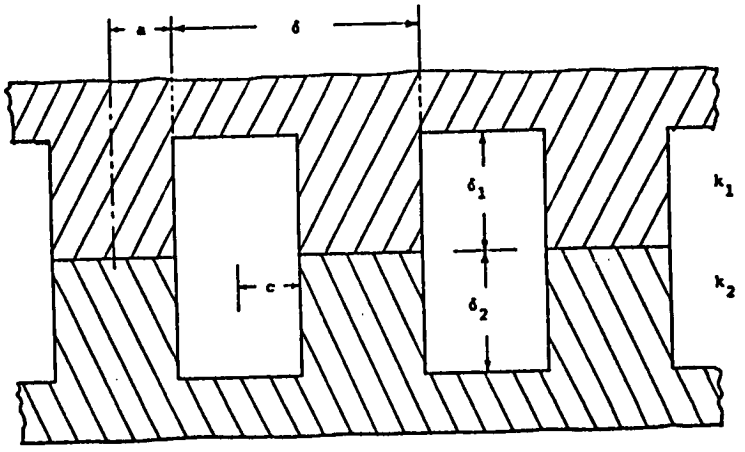


Figure 7. A Simple Thermal Contact Resistance Model

Let surfaces contact each other with surface roughness $\delta_1$ and $\delta_2$ and thermal conductivities $k_1$ and $k_2$, respectively. Assume the contacting area per periodic contact is $\pi a^2$. Then the number of contacts per unit area $n = \frac{1}{\pi a^2}$ and the total number of contacts for two surfaces with total contacting area A is $\frac{A}{\pi a^2}$. Conductance can therefore be calculated:

$$h = \frac{k_s}{\delta} \left( \frac{\epsilon^2}{1 - \epsilon^2} \right) \left( \frac{\eta}{\epsilon + \eta} \right) \tag{6}$$

where

$$\frac{1}{k_s} = \frac{1}{2} \left( \frac{1}{k_1} + \frac{1}{k_2} \right)$$

$\delta = \delta_1 + \delta_2$ ($\simeq 2\delta_1$ or $2\delta_2$)

$\eta = 2.13\delta \sqrt{n}$ , where $\eta$ is a parameter for roughness

$\epsilon = \frac{c}{a + c}$ , where c is the half-width of the surface cavity

$n = \frac{1}{\pi a^2}$ = number of contacts per unit area

$k_1, k_2$ = thermal conductivity of nodes 1 and 2

$\delta_1, \delta_2$ = root mean square surface roughness of nodes 1 and 2

A = total node interface area

a = radius of a contacting point

For the radiative interchanges in an enclosure including both specular and diffuse surfaces, a radiative property such as a reflectance, $\rho$, can be divided into a diffuse and a specular component as well as shortwave and long-wave bands.

That is, for shortwave bands:

$$\rho_s = \rho_s^d + \rho_s^s$$

and for longwave bands:

$$\rho_\ell = \rho_\ell^d + \rho_\ell^s$$

where the superscripts, d and s, signify the diffuse and specular, and the subscripts the short and longwave bands. For a semi-transparent or an absorbing medium, the radiative properties have the following relationship among the reflectance $\rho$, emittance or absorptance $\varepsilon$, and transmittance, $\tau$.

$$\varepsilon_s + \rho_s + \tau_s = 1 \quad \text{for shortwave}$$

$$\varepsilon_\ell + \rho_\ell + \tau_\ell = 1 \quad \text{for longwave}$$

The energy fluxes incident upon and leaving a typical semi-transparent surface of the enclosure are described in Figure 8. Consider the $i^{th}$ inside surface area, $A_i$, of the enclosure which neighbors with other enclosures. The quantities $E_i$ and $M_i^*$ are the rates of incoming and outgoing radiant energy while considering diffuse and specular reflectance of the surface per unit inside area, respectively. The quantity $M_i^*$ does not include the rate of transmitted incident radiant energy from the other neighboring enclosures. The quantity $\tilde{E}_i$ is the rate of incoming radiant energy to the non-opaque boundary surface from the neighboring enclosure. The quanitity $\phi_i$ is the energy flux supplied by some external means to the surface to make up for the net radiative loss and thereby maintain the specified surface temperature. A heat balance at the surface provides the relation

$$\phi_i = E_i - M_i \tag{7}$$

A second equation results from the fact that the energy flux leaving the

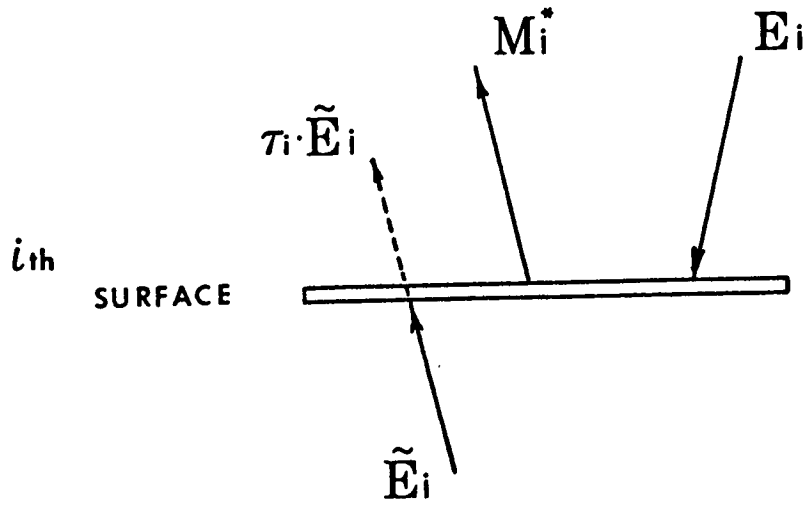


FIGURE 8. Radiation Flux Interchange

surface having diffuse and specular characteristics is composed of directly emitted plus reflected energy. This gives

$$M_i^* = \varepsilon_i \sigma T_i^4 + \rho_i^d E_i + \rho_i^s E_i \tag{8}$$

Equation 8 is called an opaque radiosity. The total radiosity, considering the rate of transmitted radiant energy which is originally coming from the neighboring enclosure, is composed of the opaque radiosity $M_i^*$ plus the energy flux transmitted through the surface with transmissivity, $\tau_i$. This gives

$$M_i = M_i^* + \tau_i \tilde{E}_i \tag{9}$$

The diffuse total radiosity considering only a diffuse factor in Eq. 9 and excluding the specular reflection term is described as the following

$$M_i^d = \varepsilon_i \sigma T_i^4 + \rho_i^d E_i + \tau_i \tilde{E}_i \tag{10}$$

The contribution to $E_i$ from the other diffusely reflecting surfaces in an enclosure can be represented in accordance with the relationship defined by the configuration factors in an enclosure with diffuse surfaces, except that now the configuration factors are replaced by the exchange factors, or

$$E_i = \sum_j \bar{F}_{ij} M_j^d \tag{11}$$

where $\bar{F}_{ij}$ is the exchange factor defined between i element and j element through j's images on the element i. Equations 7 through 11 can be represensted by the short and longwaves, respectively.

To obtain the heat balance (Eq. 7) as functions of surface temperatures in an enclosure and the irradiance, or incident radiation, from the target source at the field-of-view limiter of the radiometer models, first Eq. 9 is substituted into Eq. 7, yielding

$$\phi_i = (1 - \rho_i^d - \rho_i^s)\, E_i - \varepsilon_i\, \Omega_i - \tau_i\, \tilde{E}_i$$

in which $\rho_i^d + \rho_i^s = \rho_i$ where $\rho_i$ is the total reflectance of the surface and $\Omega = \sigma\, T^4$.

Thus

$$\phi_i = (1 - \rho_i)\, E_i - \varepsilon_i\, \Omega_i - \tau_i\, \tilde{E}_i \tag{12}$$

Then, combining Eqs. 10 and 11 and rearranging, yields the following equation

$$E_i = \sum_j (\delta_{ij} - \bar{F}_{ij}\, \rho_i^d)^{-1}\, \bar{F}_{ij} (\varepsilon_j\, \Omega_j + \tau_j\, \tilde{E}_j). \tag{13}$$

For brevity, we introduce new variables from Eq. 13, that is

$$A_{ij} = (\delta_{ij} - \bar{F}_{ij}\, \rho_j^d)^{-1}\, \bar{F}_{ij}\, \varepsilon_j. \tag{14}$$

$$C_{ij} = (\delta_{ij} - \bar{F}_{ij}\, \rho_j^d)^{-1}\, \bar{F}_{ij}\, \tau_j. \tag{15}$$

Thus, Eq. 12 with the above constants can be written

$$E_i = \sum_j A_{ij}\, \Omega_j + C_{ij}\, \tilde{E}_j \tag{16}$$

Equation 16 has an important role to couple an enclosure with the neighboring enclosures through a semi-transparent or transparent boundary surface.

The above relation (Eq. 16) can be used for the cases when an enclosure is partly or totally surrounded by the neighboring enclosures and also when part or all of the surfaces of the enclosure are non-opaque, i.e., semi-transparent or transparent. To include all the configurations of the enclosures and to couple them together through interactive boundary surfaces, the above relation (Eq. 16) can be generalized in the matrix form, that is,

$$E = \bar{A}\, \Omega + \bar{C}\, \tilde{E} \tag{17}$$

where $\bar{A}$ and $\bar{C}$ denote Eqs. 14 and 15, respectively. The bars above the notation A and C are to distinguish Eq. 14 and 15 from the notation for the area and the conduction constant of governing equation to be discussed in the Section 2.1.4.

### 2.1.3 Coupling Enclosures

In the above Eq. 17, $\tilde{E}$ can be directly related to E by defining the geometrical coupling factor. The relationship between E and $\tilde{E}$ is apparently dependent on the geometrical formation of enclosures through the interactive (non-opaque) surfaces as in the following example. Consider the system shown in Fig. 9 which consists of nine enclosures and interacts at the boundaries with the incident radiation from the environment. The incoming radiation E can be written

$$E = \begin{bmatrix} E^1 \\ E^2 \\ E^3 \\ \cdot \\ \cdot \\ \cdot \\ E^m \end{bmatrix} \tag{18}$$

where the superscript m denotes the number of enclosures in the prescribed system. Each enclosure of the system has a certain number of interacting surfaces. In such a case, the incident radiation upon the surfaces of the $i^{th}$ enclosure can be described by

$$E^i = \begin{bmatrix} E_1^i \\ E_2^i \\ E_3^i \\ \cdot \\ \cdot \\ \cdot \\ E_n^i \end{bmatrix} \qquad \text{and } 1 \leq i \leq m \tag{19}$$

where the subscript n denotes the number of a surface in an enclosure of the system. As shown in Fig. 9, $E_4^1$ and $E_2^2$ define the incident radiation on an interactive boundary surface between the first and second enclosures. The subscripts 4 and 2 here, respectively denote the surface numbers as seen or counted from each enclosure. These surfaces designated by 4 and 2 in the enclosure 1 and 2, respectively, are supposed to be the interactive boundary surface co-owned by enclosures 1 and 2. On the contrary, incident radiation $\tilde{E}$ coming from the opposite, or neighboring, enclosure upon the boundary surface is defined by $\tilde{E}_2^2$ and $\tilde{E}_4^1$, respectively. Accordingly, observing enclosures 1 and 2 with respect to the incident radiation on the interactive boundary surface, we find the following coincidences:

$$E_4^1 = \tilde{E}_2^2 \quad \text{and} \quad E_2^2 = \tilde{E}_4^1 \quad . \tag{20}$$

Equation 20 tells us that the incident radiation $E_4^1$, upon the interactive boundary surface of the first enclosure is virtually regarded as the opposite of incident radiation $\tilde{E}_2^2$, on the back surface of the same boundary, whether the second enclosure is considered to be formulated or vice versa. This coincidence on each interactive boundary surface is uniquely determined by the formation of the enclosure in a given system.

To generalize the above relationship, Eq. 20, for the enclosure which has interactive boundaries and also system boundaries, let us consider the first enclosure shown in Figure 9. The first enclosure has not only two interactive boundaries at 3rd and 4th surfaces, but also two system boundaries at 1st and 2nd surfaces (Fig. 9). Extending the above relationship (Eq. 20) to include the system boundaries and describing it in a matrix form, we have

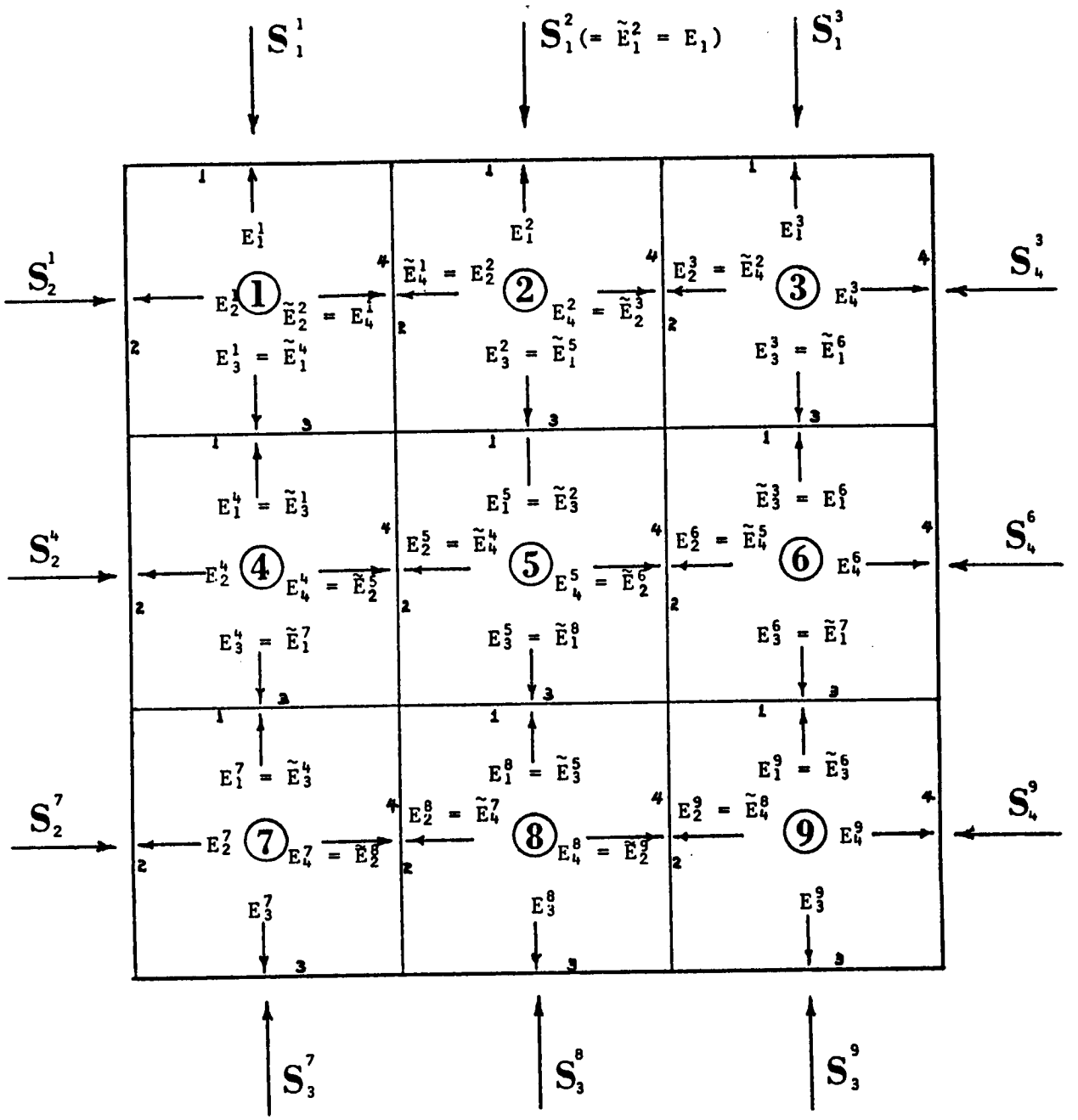


FIGURE 9. Interactive Enclosure Model

$$E^1 = \begin{bmatrix} 0 & 0 & 0 & 0 \\ 0 & 0 & 0 & 0 \\ 0 & 0 & 0 & 0 \\ 0 & 1 & 0 & 0 \end{bmatrix} E^2 + \begin{bmatrix} 0 & 0 & 0 & 0 \\ 0 & 0 & 0 & 0 \\ 1 & 0 & 0 & 0 \\ 0 & 0 & 0 & 0 \end{bmatrix} \cdot E^4 + \begin{bmatrix} 1 & 0 & 0 & 0 \\ 0 & 1 & 0 & 0 \\ 0 & 0 & 0 & 0 \\ 0 & 0 & 0 & 0 \end{bmatrix} S \qquad (21)$$

Likewise, the other enclosures have the same expression as depicted for the first enclosure. Thus, introducing a new variable D for the enclosure coupling factor, the relationship (Eq. 21) can be written

$$\tilde{E} = DE + FS \qquad (22)$$

where D is a matrix representing the enclosure coupling factors through the interactive boundaries, F is a matrix representing the system boundary conditions imposed by surroundings, and S is a column vector of the heat fluxes arriving at the system boundaries. Now substituting Eq. 22 into Eq. 17 and collecting the same variables, we have, with I being an Identity matrix

$$E = (I - \bar{C}D)^{-1} \bar{A}\Omega + (I - \bar{C}D)^{-1} \bar{C}FS \qquad (23)$$

Equation 23 illustrates that the incident radiation E upon a surface of the enclosure accounts for all the effects of radiation from the surfaces with different temperatures not only in its own enclosure, but also in neighboring enclosures, and the heat flux at the system boundaries.

The energy balance at a node or a surface in the enclosure due to the incident radiation is then described by inserting Eqs. 22 and 23 into Eq. 12. Then, by eliminating E and $\tilde{E}$ from Eq. 12, the radiative energy balance is obtained as only functions of the temperatures of enclosure surfaces and the irradiance from the target source or any other kinds of heat flux which interacts with the system boundaries. That is,

$$\phi = \left[(I - \rho - \tau D)(I - \bar{C}D)^{-1} \bar{A} - \varepsilon \quad \Omega\right]$$

$$+ \left[(I - \rho - \tau D)(I - \bar{C}D)^{-1} \bar{C} - \tau \quad FS\right] \tag{24}$$

When the radiative energy balance described by Eq. 24 is applied to the enclosures obtained by properly dividing the geometry of the system, the number of the radiative energy balance equations, $\phi$, obtained from Eq. 24 is more than the number of nodal points because consideration is given twice to the interactive boundary between two enclosures. Accordingly, in the multiple-enclosure system the radiative energy balance is calculated for each surface of enclosures. Then, for the overlapped boundary surface, the radiative energy balances from both enclosures are added together. The radiative energy balance (Eq. 24) is then plugged into the energy equation (Eq. 3) of the system.

The enclosure coupling technique developed here has many potential applications and advantages over the conventional methods currently used.

Among the advantages, this technique can be used for any kind of geometry by only setting up enclosures via dividing the geometry and defining the D and F matrices in Eq. 22. The enclosure space with irregular geometry can be properly divided into many smaller regular sub-spaces to adopt the enclosure coupling technique. For an enclosure with complicated geometry, the division of the space geometry into well-defined sub-spaces facilitates the computation of the configuration factor or the exchange factor, especially for an enclosure with specular surfaces which is totally dependent on the geometry.

This technique can also be extended to treat radiation interactions including the scattering and absorption with optically thin or thick participating media in an enclosure. Even though there are temperature and density gradients in participating media, by dividing the enclosure space into sub-spaces which are small enough to assume the sub-spaces to be isothermal and isotropic, the

enclosure theory can be directly applied for the system without loss of generality.

In short, the advantages and potential applications of the enclosure coupling technique are listed below.

ADVANTAGES:

1. It minimizes the effort required to define the exchange factors among the surfaces in an enclosure with complex geometry, and so may be able to decrease a degree of possible approximation in the computation of exchange factors.
2. It may take the wavelength characteristics of materials or participating media into account in a simple manner.
3. It can be easily coupled with the thermal model of the system so that the material and thermal properties are considered in the coupled dynamic system without approximations and assumptions such as those in the boundary definitions.
4. It enables the system to deal with any imposed initial conditions and prescribed boundary conditions.
5. It may enhance the accuracy in the computation of a geometrically partitioned conductive and radiative model.
6. As a consequence, this technique can avoid the length of time for computation and a cumbersome manipulation which is often revealed in the other methods such as ray tracing or Monte Carlo methods.

APPLICATIONS:

1. It can be used for any enclosure geometry.
2. It can be used for either the enclosure with a vacuum space or the enclosure with participating media (solid, liquid or gas).

3. It can be applied to any optical system's anslyses and design regardless of the directional, spectral, and/or temperature dependences of its enclosure spaces.
4. Applications of the enclosure coupling technique to optical systems may vary from a typical radiometer to any waveguide system.

### 2.1.4 Governing Equation

The governing equation which describes the performance of a radiometer that has a dynamic response to an incoming radiance can be obtained by substituting Eqs. 4 and 24 into Eq. 3 and collecting terms. Then we can separate the incoming radiation flux from the radiation balance term. The equation can be written in a general form to describe the energy balance in a node as follows

$$\dot{T} = AT + DT^4 + BE + B_Q\dot{Q} + b + e \tag{25}$$

where

$$A = \frac{1}{MR}$$

$$D = \frac{\sigma A_r}{M}\left[(I - \rho - D)(I - \bar{C}D)^{-1}\bar{A} - \varepsilon\right]$$

$$B = \frac{A_r}{M}\left[(I - \rho - D)(I - \bar{C}D)^{-1}\bar{C} - \tau F\right]$$

$$B_Q = \frac{A_c}{M}$$

b = a bias term

e = a noise term

R = the thermal resistance between nodes (see Eq. 5)

$M = V\gamma C$

$A_r$ = the area for the radiative interaction

$A_c$ = the node area covered by the heat sink heater

Equation 25 represents a general form that consists of a set of equations for a multinode system. Considering only the thermal model for the nonscanner total radiometer which is divided into 8 nodes, we have a set of 8 equations which represent the energy balance in each node separately. The inclusion of the electronic thermal control system equations will increase the total system by the number of the transfer functions. The constants of Eq. 25 for the nonscanner, the scanner, and the solar monitor are described in Appendices C, D, and E.

### 2.1.5 Electronic Control System Model for the Nonscanner

The block diagramshown in Fig. 10 illustrates the nonscanner ACR control system model. The control electronics transfer function is of the form (cf. ERBE Instruments, Monthly Status Report - Vol. 1, Nov. 1980, unpublished)

$$F_E(s) = \frac{K_E(\tau_1 S + 1)(\tau_2 S + 1)}{S(\tau_3 S + 1)(\tau_4 S + 1)} \tag{26}$$

To obtain the differential equations describing the electronics transfer function, we define the state variables $T_{10}$, $T_{11}$, $T_{12}$, as follows

$$\dot{T}_{10} = V_B K_a K_E \left[ \frac{R_r(T_3)}{R_a(T_1) + R_r(T_3)} - B_E \right] + K_E n_E \tag{27}$$

Note $B_E = \frac{R_4}{R_3 + R_4}$ is an input constant, where $R_3$ and $R_4$ are the bridge resistances.

$$R_i(T_j) = A_i + B_i T_j + C_i T_j^2, \qquad i = a, r; \quad j = 1,3 \tag{28}$$

$$\dot{T}_{11} = \frac{1}{\tau_3} (-T_{11} + T_{10} + \tau_1 \dot{T}_{10}) \tag{29}$$

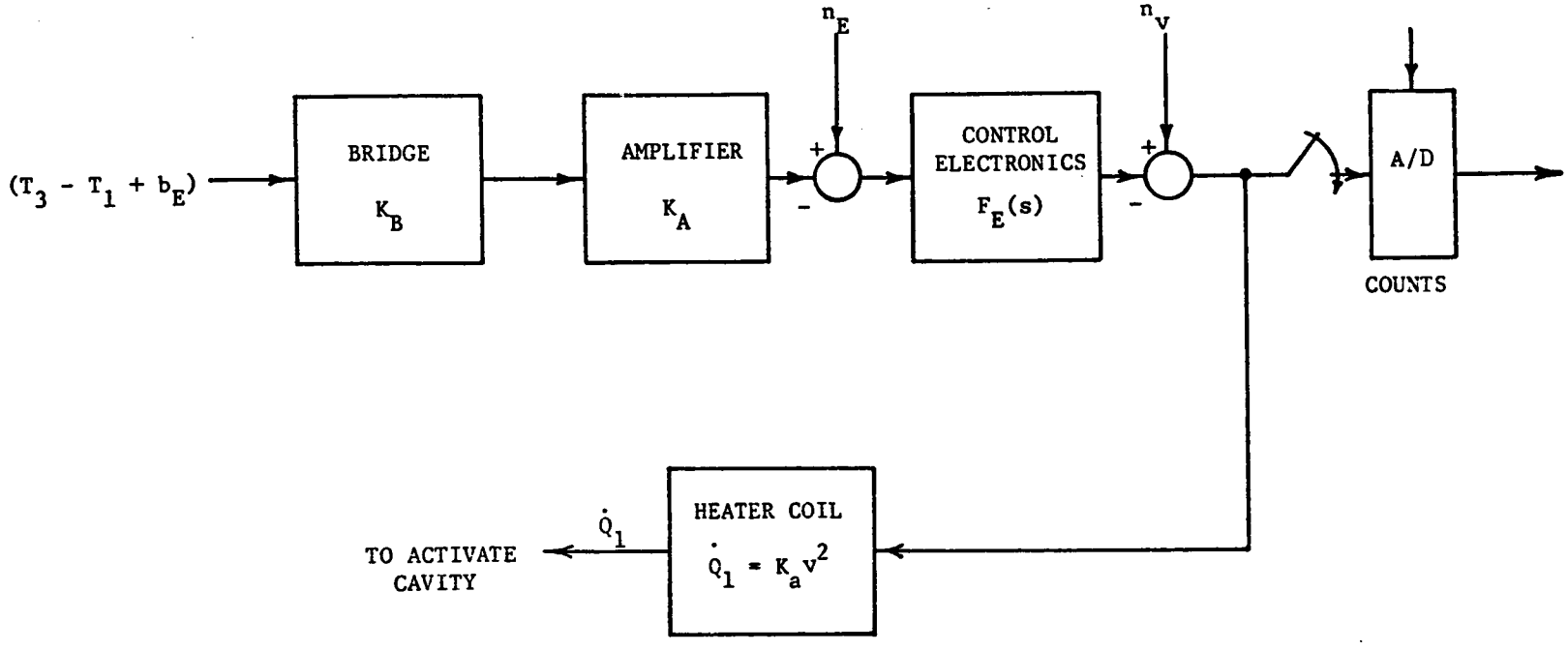


FIGURE 10. Active Cavity Radiometer (ACR) Control System Model

Substituting Eq. 27 into Eq. 29 gives

$$\dot{T}_{11} = \frac{1}{\tau_3}(-T_{11} + T_{10}) + \frac{\tau_1}{\tau_3} V_B K_a K_E \left[\frac{R_r(T_3)}{R_a(T_1) + R_r(T_3)}\right] + \frac{1}{\tau_3} K_E n_E \qquad (30)$$

$$\dot{T}_{12} = \frac{1}{\tau_3}(-T_{12} + T_{11} + \tau_2 \dot{T}_{11}) \qquad (31)$$

For full expression, substitute $\dot{T}_{11}$ in Eq. 30 into Eq. 31.

Note that $T_{12}$ is now the output of the electronics, so that the voltage output is

$$v = T_{12} + n_v \ . \qquad (32)$$

To convert to counts, C, use the following relation:

$$C = K_c v = K_c T_{12} + K_c n_v, \qquad K_c = 819.1 \text{ counts/volt.}$$

The heat flow provided to the active cavity to maintain its temperature at a constant level is given by

$$\dot{Q}_1 = K_a v^2 = K_a T_{12}^2 + 2K_a T_{12} n_v + K_a n_v^2 \qquad (33)$$

This expression for $\dot{Q}_1$ brings to light the major effects that the noise terms introduce into the operation of the radiometer. Note that due to the use of square feedback, the linear noise terms acquire a gain of $2K_a T_{12}$, while a quadratic noise term (having non-zero mean) is introduced. Coils which are wrapped around the active and reference cones generate heat and are expressed by the following terms.

$$\dot{Q}_{J_1} = V_B^2 \frac{R_a(T_1)}{[R_a(T_1) + R_r(T_3)]^2}$$

$$\dot{Q}_{J_3} = V_B^2 \frac{R_r(T_3)}{[R_a(T_1) + R_r(T_3)]^2}$$

To obtain the closed-loop system, the expression Eq. 33 is simply substituted into the equation governing the active cavity temperature.

$$\dot{T}_1 = A_{12}(T_2 - T_1) + \sum_k D_{ik} T_k^4 + B_1 E + \frac{k_a}{M_1} T_{11}^2 + \frac{2K_a T_{11} n_v}{M_1}$$

$$+ \frac{K_a n_v^2}{M_1} + V_B^2 \frac{R_a(T_1)}{[R_a(T_1) + R_r(T_3)]^2} \tag{34}$$

The block diagram shown in Fig. 11 illustrates the non-scanner ACR heat sink heater control system model.

The control electronics transfer function can be approximated in the form

$$F_{HE}(s) = K_{HE} \frac{(\tau_H s + 1)}{s} \tag{35}$$

The differential equations describing the heat sink heater controller can be expressed as

$$\dot{T}_{13} = K_{H_{13}} K_{HE} (T_H - T_2) + K_{HE} n_H \tag{36}$$

$$v_H = T_{13} + T_H K_{HE} K_{H_{13}} (T_H - T_2) + \tau_H K_{HE} n_H \tag{37}$$

$$\dot{Q}_2 = K_H v_H^2 \tag{38}$$

In Eq. 25 the heat source term, $\dot{Q}$, is substituted by Eq. 38 for the aluminum and copper heat sinks.

### 2.1.6 Simulation of the Nonscanner Model

The simulation of the ERBE nonscanner sensors is divided into two major parts; the first determines the coefficients of the system, the second solves the systems over time and plots the results. Figure 12 is a flow diagram

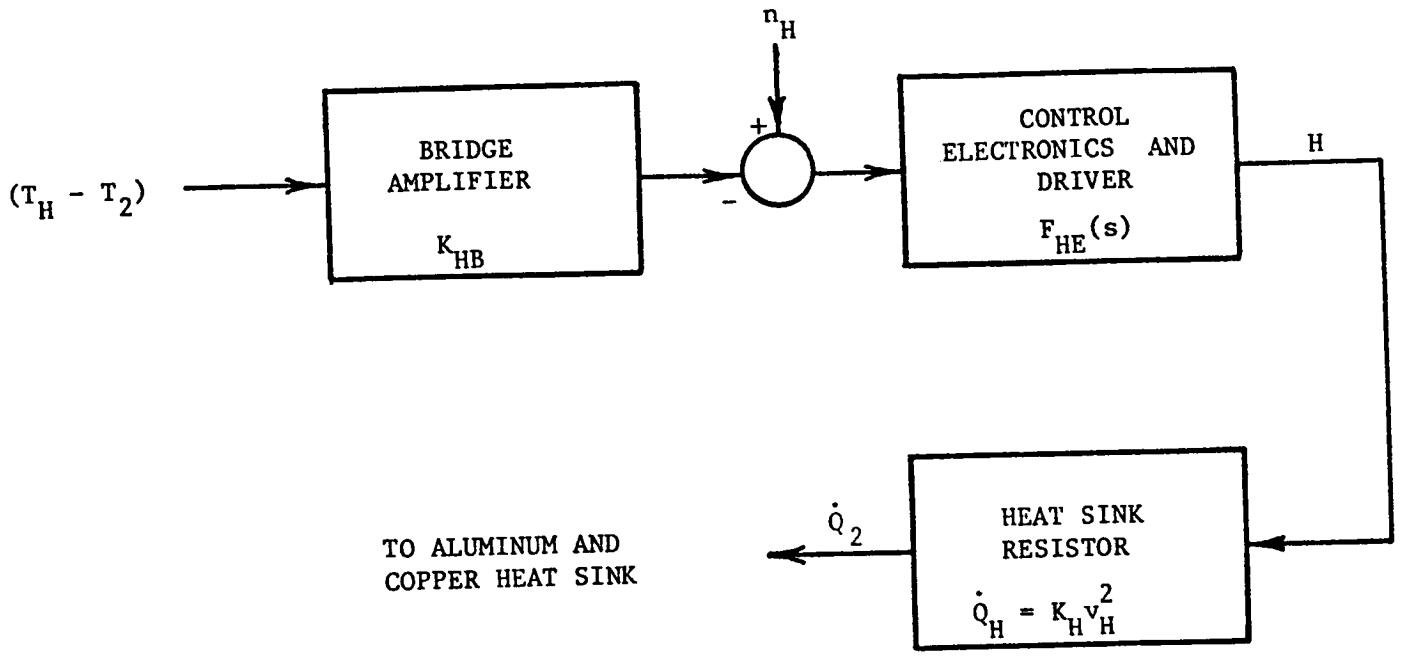


FIGURE 11. Nonscanner Heat Sink Heater Control System Model

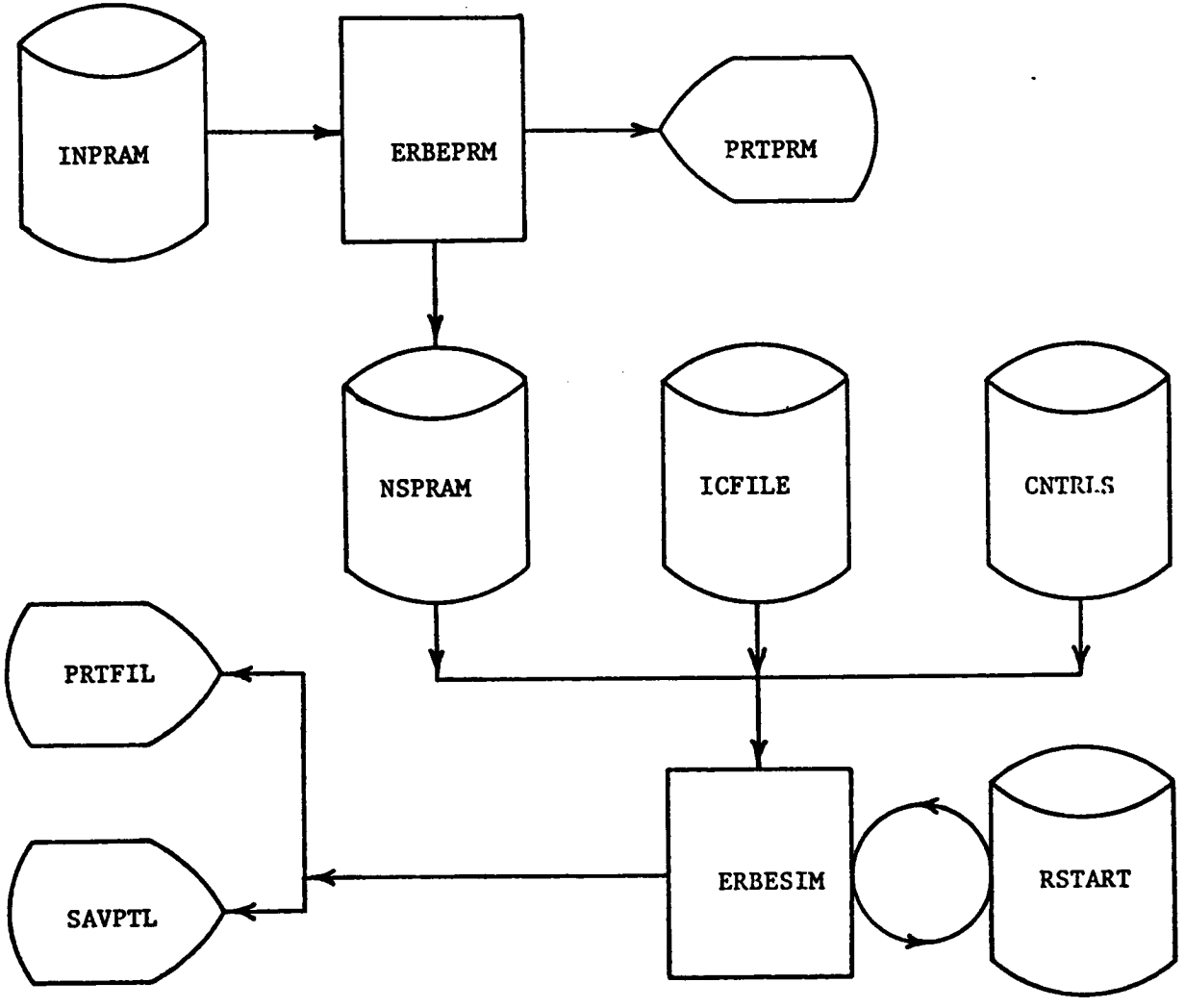


FIGURE 12. Flow Diagram Indicating File and Program Usage in Simulation

indicating file and program usage. The equation describing the change of temperature in a given node at time i is

$$\dot{T}(i) = AT(i) + DT^4(i) + BE + B_Q\dot{Q} + B_n n \qquad (39)$$

Where A is the conductance coefficient matrix, D is the radiative coefficient matrix, B is the irradiance source vector and $B_Q$ is a vector of coefficients which describe heating contributions from the control system. T(i) represents either the temperature change for a thermal node or a voltage change for an electronic node. The general method of solution is a fourth order Runge-Kutta algorithm, all of which is discussed in great detail in the following sections.

2.1.6.A Parameter and Coefficient Determination

The coefficient matrices and vectors are determined in the first program in the sequence ERBEPRM. The data inputted to this is determined from material specifications and engineering drawings supplied by the manufacturer. The code is partitioned into 5 major sections, not including the program input/output. The first of these is the subroutine "COMPUTA". This routine takes the heat capacities and node to node thermal resistances and returns the conductance coefficient matrix. The program then enters the routine ADDELC which is designed to modify the conductance matrix in such a way as to allow the ACR heater controls to use the same equations in the simulation as the node temperatures. The output from this routine is an enlarged conductance matrix and several electronic vectors. Once these two routines have been computed COMPUTH calculates the radiative exchange coefficient between surfaces for each cavity. Due to the linking of cavities a and b, as defined in Appendix C, dome filter or fictitious surfaces, the radiative exchange coefficients for these cavities

are stored for later use. The results of COMPUTH are then added together to give the total radiative exchange coefficient matrix in COMPUTD, COMPUTB and CMPUTBP. The results are then issued to two files, one formatted for inspection and one binary for use by the simulation program.

### 2.1.6.B Instrument Simulation

The program consists of four logical sections, an Input, the Integration, the intermediate Output and the Plotting section. The actual solution to the system of equations that describes each instrument is accomplished by the program ERBESIM. The program steps through a determined time interval using an evenly spaced discrete time step and solves each system using a Fourth Order Runge-Kutta scheme to evaluate the system at the next step. Each system is sampled at another rate controlled by the user until 20 samplings are taken or the end of simulated time is reached. The results are then stored on magnetic medium for use by the plotting routines. The final product is the sensor's resposne described by plots and tables of the modeled response of the instrument, i.e., time-dependent temperatures of the nodes, instrument response (in counts), electronic voltages (in volts) and input source irradiance (in $W/m^2$).

The first section of the program reads the coefficient matrices and vectors, intitial conditions from binary files, and the simulation control variables from a namelist file. The Namelist file contains variables for controlling simulation time step size, sampling rates and the combination of instruments and radiation profiles, etc. which are to be simulated. The simulation is

capable of allowing the user to choose either a sawtooth, Fourier series, step function, constant or ramp radiance profile.

The Runge-Kutta method used was developed by Fehlberg and solves the system

$$Y_{i,m+1} = Y_{i,m} + h \sum_{j=0}^{5} A_j K_{ji}, \quad i = 1, 2, 3, \ldots \text{ number of nodes}$$

where

$$K_{ji} = f(t_m + C_j h, y_m + h \sum_{\ell=0}^{i} b_{j\ell} K_{\ell j})$$

where f is the function describing T(i) from Eq. 39 as functions of time and temperature, $a_j$, $b_{j\ell}$, and $C_j$ are constants determined by Fehlberg for solving first order non-stiff systems of ordinary differential equations.

### 2.1.7 Count Conversion for Nonscanner

#### 2.1.7.A Nonscanner Total Channel

In the active cavity radiometers, the electronics control the amount of heat added to the active cavity to maintain the temperature of the cavity about half a degree above the reference cavity. The control of the heat input to the active cavity is inversely proportional to the incident radiation entering through the field of view and precision aperture from a given source. In other words, the control system provides more heat input for the weak incident radiation and less heat input for the strong incident radiation. Thus, the voltage driving the active cavity heater provides the sensor output proportional to the incident radiation. The voltage reading, after A/D conversion, provides the sensor output in counts. The sensor output in counts is then converted into engineering units. The algorithms for the count conversion are of the gain/offset type, and are derived based on the sampled instrument data, e.g., sensor response (in counts), HK temperatures, etc. and the instruments radiative and conductive interactions.

The following is the count conversion equation for NS total channels.

$$E(t - \tau) = A_v v^2(t) + A_H\left[T_H(t) - T_{H_o}\right] + A_A\left[T_A(t) - T_{A_c}\right] + A_F\left[T_F(t) - T_{F_o}\right] + B \tag{40}$$

The constants in Eq. 40 are defined as follows

$$A_v = - \frac{B_a K_a}{B_1} \tag{41}$$

$$A_H = - \frac{4}{B_1} \sum_{k \neq A,F} D_{1k} T^3_{k_o} \tag{42}$$

$$A_A = - 4 \frac{D_{18}}{B_1} T^3_{8_o} \tag{43}$$

$$A_F = - 4 \frac{D_{16}}{B_1} T^3_{6_o} \tag{44}$$

$$B = \frac{A_{12}}{B_1} b_E - \sum_{k=1}^{n} \frac{D_{1k}}{B_1} T^4_{k_o} - \frac{V_B^2}{4 R_B M_1 B_1} \tag{45}$$

where

$V$ = instrument output (in volts)

$T_H$ = measured heat sink temperature ($^oK$) at time t

$T_A$ = measured precision aperture temperature ($^oK$) at time t

$T_F$ = measured FOV limiter temperature ($^oK$) at time t

The remaining quantities, i.e., $B_a$, $K_a$, $B_1$, T, $D_{ik}$, $A_{12}$ and $b_E$ are constants which are specified for each instrument. These constants for the count donversion equations are determined for the simulation study of the instrument model using ground and inflight calibration data. These parameters or constants

may be altered at various points in time, usually after a flight calibration, in order to reflect any changes in the instrument characteristics.

### 2.1.7.B Nonscanner Filtered Channel for Shortwave

For the filtered channels, the count conversion has a set of two equations for short and longwaves as follows:

$$\alpha_{11}\,\hat{E}_s + \alpha_{12}\,\Delta T_9 = \beta_1 \tag{46}$$

$$\alpha_{21}\,\hat{E}_s + \alpha_{22}\,\Delta T_9 = \beta_2 \tag{47}$$

The coefficients of the terms in the above equations are given by the following equations,

$$\alpha_{11} = B_{1s} - B_{1\ell} \tag{48}$$

$$\alpha_{12} = 4D_{1,9}\,T_{9_o}^3 \tag{49}$$

$$\alpha_{21} = B_{9\ell} - B_{9s} \tag{50}$$

$$\alpha_{22} = A_{9,4} + A_{9,8} - 4D_{9,9}\,T_{9_o}^3 \tag{51}$$

$$\begin{aligned}\beta_1 = {} & \left(A_{12}\,b_E - \sum_{k=1}^{n_s} D_{i1}\,T_{k_o}^4 - \frac{V_B^2}{4R_B\,M_1}\right) - 4\left(\sum_{k\neq 8,6}^{} D_{ik}\,T_{k_o}^3 - \frac{V_B^2\,\beta_r}{16R_B^2\,M_1}\right) \\ & * (T_H - T_{H_o}) - 4D_{18}\,T_{8_o}^3\,(T_A - T_{A_o}) - 4D_{16}\,T_{6_o}^3\,(T_F - T_{F_o}) \\ & - B_a\,K_a\,v_s^2 - B_{ie}\,\hat{E}\end{aligned} \tag{52}$$

$$\begin{aligned}\beta_1 = {} & \sum_{k=1}^{n_s} D_{9k}\,T_{k_o}^3 + A_{98}(T_A - T_{9_o}) + A_{d8}(T_H - T_{9_o}) + 4\left(\sum_{k\neq 4,8,9}^{n_s} D_{9k}\,T_{k_o}^3\right) \\ & * (T_H - T_{H_o}) + 4D_{98}\,T_{8_o}^3\,(T_A - T_{A_o}) - 4D_{16}\,T_{6_o}^3\,(T_F - T_{F_o}) + B_{1\ell}\,E\end{aligned} \tag{53}$$

The filtered channel count converstion is obtained from the solution of two simultaneous equations (Eqs. 46 and 47). Thus the solution to the equations is given by

$$\hat{E}_s = \frac{1}{\alpha_{11}\,\alpha_{22} - \alpha_{12}\,\alpha_{21}} (\alpha_{22}\,\beta_1 - \alpha_{12}\,\beta_2) \tag{54}$$

$$T_9 = \frac{1}{\alpha_{11}\,\alpha_{22} - \alpha_{12}\,\alpha_{21}} (-\alpha_{21}\,\beta_1 + \alpha_{11}\,\beta_2) \quad . \tag{55}$$

The longwave incident radiation estimate is then defined by subtracting the shortwave incident radiation from the total incident radiation estimate. That is,

$$\hat{E}_\ell = \hat{E} - \hat{E}_s \tag{56}$$

The constants in Eqs. 46 - 56 are

$v_s$ = shortwave channel output (in volts)

$\hat{E}_s$ = shortwave incident radiation estimate ($W/m^2$)

$\hat{E}_\ell$ = longwave incident radiation estimate ($W/m^2$)

$\hat{E}$ = total incident radiation estimate ($W/m^2$)

The temperatures of the heat sink, aperture and FOV limiter, $T_H$, $T_A$, and $T_F$, are measured as before in total NS channel.

### 2.1.8 Solar Monitor Model Analysis

The solar monitor is different from the nonscanner in size, shape and design feature as shown in Figure 6. It has a barrel structure ~ 9.5 cm long between the primary and secondary apertures. The tail of the core body of the instrument is attached to the housing and includes the primary and secondary apertures, barrel, heat sink and active and reference cavities. This instrument has a shutter located in front of the secondary aperture. The shutter operates on a 64 second "on and off" cycle in which it is open for 32 seconds and then closed for 32 seconds.

Since this instrument deals with a strong intensity of the incident radiant energy and does not have the heat sink temperature controller, the heat sink has a larger heat capacity for damping out the effect of large input temperature gradients.

However, it is desirable to check whether there is any transient effect due to the periodical on and off mode of the shutter, the strong intensity of solar radiation, and the excessively long barrel geometry. In other words, it is desirable to check whether the steady-state approximation is appropriate to develop the count conversion algorithm for the solar monitor. Thus, we introduce two simplified geometries here to check how fast the temperature reaches a stable condition, as every 32 seconds the solar radiation is viewed.

First, let us assume that the shutter has a rectangular shape of thin aluminum plate and the shutter is partly exposed to the incident solar radiation for a 32 second interval of the full 64 second cycle and has a radiation interaction with the isothermal neighboring components at any time. Figure 13 shows

the shutter model.

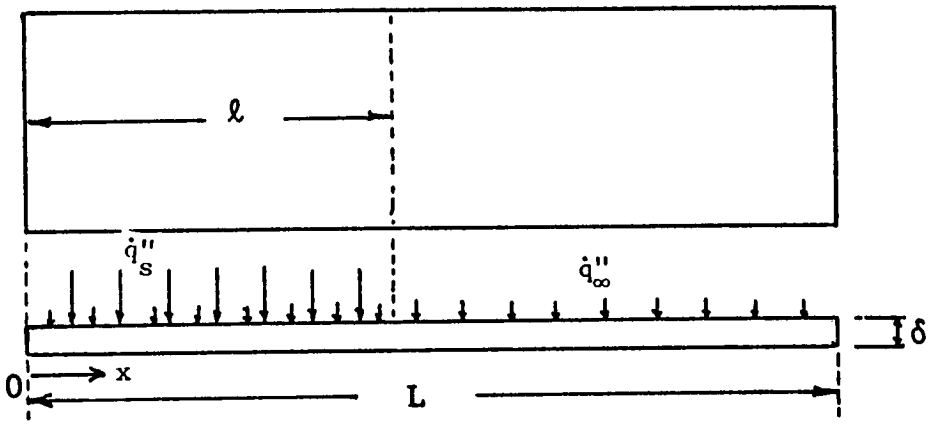


FIGURE 13. The Shutter Model

It is assumed that the left end of the shutter is insulated and the right end is attached to a temperature reservoir which has a large heat capacity. Then the energy balance equation, the initial and boundary conditions governing the above model can be written as

$$\text{G.E.} \qquad \rho C \frac{\partial T}{\partial \tau} = \frac{k}{\rho C} \frac{\partial^2 T}{\partial x^2} + \frac{\dot{q}''}{\delta} \tag{57}$$

$$\text{I.C.} \qquad T(\tau = 0) = T_o$$

$$\text{B.C.} \qquad T_x(x = 0, \tau) = 0$$

$$T_x(x = L, \tau) = T_b$$

The above equation with Neumann and Dirichlet boundary conditions can be easily solved by introducing a new variable and separating the variables. Thus the solution to the equation is described by

$$T(x, \tau) = T_b + 2(T_o - T_b) \sum_{n=0}^{\infty} \frac{(-1)^n}{(\lambda n L)} e^{-a\lambda n^2 \tau} \cos(\lambda n x)$$

$$+ \frac{\dot{q}'' L^2}{2k\delta} \left\{ \left[ 1 - \left(\frac{x}{L}\right)^2 \right] - 4 \sum_{n=0}^{\infty} \frac{(-1)^n}{(\lambda n L)^3} e^{-a\lambda n^2 \tau} \cos(\lambda n x) \right\} \tag{58}$$

where $T_o$ is an initial temperature set by 273.16 $^oK$, L the total length of the shutter (6.5 cm), $\delta$ the thickness of the shutter (0.2 cm), k the thermal conductivity (1.557 w/cm$^oK$), $\ell$ the exposure length to solar radiation (2.5 cm), $\rho$ the density of the shutter (2.713 g/cm$^3$), c the specific heat of the shutter (0.887 J/g$^oK$), a the thermal wave velocity (0.647 cm$^2$/sec)

$\lambda_n = \frac{(2n+1)\pi}{2L}$ n = 0, 1, 2, ...

$\dot{q}''_s$ is the solar flux (0.142 w/cm$^2$) x 0.2

$\dot{q}''_\infty = F \varepsilon \sigma [T_\infty^4 - T^4]$

$\dot{q}'' = \dot{q}''_s\, u(\ell-x)\, u(32-\tau) + \dot{q}''_s\, u(\ell-x)\, u(\tau-64)\, u(96-\tau) \ldots + 2\, \dot{q}''$

F the configuration factor between the shutter and the neighboring components (0.85)

$\varepsilon$ the emissivity of the shutter surface (0.8)

$\sigma$ = the Stephan-Boltzmann constant

$T_\infty$ = the ambient temperature (use $T_\infty = T_b$)

$T_b$ = the reservoir temperature set by 273$^oK$,

T = current shutter temperature, but use $T(\tau-1)$

u(x) = the unit step function.

The graphical description of the solution is shown in Figures 14 and 15. Figure 14 shows that the shutter temperature not only responds to the on and off mode of the solar flux, but the peak temperatures as well as the minimum temperatures of each cycle (64 sec) also stay at the same ranges. That is, the time averaged temperature of the shutter does not change sifnificantly. And Figure 14 also shows that the temperatures before reaching minimum and maximum points become stable. Figure 15 shows the temperatures along the length of the shutter after 100 seconds passed.

Secondly, the long barrel which is placed in the housing and is between the primary and secondary apertures is considered by the following assumptions:

1) no direct exposure to the solar flux

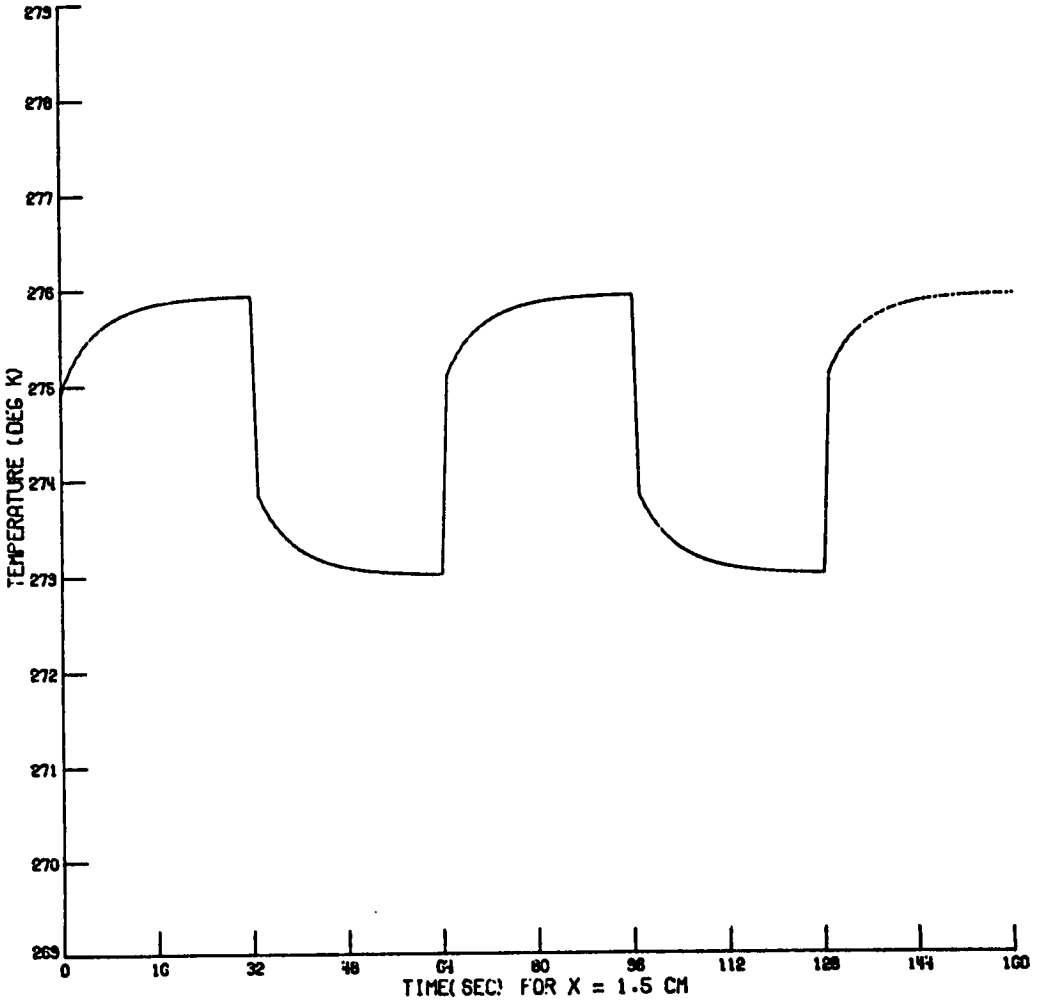


FIGURE 14. SHUTTER TEMPERATURE AT X = 1.5 CM WITH 20% ABSORPTION OF SOLAR FLUX $\ddot{Q}s = 0.142\ W/CM^2$.

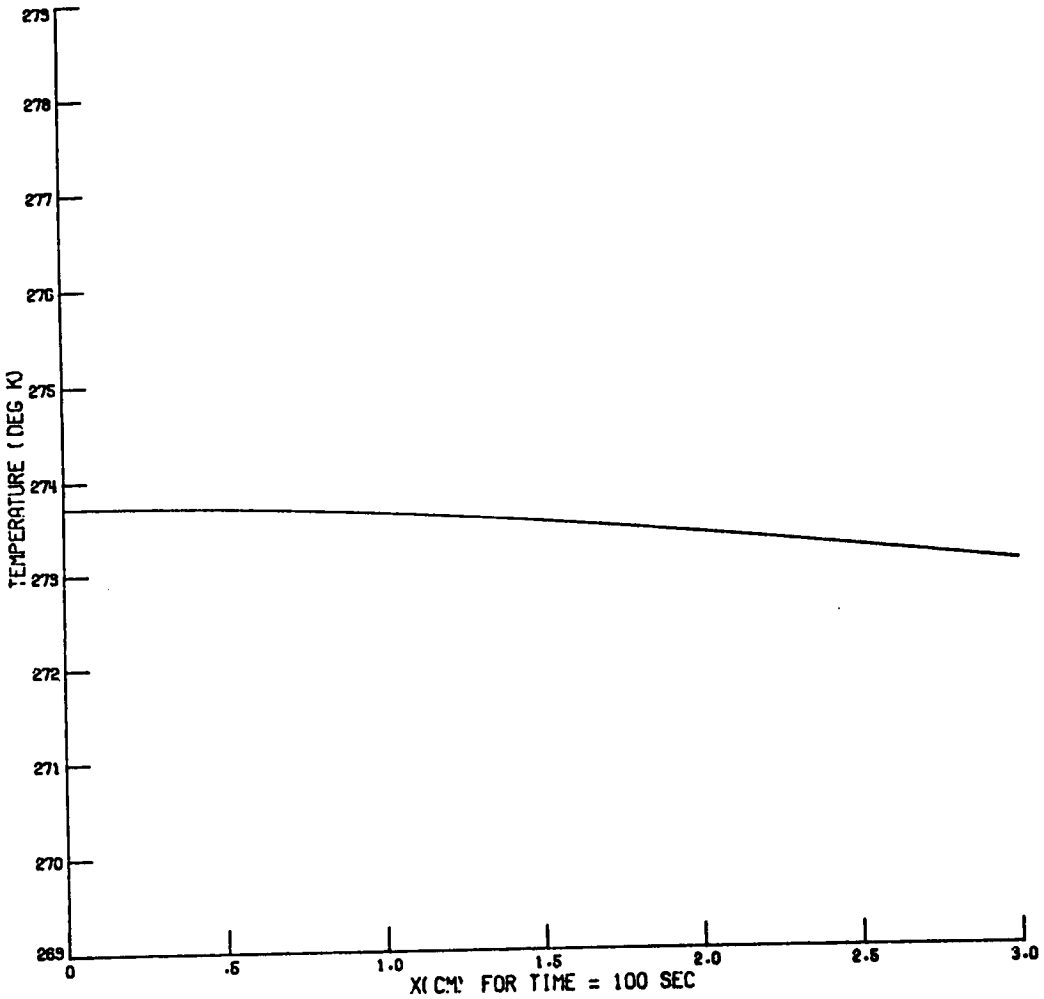


FIGURE 15. SHUTTER TEMPERATURE AT 100 SECONDS WITH 20% ABSORPTION OF SOLAR FLUX $\ddot{Q}s = 0.142$ W/CM$^2$.

2) radially uniform temperature since the wall thickness is thin

3) no circumferential temperature gradient

4) radiation exchanges only at inside and outside walls

The configuration of the model is shown in Figure 16.

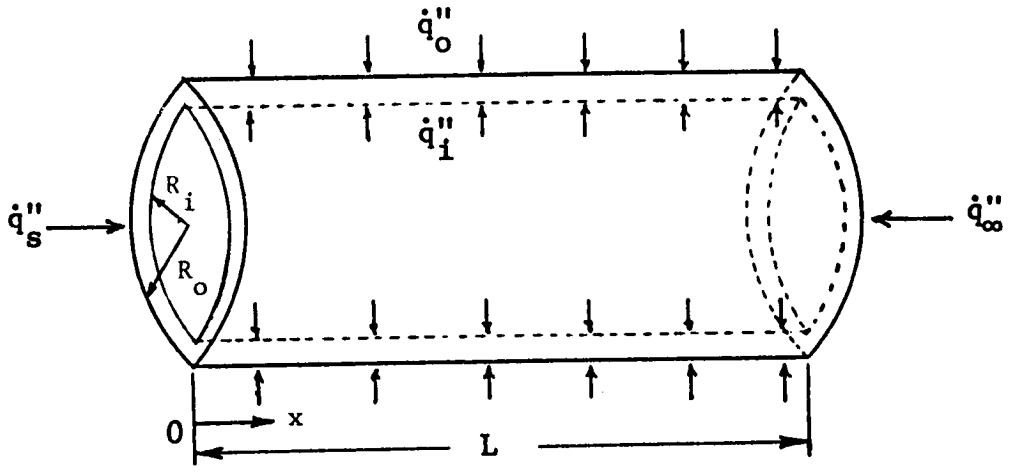


FIGURE 16. A SIMPLIFIED CONFIGURATION OF SOLAR MONITOR BARREL

The equations and boundary conditions governing the thermal conditions imposed upon the above geometry can be written as

$$\text{G.E.} \qquad \rho c \frac{\partial T}{\partial \tau} = k \frac{\partial^2 T}{\partial x^2} + \frac{\dot{q}''}{R_o - R_i} \tag{59}$$

$$\text{I.C.} \qquad T(\tau=0) = T_b$$

$$\text{B.C.} \qquad T_x(x=0) = \dot{q}''_\infty \quad \text{(set to be constant)}$$

$$T(x=L) = T_b \ .$$

Then the solution to the equation is obtained as

$$T = T_b + \frac{\dot{q}'' L^2}{2k(R_o - R_i)} \left\{ \left[ 1 - \left(\frac{x}{L}\right)^2 \right] - \frac{2k(R_o - R_i)\ \dot{q}''_\infty}{\dot{q}'' L} \left(1 - \frac{x}{L}\right) \right.$$

$$\left. - 2 \sum_{n=0}^{\infty} \left[ \frac{(-1)^n}{(L\lambda n)^3} - \frac{2k(R_o - R_i)\ \dot{q}''_\infty}{\dot{q}'' L} \frac{1}{(L\lambda n)^2} e^{-a\lambda n^2 t} \cos(\lambda n x) \right] \right\} \tag{60}$$

where

$$\dot{q}'' = \dot{q}_i'' + \dot{q}_o''$$

$$\dot{q}_o'' = F_{1-1}\varepsilon_1\alpha[(T^4(x, t-5) - T^4(x, t-1))]$$

$$\dot{q}_i'' = |\dot{q}_s'' - \dot{q}_\infty''|\varepsilon_2 F_{1-2}$$

$$\dot{q}_\infty'' = F_{1-3}\varepsilon_3\sigma[T_{av}^4(\text{in } x) - T^4(x=0, t-1)][u(64-\tau)\, u(\tau-32) + u(128-\tau)\, u(\tau-96) + \ldots]$$

$T_b = 273.16\ ^oK$

$L = 10$ cm

$k = 1.557$ w/cm $^oK$

$a = 0.647\ cm^2/sec$

$Ro-Ri = 0.5$ cm

$$\lambda_n = \frac{(2n+1)}{2L}\pi$$

$$\dot{q}_s'' = 0.146\left[u(32-\tau) + u(\tau-64)\, u(96-\tau) + \ldots\right]$$

$F_{1-1} = 0.75$

$\varepsilon_1 = 0.8$

$F_{1-2} = 0.4$

$\varepsilon_2 = 0.08$

$F_{1-3} = 0.4$

$\varepsilon_3 = 0.5$

The above values are used in both the shutter and barrel cases. These estimates were selected to best represent the solor monitor based on the material and thermal properties of the shutter and barrel. The results of the calculations described in Figures 17 and 18 demonstrate that the temperatures do not change very much with respect to time or in the axial direction of the barrel since they exhibit only about a half degree of temperature change in both cases.

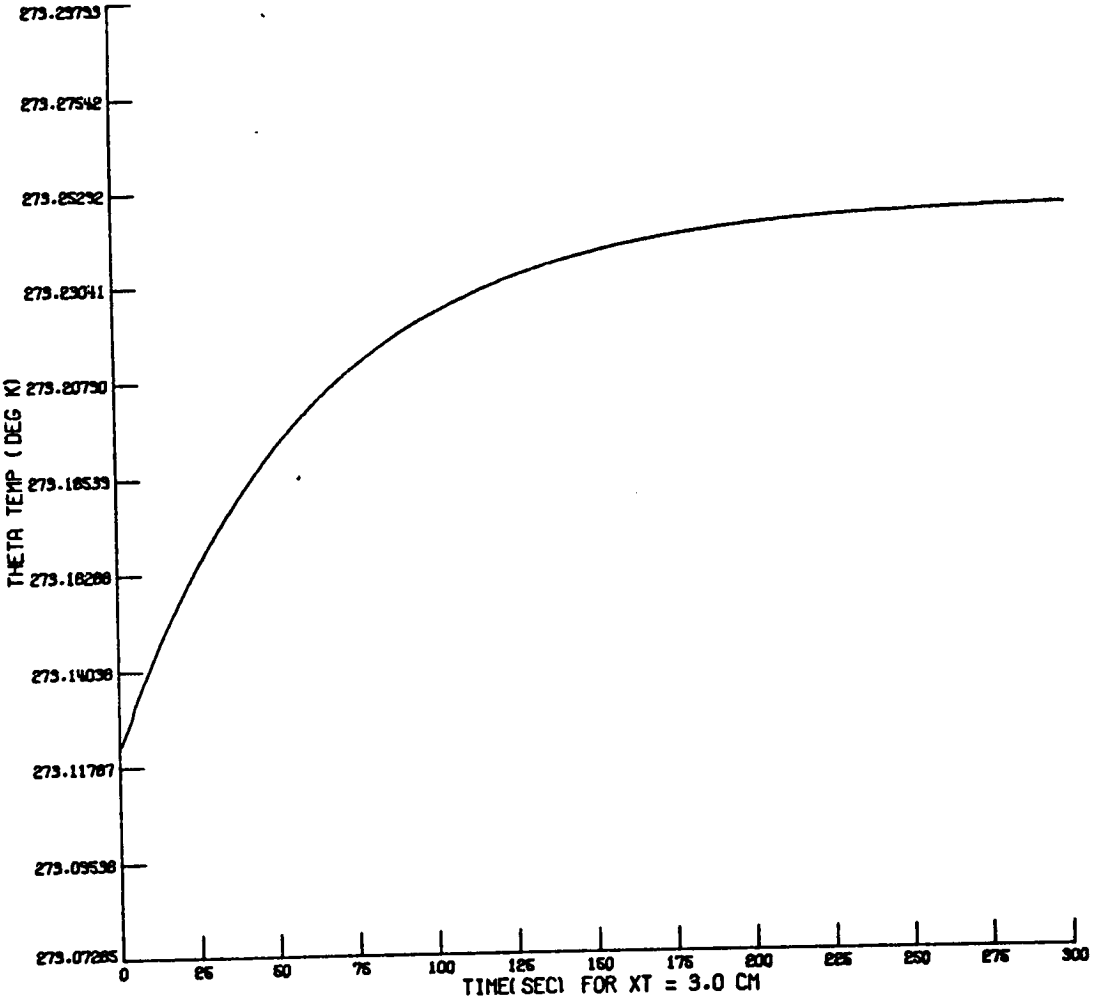


FIGURE 17. BARREL TEMPERATURE WRT TIME AT X=3 CM FROM THE SECONDARY APERTURE.

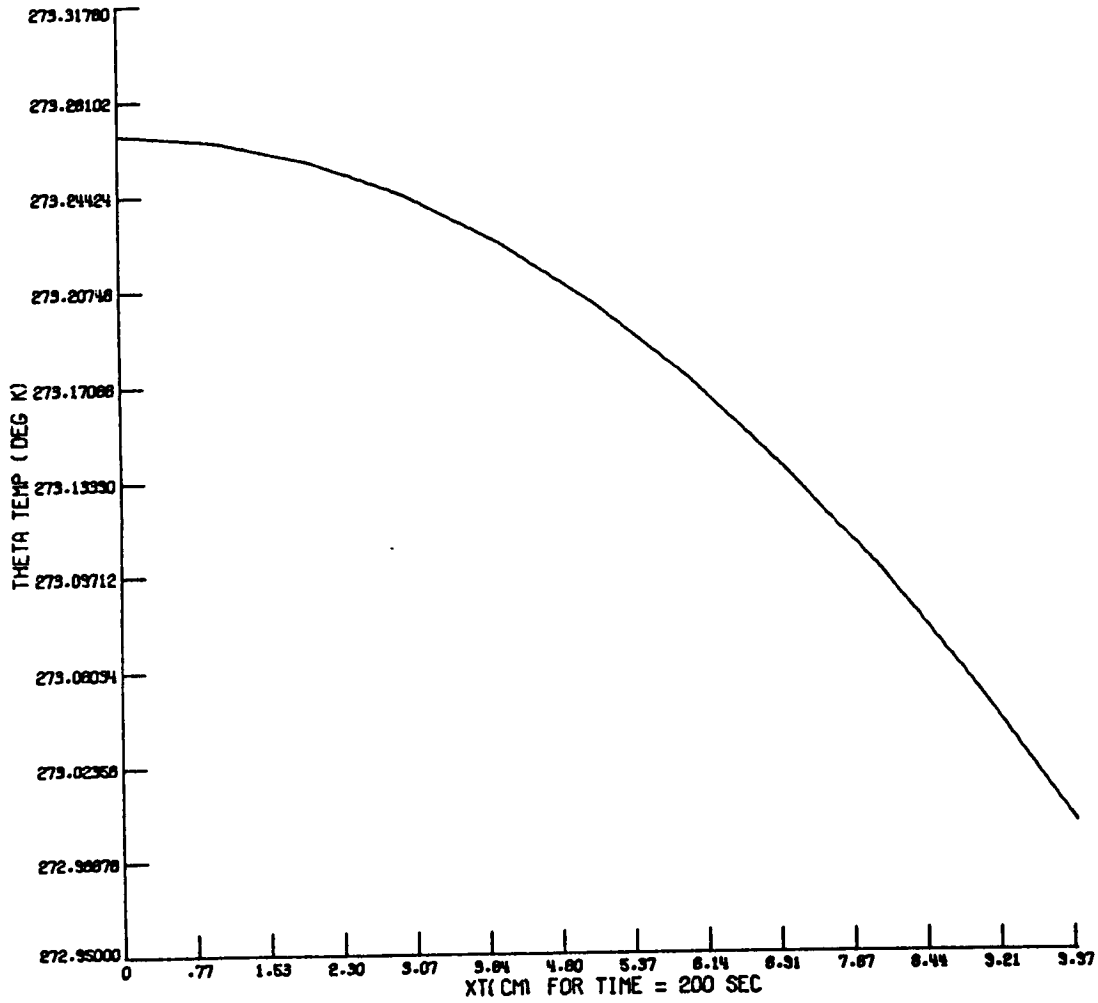


FIGURE 18. BARREL TEMPERATURE ALONG THE AXIAL DIRECTION AT THE TIME OF 200 SECONDS.

Therefore, these results show that the steady-state approximation for the count conversion algorithm does not contain any crucial errors. Therefore, the open and closed modes of the shutter were considered in the algorithm development. Namely, the output responds to the direct radiation which falls into the active cavity according to the shutter's on and off modes. Even though the instrument has a small time constant and hence it is stabilized quickly, within the 32 seconds of a half cycle, the output data which is used for the conversion algorithm has to be picked up at the near-end of a half cycle just before the shutter closes the aperture.

### 2.1.9 Solor Monitor Count Conversion Algorithm

The approximations made here including the steady-state approximation are the following:

1. The nodal points are selected to be adjacent to where the temperature probes are so that the temperatures measured by the probes may be regarded as the temperature of the nodes.
2. $T_1 = T_2 + b_E$ where $b_E$ is the electronical bias.
3. The temperature of the reference cavity is the same as that of the heat sink, that is, $T_2 = T_3$. Accordingly, $T_{1o} = T_{3o} + b_E$ where the subscript o signifies the initial temperature.
4. $T_1 - T_{1o}$ can be replaced by $T_3 - T_{3o}$.

With the above approximations, the equation for count conversion was derived as

$$\hat{E}(t-\tau) = A_v V^2(t) + A_3 \left[T_3(t) - T_{3o}\right] + A_5 \left[T_5(t) - T_{5o}\right] + A_7 \left[T_7(t) - T_{7o}\right] + B \tag{61}$$

where $T_3$, $T_5$, and $T_7$ are temperatures in $^{o}K$ which are measured in the instrument. These temperatures are measured and telemetered every 16 seconds. If these temperatures are measured twice during the open period of the shutter, then the second measured temperatures can be used for the count conversion algorithm. Otherwise, as the temperatures are measured arbitrarily without regard to the shutter on-and-off mode, the temperature measured at or near the time before the shutter closure must be used. As well as the temperatures measured, the count has to be picked up at every 40th data point or near the time before the shutter closure. V(t) in the equation is the instrument output in volts and is telemetered at every 0.8 second intervals. The constants in the equations are obtained from the thermal control electronics and conductive and radiative heat transfer, all of which interact with the active cavity and the nodes

which have temperature probes. In the equation,

$$A_v = -\frac{B_a K_a}{B_1} \tag{62}$$

$$A_3 = -\frac{4}{B_1}\left[D_{1-1}T_{1o}^3 + D_{1-2}T_{2o}^3 + D_{1-3}T_{3o}^3 + D_{1-4}T_{4o}^3 + D_{1-6}T_{6o}^3 + D_{1-18}T_{18o}^3 + D_{1-19}T_{19o}^3\right] \tag{63}$$

$$A_5 = -\frac{4}{B_1}\left[D_{1-5}T_{5o}^3 + D_{1-6}T_{6o}^3\right] \tag{64}$$

$$A_7 = -\frac{4}{B_1}\left[D_{1-7}T_{7o}^3 + D_{1-8}T_{8o}^3 + D_{1-9}T_{9o}^3 + D_{1-11}T_{11o}^3 + D_{1-14}T_{14o}^3 + D_{1-15}T_{15o}^3 + D_{1-17}T_{17o}^3\right] \tag{65}$$

$$B = \frac{A_{13}}{B_1} b_E - \Sigma_k \frac{D_{1k}}{B_1} T_{ko}^4 - \frac{B_J K_J V^2}{B_1} - \frac{\varepsilon}{B_1}. \tag{66}$$

the quantities such as $B_a$, $B_J$, $K_a$, $K_J$, V, $B_1$, T, $D_{ik}$, $T_{k_o}$, $A_{13}$ and $b_E$ are the constants to be specified for the instrument.

2.1.10 Scanner Control Electronics

The control electronics for the scanner have a different feature from that of the nonscanner. The difference between them is attributed to the type of sensor in the scanner. The scanner uses thermister blolometers for both active and reference flakes. When the temperature of the thermister varies due to the energy exchange, the current through the thermister varies with the change of the temperature-dependent thermister resistance. In the scanner instrument, the active flake that is attached to the heat sink indirectly responds to the incident radiation from the source through its optical arrangement. The reference flake is also attached to the heat sink and is placed where the space is totally sealed by the surrounding materials such as the heat sink and housing. Thus it is assumed that the reference flake's temperarture is equal to that of the heat sink and its housing. Accordingly, the observed difference in resistances between the active and reference flakes, is proportional to the incoming radiation.

Figure 19 is the block diagram for the scanner control electronics and their transfer functions.

The thermister resistance as a function of temperature is given by

$$R_i(T) = R_i(T_o) \text{ EXP } \beta_i\left(\frac{1}{T_i} - \frac{1}{T_o}\right) \quad , \qquad i = 1, 3 \tag{67}$$

Using the polynominal expansion of the exponential in Eq. 67, the difference in resistances between the active and reference flakes is approximated as

$$R_1(T_1) - R_3(T_3) = \frac{R_{1_o}\,\beta_1}{T_o^2}\;T_1 + \frac{R_{3_o}\,\beta_3}{T_o^2}\;T_3 + \frac{R_{1_o}\,\beta_1 - R_{3_o}\,\beta_3}{T_o} \tag{68}$$

The constant in the bridge is defined by

$$K_B \simeq \frac{2v_B}{R_o}\;\frac{k(1+k)}{(1+2k)^2} \tag{69}$$

The transfer function of the bridge is transformed into a differential equation as shown in the following

$$\tau_1\,\dot{x}_1 + x_1 = K_B(R_1 - R_3) \tag{70}$$

where $\tau_1$ is a time constant which, for the case of the scanner is less than 10 ms.

For the preamplifier, we end up with the equation

$$\tau_2\,\dot{x}_2 + x_2 = x_1 + \tau_3\,x_1 - K_c\,C_B + (E_{os} + n) + \tau_3(\dot{E}_{os} + \dot{n}) \tag{71}$$

Thus, the following equations describe the energy balance equation (Eq. 72) and the differential forms of the transfer functions, (Eq. 73) which include generalized forms of the amplifier and filter and a model of each scanner channel

$$\dot{T} = AT + DT^4 + B_Q\,\dot{Q}_8 + BE \tag{72}$$

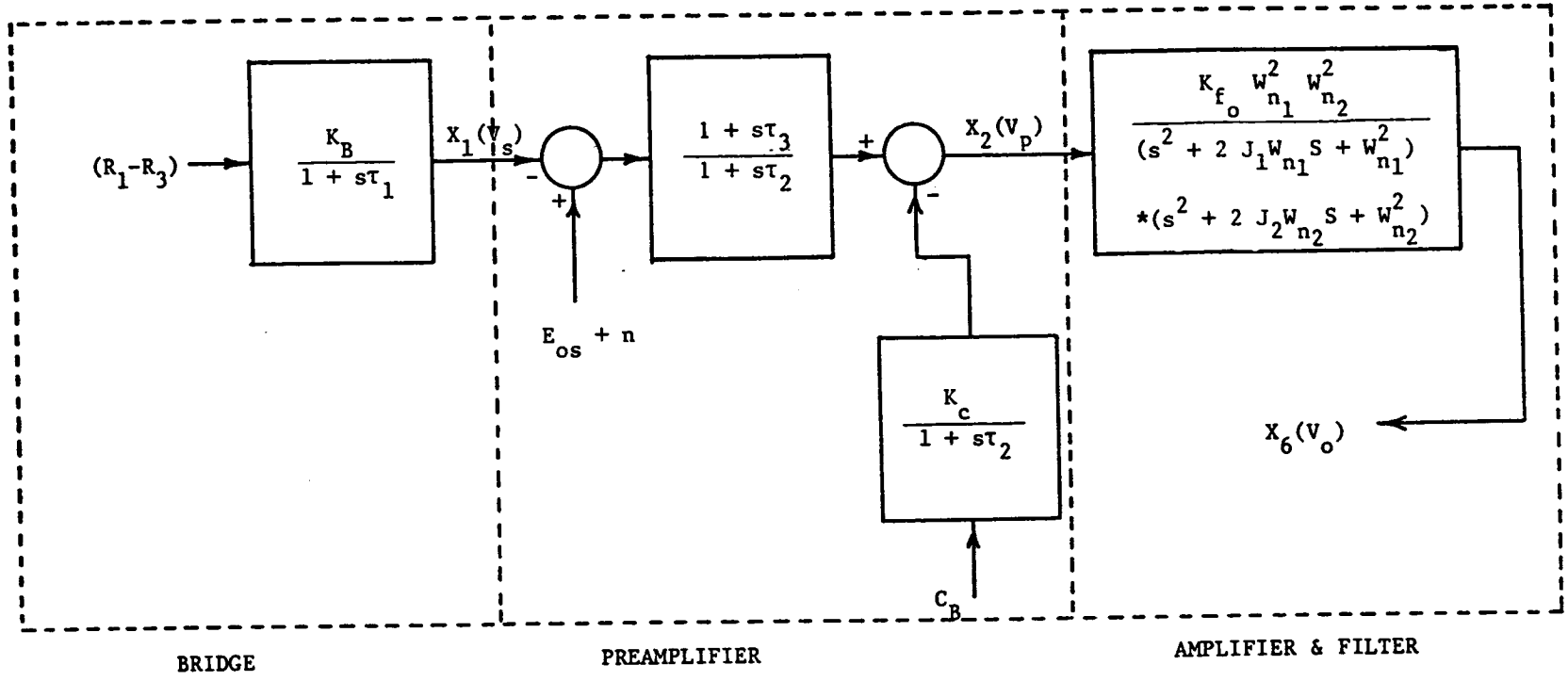


FIGURE 19 Scanner Electronic Control Model

$$\dot{x} = A_x\, x + B_T + B_{os}(E_{os} + n) + B_c\, C_B + b \tag{73}$$

where T is a 14 component vector consisting of node temperatures, x is a 6 component vector consisting of electrical signal processing variables, $\dot{Q}_8$ is the heater heat flow rate, $E_{os}$, $C_B$, and b are electrical and flake related variables, n is the total noise as viewed at the preamplifier input, and E is the incoming radiant incidence vector. The measured quantities which are telemetered to ground are the raw counts, $x_6$, and the heat sink temperature $T_7$, measured by a thermister.

$$y = \begin{bmatrix} x_6 \\ T_7 \end{bmatrix} + v \tag{74}$$

where v is the measurement noise including quantization error due to A/D conversion.

### 2.1.11 Scanner Steady-State Analysis

Two types of transient behavior will be noticeable in the instruments. One type occurs when the heater $\dot{Q}_8$ is activated, i.e., when the instrument is turned on. The transient behavior in this case is rather slow, as the heat sink time constant is large and the conductivity of the filters (for SW and LW instruments) is low. Thus, the time period necessary for the various node temperatures to reach their relatively steady operating temperatures, particularly the filters, will be long. The precise period can be determined by simulation or measurement.

The second and more important transient behavior is due to quick variations in the input (or observed) radiation incidence, E, after the operating condition has been reached. The time constants, in this case, are determined largely by the electronic signal processing parameters and the

flake characteristics. After the operating condition has been reached, the temperature variations of most nodes should be negligible. The active flake temperature then varies with the incoming radiation. The flake resistance and other electrical variables also vary with the incoming radiation and can produce transient behavior which can be observed if the target level is changed suddenly, as a step function. On the other hand, if the incoming radiation varies slowly relative to the system time constants, then the system will operate in quasi-steady state condition. A preliminary analysis indicates that, for the parameters selected by the designer, the applicable time constants are in the vicinity of 10 ms. Thus, if the input radiation does not contain frequencies above 10 Hz, the transient will be negligible, while frequencies above 17 Hz, will be attenauted. Whereas the earth scan may have low content in the high frequencies (which are of less interest to ERBE), the transition from space to Earth may produce a necessarily short period of transient behavior. It may be of interest to analyze the magnitude and duration of such transients, which probably last less than 50 ms.

Since the quasi-steady state condition is of interest to this analysis, let us first consider one scan period. The scanner looks at space for a period "sufficient" for the transient effect to die down and obtains an average of the last few values (to reduce noise and errors) as the "space clamp". Then the scanner sees the Earth and atmosphere, then looks at two black bodies at ambient, but known, temperatures as well as the SWICS in the off condition. The $k\Delta t$ correspond to the kth space clamp, so that $T(k\Delta t)$ and $x(k\Delta t)$ are the temperature and electronic vectors at the space clamp measurement. Now let

$$\Delta x(t) = x(t) - x(k\Delta t),\ \Delta T(t) = T(t) - T(k\Delta t),\quad k\Delta t \le t \le (k+1)\Delta t. \qquad (75)$$

From Eq. 72 and Eq. 73

$$\Delta\dot{T} \simeq A\Delta T + 4D\, T_k^3\, \Delta T + B_Q\, \Delta\dot{Q}_8 + BE \tag{76}$$

$$\Delta\dot{x} \simeq A_x \Delta x + B_T \Delta T + \Delta d + B_{os} \Delta n, \tag{77}$$

where it has been assumed that the thermal and radiative properties are included in A, D, $B_Q$ and B and the time constants for the electronics in $A_x$, $B_{os}$ and $B_c$ have remained unchanged over the scan period of 4 seconds. Also we can define $\Delta d$, the drift component of the voltage as,

$$\Delta d = \Delta B_T\, T(k\Delta t) + B_{os}\, \Delta E_{os} + \Delta b + B_C\, \Delta C_B \tag{78}$$

Considering the amplifier and Bessel filter to be in a quasi-steady state condition, it can be seen that

$$\Delta x_6(t) \simeq K_{f_o}\, \overline{\Delta x}_2(t) + K_{f_o}\, \tilde{\Delta x}_6(t) \tag{79}$$

where $\overline{\Delta x}_2(t)$ is the part of $\Delta x_2(t)$ with lower frequency content (below 10 Hz) consisting of an averaged part of $\Delta x_2(t)$, which may be considered the signal part, and $\tilde{\Delta x}_6(t)$ is the part of $\Delta x_6(t)$ consisting largely of noise and irradiance variations over short distances at the top of the atmosphere with zero mean. As the filter attenuates high frequencies, $\tilde{\Delta x}_6(t)$ will have a low amplitude.

The preamp equations are expressed as

$$\tau_2\, \Delta\dot{x}_2 + \Delta x_2 = \Delta x_1 + \tau_3\, \Delta\dot{x}_1 + \Delta E_{os} + \Delta n + \tau_3(\Delta\dot{E}_{os} + \Delta\dot{n}), \quad - K_c\, \Delta C_B \tag{80}$$

Now assume that

$$\tau_2\, \dot{\overline{\Delta x}}_2 - \tau_3\, \Delta\dot{E}_{os} \simeq 0 \tag{81}$$

then

$$\overline{\Delta x}_2 = \overline{\Delta x}_1 + \tau_3\, \dot{\overline{\Delta x}}_1 + \Delta E_{os} - K_c\, \Delta C_B + \overline{\Delta n} \tag{82}$$

where $\overline{\Delta x}_1$ is the low frequency portion of $\Delta x_1$, and where it has been assumed that $\Delta E_{os}$ and $\Delta C_B$ are baseband signals. Note that

$$\Delta x_2 = \overline{\Delta x}_2 + \tilde{\Delta x}_2, \tag{83}$$

where $\tilde{\Delta x}_2$ contains the higher frequency components of $\Delta x_2$ and causes the term $\tilde{\Delta x}_6$. The bridge equations are now expressed as

$$\tau_1 \dot{\Delta x}_1 + \Delta x_1 = \tau_1 B_{T_{11}} \Delta T_1 + \tau_1 B_{T_{13}} \Delta T_3 + \Delta b_1 + \tau_1 \Delta B_{T_{11}} T_1$$

$$+ \tau_1 \Delta B_{T_{13}} T_3 + \tau_1 \Delta B_{T_{11}} \Delta T_1 + \tau_1 \Delta B_{T_{13}} \Delta T_3 \tag{84}$$

It is assumed that the only variable on the RHS containing higher frequency components is $T_1$, whereas the remaining variables are slow moving drift components.

$$\overline{\Delta x}_1 = \tau_1 (B_{T_{11}} \overline{\Delta T}_1 + B_{T_{13}} \Delta T_3 - \dot{\overline{\Delta x}}_1) \tag{85}$$

Combining Eqs. 85, 82, and 79,

$$\overline{\Delta x}_2 = \tau_1 (B_{T_{11}} \overline{\Delta T}_1 + B_{T_{13}} \Delta T_3) + (\tau_3 - \tau_1) \dot{\overline{\Delta x}}_1 - \tau_2 \dot{\overline{x}}_2$$

$$+ E_{os} - K_c \Delta C_B + \overline{\Delta n} \tag{86}$$

$$\Delta x_6 = K_{f_o} \tau_1 (B_{T_{11}} \overline{\Delta T}_1 + B_{T_{13}} \Delta T_3)$$

$$+ K_{f_o} \left[ (\tau_3 - \tau_1) \dot{\overline{\Delta x}}_1 - \tau_2 \dot{\overline{x}}_2 + \Delta E_{os} - K_c \Delta C_B + \overline{\Delta n} + \tilde{\Delta x}_6 \right] \tag{87}$$

Now consider the thermal equation

$$\dot{\Delta T}_1 = A_{12} (\Delta T_2 - \Delta T_1) + 4 \sum_{k=1}^{N} D_{ik} T_k^3 \Delta T_k + B_1 E \tag{88}$$

$$B_1 \bar{E} = A_{12} (\Delta \bar{T}_1 - \Delta T_2) - 4 \sum_{k=1}^{N} D_{1k} T_k^3 \Delta T_k + \dot{\bar{T}}_1 \tag{89}$$

$$\Delta\bar{T}_1 = \frac{1}{K_{f_o}\,\tau_1\,B_{T_{11}}}\,\Delta x_6 - \frac{B_{T_{13}}}{B_{T_{11}}}\,\Delta T_3 - \frac{1}{\tau_1\,B_{T_{11}}}\,\delta_1 \tag{90}$$

$$\delta_1 = (\tau_3 - \tau_1)\,\dot{\bar{x}}_1 - \tau_2\,\dot{\bar{x}}_2 + \Delta E_{os} - K_c\,\Delta C_B + \Delta\bar{n} + \Delta\tilde{x}_6 \tag{91}$$

Substituting Eq. 88, 90, and 91 into Eq. 89, we have

$$B_1\bar{E} = \frac{(A_{12} - 4\,D_{11}\,T_1^3)}{K_{f_o}\,\tau_1\,B_{T_{11}}}\,\Delta x_6 - A_{12}\,\Delta\dot{T}_2 - \frac{B_{T_{13}}}{B_{T_{11}}}\,(A_{12} - 4\,D_{11}\,T_1^3)\Delta T_3$$

$$- \sum_{k=2}^{N} 4\,D_{ik}\,T_k^3\,\Delta T_k + \Delta\dot{\bar{T}}_1 - \frac{(A_{12} - 4\,D_{11}\,T_1^3)}{\tau_1\,B_{T_{11}}}\,\delta_1 \tag{92}$$

## 2.1.12 Scanner Count Conversion

The scanner count conversion algorithm below is based on steady state approximation. The structure (i.e., the form of the equations) of the algorithm is the same for each of the three scanner channels. The parameters have different values for each channel.

The average of scan points during space clamp is given below

$$\bar{v}(t_k) = \frac{1}{n}\sum_{i=1}^{n} v(t_{ki}), \qquad n = 8 \tag{93}$$

The mean variance of the counts compared with the space clamp during a scan cycle is obtained by the equation

$$\sigma_k^2 = \frac{1}{n}\sum_{i=1}^{n}\left[v(t_k) - \bar{v}(t_k)\right]^2 \tag{94}$$

The scanner count conversion equation is then defined by the following equations

$$E(t - \tau) = A_v\left[v(t) - v(t_k)\right] + A_H\left[T_H(t) - T_H(t)\right] + A_\delta\,\delta_k\,\frac{t - t_k}{\Delta t}\,,$$

$$t_{k-1} \le t \le t_k \tag{95}$$

The coefficients in Eq. 95 are the following

$$A_v = \frac{A_{12} - 4\, D_{11}\, T_1^3}{K\, K_{f_o}\, \tau_1\, B_{T_{11}}} \quad \frac{V_{B_o}}{V_B(t)} \tag{96}$$

$$A_H = -\ \frac{1}{k}\, 4 \left[ D_{11}\, T_1^3 + D_{12}\, T_2^3 + D_{13}\, T_3^3 + D_{14}\, T_4^3 + D_{15}\, T_5^3 + D_{16}\, T_6^3 + D_{18}\, T_8^3 + D_{113} T_{13}^3 \right] - A_{12}\left(1 + \frac{B_{T_{13}}}{B_{T_{11}}}\right) \frac{1}{K} \tag{97}$$

$$A = c\, \frac{A_{12} - 4\, D_{11}\, T_1^3}{K\, \tau_1\, B_{T_{11}}} \quad \frac{V_{B_o}}{V_B(t)} = c\, K_{f_o}\, A_v \tag{98}$$

$$\delta_k = \frac{1}{K_{f_o}} \left[ \bar{v}(t_k) - \bar{v}(t_{k-1}) \right] - \tau_1 (B_{T_{11}} + B_{T_{13}}) \left[ T_H(t_k) - T_H(t_{k-1}) \right] - \frac{\tau_1}{V_{B_o}} (B_{T_{11}}\, T_1 + B_{T_{13}}\, T_3) \left[ V_B(t_k) - V_B(t_{k-1}) \right] + K_d \left[ V_d(t_k) - V_d(t_{k-1}) \right] \tag{99}$$

$$t_k = t_{k-1} + \Delta t \tag{100}$$

In the last term of Eq. 95, $(t-t_k)/\Delta t$ can be replaced by the number of measurements in the scan mode as follows:

$$\frac{t - t_k}{\Delta t} \simeq 0.0135\ (J-8) \tag{101}$$

where J is the number of measurements in the scan mode. The constants in the above equation are the following:

$\bar{v}(t_k)$ = space clamp value at time $t_k$

$v(t_{ki})$ = instrument output (in volts) when viewing space at $t_k$

$\sigma_k^2$ = noise variance estimate during space look

$v(t)$ = instrument output sample at time t

$T_H(t)$ = heat sink temperature measurement at t or most recent value ($^oK$)

$\Delta t$ = total scan period (4 sec.)

$t_k$ = time at end of space look (sec.)

t = sampling instant (sec.)

$V_B(t)$ = detector bridge bias voltage measurement at time t or most recent value (v)

$V_d(t_k)$ = drift balance DAC voltage measurement at time t or most recent value (v)

$\delta_k$ = estimate of unaccounted drift during $k^{th}$ scan period (V)

$\tau$ = average time lag (sec.)

$k_{f_o}$ = post amplification gain

Note that to compute $\delta_k$, it is necessary to have the following space clamp value; i.e., $\bar{v}(t_k)$. If the term with $\delta_k$ in Eq. 95 is neglected, then the count conversion may be done without using $\bar{v}(t_k)$. The variance $\sigma_k^2$ is computed for diagnostic purposes and should be output as described below. The converted value $E_i(t - \tau)$, i = s,ℓ, T (for shortwave, longwave, and total, respectively) can be interpreted as follows

$$E_i(t) = \int \tau_i(\lambda)\, E_\lambda(t)\, d\lambda + e_i(t) \qquad (102)$$

where $\tau_i(\lambda)$ is the transmittance of the $i^{th}$ channel, $E_\lambda(t)$ is the spectral irradiance at the instrument due to radiation from the footprint at time $t_1$

and $e_i(t)$ is the error in the measurement combined with the count conversion process, and can be estimated through analysis of calibration data and model results.

### 2.1.13 Accuracy and Diagnostic Checks

During each scan, the instruments view two black bodies at ambient, but known temperatures. These data can be used to determine if the basic operation of the instruments have changed as well as provide an approximate accuracy check of the combined error $e_i(t)$ in Eq. 101.

1. Store a table of elements

$(v_{Bs}(T_B), v_{B\ell}(T_B), v_{BT}(T_B), E_{Bs}(T_B), E_{B\ell}(T_B), E_{BT}(T_B))$ where $T_B = T_{Bj}$, $1 \le j \le N$. The values $v_{Bi}(T_B)$ represent the steady state output of the $i^{th}$ channel when viewing the black body at temperature $T_B$, and may be obtained in calibration tests. The values $E_{Bi}(T_B)$ represent the output of count conversion when viewing the black body at temperature $T_B$, given by

$$E_{Bi}(T_B) = \int \tau_i(\lambda)\, E_{B\lambda}(T_B)\, d\lambda \tag{103}$$

where $E_{B\lambda}(T_B)$ is the spectral irradiance from the black body at temperature $T_B$.

2. Compute $E_{Bi}$ using the measured black body temperature $T_B(t)$ as

$$E_{Bi}(T_B(t)) \simeq E_{Bi} + \frac{T_B(t) - T_{B1}}{T_{B2} - T_{B1}} \left[ E_{Bi}(T_{B2}) - E_{Bi}(T_{B1}) \right] \tag{104}$$

where $T_{B1} \le T_B(t) \le T_{B2}$

3. Compute $\hat{E}_i(t)$ using the count conversion algorithm with the corresponding value $v_i(t)$.

4. Plot $v_i(t)$ and $v_{Bi}(T_B(t))$ on same axes.

5. Plot $\hat{E}_i(t)$ and $E_{Bi}(T_B(t))$ on same axes.

6. Compute and plot $\sigma_k^2$, and

$$\bar{e}_{v_i,k+1} = a_{v_i k} + (1 - a)(v_1(t) - v_{Bi}(T_B(t))) \tag{105}$$

$$\bar{e}_{i,k+1} = a\,\bar{e}_{ik} + (1 - a)(\hat{E}_i(t) - E_{Bi}(T_B(t))) \tag{106}$$

$$\sigma^2_{x_i,k+1} = a\,\sigma^2_{v_i k} + (1 - a)\left[(v_i(t) - v_{Bi}(T_B(t)) - \bar{e}_{v_i,k+1}\right]^2 \tag{107}$$

$$\sigma^2_{i,k+1} = a\,\sigma^2_{ik} + (1 - a)\left[(\hat{E}_i(t) - E_{Bi}(T_B(t)) - \bar{e}_{i,k+1}\right]^2 \tag{108}$$

## 3. INSTRUMENT PERFORMANCE AND COUNT CONVERSION TEST

The instrument models developed for the non-scanner, the scanner, and the solar monitor are based upon the theoretical approach with a certain degree of approximation. For instance, the energy equations for the instruments were formulated with the assumptions that the node (or control volume) has uniform temperature and homogeneous thermal and radiative properties. However, this lumped geometry of the node, in reality, cannot hold the uniform temperature through the node geometry unless the temperatures of the neighbor nodes are the same, or the node boundaries are perfectly insulated, or the thermal conductivity of the node material is infinity. Otherwise, if there is any heat flux allowed into or from the node, a temperature gradient from the center of node to the boundary will exist.

The radiative properties that are used in the ERBE radiometer instrument models may be the values picked out of the handbook or measured and averaged values over a certain band of wavelength. No matter where these values were obtained, they would introduce some errors when they are used for the computation of the radiation exchange between the surfaces. The spectral distribution of the emissive energy flux from a source of radiation such as MRBB may lie on the limited range of wavelength in which the averaged radiative properties used may be far above or below the real values within the spectral energy distribution. Therefore, the averaged values may not represent reality in instrument performance. Also, during long term operation in space, these properties will be subject to changes due to various reasons such as thermal and environmental contamination, and aging effect.

The electronic systems are used in the radiometer to measure the temperature difference between the active and reference cavities or flakes, and to

digitize the signal, then to transmit it through a telemetry system. The parts such as resistors of this electronic system are sensitive to a wide range of temperature changes. For instance, if the resistance of the bridge slightly changes from the reference point, then the error in irradiance measurement due to this temperature change may be in error by a few watts per square meter. Although the instrument models are well-conceptualized and designed, the real behavior of the radiometers are, as expected, different from what is was designed to be.

Other factors to be considered, which influence the sensor performance and measurement accuracy, are the inflight changes from the states that the sensor normally operates in and the calibration source variability in its operation mode or the changes in source characteristics. An environmental change was expected in the long-term operation of the instrument due to the orbital changes which caused cyclic variations in the heat load of the instrument. Another change, was due to the contamination or degradation of then senosr surfaces due to radiative interactions with other surfaces.

The internal calibration sources such as MRBB and SWICS are also subject to change. The monitoring of the change in intensity of these sources by possible variation in power supply and shift of the spectral distribution in the source output is possible by using the SiPD, although it is also subject to change, and intercomparing calibration sources.

To account for the possible errors due to the reasons discussed above a procedure was developed to detect those errors. The procedure uses the algorithm shown in Figs. 20 and 21 for that purpose. This algorithm is capable of evaluating the sensor model, adjusting the simulation model parameters for minimum errors, and establishing confidence intervals for the

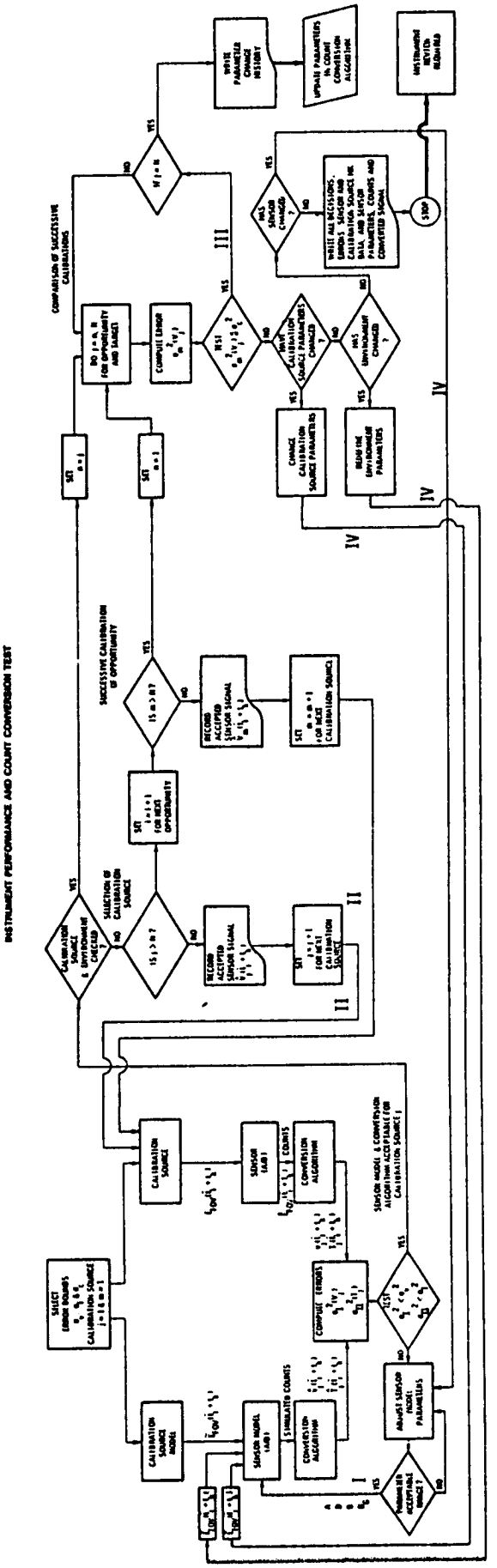


ORIGINAL PAGE IS
OF POOR QUALITY

FIGURE 20.

## ERBE INSTRUMENT VALIDATION PLAN

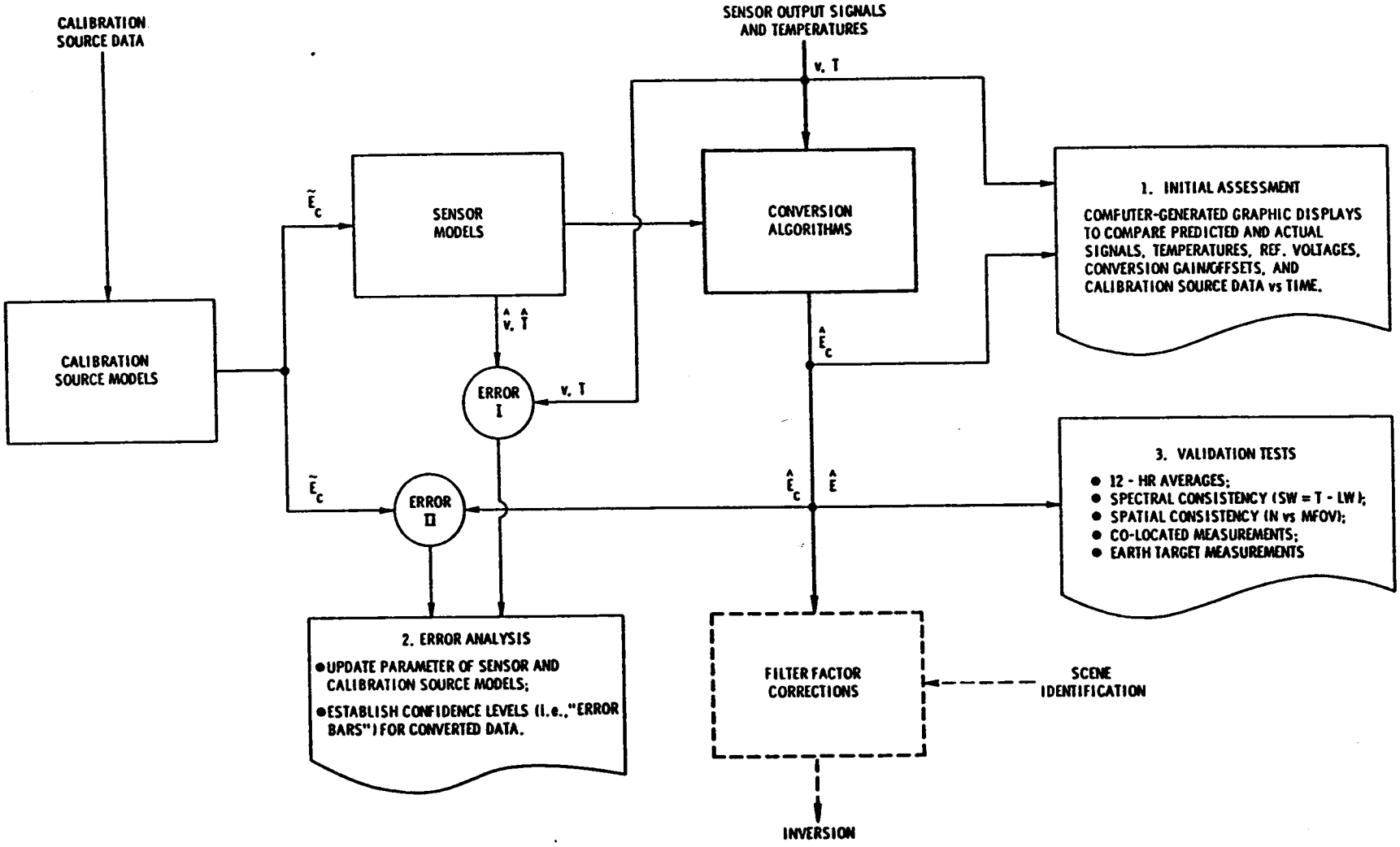


FIGURE 21.

converted data reflecting sensor characteristics and calibration sources.

The sensor simulation model responses, using known calibration sources as inputs to the model, are checked against the instrument calibration output. Any differences in the slope, offset and curvature between the simulation and calibration results were interpreted as uncertainties of the model simulating the instrument. These differences, however, generally reflect the problems discussed earlier. In the algorithm, these differences are narrowed by checking and adjusting the sensor model, source, and environmental parameters to minimize the errors. However, the estimated parameters must stay within the tolerance that can be allowed by the approximations made in the modeling or by the nature of reasons described earlier.

The algorithm consists of three parts (see Fig. 20):

The first part is a routine to adjust the sensor model parameters by comparing sensor simulation outputs such as counts and HK temperatures to the inflight and ground calibrations obtained for the known sources.

The second part is a procedure to check the errors generated by simulating a sensor by comparing them to the calibration data for the known sources. It checks the error generated from the sensor simulation target source, or envrionment at different time intervals for the same known irradiance source as in the inflight calibration.

The third part consists of routines to search for any changes in the target, environment and sensor performance due to the degradation of the instrument surface, vibration, contaminations, and thermal and aging effects on the radiation interactive surfaces.

To do the above job, the algorithm has been designed to have the following capabilities:

1. to adjust the sensor model parameters in comparison with the calibration data from known sources to minimize the error between the sensor model and the calibration data,
2. to periodically check any changes in sensor, target and environment parameters between inflight calibrations by comparing the calibration data for the same sources at different time intervals (e.g., 1 or 2 week periods),
3. to re-define the sensor, target and environment parameters, if they have been changed,
4. to test and check any differences between calibration data and responses from the simulated sensor model for the same known sources,
5. to repeat the routines 1 through 4 until the errors produced by step 4 are minimized,
6. to generate the count conversion parameters.

## 3.1 Description of Routines

### 3.1.1 Routine I

The calibration sources identified during either ground or inflight calibrations are numbered by j = 1, N at time $t_i$ and $t_{i+1}$ where i = 1, n. The sensor simulation model generates temperatures and sensor responses corresponding to the calibration sources at a time $t_i$. These temperatures and sensor responses, which are obtained from the model simulation, are compared with measured data to compute errors of the simulation model. Once these errors fall within the predetermined error bounds (after repetitive refinement of simulation parameters), then these errors will be used as criteria to determine the measurement errors

against known targets on the ground. If not, the parameters for both the target source and environment effects will be checked; then in turn the sensor parameters will be checked and adjusted, in case when the computed parameters are not within the acceptable range based on the materials properties, e.g. its optical properties. Such a routine will inlcude a decision block to check targets and environmental effects to avoid unnecessary adjustments of sensor parameters when the errors may be caused by and come from the target and environment parameters.

### 3.1.2 Routine II

If the errors are within bounds, the sensor responses $V_j$, j = 1, N at different times $t_i$ and $t_{i+1}$ will be sorted and evaluated in Routine I to check the errors from the sensor simulation model for the targets at different times $t_i$ and $t_{i+1}$.

### 3.1.3 Routine III

After finishing Routine II, using all the target sources at different times, $t_i$ and $t_{i+1}$, Routine III checks the sensor respones of the same target at a different time and computes the errors. If the error of the same target at a different time falls within the error bounds, the Routine will check the next target. If not, the history of target source variation will be studied, and at the same time the sensor and environmental conditions will be rechecked to determine the source of errors. This evaluation in Routine I is performed whenever the error signals the flag. The process continues until the error source is recognized and its correction of error is made by adjusting the related parameters in the simulation model. When this Routine finishes satisfactorily evaluating all of the target sources, the program will print all the decisions, errors, sensor

and calibration source HK data, sensor parameters and counts and will supply the final results to the count conversion algorithm.

### 3.1.4 Routine IV

If the error does not fall within the prescribed error bounds, the target and environment parameters are checked in order to find whether changes in these parameters created pseudo-errors in the sensor responses. If there has been a change in either the target or environmental parameters, they are re-defined and re-input to Routine I. In spite of repeated checks, if the error cannot be minimized, then the thorough review of instruments will be required to determine whether the error bounds are to be reassessed. In this routine, when the target and environment are checked and relatively free from the erroneous performance then we would postulate that the instrument's measurement capability might be deteriorated due partially to the thermal and environmental contamination or by other means such as aging of the parts and so on.

## 4. DISCUSSION OF PARAMETER ESTIMATION

The simulation code was developed to study the sensor instrument responses and behavior during the ground and inflight calibration procedures as described earlier in Section 2.1.6. This simulation code uses the irradiance at the FOV limiter of the instrument as the input data. All the constants representing the instrument geometry, material, thermal and radiative properties and the electronic thermal control systems are parameterized to be used as coefficients in the system of equations. Then the simulation code generates the counts and the nodal temperatures of the model corresponding to the input irradiance. When the simulation code uses the input irradiance which is the same as the calibration source, the results of counts and housekeeping temperaures from the simulation are compared to the calibation results. If the differences from these comparisons for various levels of irradiance are wide, then the simulation model parameters are adjusted to minimize those differences. This procedure for estimating the model parameters is repeated until the differences can no longer be reduced. These estimations also continue for various calibration sources until systematic response patterns for each calibration source are established. All procedures mentioned above are performed for each individual radiometer sensor. Even though two instruments of the same type are used in the calibration procedure, for example, the results may differ due to the inherent differences in the many factors involved, e.g. slight differences in the sensor assembly process of uniform surface roughness, coatings, glue or contact areas.

The following is an example that shows how the parameters for the nonscanner total channel are selected. Assume that the instrument output derived from calibration input irradiances are linear; then the factors which determine the slope and offset of the curve for simulated results would be judged to be the

offset temperature between the active and reference cavities, and the radiative constant for the term of irradiance in Eq. 34, i.e. $B_1$. To determine these two factors using the measurement data, the linear form of Eq. 34 can be written

$$\alpha x = \beta \tag{109}$$

where x is a column vector consisting of the offset temperature and radiative constant, and $\alpha$ and $\beta$ are defined later. The solution to Eq. 108 is

$$x = (\alpha' \alpha)^{-1} \alpha' \beta \tag{110}$$

where $\alpha'$ is the transpose of $\alpha$.

The constant $\alpha$ is a matrix defined by

$$\alpha_{ij} = \begin{bmatrix} A_{12} + 4 D_{11}(T_2^3)_1, & E_1 \\ A_{12} + 4 D_{11}(T_2^3)_2, & E_2 \\ \vdots & \vdots \\ A_{12} + 4 D_{11}(T_2^3)_i, & E_i \end{bmatrix}$$

where i is the calibration sequence.

The constant $\beta$ is a column vector

$$\beta_i = \begin{bmatrix} \beta_1 \\ \beta_2 \\ \vdots \\ \beta_i \end{bmatrix}$$

$\beta$ as an explicit form is

$$\beta_1 = - B_a K_a V_i^2 - \phi_i - B_{J_1} \dot{Q}_{J_1} \tag{111}$$

$$\phi_1 = \sum_k D_{1k} T_{ki}^4 , \quad \text{only when } k = 1, \text{ replace } T_{1i} \text{ by } T_{2i} \quad . \tag{112}$$

The nominal values are used for unmeasured $T_{ki}$ and $\dot{Q}_{J_1}$ except $T_3 \simeq T_2 + \delta T$. The temperature of the reference cavity is a little higher than the heat sink temperature due to the Joule heating by electric current flowing probe wire of reference cavity. The temperature difference, $\delta T$, due to the Joule heating cannot be directly measured but can be observed from the simulation results.

The plots of the calibration and simulation results show that they are not actually linear but could be considered to be linear for estimation (see for instance, the steady-state response comparison of simulation of calibration data for the NS WFOVSW sensor on page 100 in Appendix A). Therefore, the above approach can still adjust the overall slope and offset of the curve by regarding them as a linear. The linearity and adjustment can be made by adjusting other parameters. But since almost all parameters are interrelated, the selection of a parameter that mostly influences the linearity of the curve in a plot of simulation results must be cautiously taken by testing the linearity with various parameters.

Since the simulation code was developed, the calibration data for the nonscanner radiometers using MRBB as a calibration source was the only source available. Hence, the nonscanner instrument models have been simulated using MRBB data which was used in the calibration. Figure 22 shows the calibration data for the MRBB temperatures in the 1st column and the count outputs for the four nonscanner channels in the 6th through 9th columns. The 2nd column shows the blackbody radiation corresponding to the temperatures in the 1st

| 1 MRBB TEMP $^{o}K$ | 2 $\sigma_e T^4$ ($w/m^2$) | 3 MODEL % SHORT-WAVE | 4 MODEL % LONG-WAVE | 5 IRRADIANCE SW/LW ($w/cm^2$) | 6 MFOV (COUNTS) CALIB/ | 7 WFOV (COUNTS) C/M | 8 MFOVSW (COUNTS) C/M | 9 WFOVSW (COUNTS) C/M | DIFFERENCE BETWEEN CAL AND SIMULATION 10 MT/MS | 11 WT/WS |
|---|---|---|---|---|---|---|---|---|---|---|
| 188.23 / -84.93 | 71.55 | .02% | 99.980% | .0000015 / .0071535 | 8047 / 8049 | 6912 / 6912 | 6382 / 6382 | 7327 / 7327 | +2 / 0 | 0 / 0 |
| 243.4 / -29.76 | 198.95 | .243% | 99.757% | .0000483 / .0198467 | 7936 / 7924 | 6668 / 6665 | 6367 / 6373 | 7312 / 7315 | +6 / +6 | -3 / +3 |
| 275.66 / 2.5 | 327.55 | .692% | 99.308% | .0002267 / .0325283 | 7828 / 7832 | 6407 / 6407 | 6355 / 6363 | 7300 / 7301 | +4 / +8 | 0 / +1 |
| 299.36 / 26.2 | 455.25 | 1.266% | 98.734% | .0005763 / .0449487 | 7714 / 7221 | 6144 / 6139 | 6344 / 6352 | 7282 / 7285 | +7 / +8 | -5 / +3 |
| 318.56 / 45.4 | 583.77 | 1.916% | 98.084% | .0011185 / .0572585 | 7606 / 7608 | 5858 / 5857 | 6332 / 6339 | 7265 / 7266 | +1 / +7 | -1 / +1 |
| 334.77 / 61.61 | 711.72 | 2.603% | 97.397% | .0018526 / .0693194 | 7483 / 7494 | 5563 / 5563 | 6318 / 6324 | 7244 / 7245 | +11 / +6 | 0 / +1 |
| 348.86 / 75.70 | 839.62 | 3.307% | 96.693% | .0027766 / .0811854 | 7378 / 7378 | 5252 / 5252 | 6306 / 6307 | 7223 / 7221 | 0 / 1 | 0 / -2 |

EXPLANATIONS: MRBB TEMPERATURE WAS OBTAINED FROM TRW IN $^{o}C$, THE $^{o}K$ IS THE RESULT OF ADDING 273.16 HEAT SINK CONTROLLER SET AT 39.995$^{o}C$ or 313.155$^{o}K$ IN THE MODEL.

FIGURE 22.

column. The 3rd and 4th columns show the percentages for the shortwave and longwave portions of the blackbody radiation described in the 5th column, respectively. These shortwave and longwave portions were calculated by the integration of Planck's equation for blackbody radiation with respect to the wavelength from 0 to 5 μm for shortwave and from 5 μm to 1000 μm for longwave. These portions were used for the MFOV and WFOV shortwave instrument simulations. The shortwave range selection of 0 to 5 μm was simply made by the shortwave filter (suprasil) characteristics. In the 6th through 9th columns, the numbers in the bottom part of the blaock signify the output (in counts) corresponding to MRBB radiation from the simulation. The 10th and 11th columns show the differences in count between calibration and simulation tests.

## REFERENCES


1. Barkstrom, B. R., and J. B. Hall, Jr., Earth Radiation Budget Experiment (ERBE): An Overview Journal of Energy, Vol. 6, No. 2, March - April, 1982, pp. 141-146.
2. Sparrow, E. M., and R. D. Cess, Radiation Heat Transfer, Hemisphere Publishing Corporation, 1978.
3. Rohsenow, W. M., Developments in Heat Transfer, The MIT Press, 1964.

# APPENDIX A

# PRELIMINARY RESULTS ON ERBE NON-SCANNER INSTRUMENT MODELING, COUNT CONVERSION AND SENSITIVITY ANALYSIS

## GOALS

- DEVELOP A DYNAMIC SENSOR MODEL FOR EACH INSTRUMENT
- DEVELOP AN ADAPTIVE COUNT CONVERSION ALGORITHM THAT CAN ACCOMMODATE CHANGING CONDITIONS
- DETERMINE THE ACCURACY OF THE ERBE INSTRUMENTS
- DETERMINE THE ACCURACY OF THE ERBE MEASUREMENTS

## APPROACH TO ASSESSMENT OF INSTRUMENT ACCURACY

- DEVELOP A MATHEMATICAL MODEL AND COMPUTER SIMULATION FOR EACH INSTRUMENT

- COMPARE GROUND CALIBRATION DATA TO CORRESPONDING SIMULATION DATA
- MINIMIZE DIFFERENCE BY ADJUSTING MODEL PARAMETERS

- PERFORM A SENSITIVITY ANALYSIS
- ESTIMATE CONFIDENCE INTERVALS FROM GROUND CALIBRATION DATA

- REPEAT SAME PROCEDURE FOR FLIGHT CALIBRATION DATA (ERROR ANALYSIS)
- ADJUST ESTIMATE OF CONFIDENCE INTERVALS AT EACH FLIGHT CALIBRATION

## APPROACH TO ADAPTIVE COUNT CONVERSION

- DEVELOP A MATHEMATICAL MODEL AND COMPUTER SIMULATION FOR EACH INSTRUMENT

- COMPARE GROUND CALIBRATION DATA TO CORRESPONDING SIMULATION DATA
- MINIMIZE DIFFERENCE BY FINE TUNING MODEL PARAMETERS

- DEVELOP A COUNT CONVERSION ALGORITHM (CCA) BASED ON THE MODEL
- SIMULATE THE INSTRUMENT AND CCA
- ESTIMATE ERROR DUE TO CCA

- REPEAT PROCEDURE FOR EACH FLIGHT CALIBRATION
- FINE TUNE MODEL AND CCA PARAMETERS
- OBTAIN NEW ERROR ESTIMATES

# NON-SCANNER MFOV TOTAL

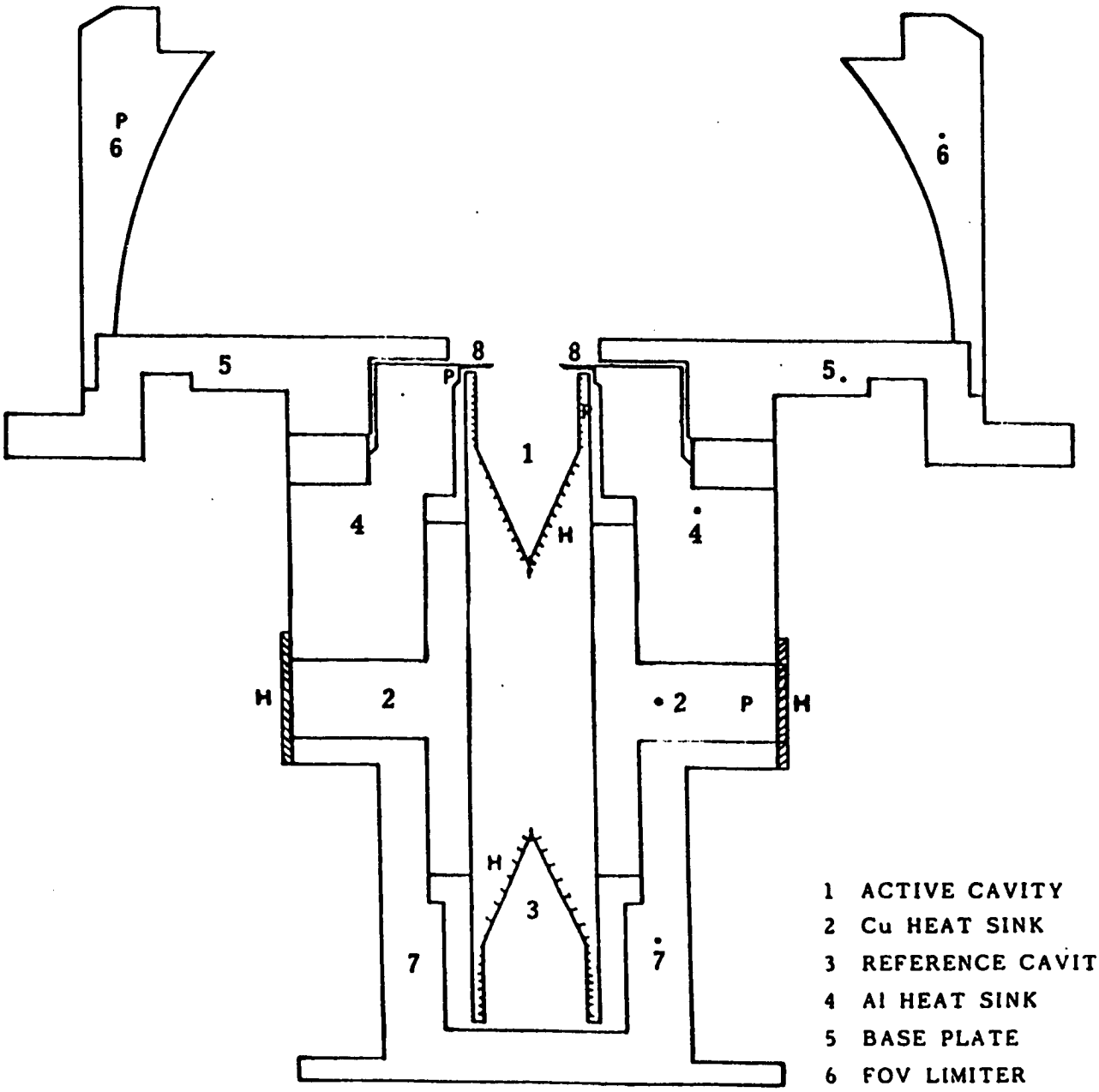


1 ACTIVE CAVITY
2 Cu HEAT SINK
3 REFERENCE CAVITY
4 Al HEAT SINK
5 BASE PLATE
6 FOV LIMITER
7 Al HEAT SINK
8 APERTURE

H HEATER
P TEMPERATURE PROBE

# NON-SCANNER WFOV SW

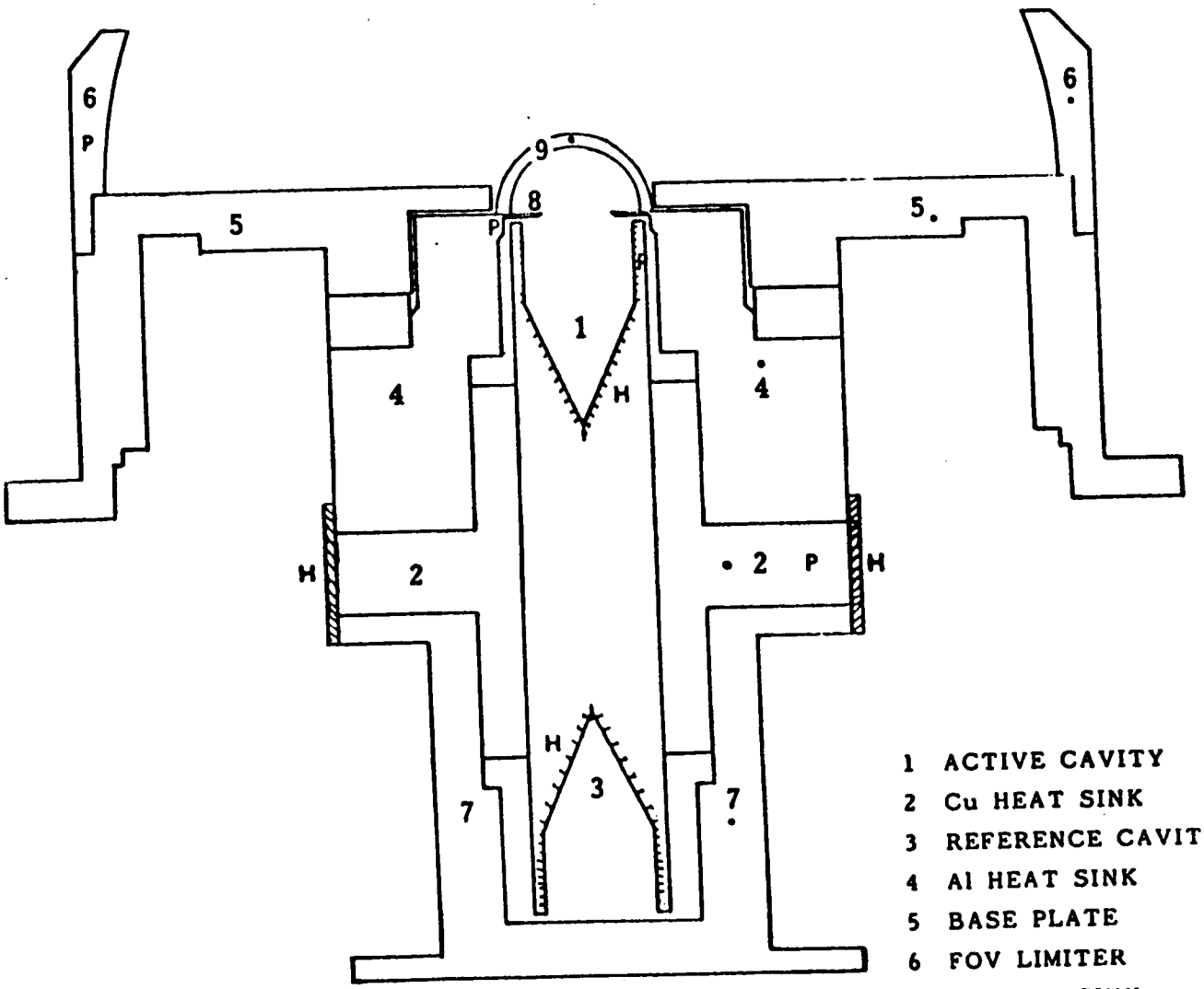


1 ACTIVE CAVITY
2 Cu HEAT SINK
3 REFERENCE CAVITY
4 Al HEAT SINK
5 BASE PLATE
6 FOV LIMITER
7 Al HEAT SINK
8 APERTURE
9 SW FILTER DOME
H HEATER
P TEMPERATURE PROBE

# NON-SCANNER ELECTRONICS (ACR)

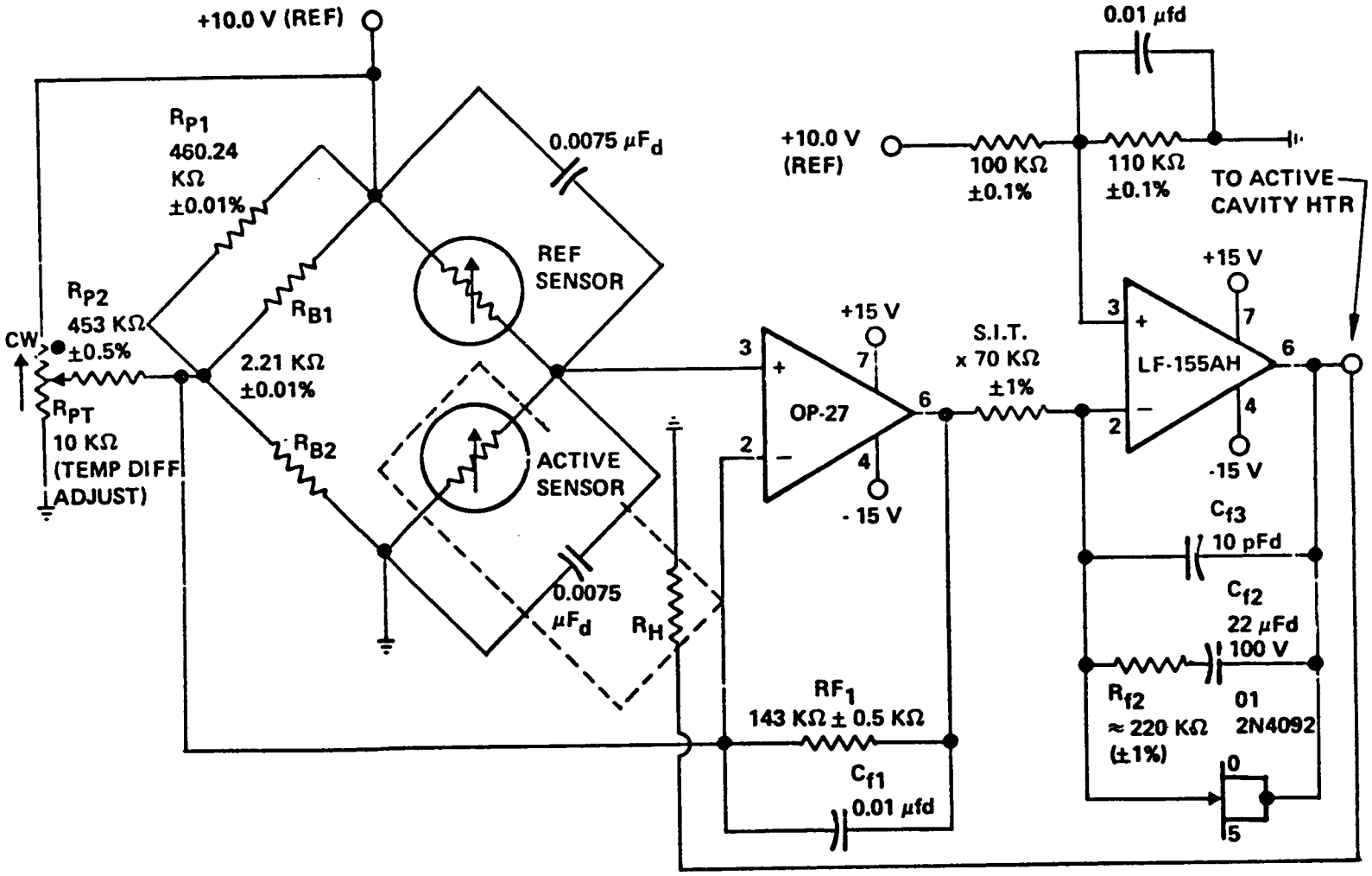

# NON-SCANNER DYNAMIC RESPONSE

WFOV TOTAL SIMULATION

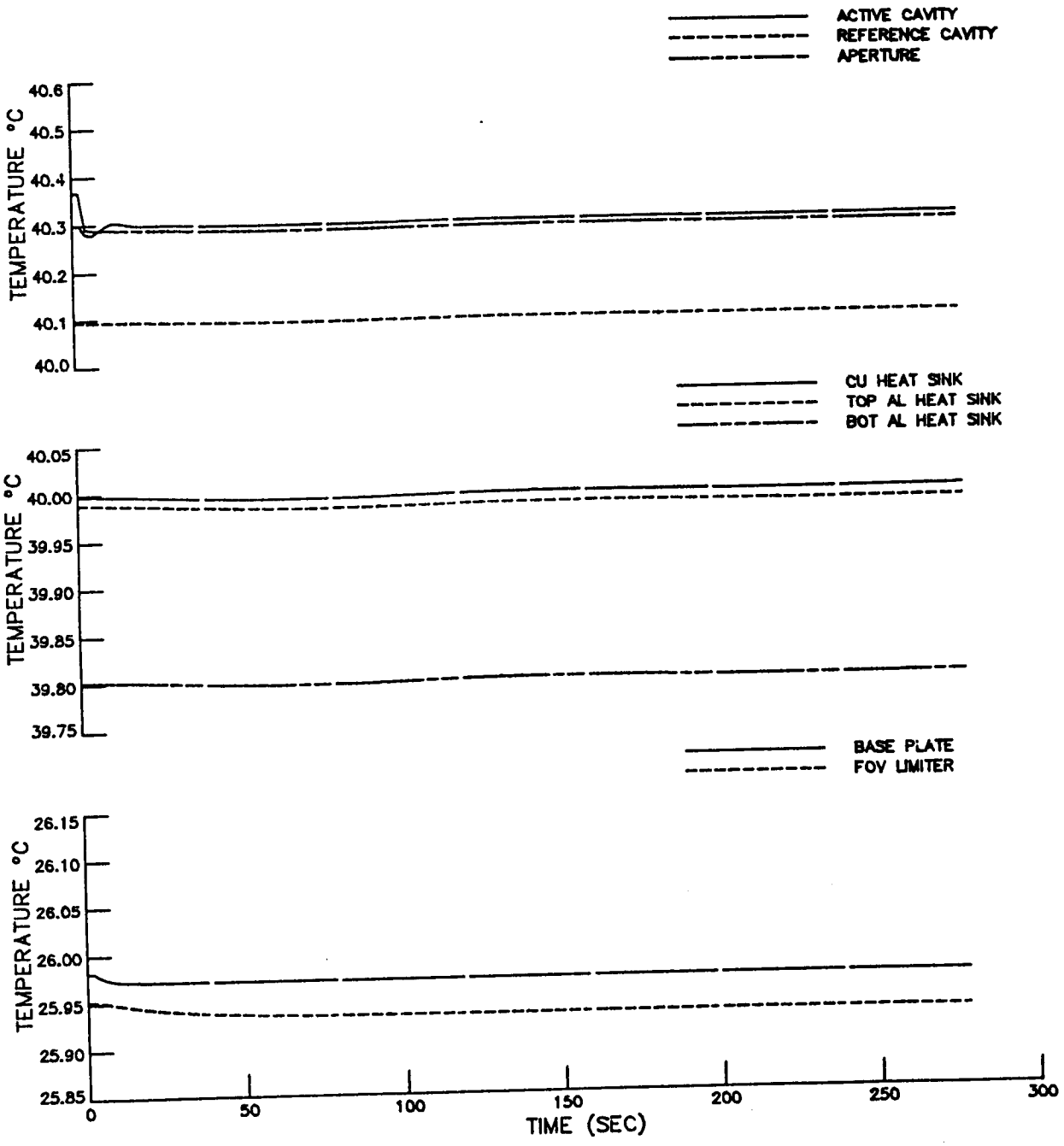

# NON-SCANNER DYNAMIC RESPONSE

WFOV TOTAL SIMULATION

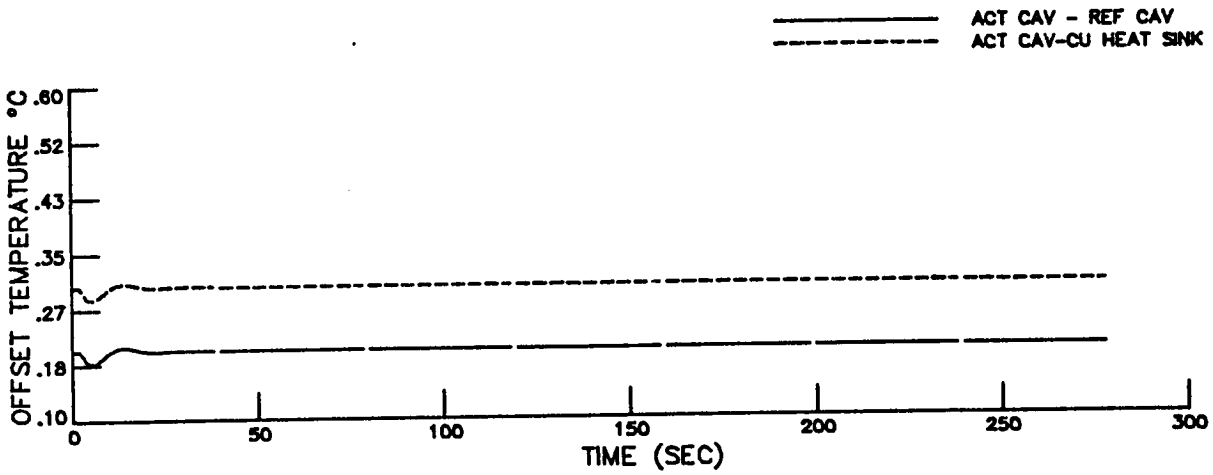

# NON-SCANNER DYNAMIC RESPONSE

WFOV TOTAL SIMULATION

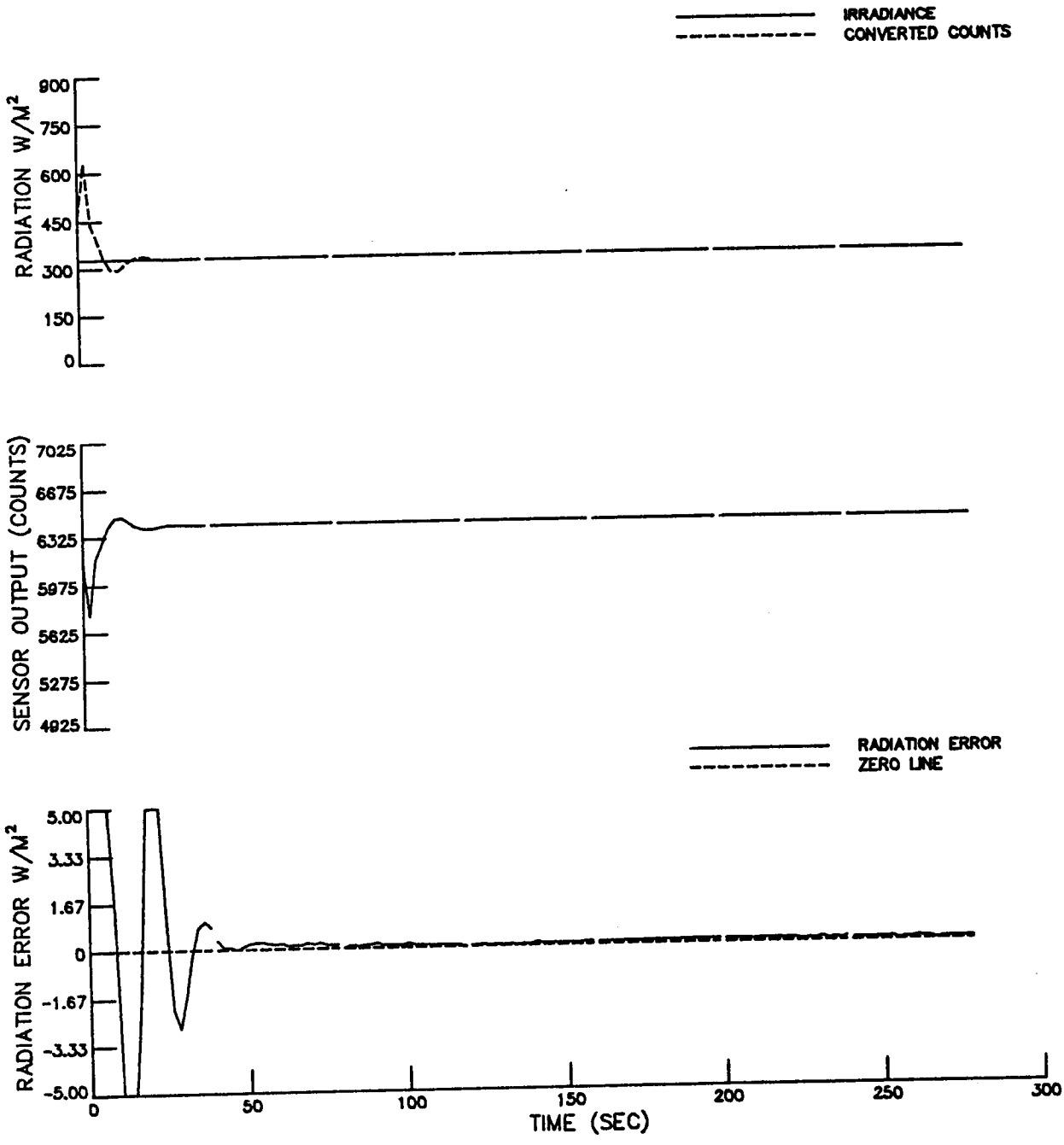

# NON-SCANNER DYNAMIC RESPONSE

WFOV FILTERED SIMULATION

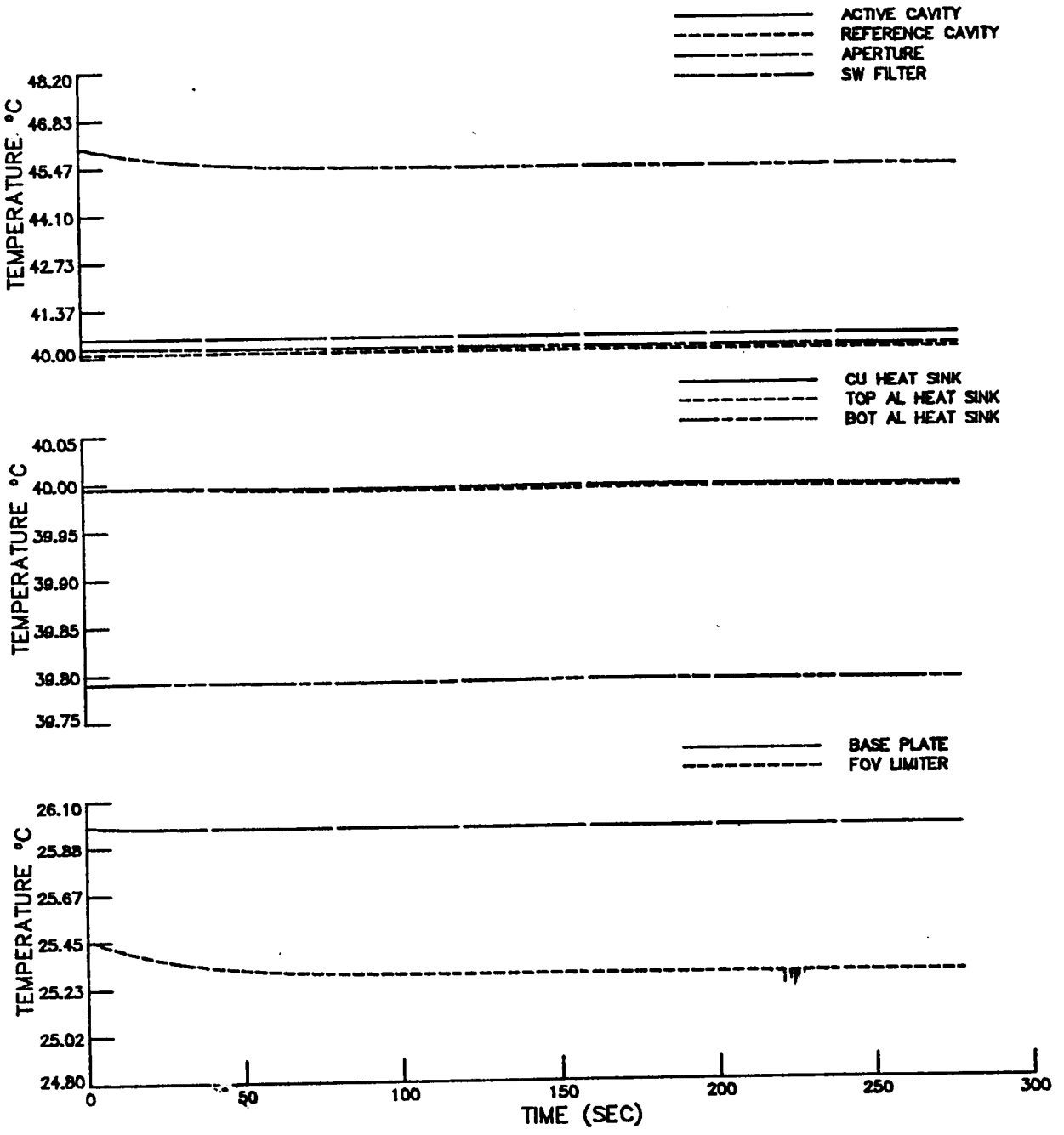

# NON-SCANNER DYNAMIC RESPONSE

WFOV FILTERED SIMULATION

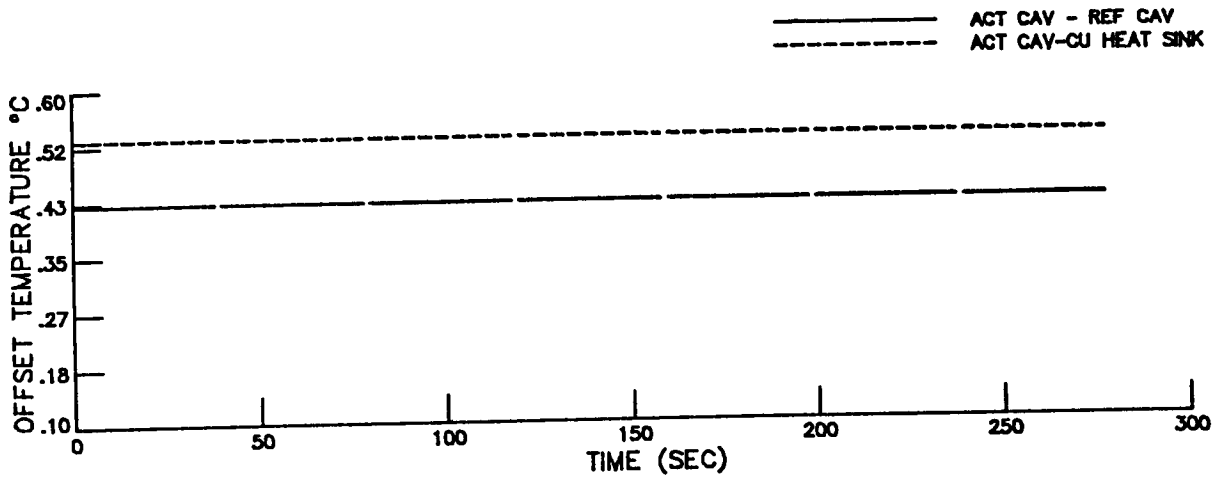

# NON-SCANNER DYNAMIC RESPONSE

WFOV FILTERED SIMULATION

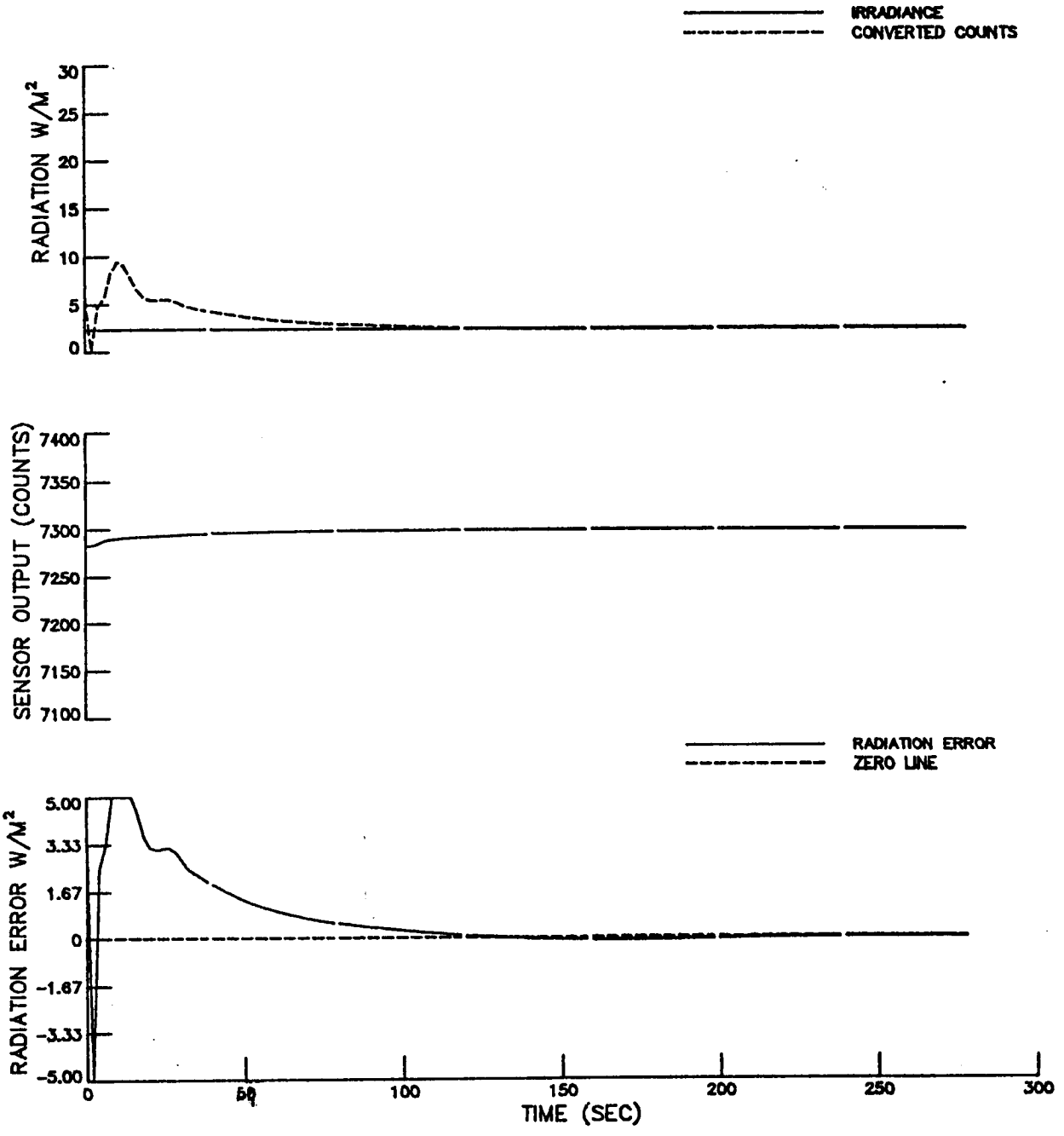

# NON-SCANNER DYNAMIC RESPONSE

MFOV TOTAL SIMULATION

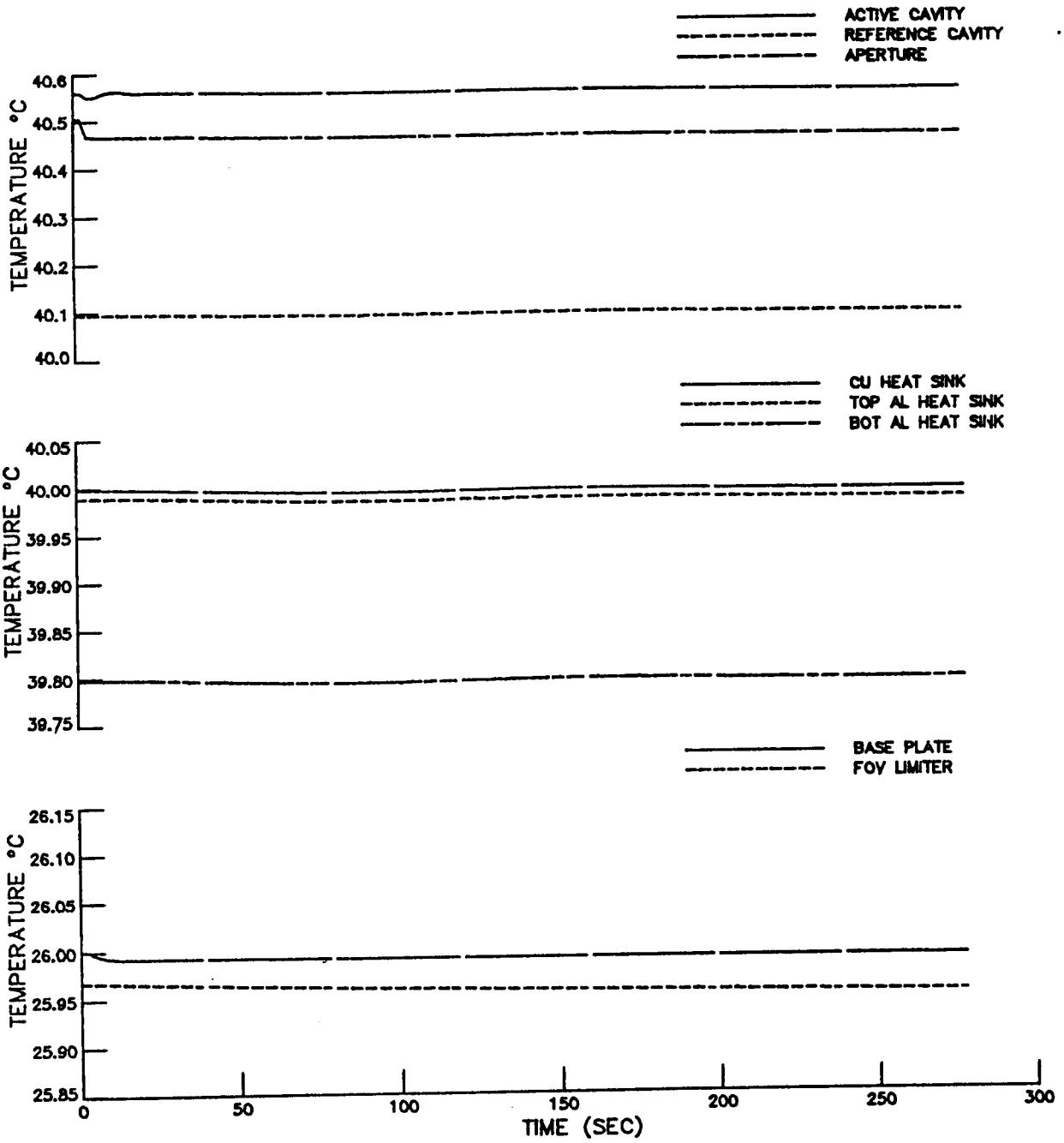

# NON-SCANNER DYNAMIC RESPONSE

MFOV TOTAL SIMULATION

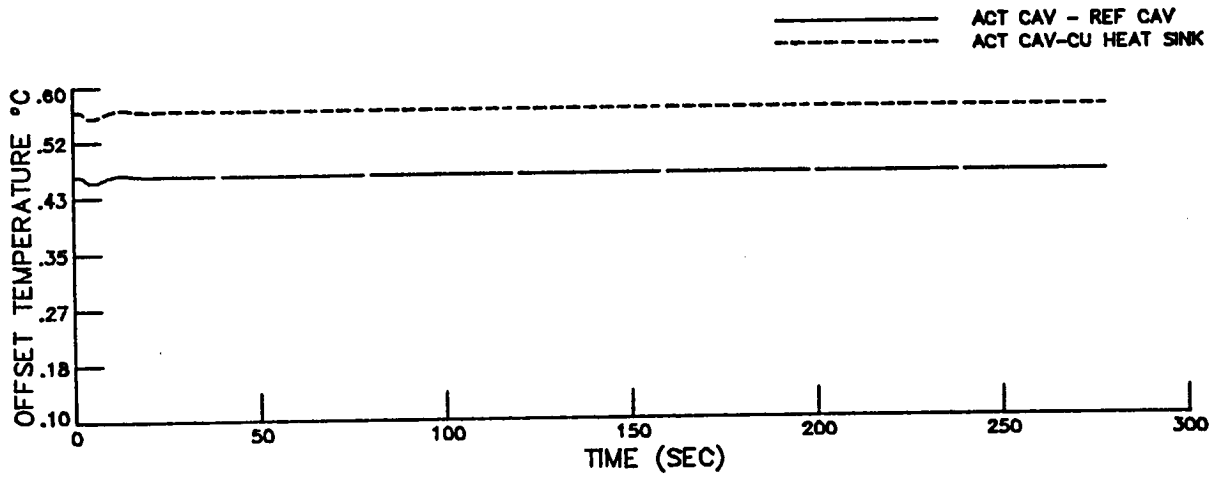

# NON-SCANNER DYNAMIC RESPONSE

MFOV TOTAL SIMULATION

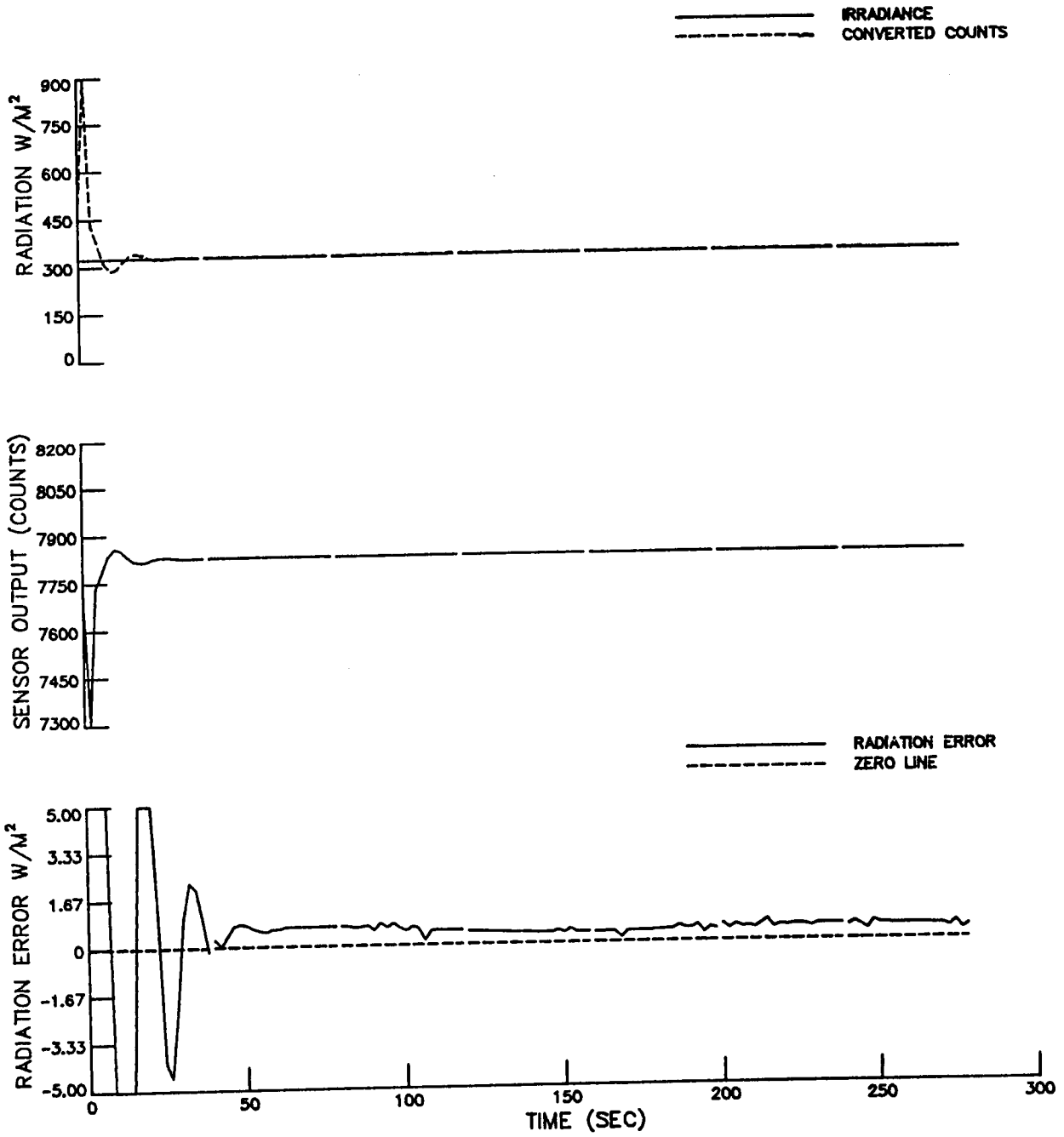

# NON-SCANNER DYNAMIC RESPONSE

MFOV FILTERED SIMULATION

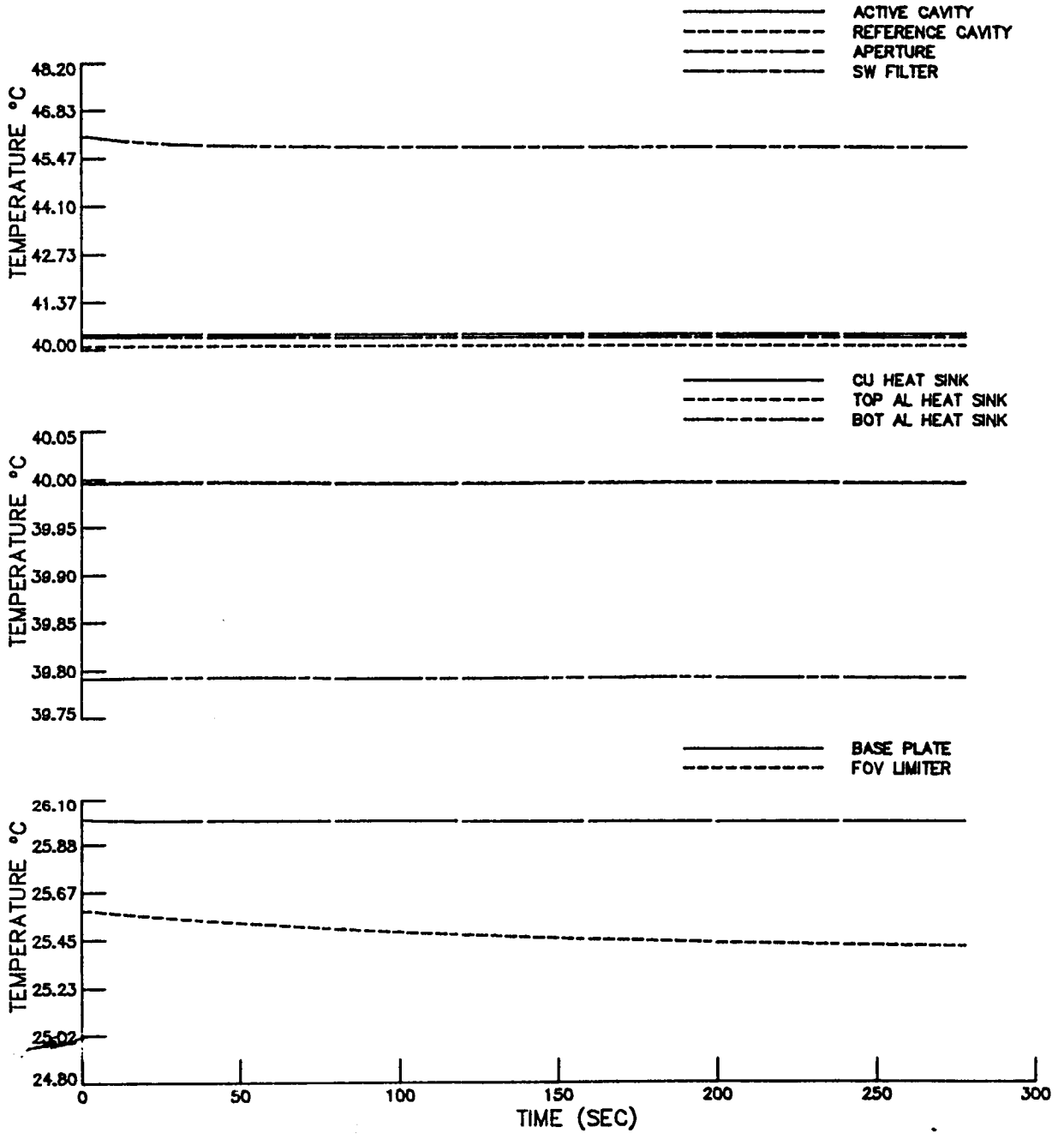

# NON-SCANNER DYNAMIC RESPONSE

MFOV FILTERED SIMULATION

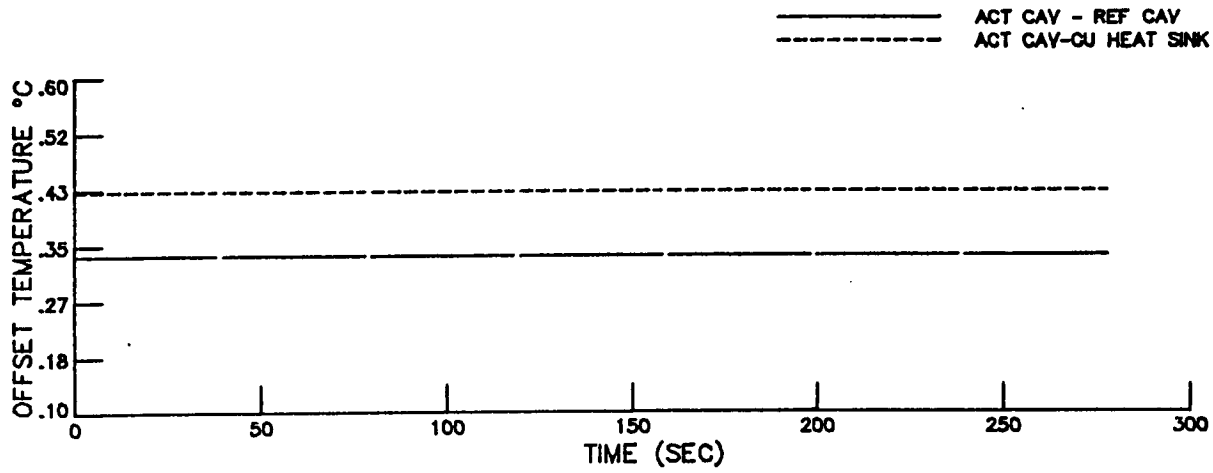

# NON-SCANNER DYNAMIC RESPONSE

MFOV FILTERED SIMULATION

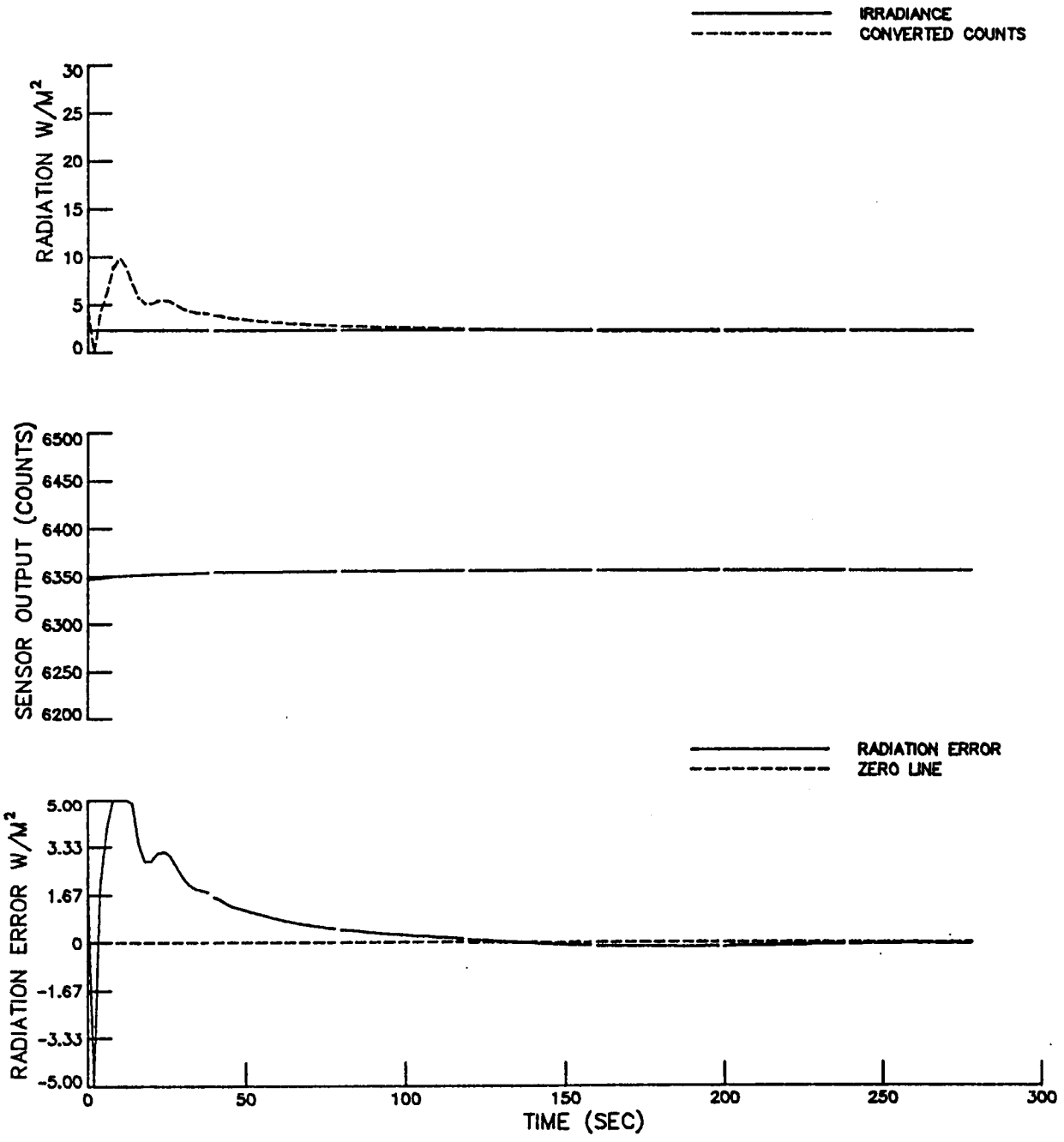

# NON-SCANNER STEADY STATE RESPONSE

## COMPARISON OF SIMULATION TO CALIBRATION DATA

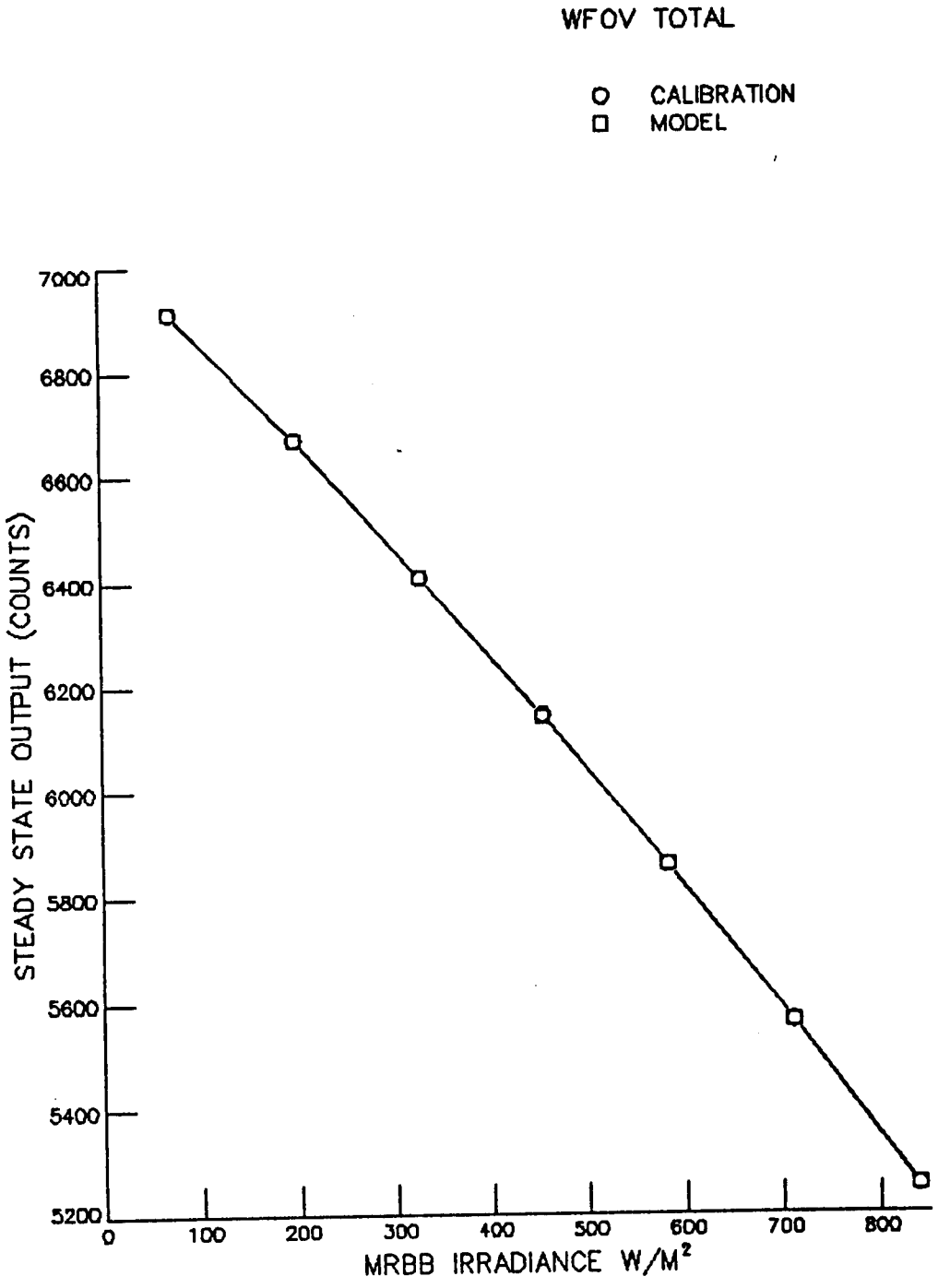

# NON-SCANNER STEADY STATE RESPONSE

## COMPARISON OF SIMULATION TO CALIBRATION DATA

WFOV TOTAL

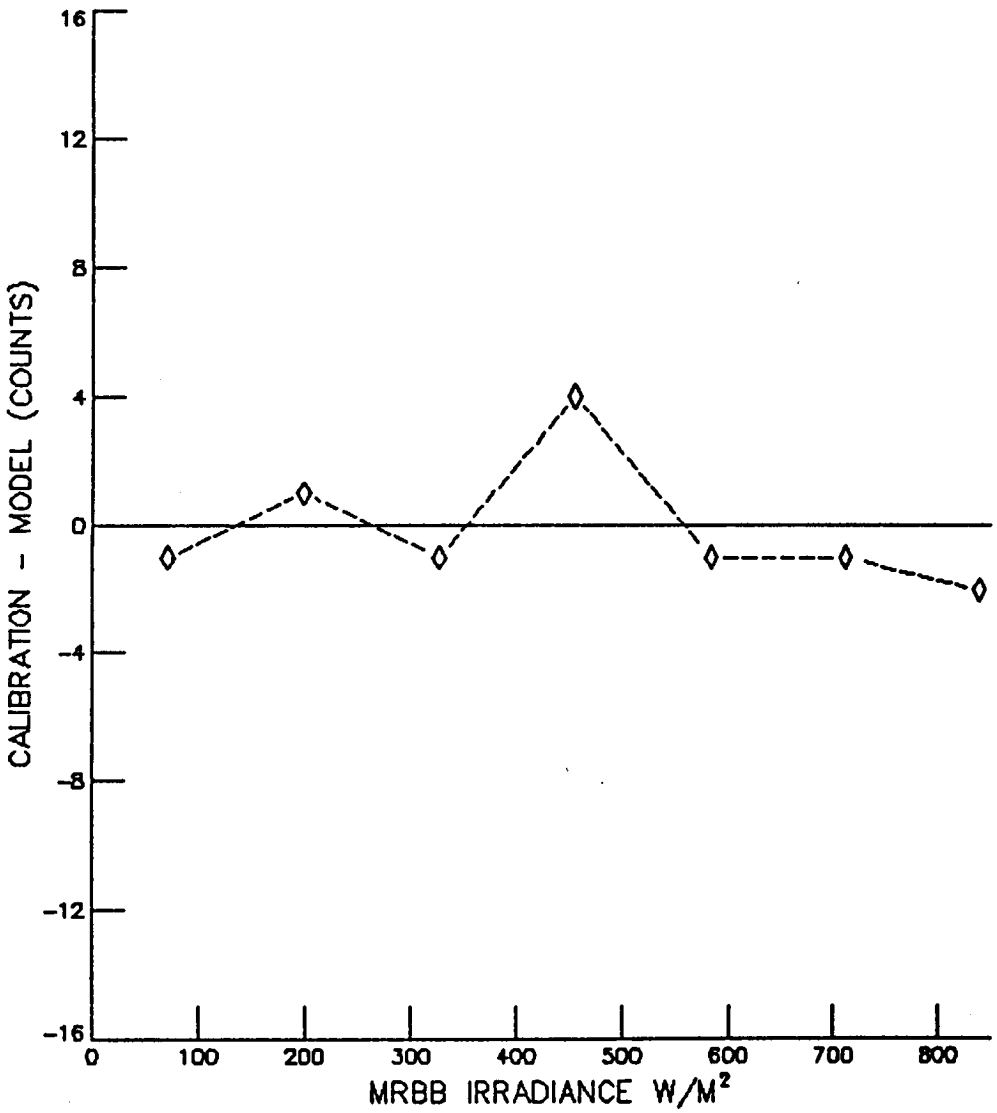

NON-SCANNER STEADY STATE RESPONSE

COMPARISON OF SIMULATION OF CALIBRATION DATA

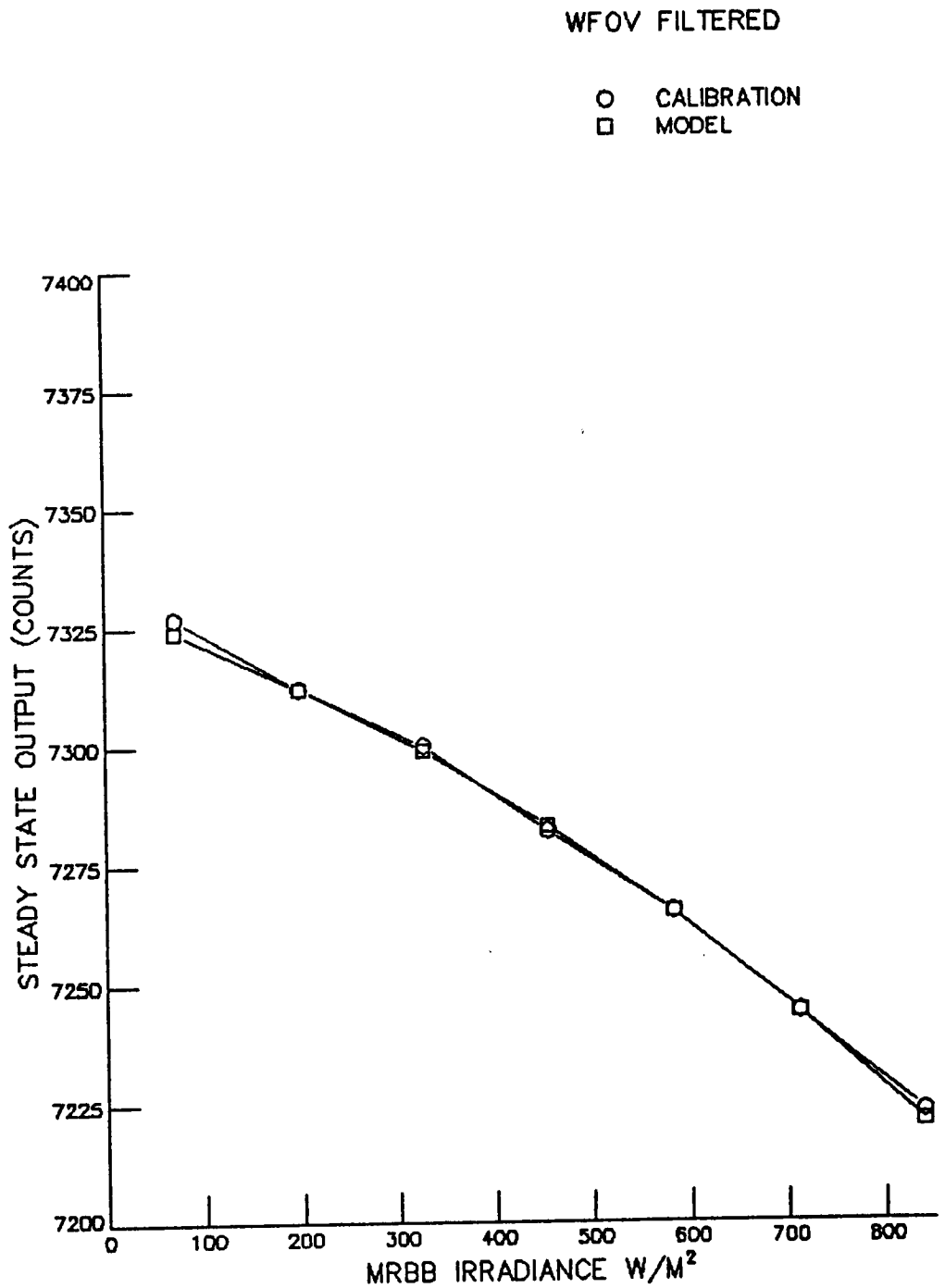

# NON-SCANNER STEADY STATE RESPONSE

## COMPARISON OF SIMULATION TO CALIBRATION DATA

WFOV FILTERED

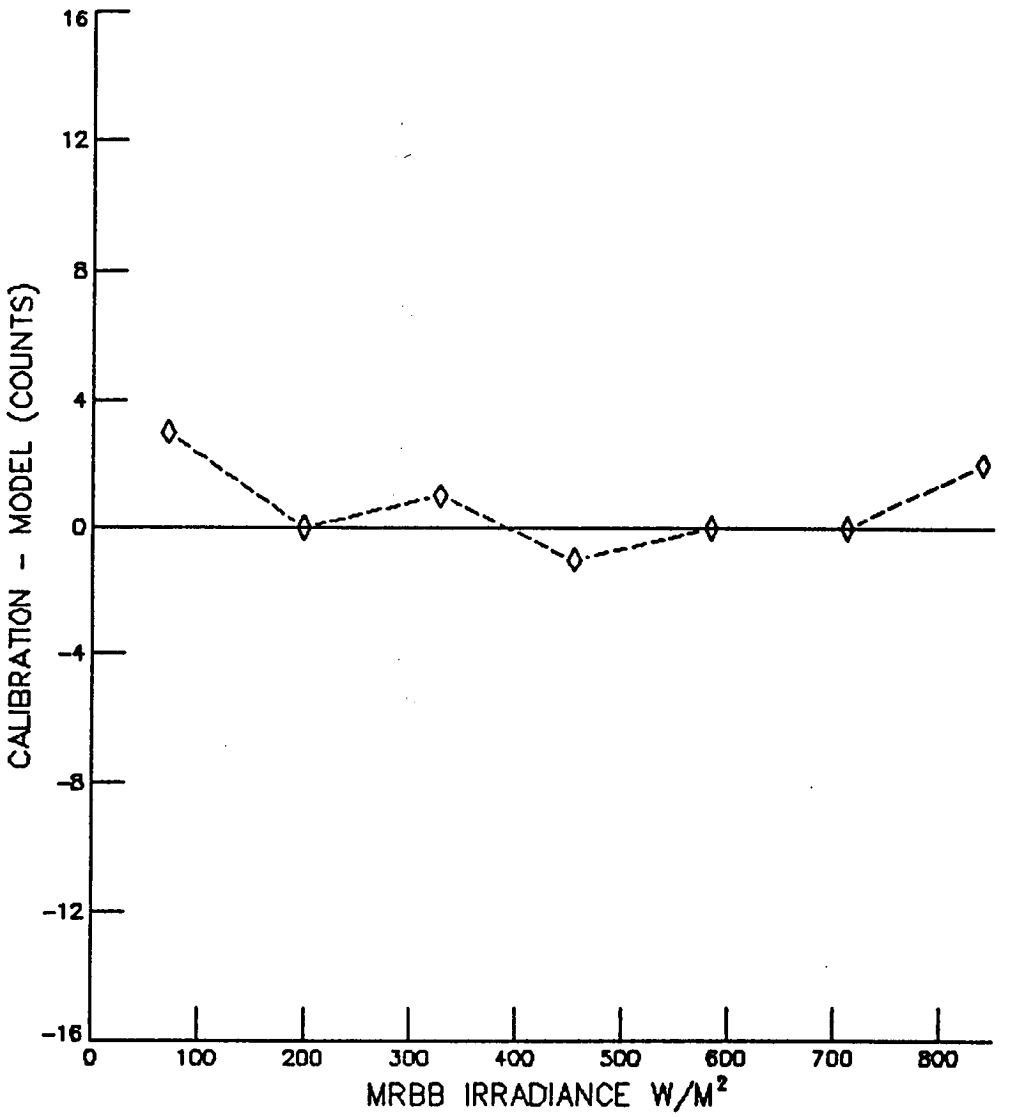

# NON-SCANNER STEADY STATE RESPONSE

## COMPARISON OF SIMULATION TO CALIBRATION DATA

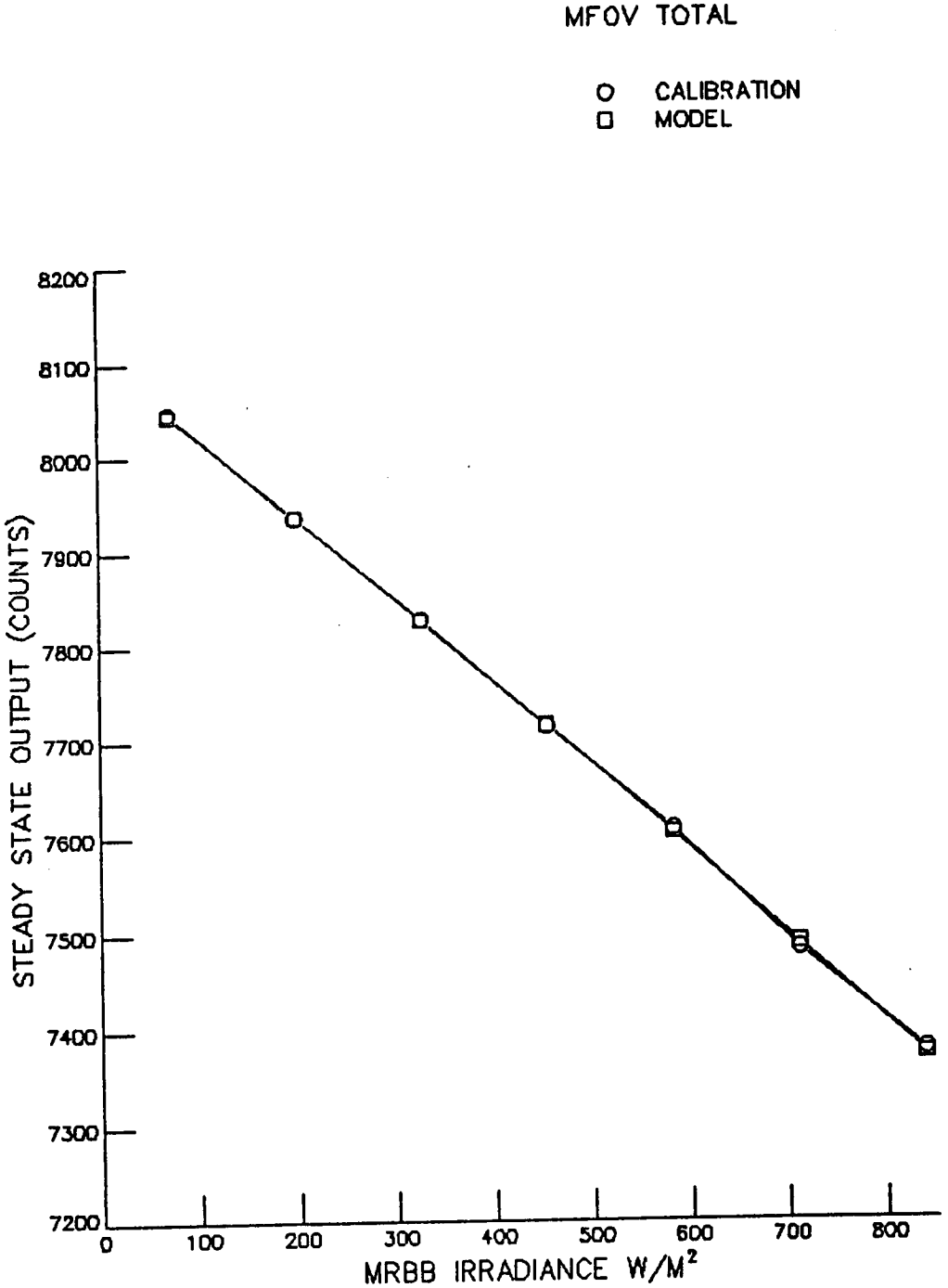

## NON-SCANNER STEADY STATE RESPONSE

## COMPARISON OF SIMULATION TO CALIBRATION DATA

MFOV TOTAL

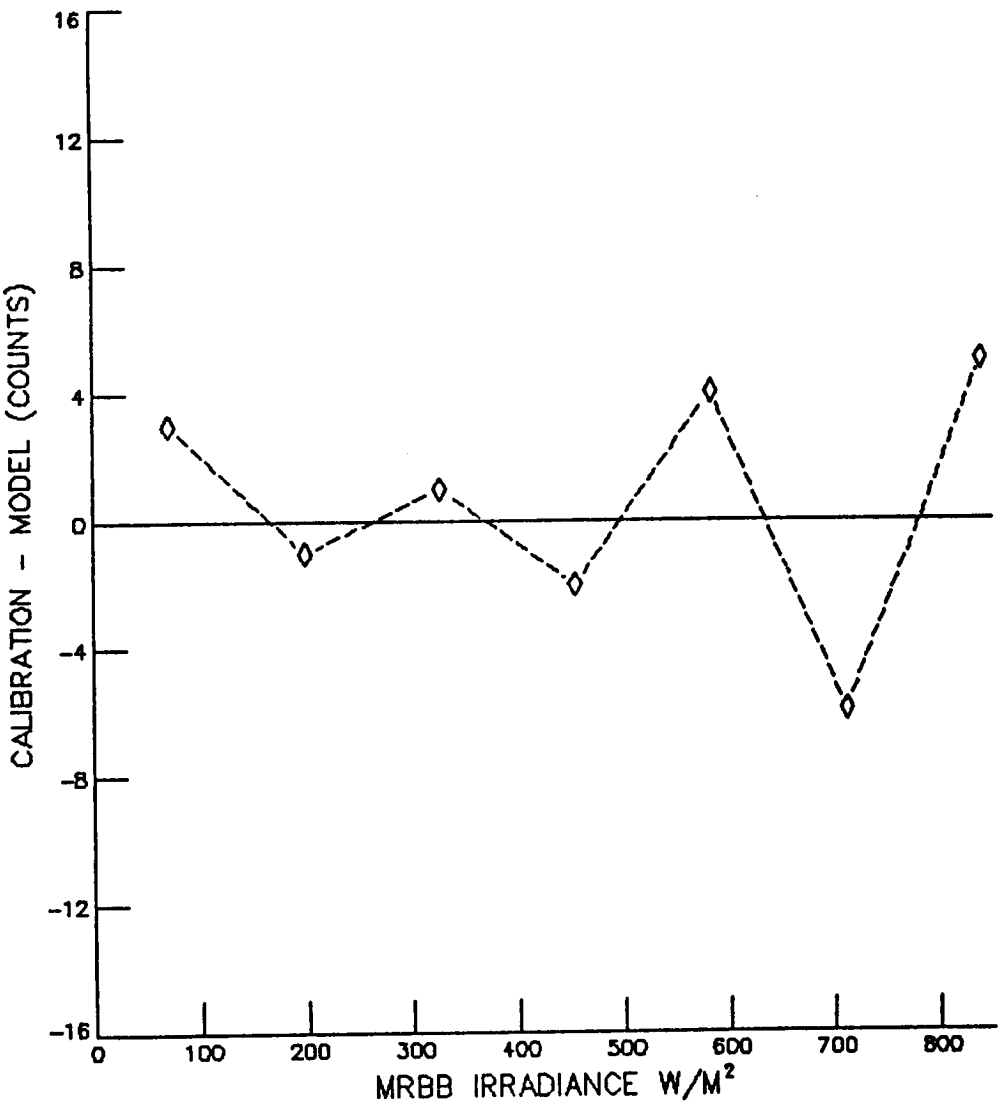

# NON-SCANNER STEADY STATE RESPONSE

## COMPARISON OF SIMULATION TO CALIBRATION DATA

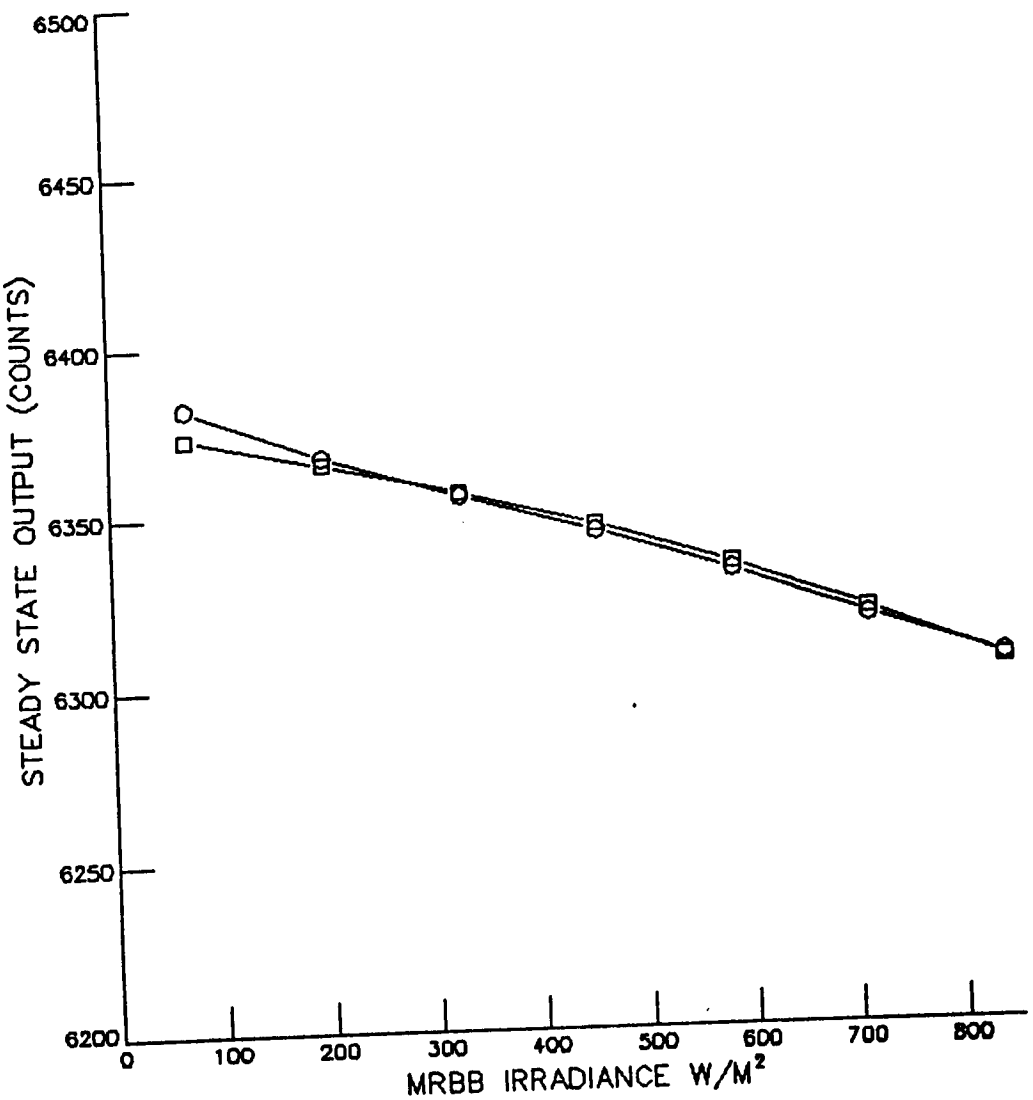

# NON-SCANNER STEADY STATE RESPONSE

## COMPARISON OF SIMULATION TO CALIBRATION DATA

MFOV FILTERED

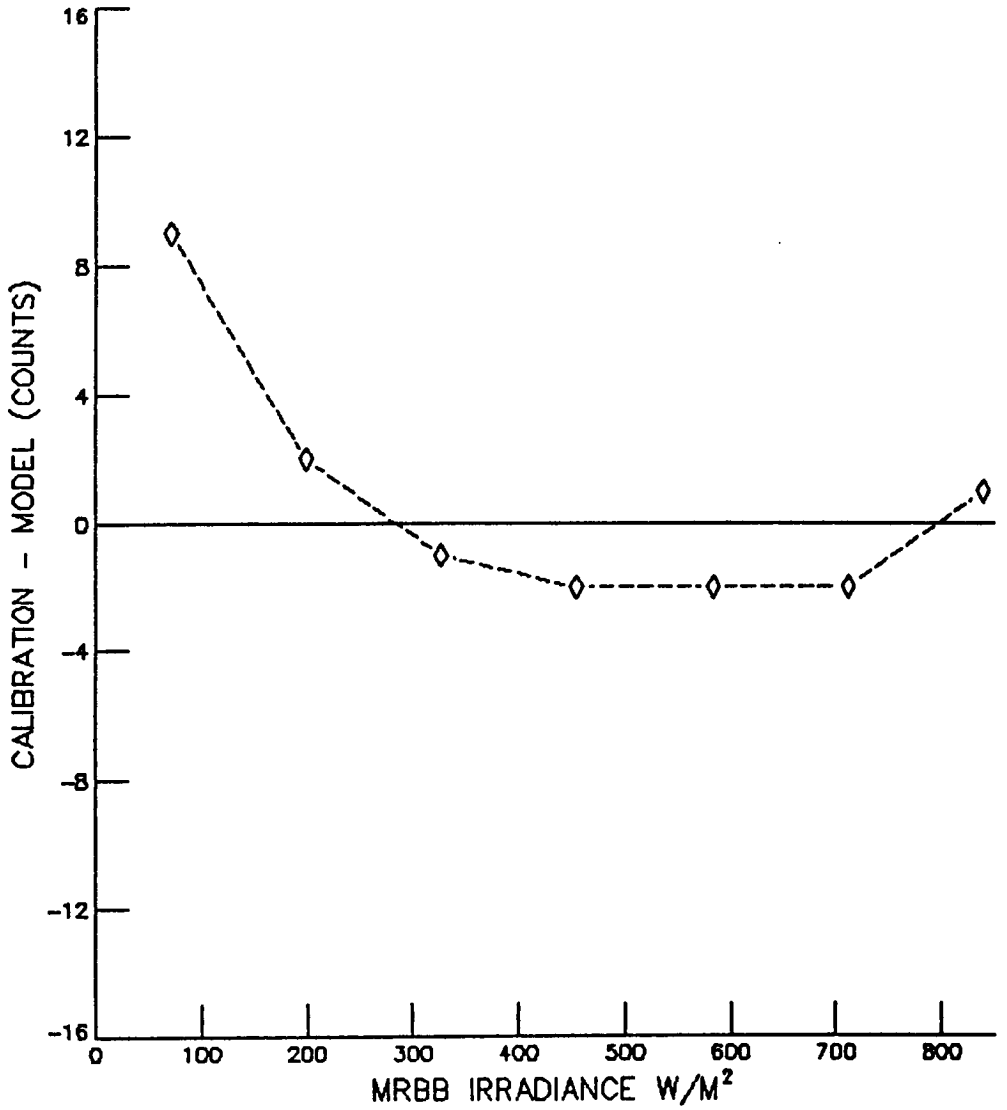

# NON-SCANNER DYNAMIC RESPONSE

WFOV TOTAL SIMULATION

TIME DELAY (LAG) ESTIMATION

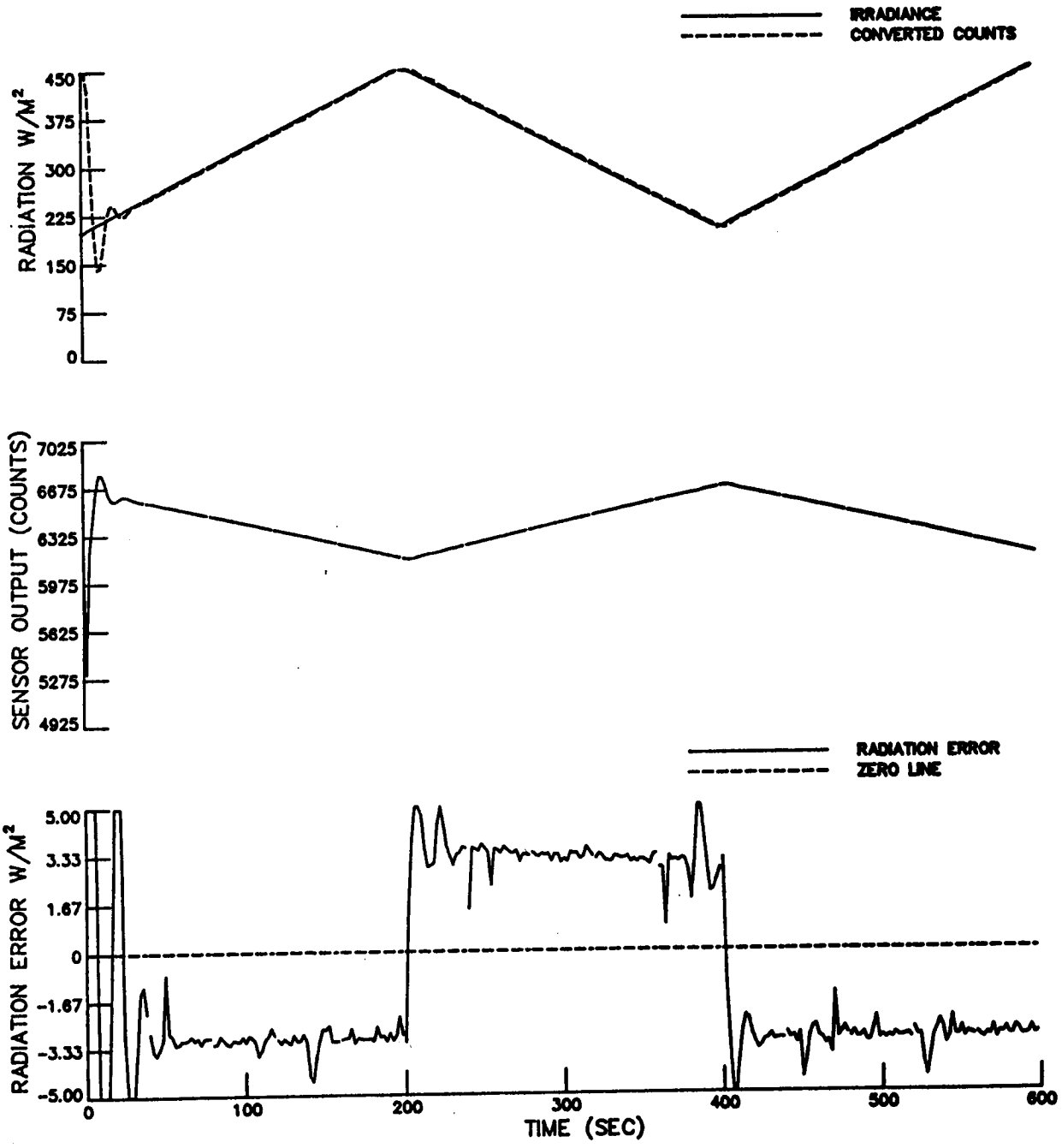

# NON-SCANNER DYNAMIC RESPONSE

WFOV TOTAL SIMULATION

TIME DELAY (LAG) ESTIMATION

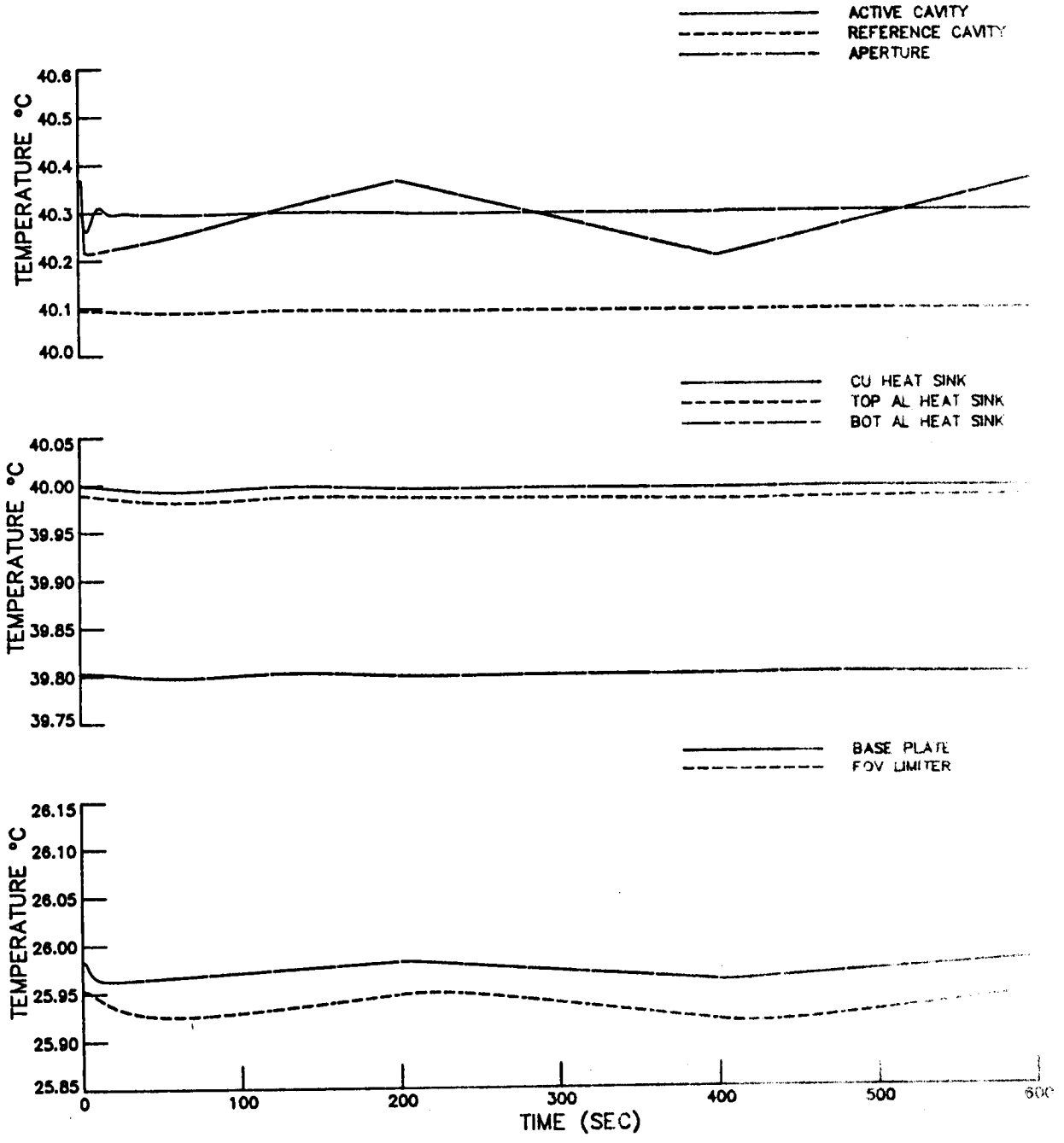

# NON-SCANNER DYNAMIC RESPONSE

WFOV TOTAL SIMULATION

TIME DELAY (LAG) ESTIMATION

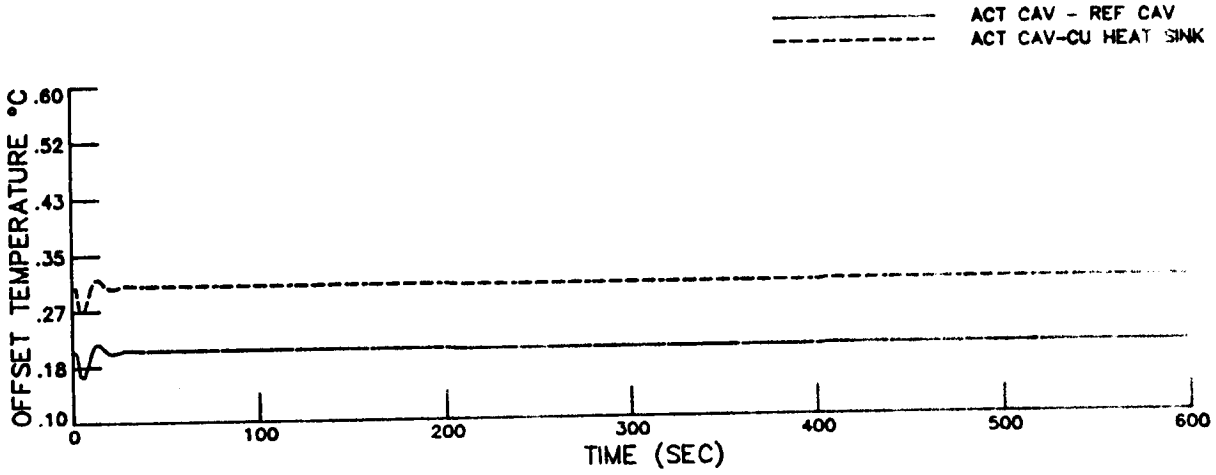

# NON-SCANNER DYNAMIC RESPONSE

MFOV TOTAL SIMULATION

TIME DELAY (LAG) ESTIMATION

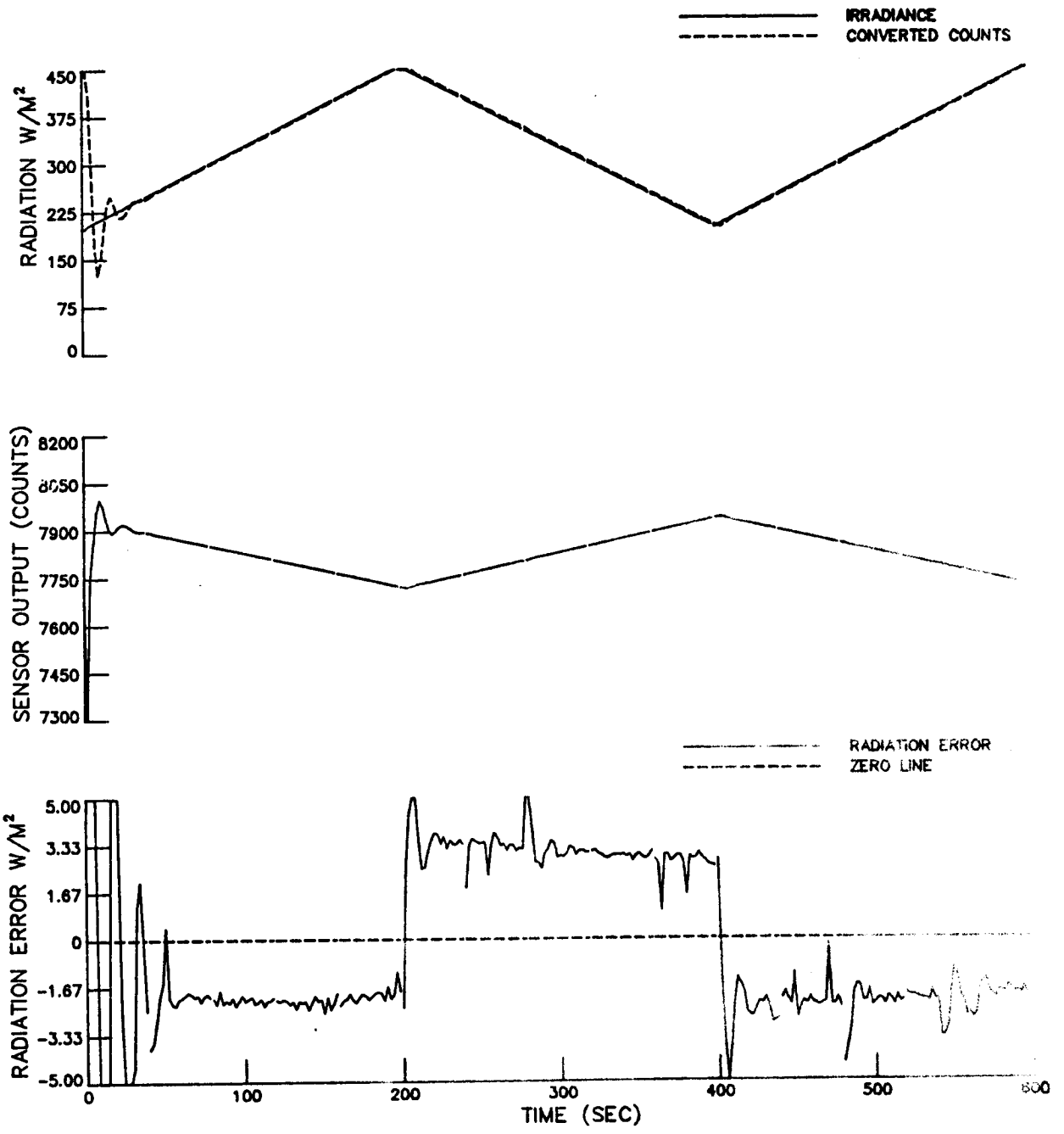

# NON-SCANNER DYNAMIC RESPONSE

MFOV TOTAL SIMULATION

TIME DELAY (LAG) ESTIMATION

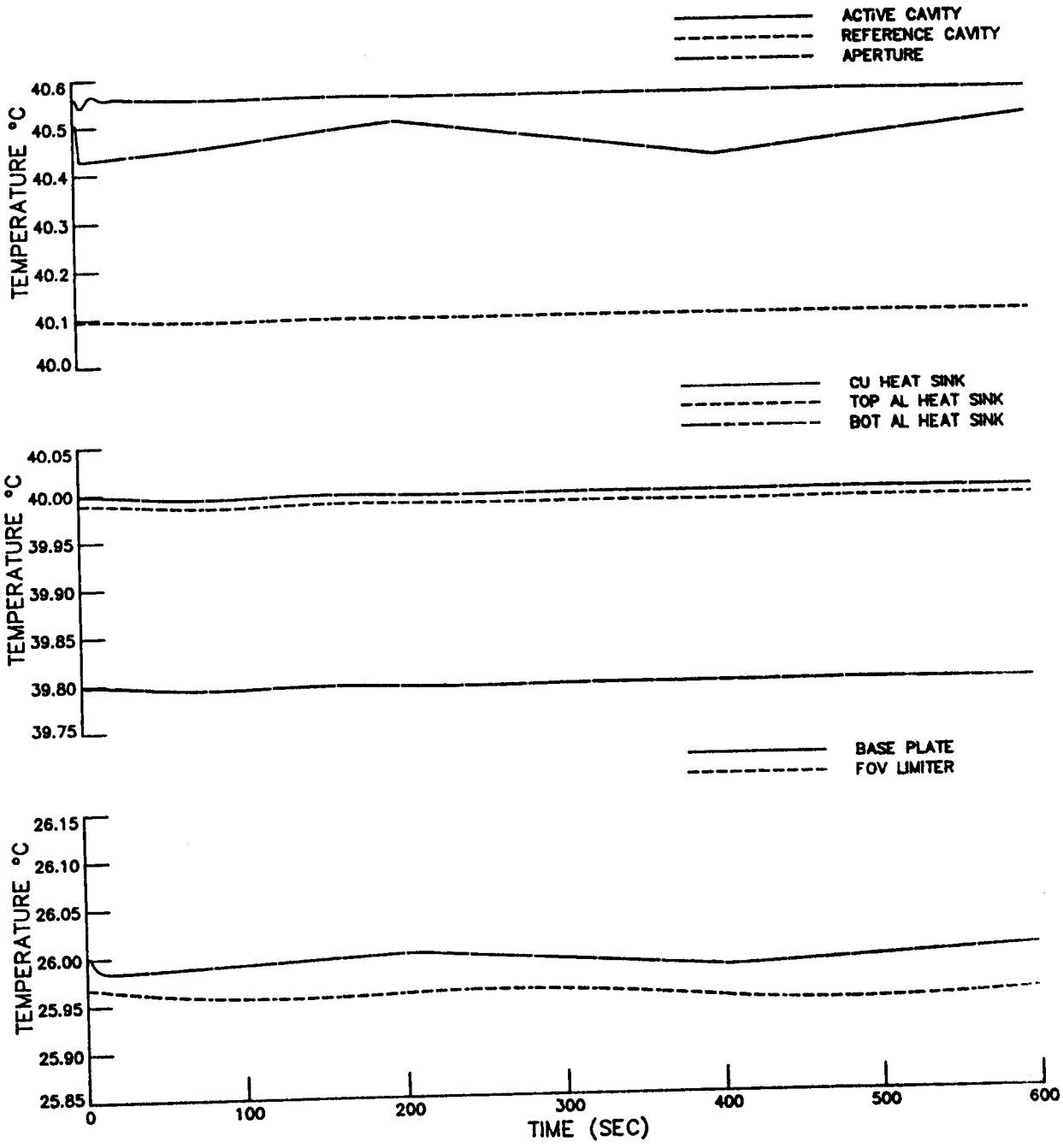

# NON-SCANNER DYNAMIC RESPONSE

MFOV TOTAL SIMULATION

TIME DELAY (LAG) ESTIMATION

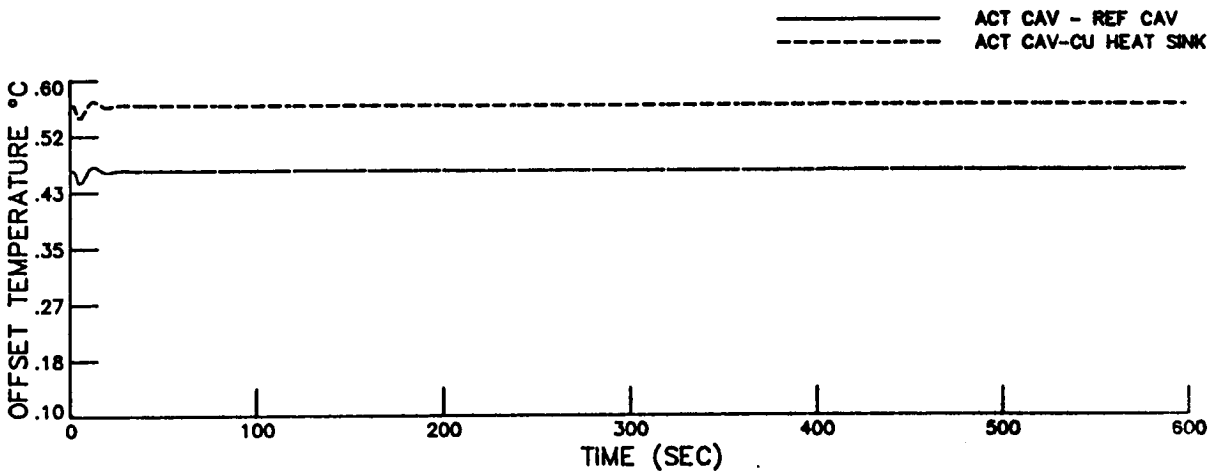

# NON-SCANNER DYNAMIC RESPONSE

WFOV FILTERED SIMULATION

TIME DELAY (LAG) ESTIMATION

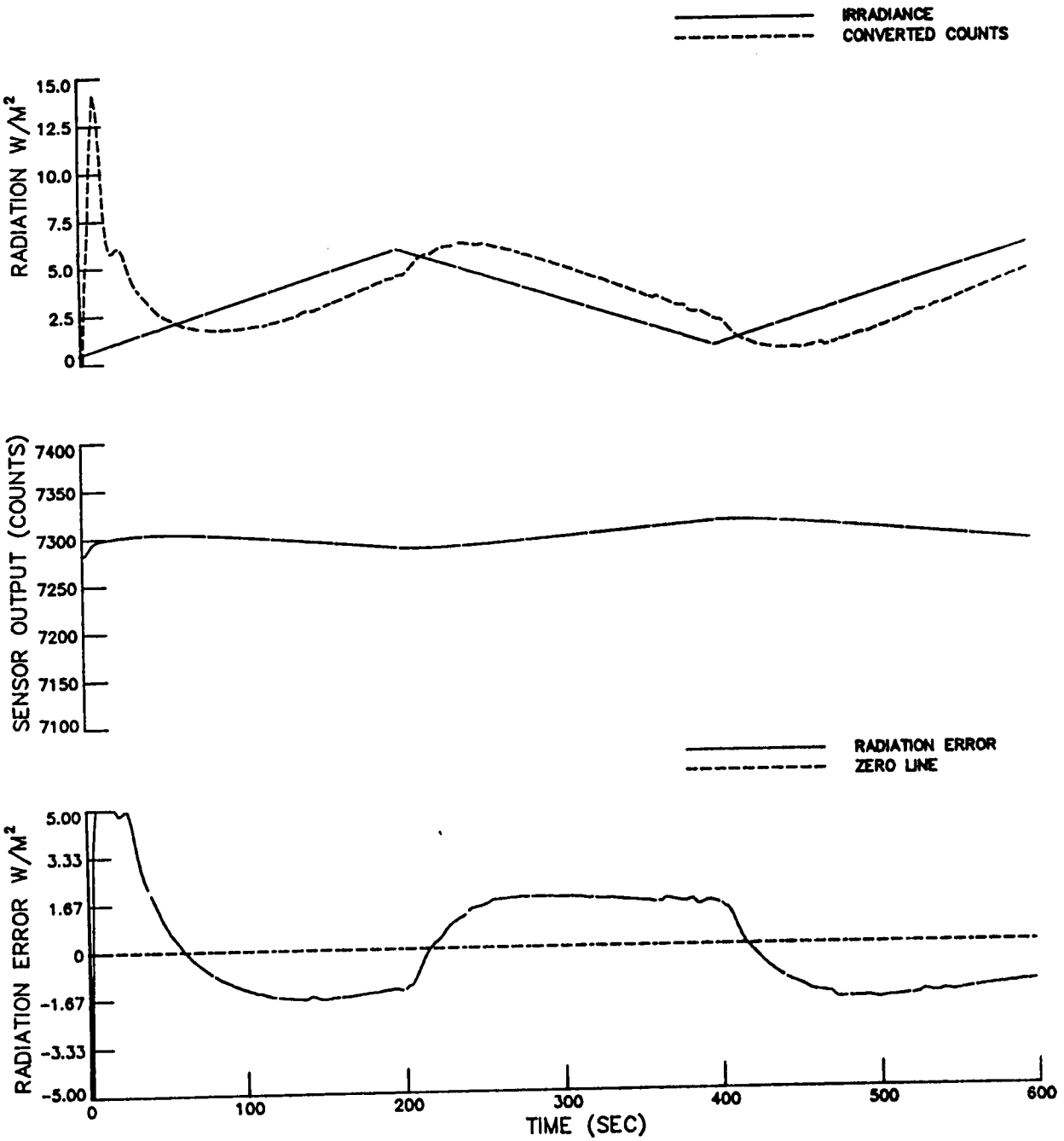

# NON-SCANNER DYNAMIC RESPONSE

WFOV FILTERED SIMULATION

TIME DELAY (LAG) ESTIMATION

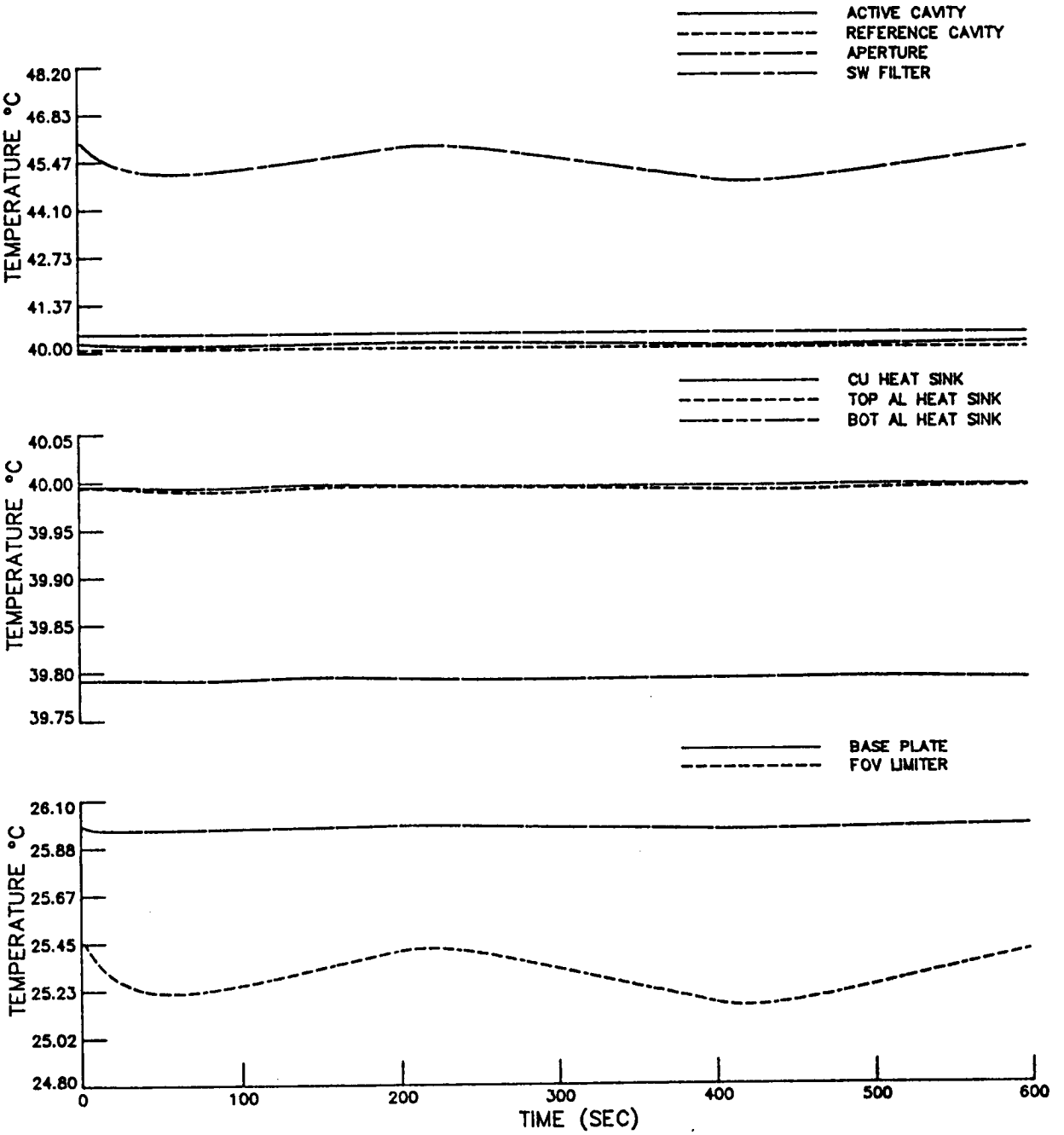

# NON-SCANNER DYNAMIC RESPONSE

WFOV FILTERED SIMULATION

TIME DELAY (LAG) ESTIMATION

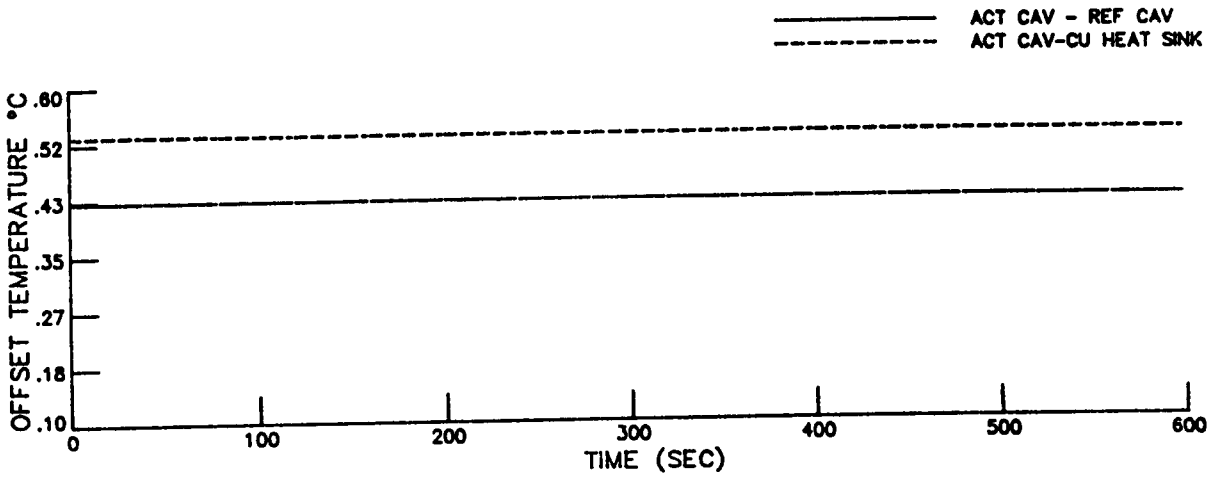

# NON-SCANNER DYNAMIC RESPONSE

MFOV FILTERED SIMULATION

TIME DELAY (LAG) ESTIMATION

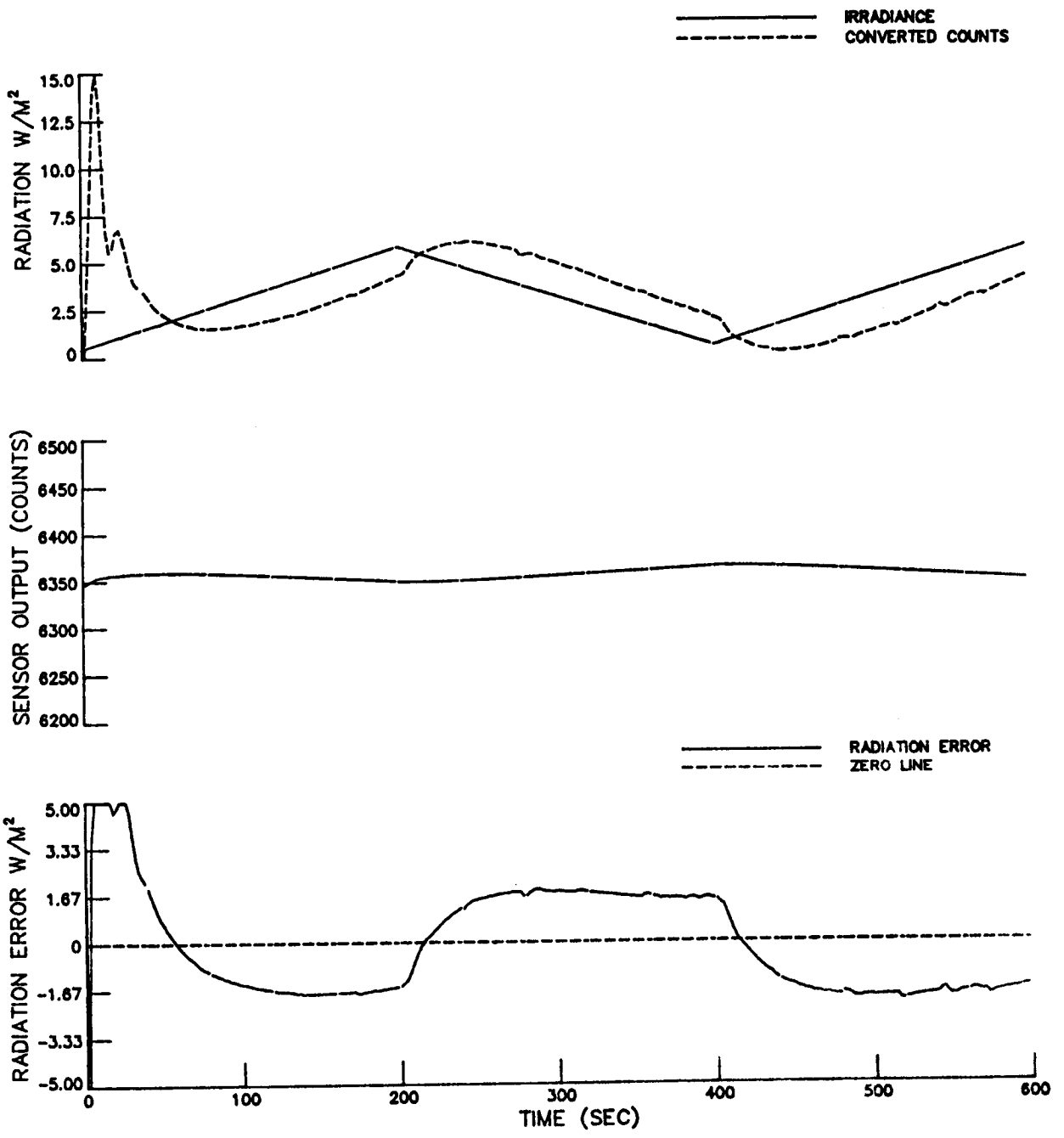

# NON-SCANNER DYNAMIC RESPONSE

MFOV FILTERED SIMULATION

TIME DELAY (LAG) ESTIMATION

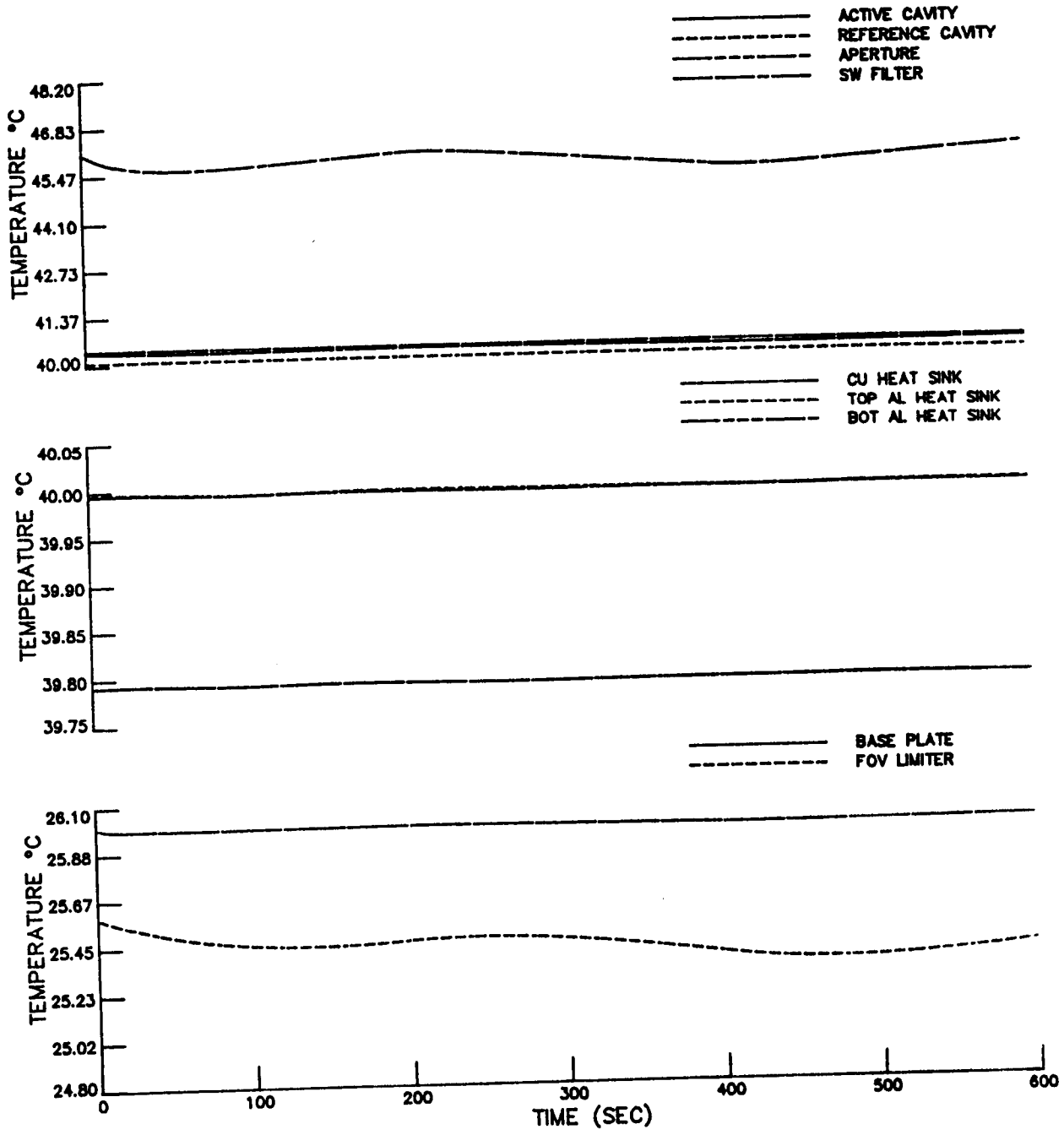

# NON-SCANNER DYNAMIC RESPONSE

## MFOV FILTERED SIMULATION

## TIME DELAY (LAG) ESTIMATION

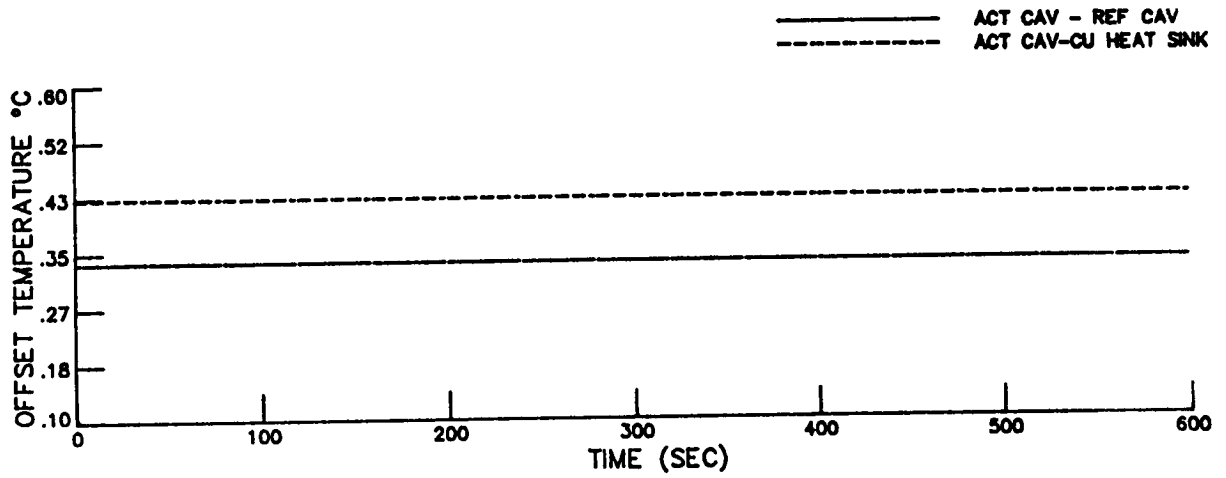

# SENSITIVITY ANALYSIS USING DYNAMIC MODEL

MFOV TOTAL SIMULATION

ACTIVE CAVITY EMISSIVITY CHANGED BY .02 (NOMINAL .92)

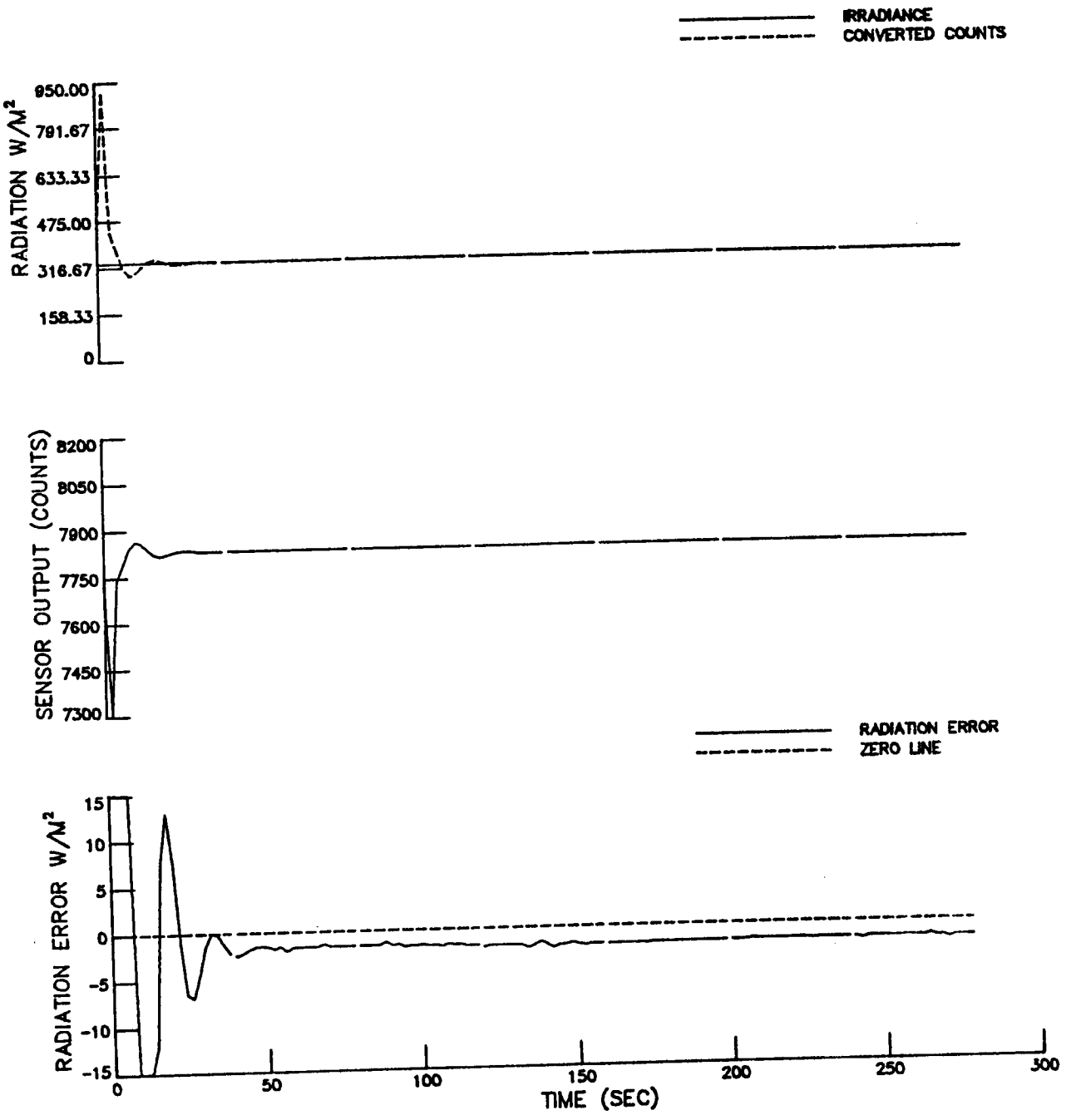

# SENSITIVITY ANALYSIS USING DYNAMIC MODEL

MFOV TOTAL SIMULATION

ACTIVE CAVITY EMISSIVITY CHANGED BY .02 (NOMINAL .92)

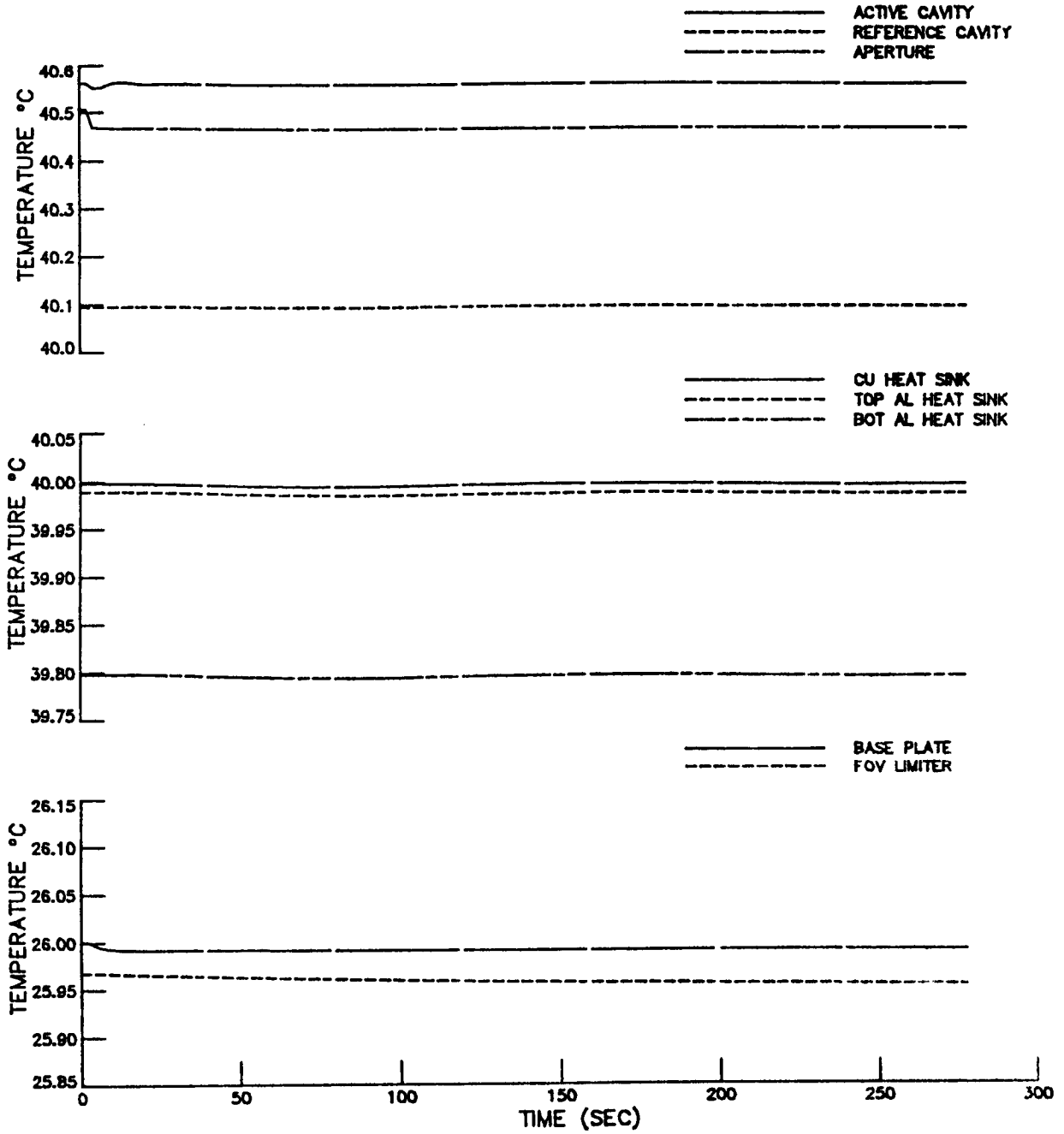

# SENSITIVITY ANALYSIS USING DYNAMIC MODEL

MFOV TOTAL SIMULATION

ACTIVE CAVITY EMISSIVITY CHANGED BY .02 (NOMINAL .92)

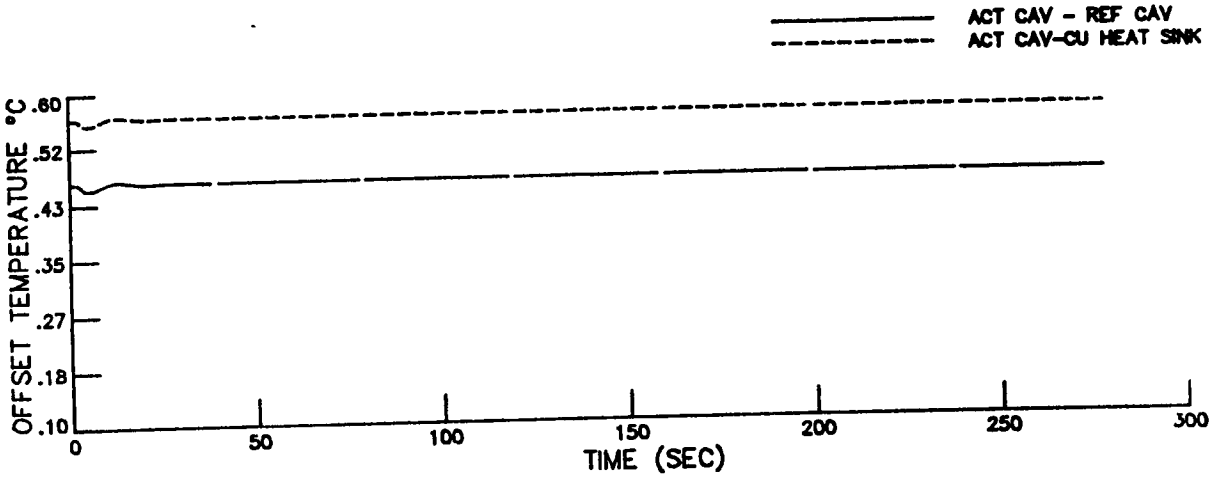

# SENSITIVITY ANALYSIS USING DYNAMIC MODEL

MFOV TOTAL SIMULATION

REFERENCE CAVITY EMISSIVITY CHANGED BY .02 (NOMINAL .95)

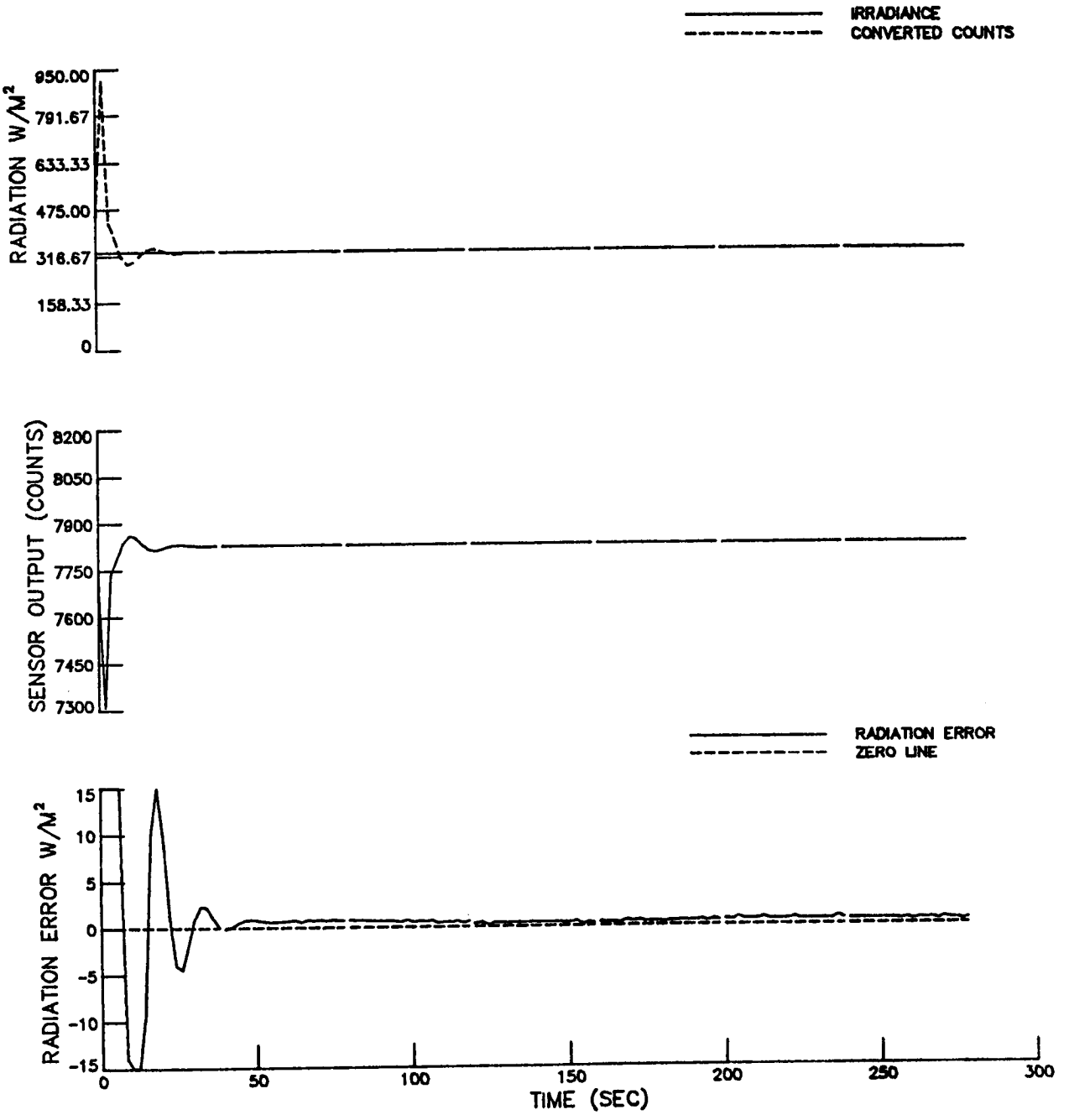

# SENSITIVITY ANALYSIS USING DYNAMIC MODEL

MFOV TOTAL SIMULATION

REFERENCE CAVITY EMISSIVITY CHANGED BY .02 (NOMINAL .95)

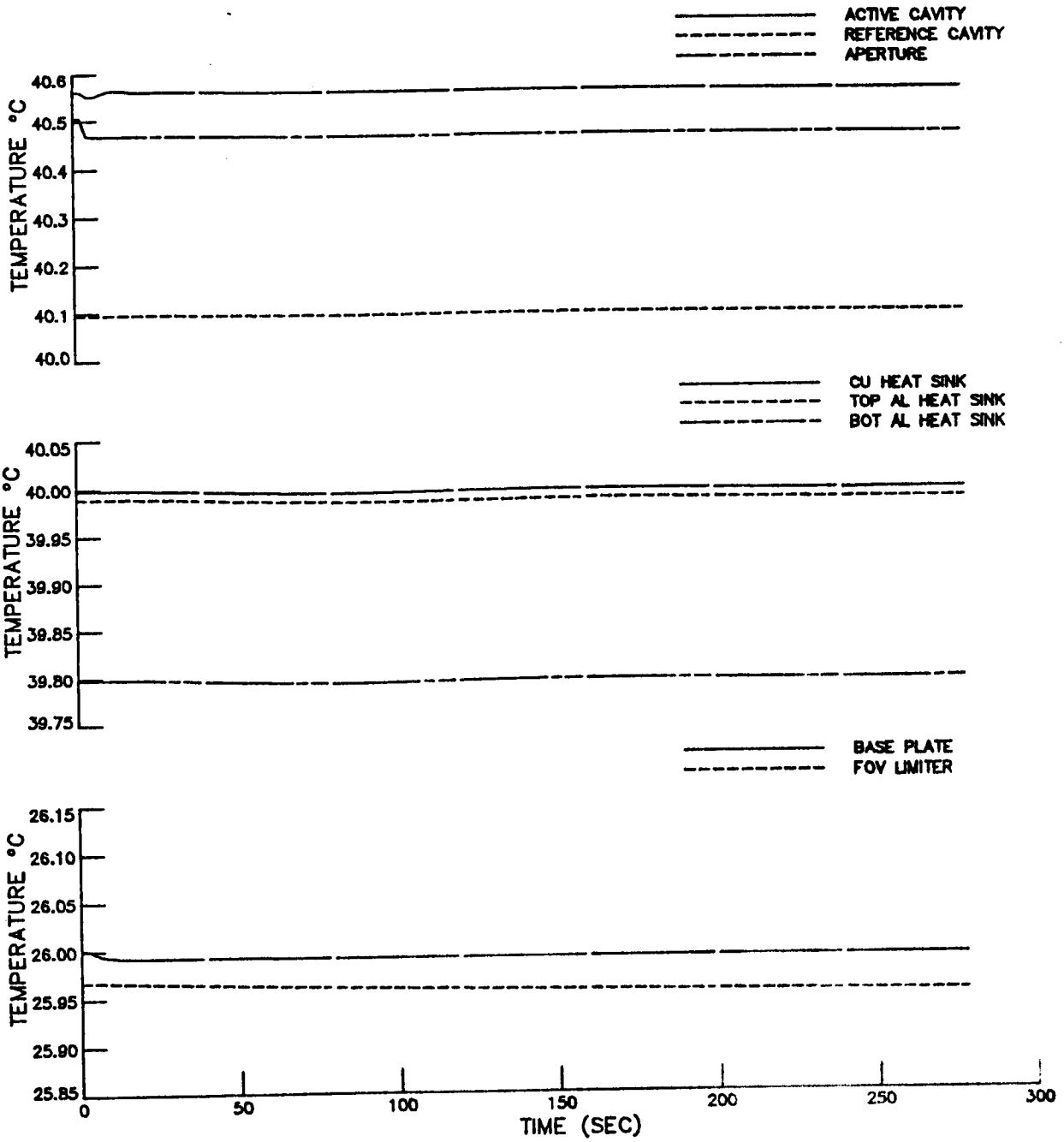

# SENSITIVITY ANALYSIS USING DYNAMIC MODEL

MFOV TOTAL SIMULATION

REFERENCE CAVITY EMISSIVITY CHANGED BY .02 (NOMINAL .95)

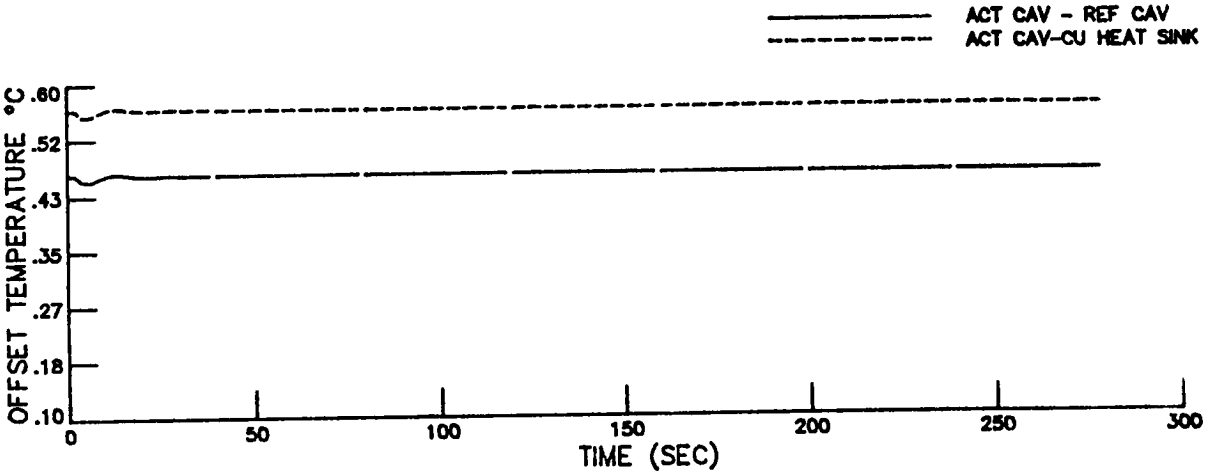

# SENSITIVITY ANALYSIS USING DYNAMIC MODEL

MFOV TOTAL SIMULATION

DOME FILTER LONG WAVE TRANSMITTANCE (LEAK) CHANGED BY .005 (NOMINAL .01)

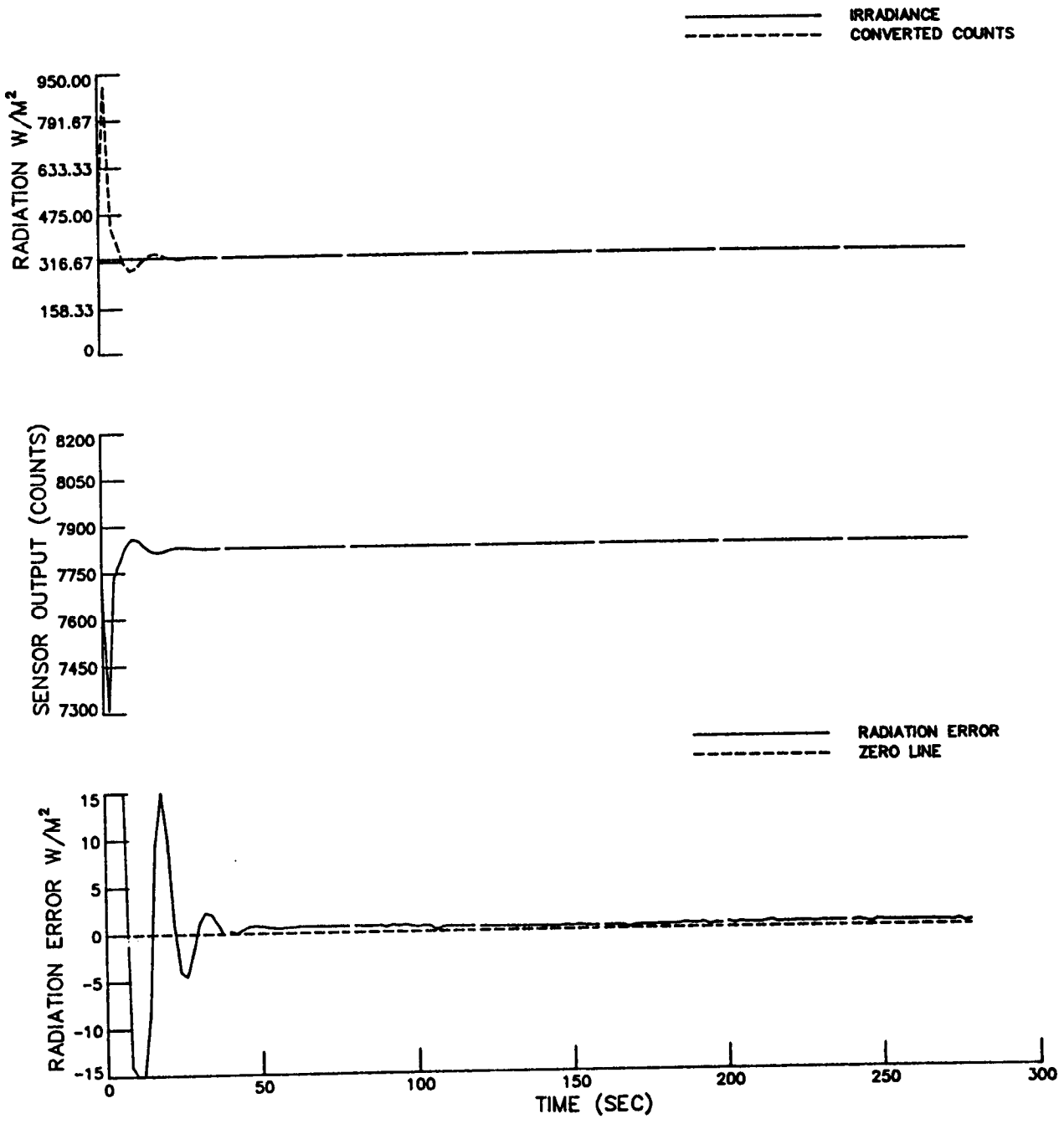

# SENSITIVITY ANALYSIS USING DYNAMIC MODEL

MFOV TOTAL SIMULATION

DOME FILTER LONG WAVE TRANSMITTANCE (LEAK) CHANGED BY .005 (NOMINAL .01)

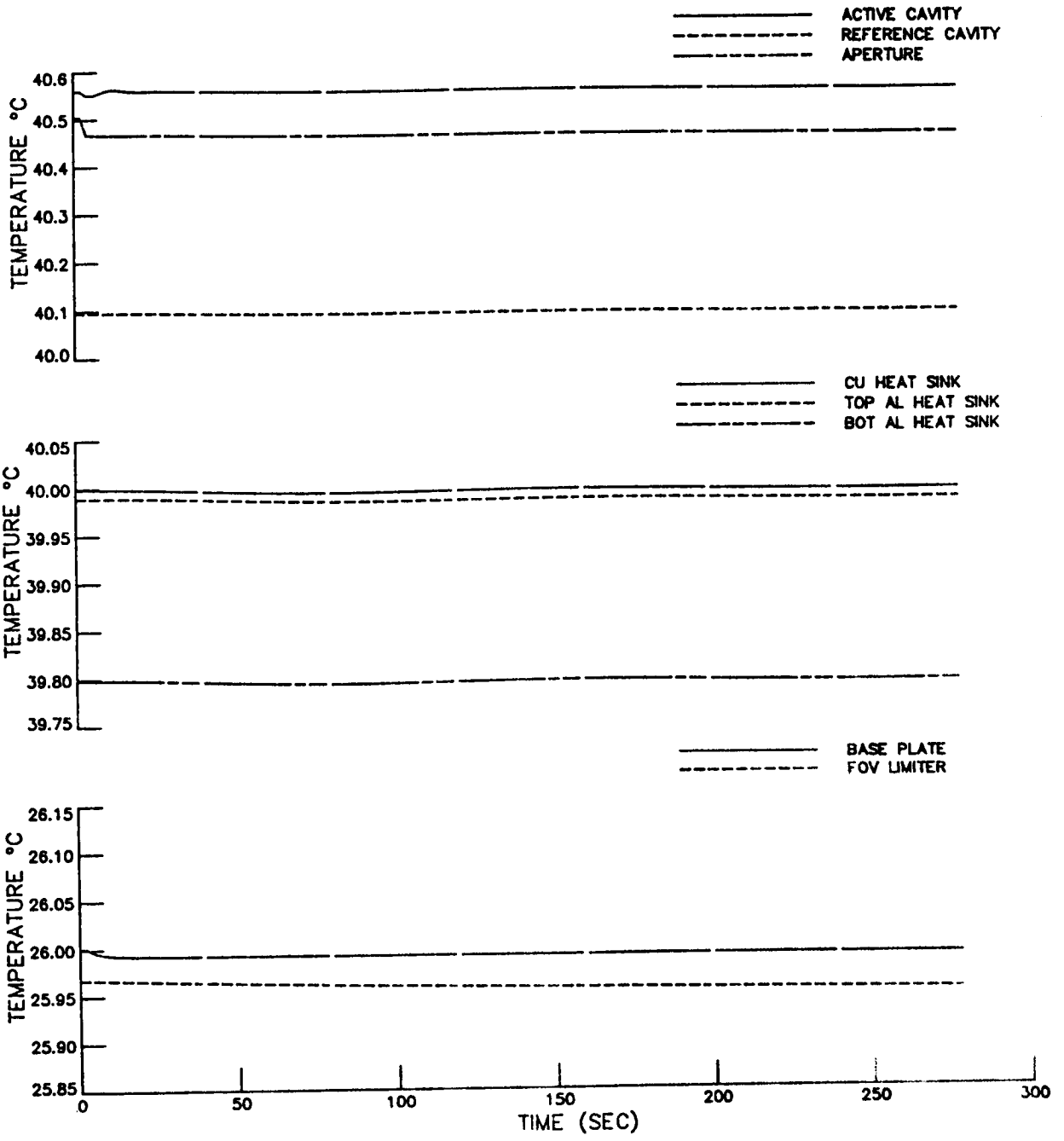

# SENSITIVITY ANALYSIS USING DYNAMIC MODEL

MFOV TOTAL SIMULATION

DOME FILTER LONG WAVE TRANSMITTANCE (LEAK) CHANGED BY .005 (NOMINAL .01)

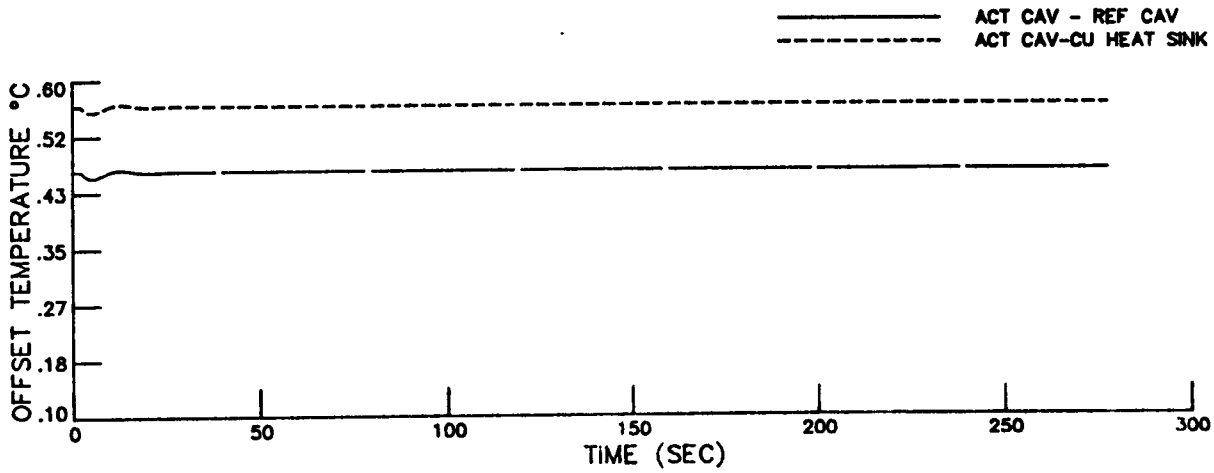

# SENSITIVITY ANALYSIS USING DYNAMIC MODEL

MFOV FILTERED SIMULATION

DOME FILTER LONG WAVE TRANSMITTANCE (LEAK) CHANGED BY .005 (NOMINAL .01)

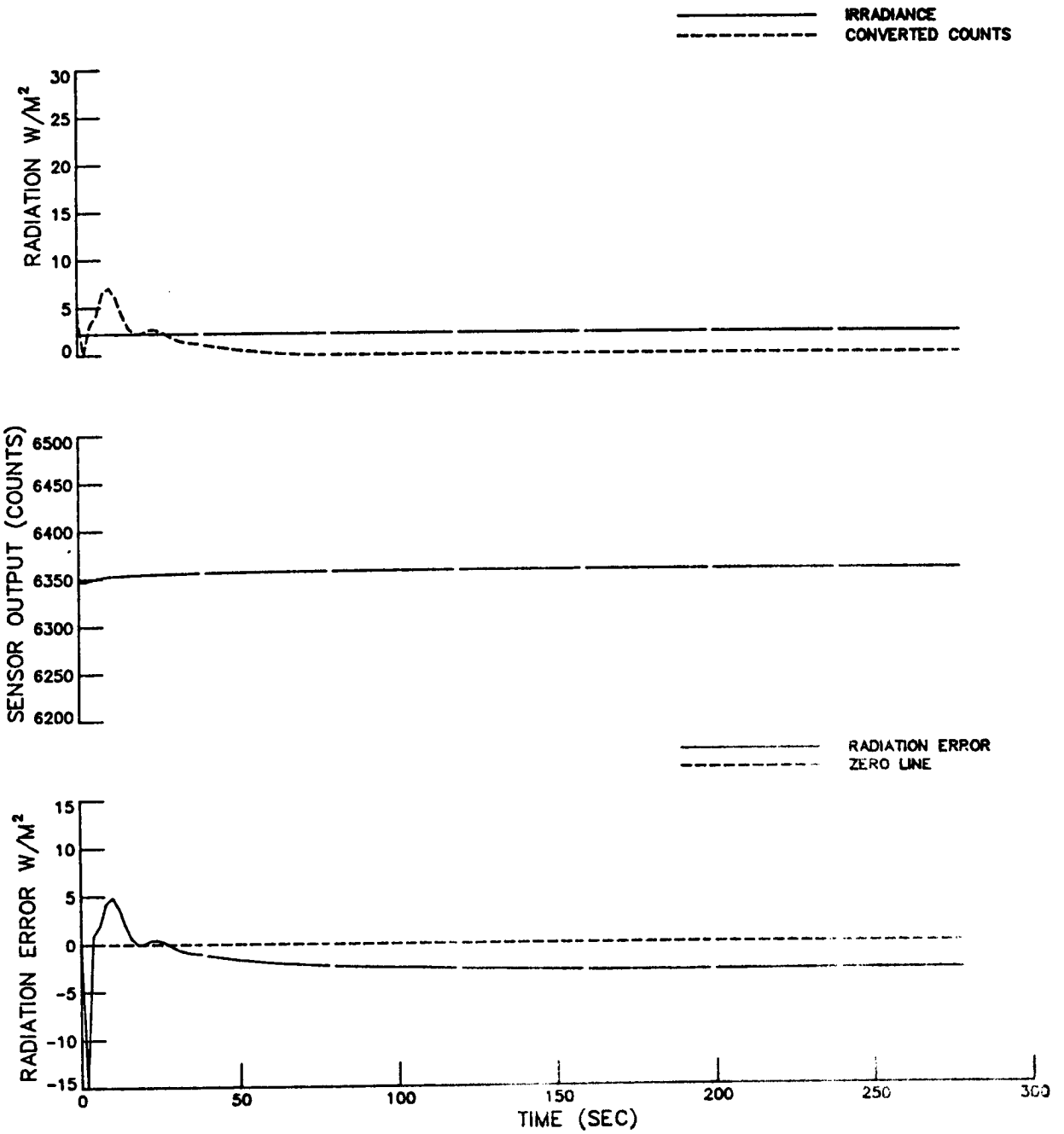

# SENSITIVITY ANALYSIS USING DYNAMIC MODEL

MFOV FILTERED SIMULATION

DOME FILTER LONG WAVE TRANSMITTANCE (LEAK) CHANGED BY .005 (NOMINAL .01)

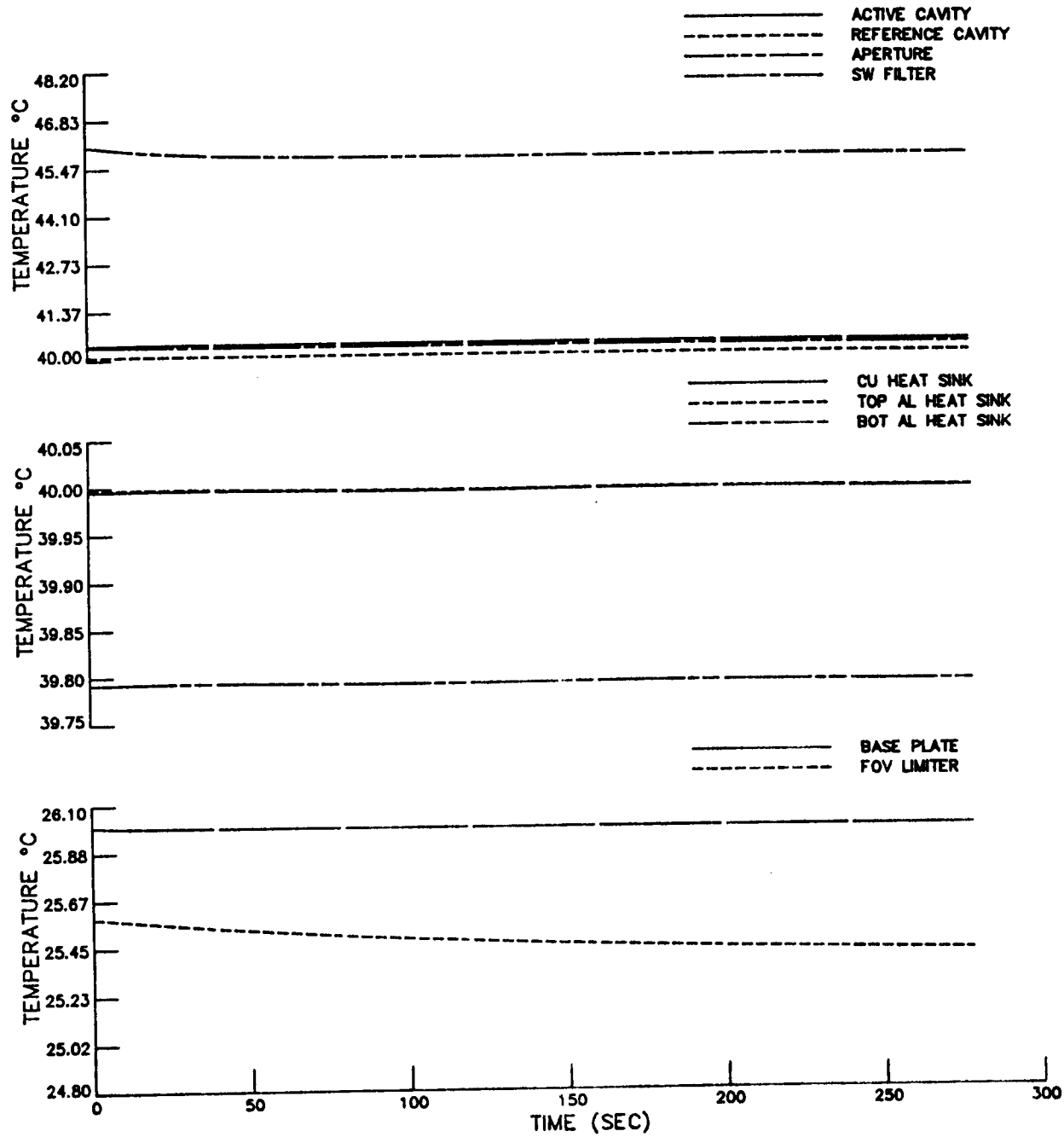

# SENSITIVITY ANALYSIS USING DYNAMIC MODEL

MFOV FILTERED SIMULATION

DOME FILTER LONG WAVE TRANSMITTANCE (LEAK) CHANGED BY .005 (NOMINAL .01)

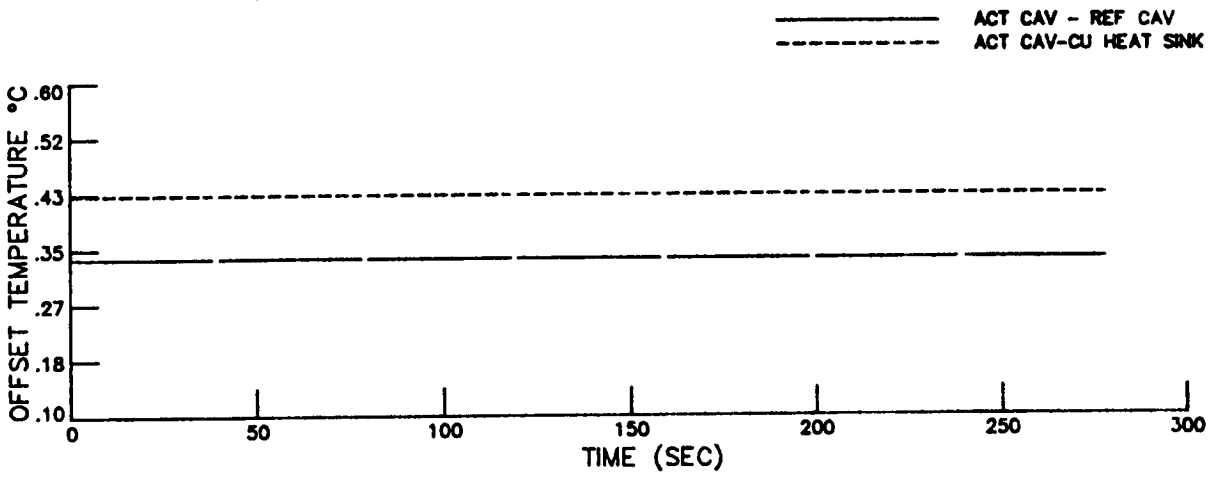

# SENSITIVITY ANALYSIS USING DYNAMIC MODEL

MFOV TOTAL SIMULATION

DOME FILTER SHORT WAVE TRANSMITTANCE CHANGED BY .005 (NOMINAL .946)

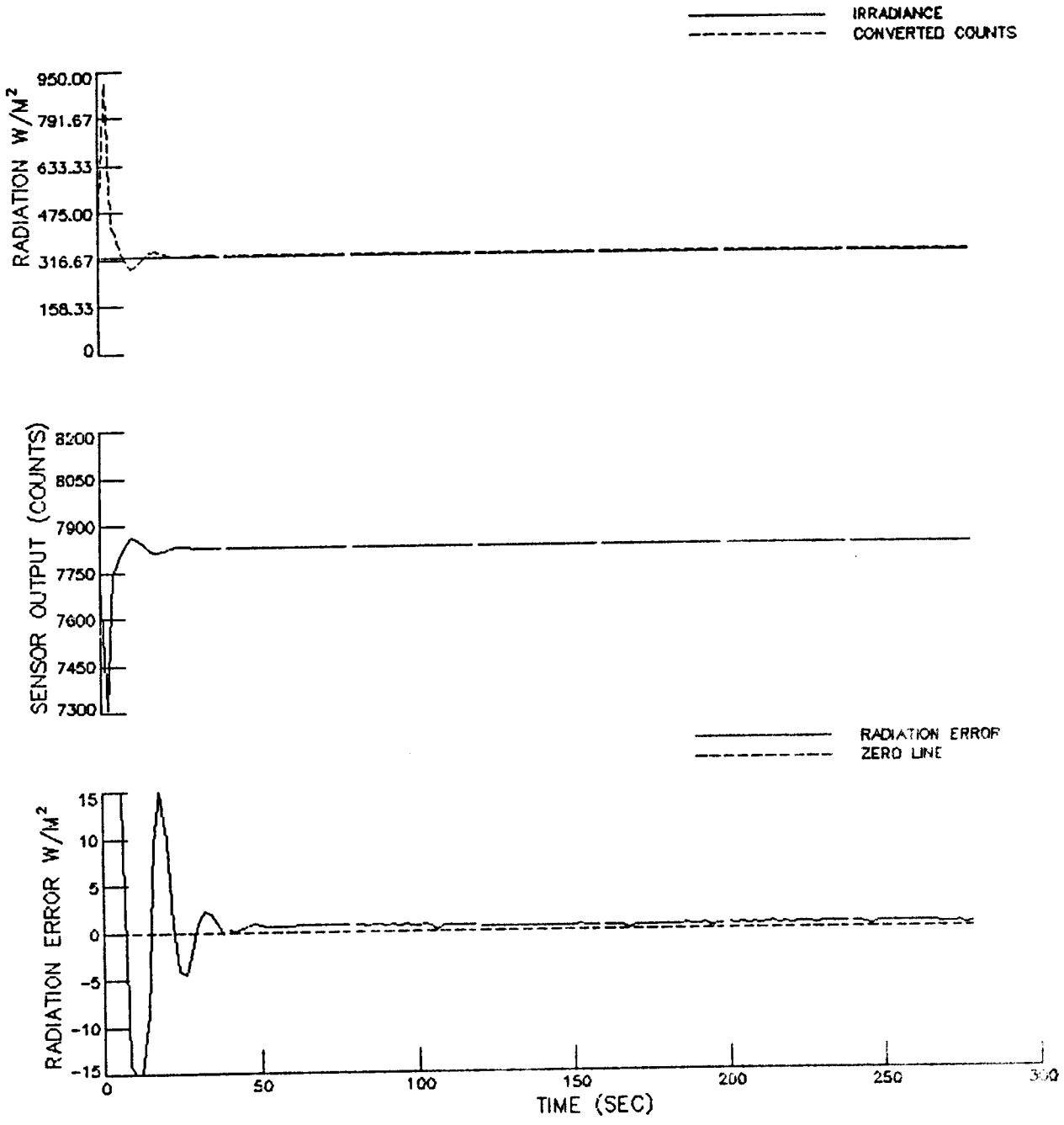

# SENSITIVITY ANALYSIS USING DYNAMIC MODEL

**MFOV TOTAL SIMULATION**

**DOME FILTER SHORT WAVE TRANSMITTANCE CHANGED BY .005 (NOMINAL .946)**

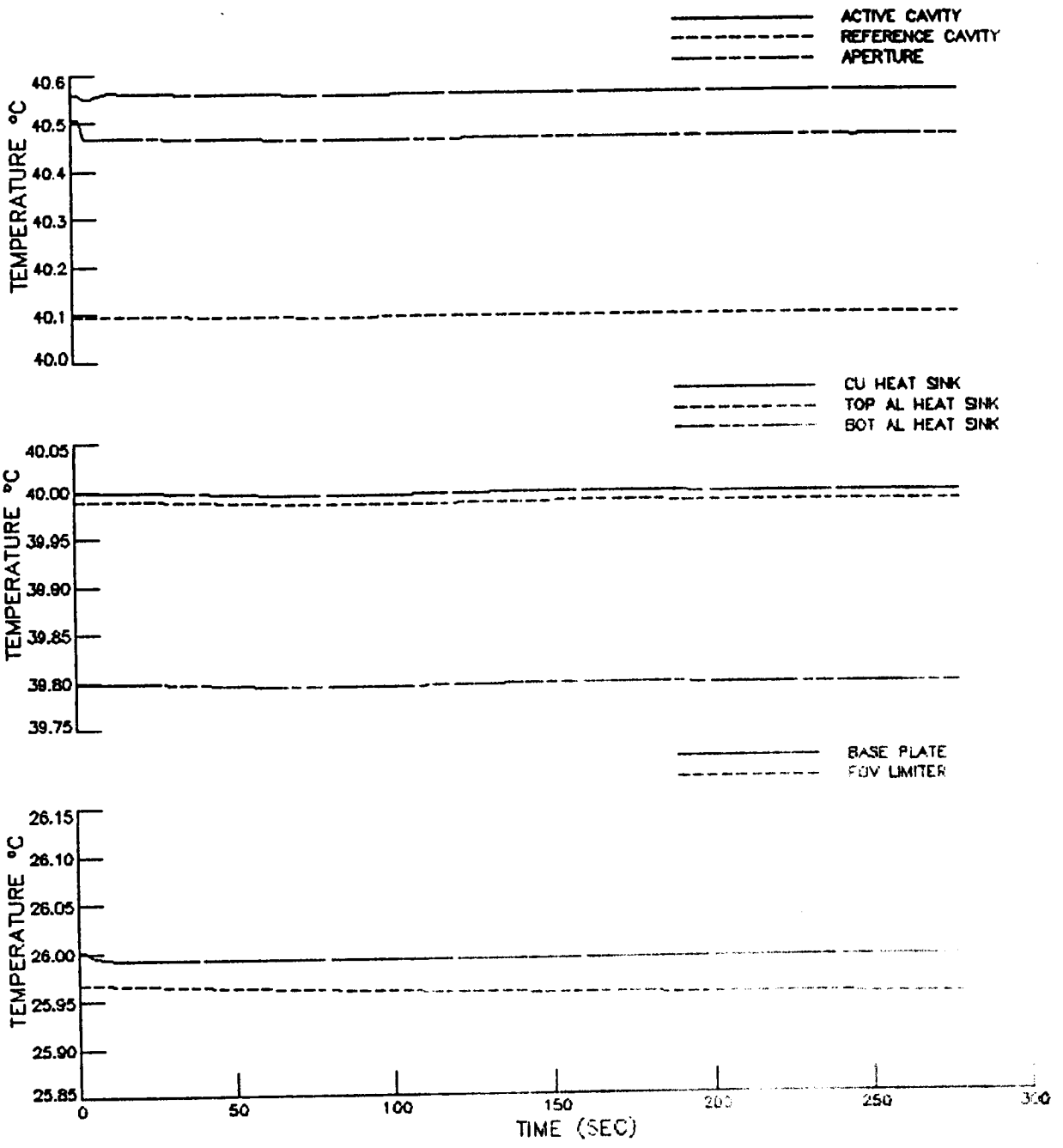

# SENSITIVITY ANALYSIS USING DYNAMIC MODEL

MFOV TOTAL SIMULATION

DOME FILTER SHORT WAVE TRANSMITTANCE CHANGED BY .005 (NOMINAL .946)

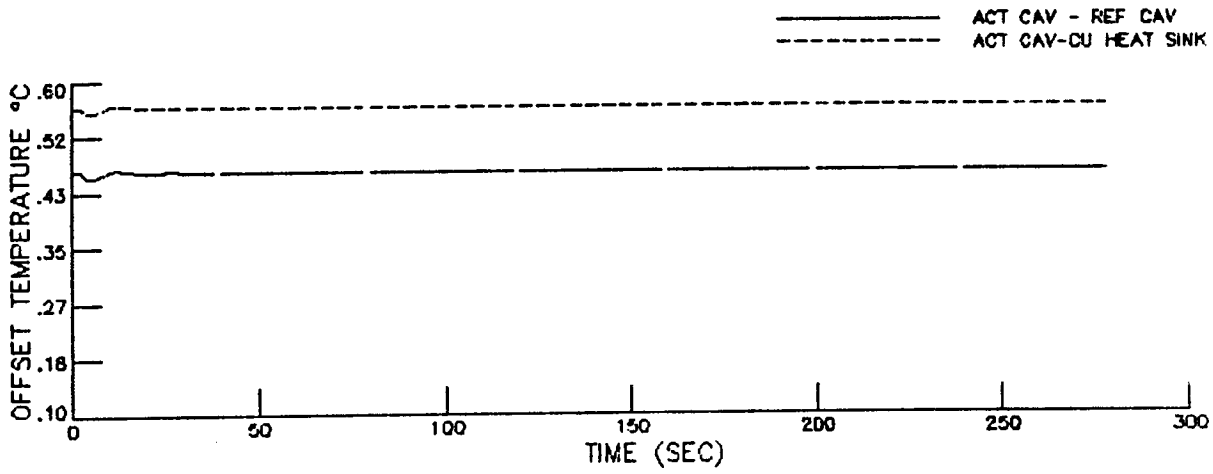

# SENSITIVITY ANALYSIS USING DYNAMIC MODEL

MFOV FILTERED SIMULATION

DOME FILTER SHORT WAVE TRANSMITTANCE CHANGED BY .005 (NOMINAL .946)

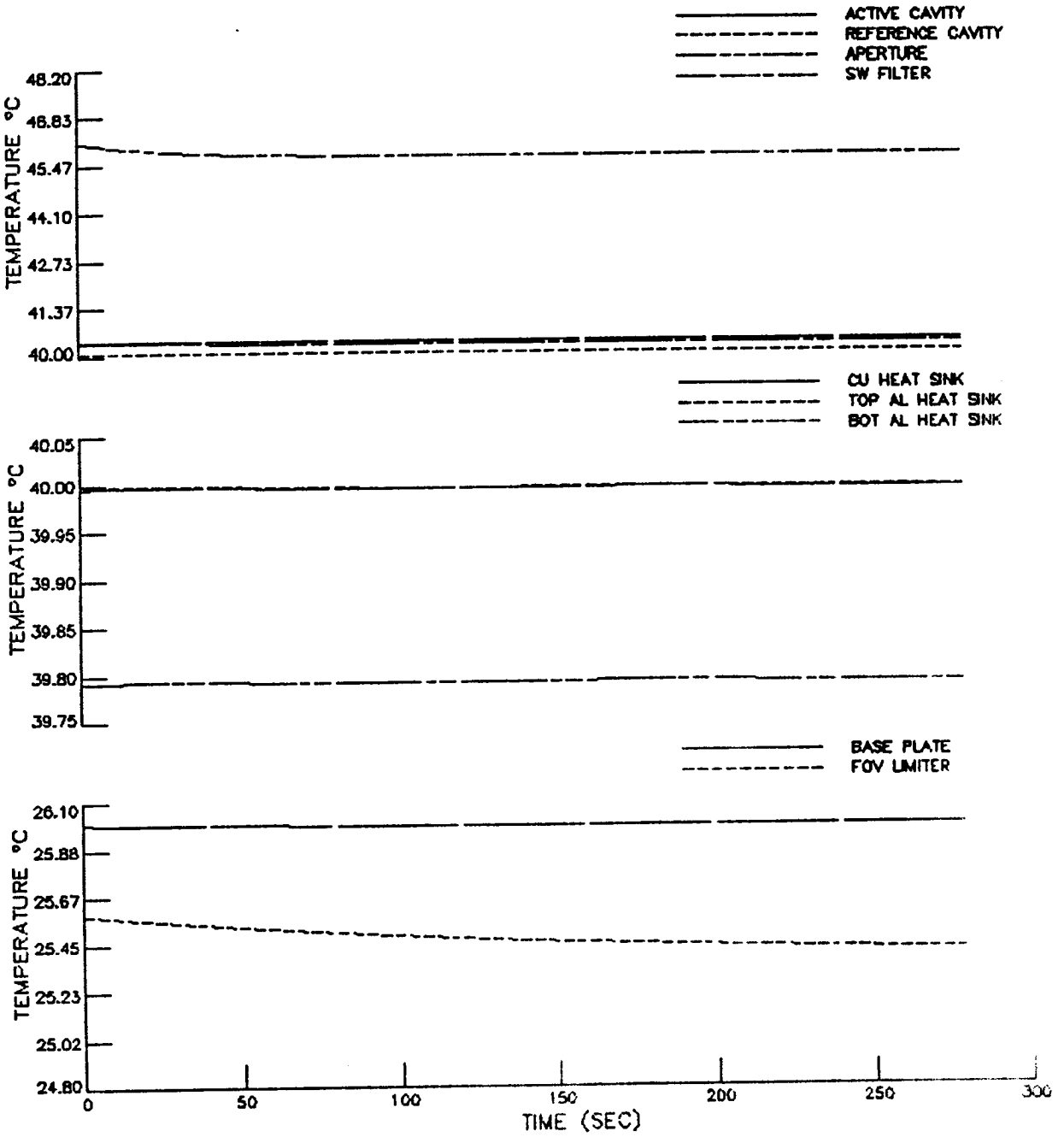

# SENSITIVITY ANALYSIS USING DYNAMIC MODEL

MFOV FILTERED SIMULATION

DOME FILTER SHORT WAVE TRANSMITTANCE CHANGED BY .005 (NOMINAL .946)

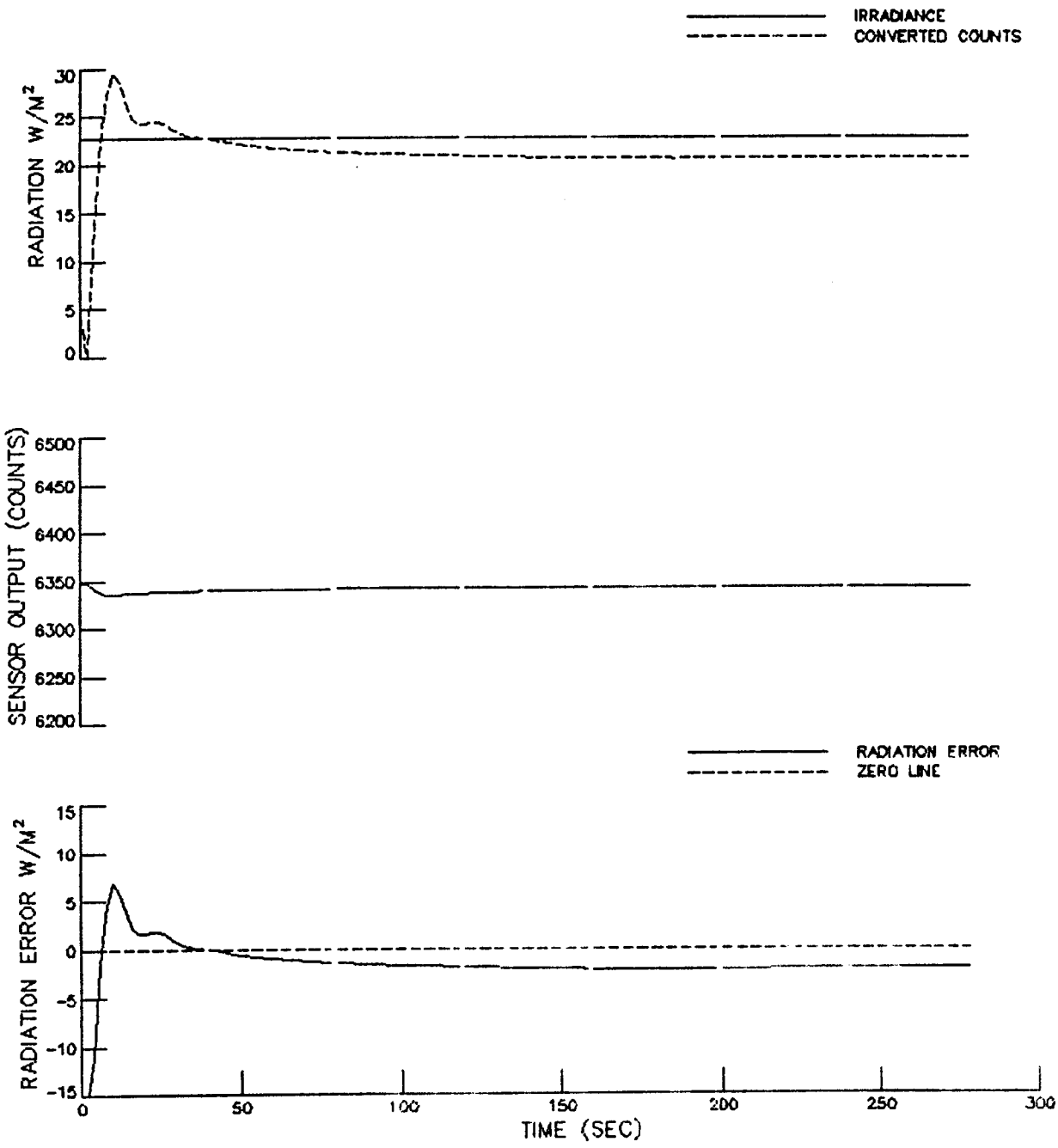

# SENSITIVITY ANALYSIS USING DYNAMIC MODEL

MFOV FILTERED SIMULATION

DOME FILTER SHORT WAVE TRANSMITTANCE CHANGED BY .005 (NOMINAL .946)

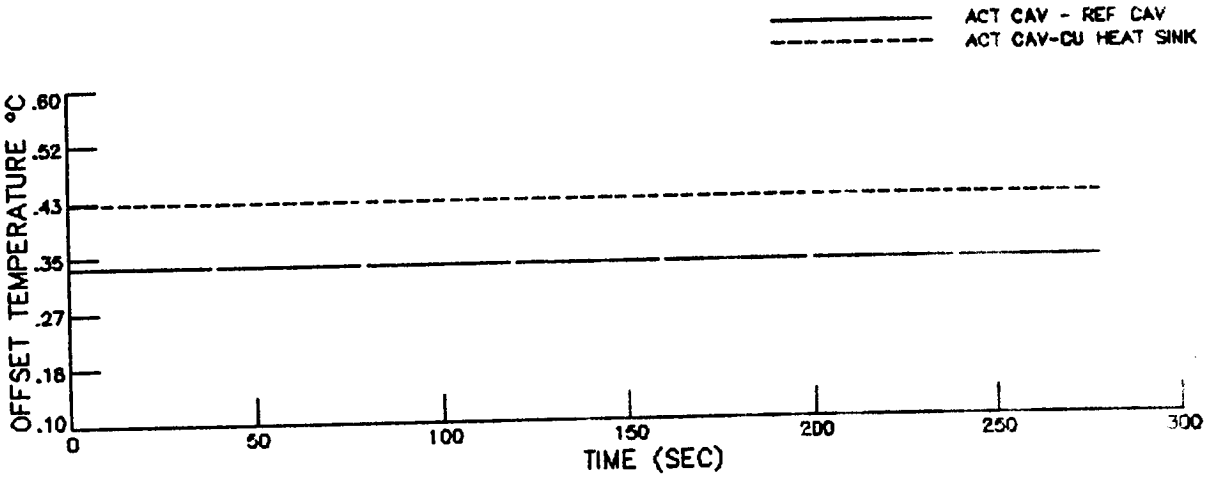

# SENSITIVITY ANALYSIS USING DYNAMIC MODEL

MFOV FILTERED SIMULATION

DOME FILTER LONG WAVE EMISSIVITY CHANGED BY .005 (NOMINAL .69)

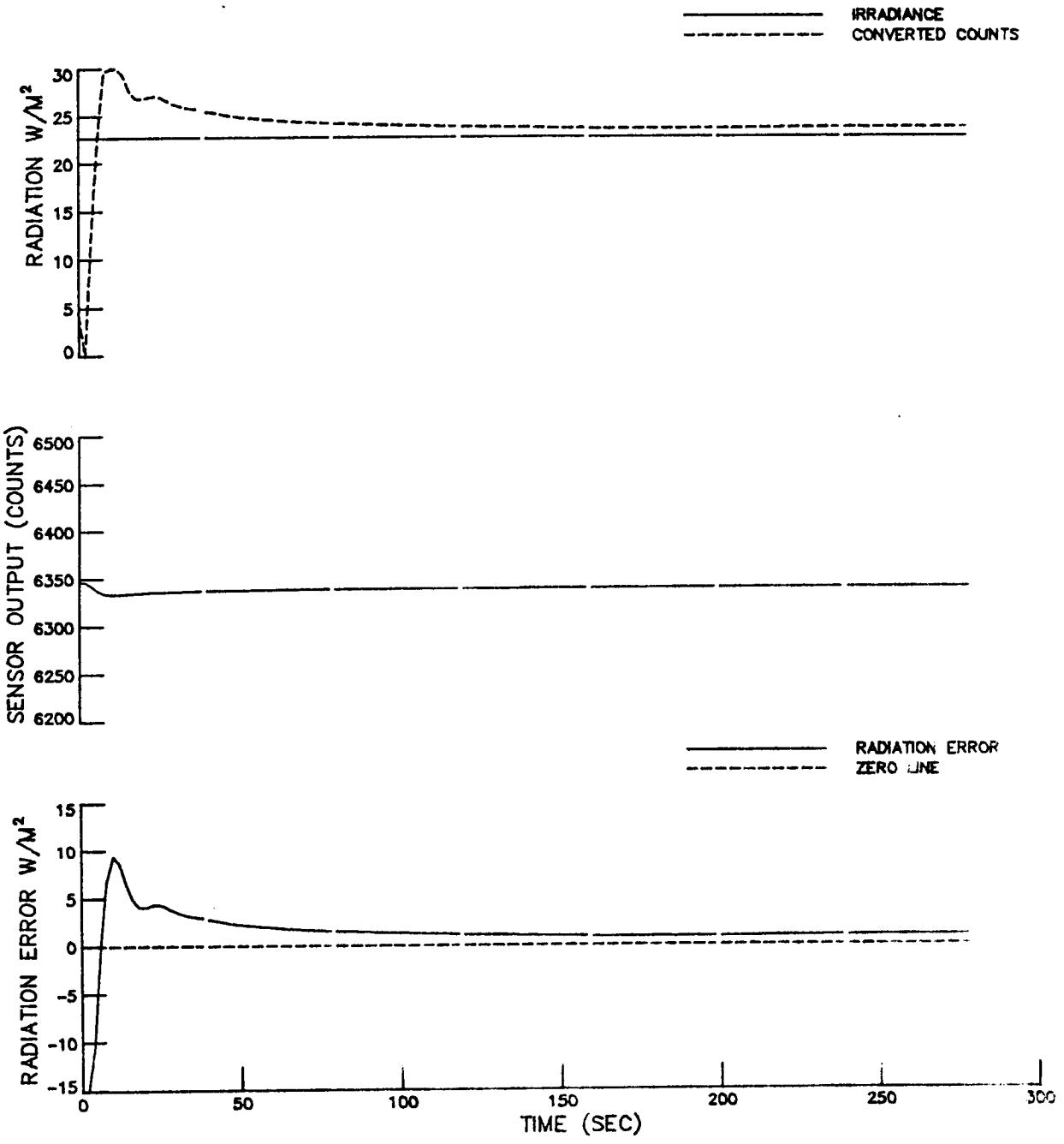

# SENSITIVITY ANALYSIS USING DYNAMIC MODEL

MFOV FILTERED SIMULATION

DOME FILTER LONG WAVE EMISSIVITY CHANGED BY .005 (NOMINAL .69)

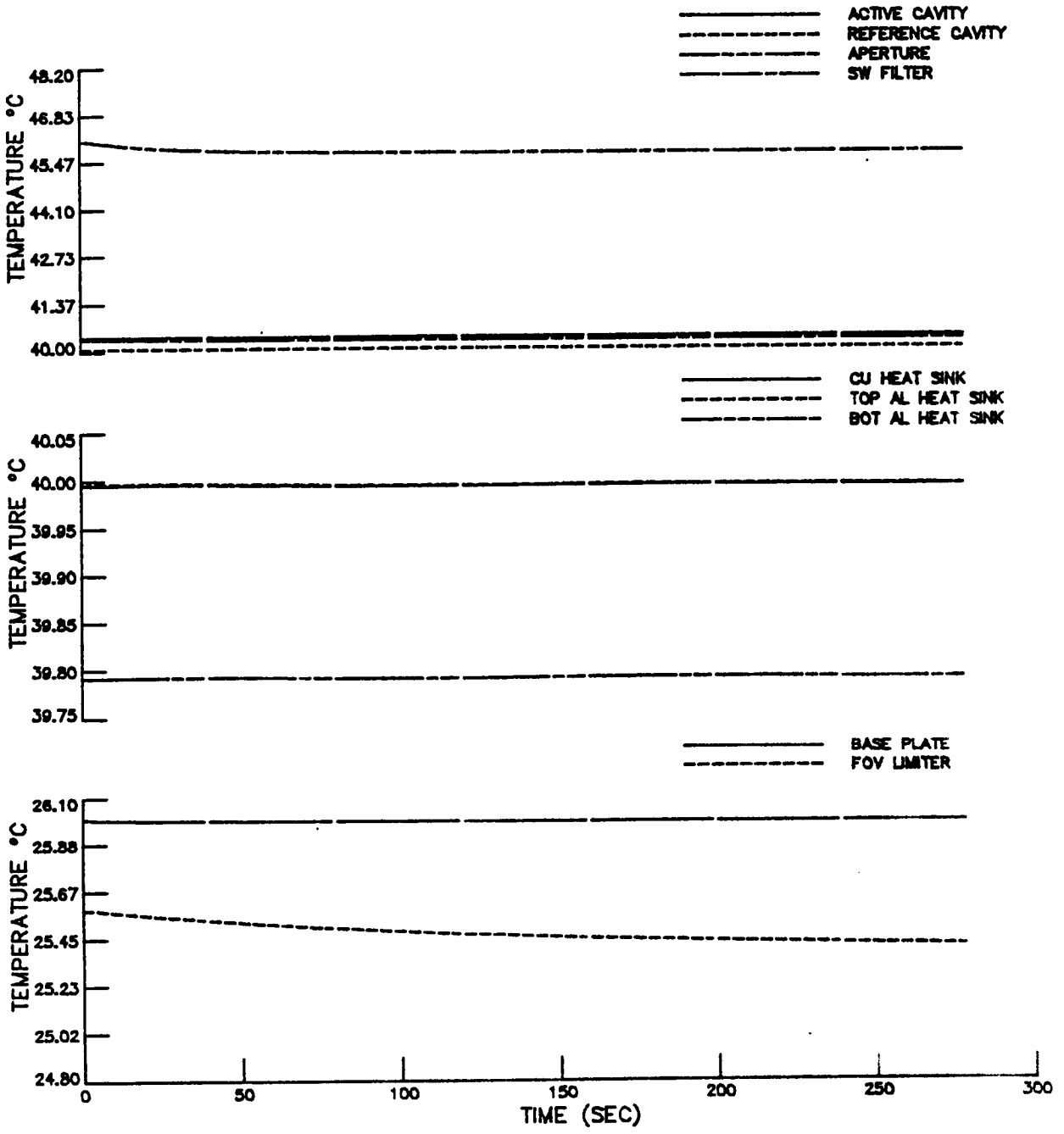

# SENSITIVITY ANALYSIS USING DYNAMIC MODEL

MFOV FILTERED SIMULATION

DOME FILTER LONG WAVE EMISSIVITY CHANGED BY .005 (NOMINAL .69)

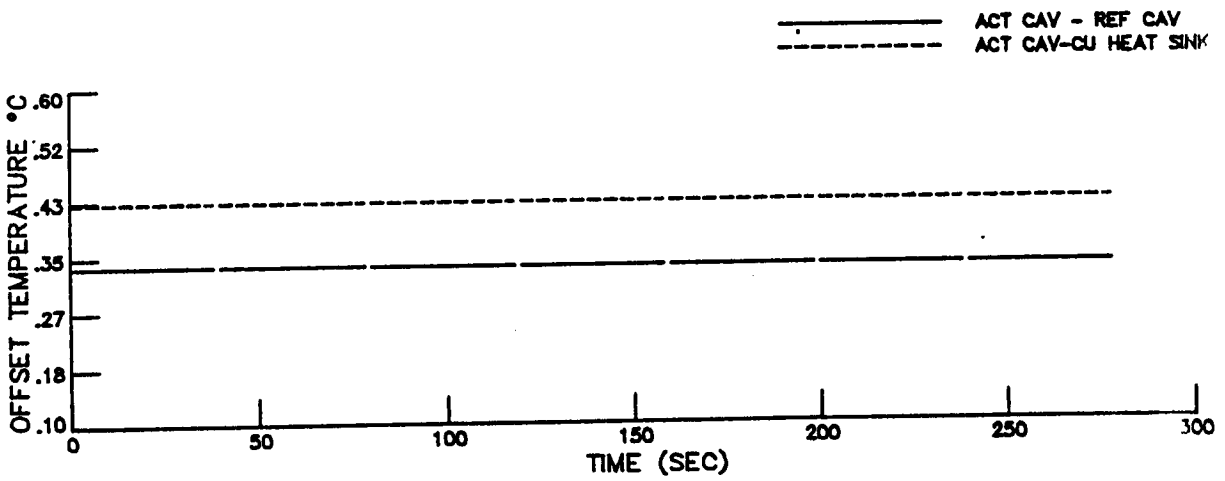

# SENSITIVITY ANALYSIS USING DYNAMIC MODEL

MFOV TOTAL SIMULATION

SENSOR BRIDGE VOLTAGE CHANGED BY .01 v (NOMINAL 10 v)

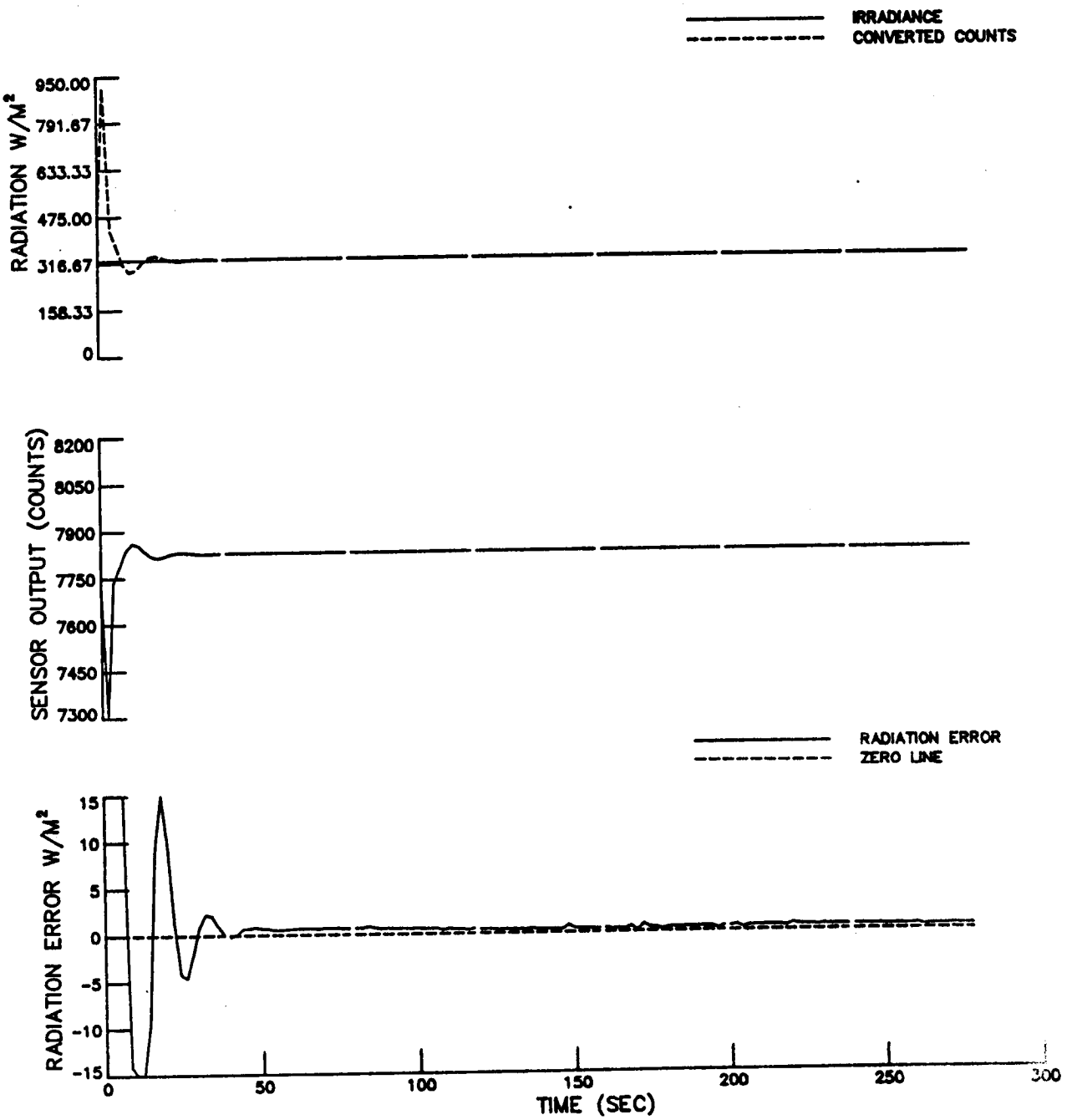

# SENSITIVITY ANALYSIS USING DYNAMIC MODEL

MFOV TOTAL SIMULATION

SENSOR BRIDGE VOLTAGE CHANGED BY .01 v (NOMINAL 10 v)

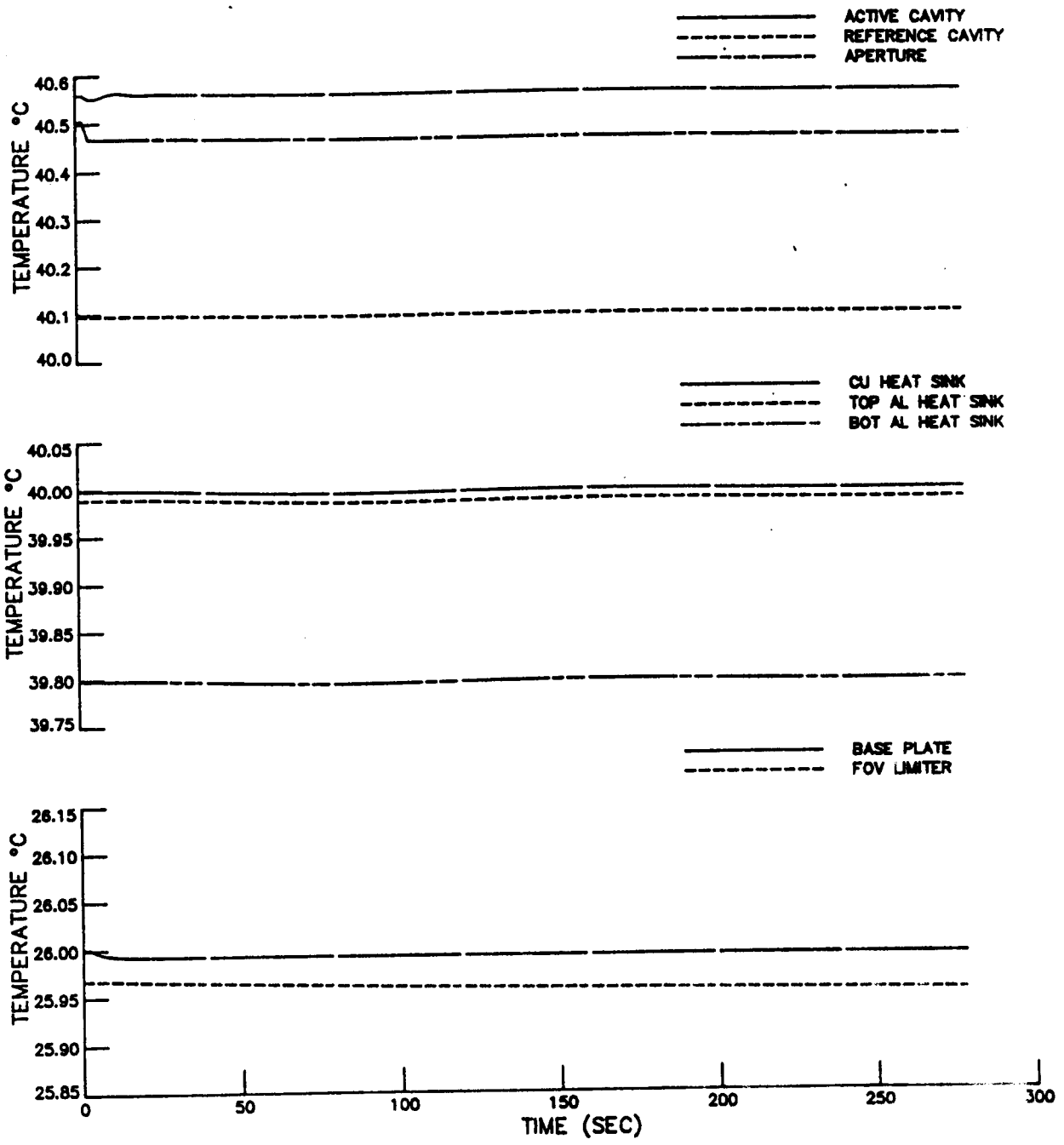

# SENSITIVITY ANALYSIS USING DYNAMIC MODEL

MFOV TOTAL SIMULATION

SENSOR BRIDGE VOLTAGE CHANGED BY .01 v (NOMINAL 10 v)

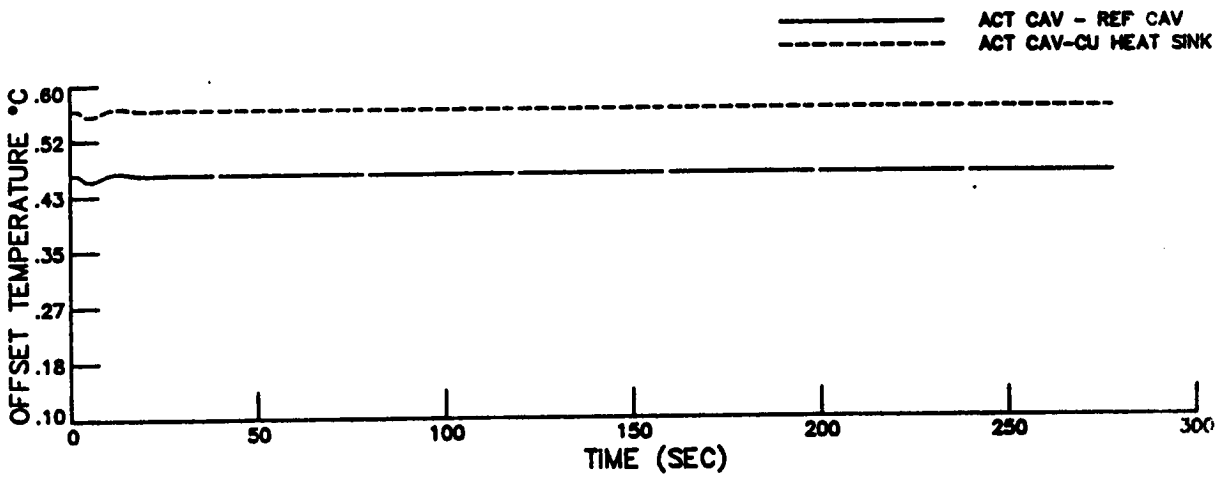

# SENSITIVITY ANALYSIS USING DYNAMIC MODEL

**MFOV TOTAL SIMULATION**

**ACTIVE CAVITY HEATER RESISTANCE CHANGED BY .1 Ω (NOMINAL 1492.3 Ω)**

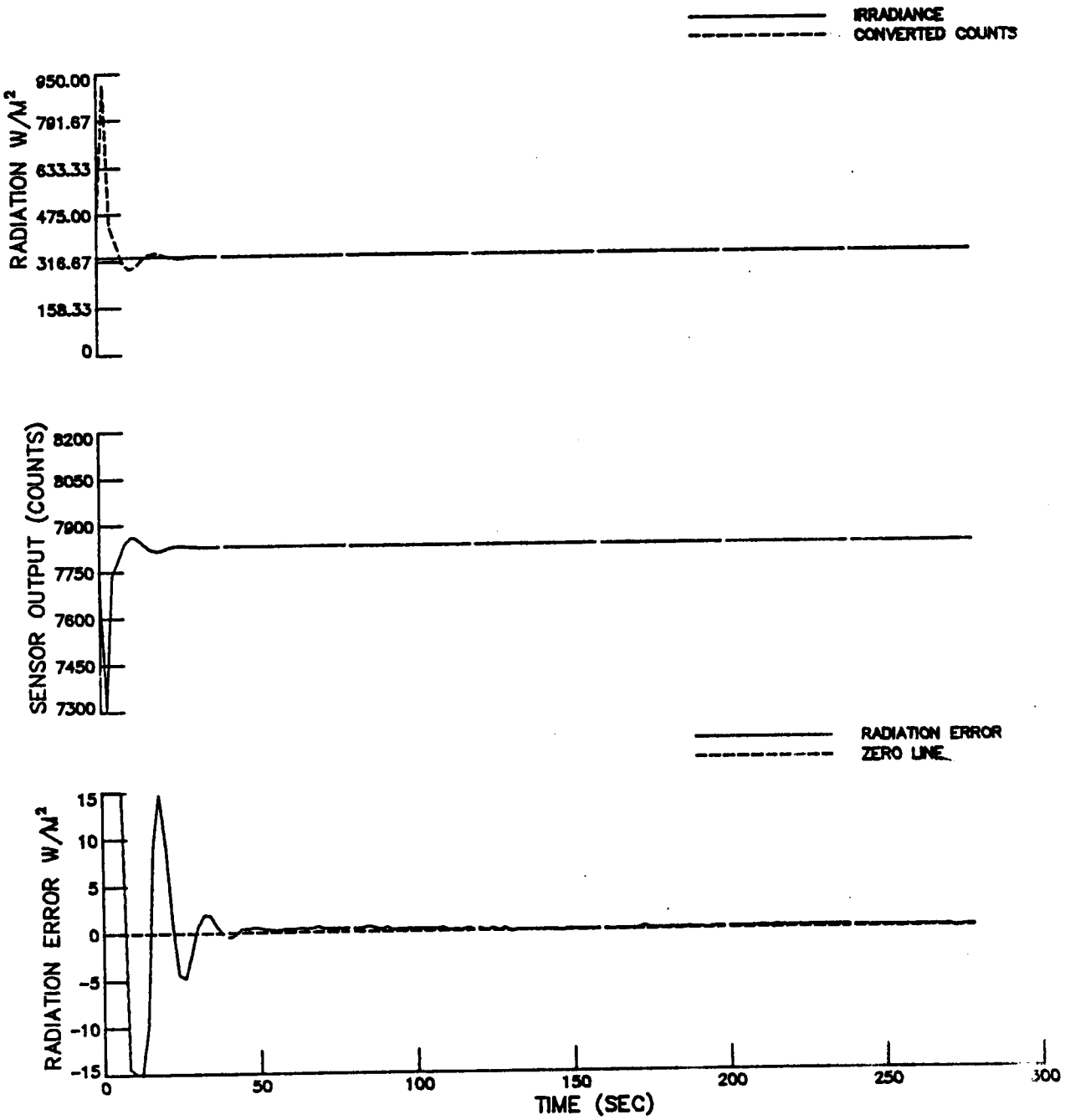

# SENSITIVITY ANALYSIS USING DYNAMIC MODEL

MFOV TOTAL SIMULATION

ACTIVE CAVITY HEATER RESISTANCE CHANGED BY .1 Ω (NOMINAL 1492.3 Ω)

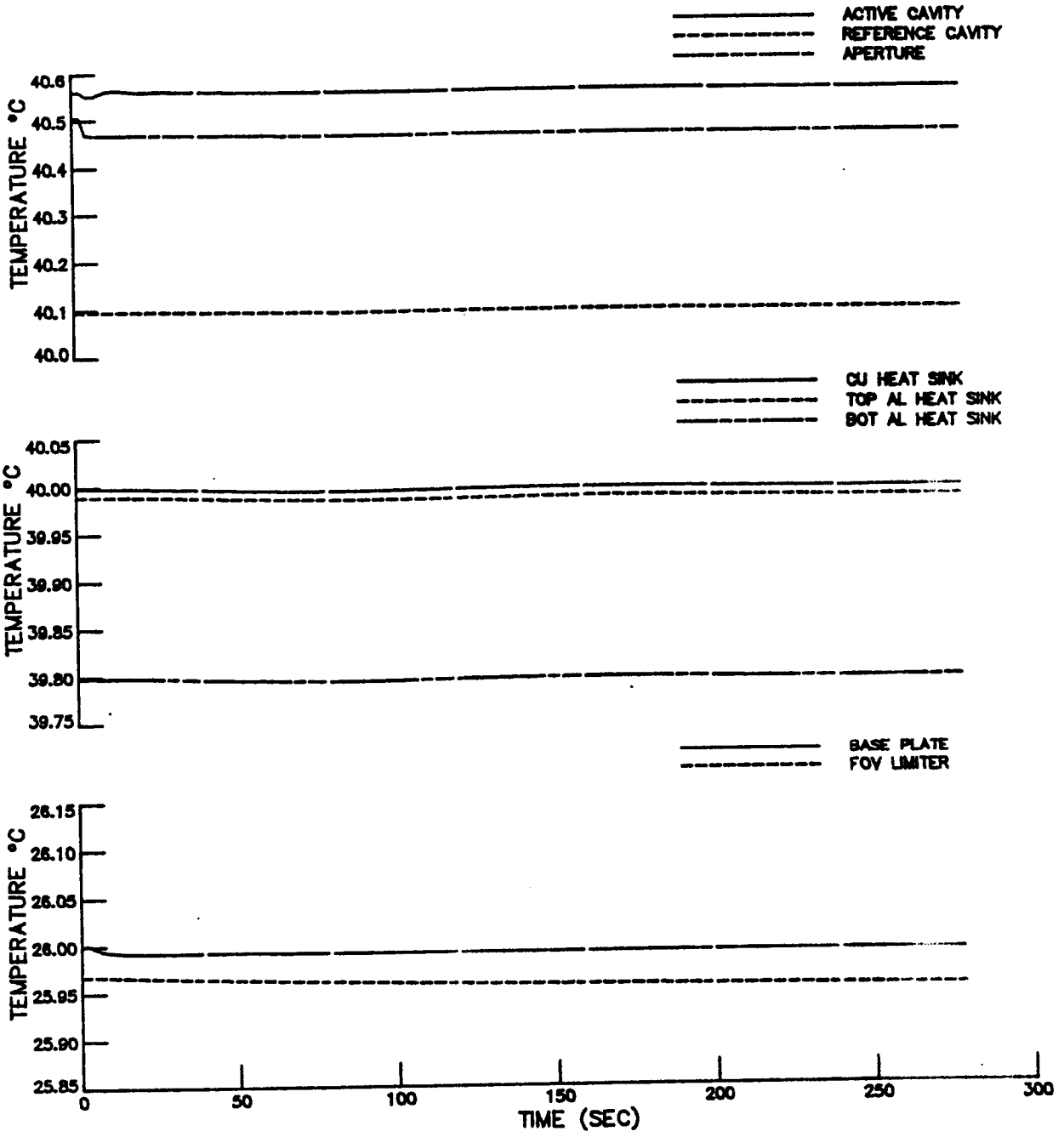

# SENSITIVITY ANALYSIS USING DYNAMIC MODEL

MFOV TOTAL SIMULATION

ACTIVE CAVITY HEATER RESISTANCE CHANGED BY .1 Ω (NOMINAL 1492.3 Ω)

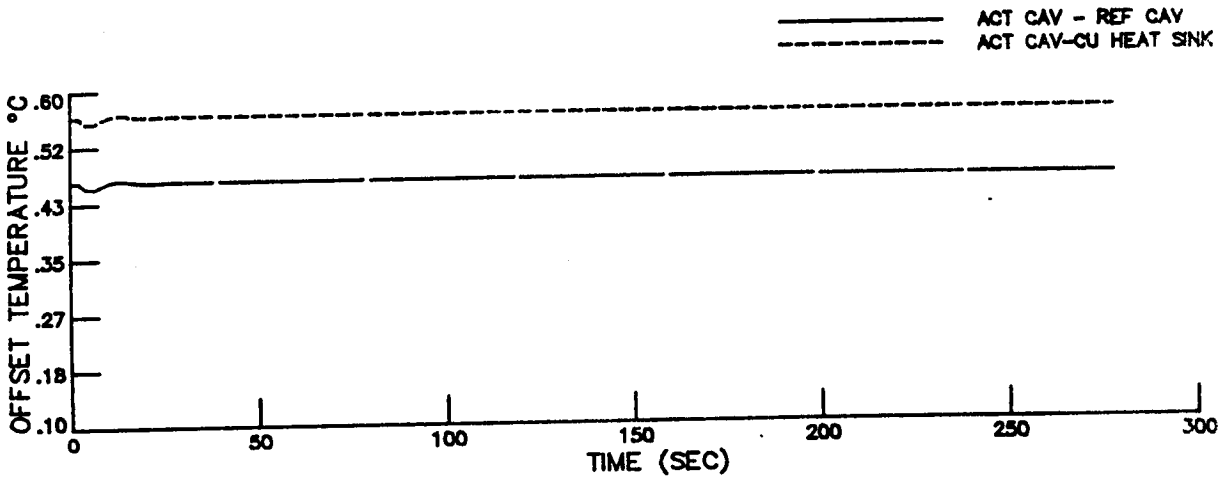

# SENSITIVITY ANALYSIS USING DYNAMIC MODEL

MFOV TOTAL SIMULATION

ACTIVE CAVITY SENSOR WIRE RESISTANCE CHANGED BY .01 Ω (NOMINAL 2319.1 Ω @ 40°C)

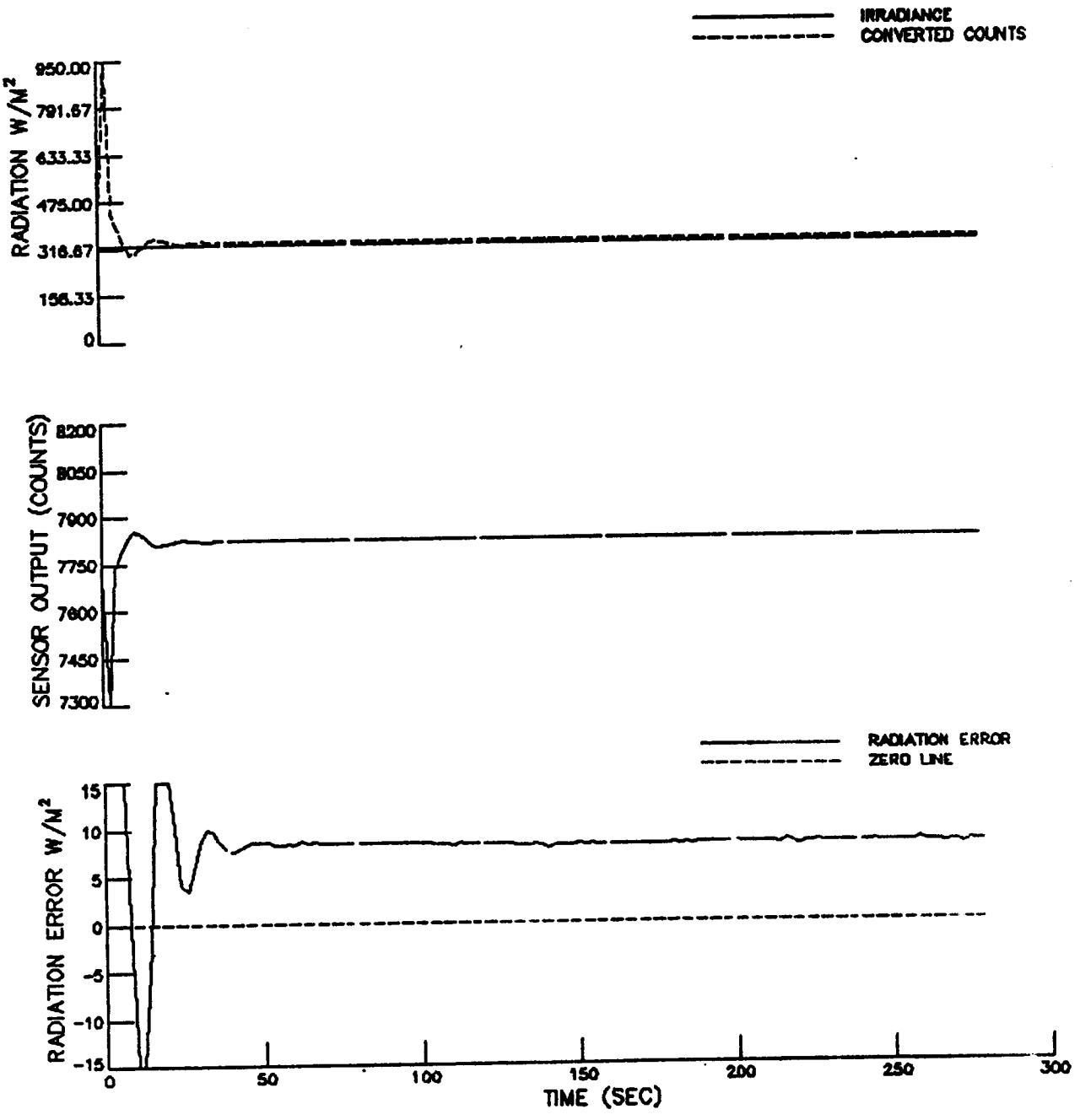

# SENSITIVITY ANALYSIS USING DYNAMIC MODEL

MFOV TOTAL SIMULATION

ACTIVE CAVITY SENSOR WIRE RESISTANCE CHANGED BY .01 Ω (NOMINAL 2319.1 Ω @ 40°C)

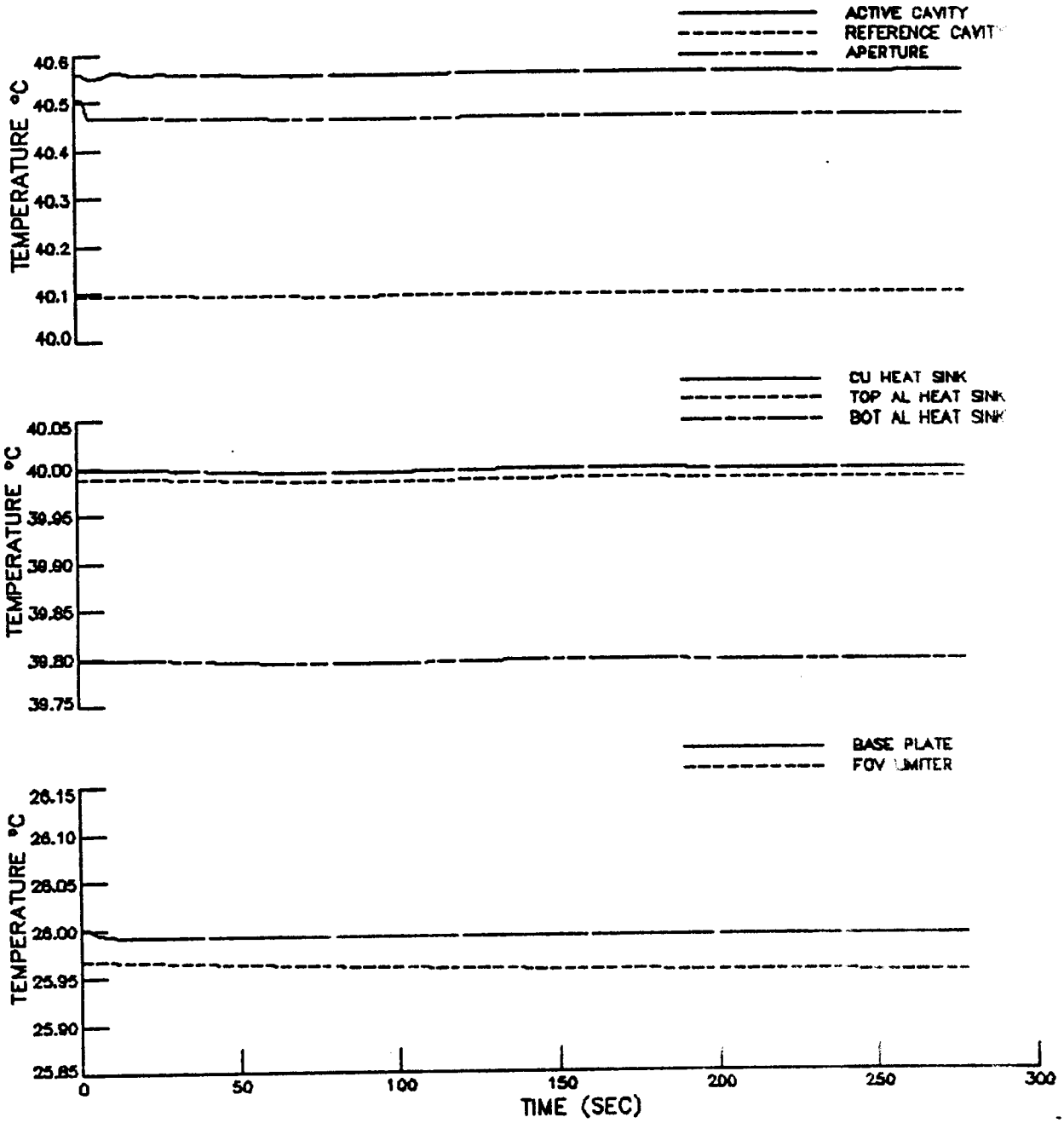

# SENSITIVITY ANALYSIS USING DYNAMIC MODEL

MFOV TOTAL SIMULATION

ACTIVE CAVITY SENSOR WIRE RESISTANCE CHANGED BY .01 Ω (NOMINAL 2319.1 Ω @ 40°C)

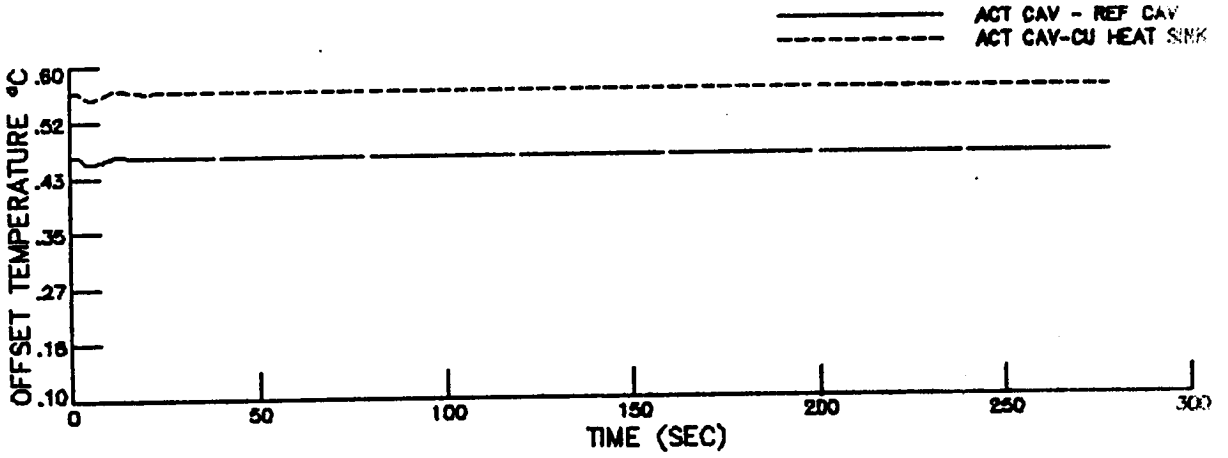

# SENSITIVITY ANALYSIS USING DYNAMIC MODEL

**MFOV TOTAL SIMULATION**

**REFERENCE CAVITY SENSOR WIRE RESISTANCE CHANGED BY .01 Ω (NOMINAL 2327.1 Ω @ 40°C)**

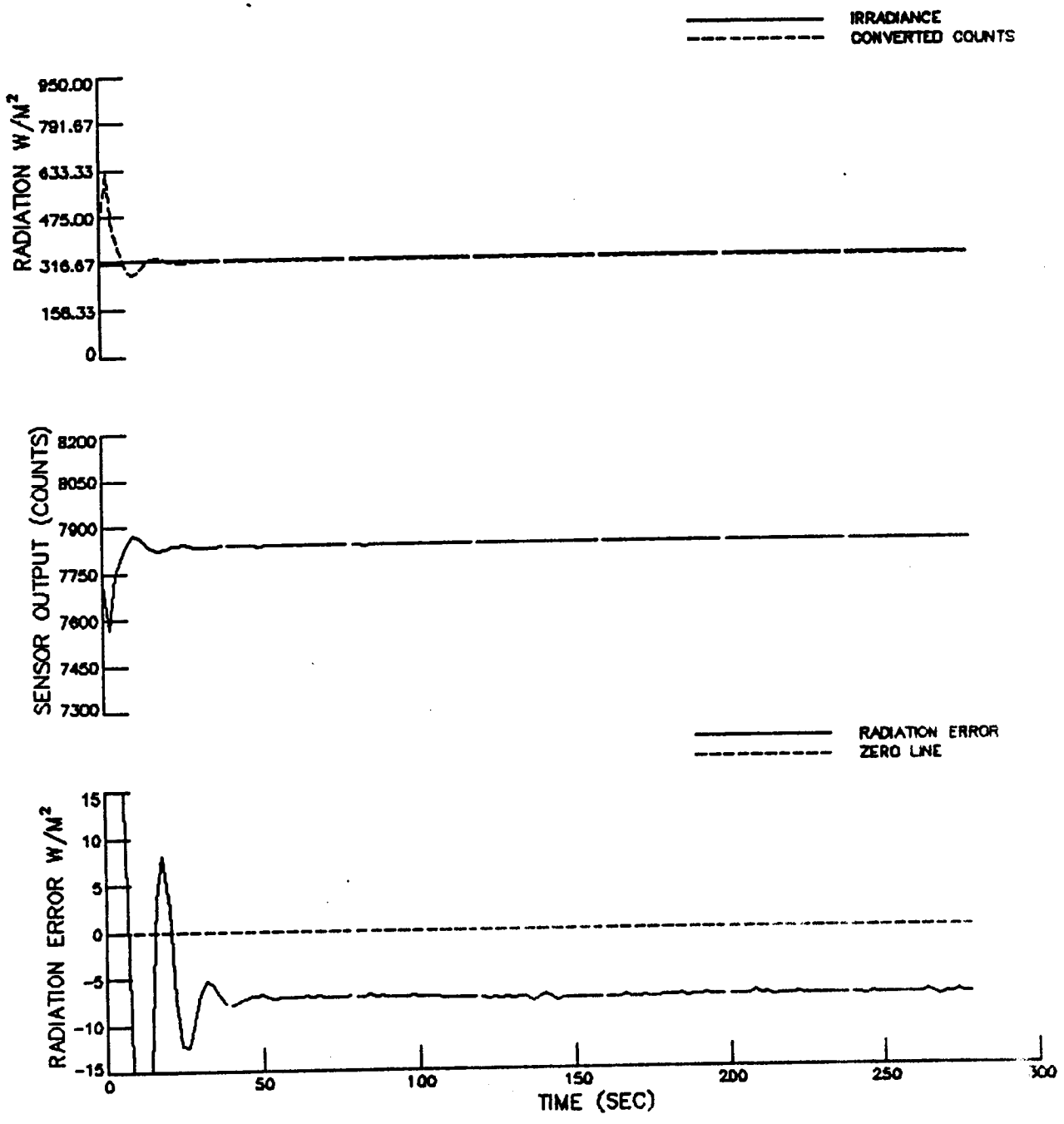

# SENSITIVITY ANALYSIS USING DYNAMIC MODEL

MFOV TOTAL SIMULATION

REFERENCE CAVITY SENSOR WIRE RESISTANCE CHANGED BY .01 Ω (NOMINAL 2327.1 Ω @ 40°C)

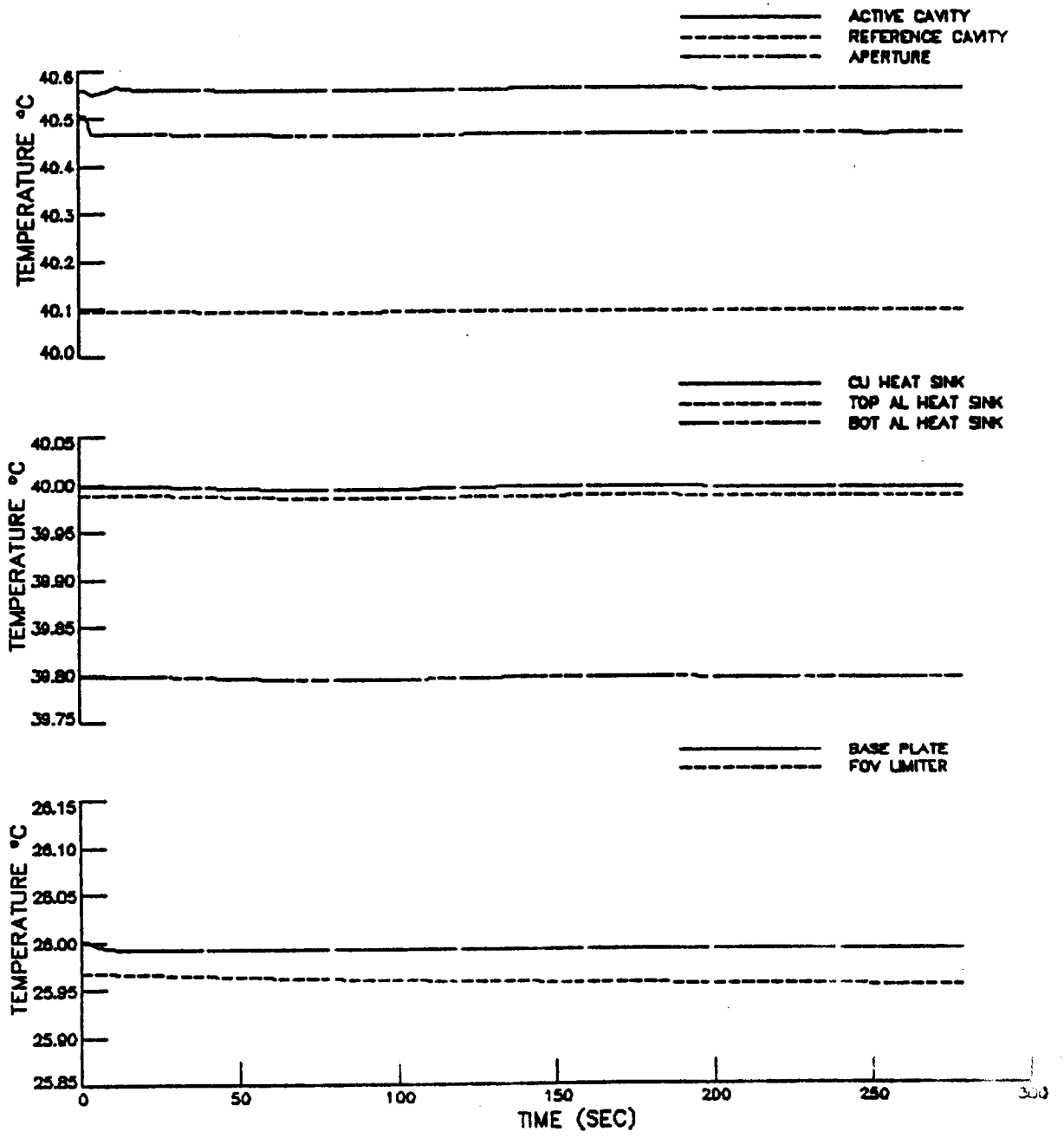

# SENSITIVITY ANALYSIS USING DYNAMIC MODEL

**MFOV TOTAL SIMULATION**

**REFERENCE CAVITY SENSOR WIRE RESISTANCE CHANGED BY .01 Ω (NOMINAL 2327.1 Ω @ 40°C)**

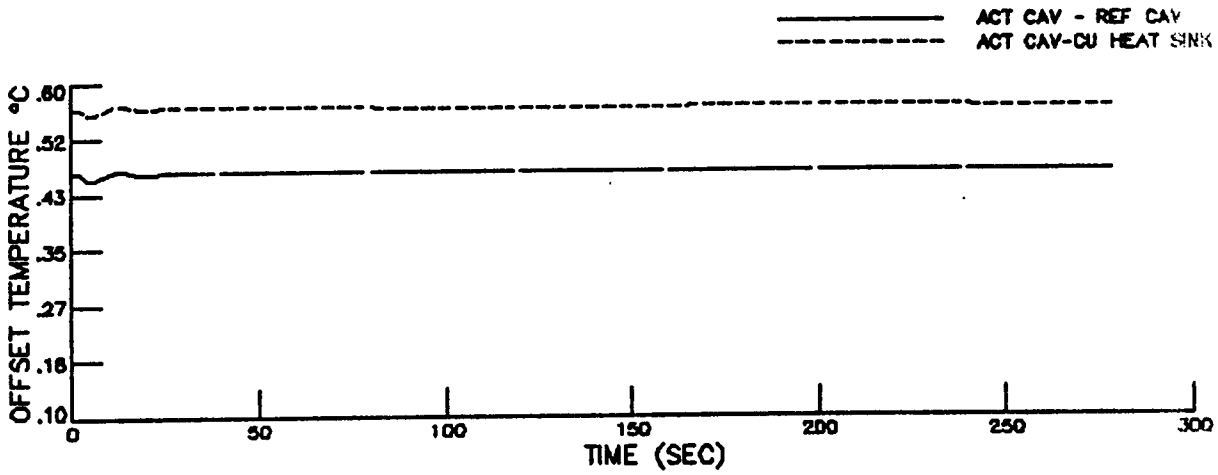

# SENSITIVITY ANALYSIS USING DYNAMIC MODEL

MFOV TOTAL SIMULATION

SENSOR BRIDGE RESISTANCE CHANGED BY .01 Ω (NOMINAL 2210 Ω)

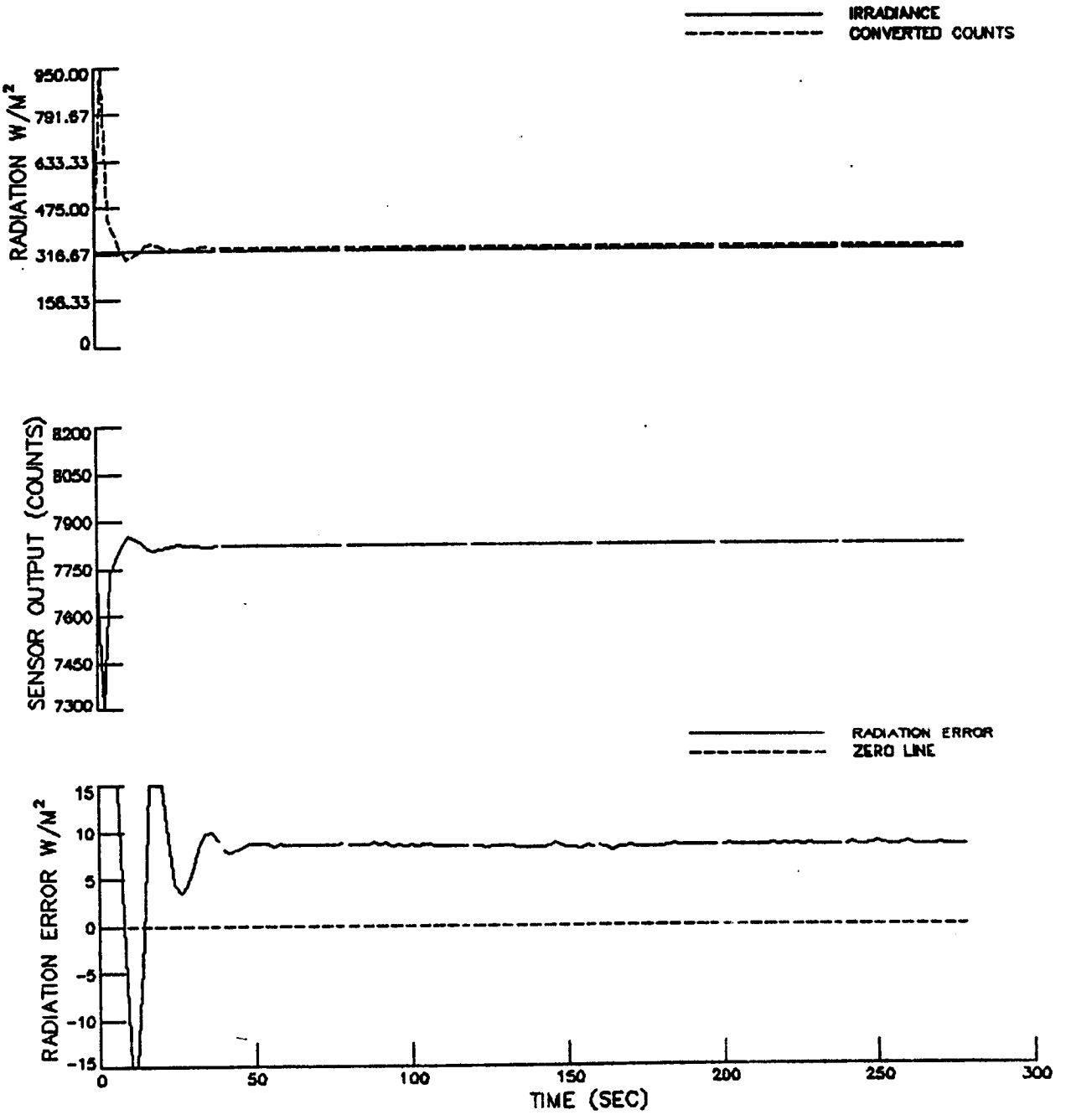

# SENSITIVITY ANALYSIS USING DYNAMIC MODEL

MFOV TOTAL SIMULATION

SENSOR BRIDGE RESISTANCE CHANGED BY .01 Ω (NOMINAL 2210 Ω)

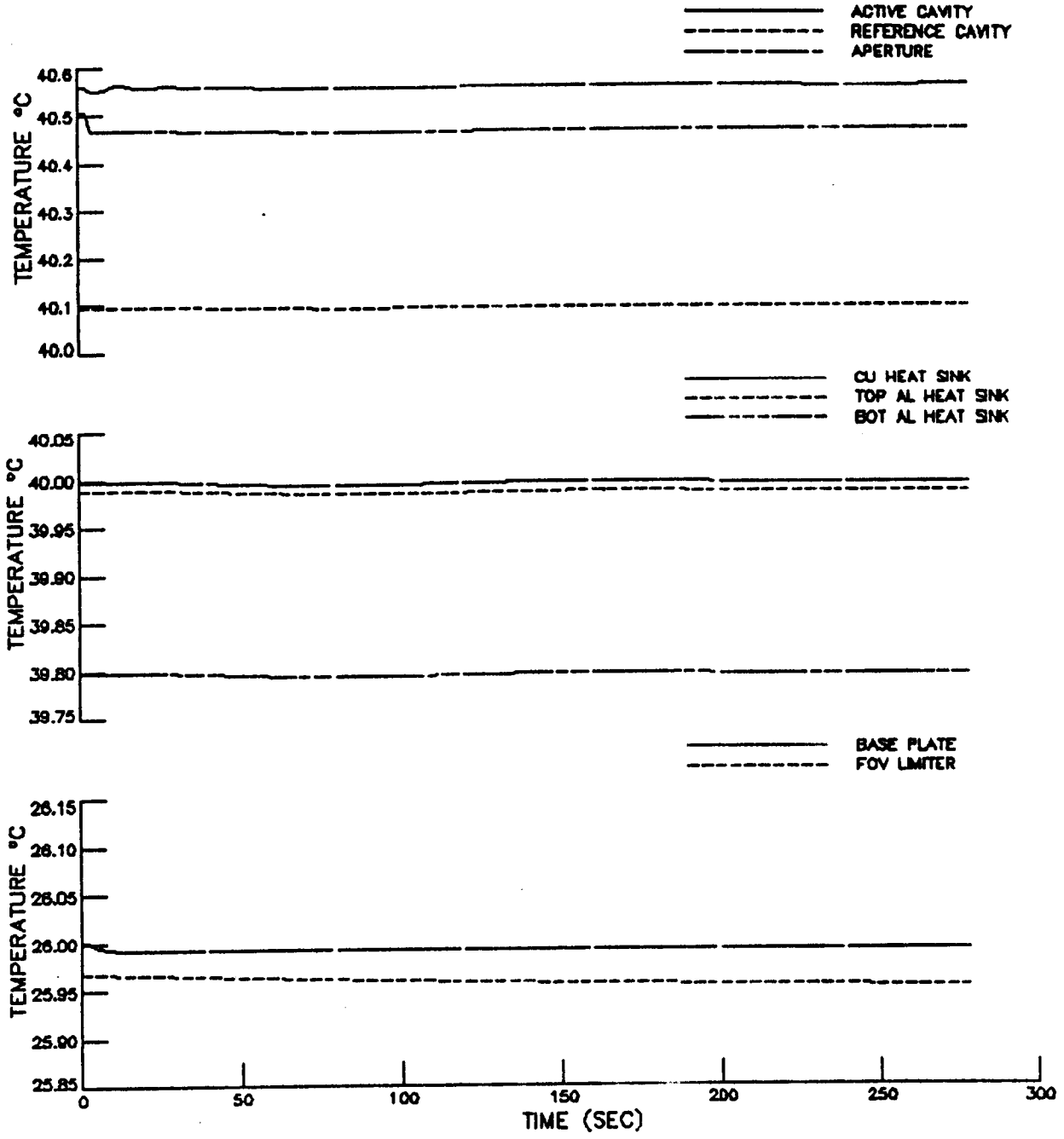

# SENSITIVITY ANALYSIS USING DYNAMIC MODEL

MFOV TOTAL SIMULATION

SENSOR BRIDGE RESISTANCE CHANGED BY .01 Ω (NOMINAL 2210 Ω)

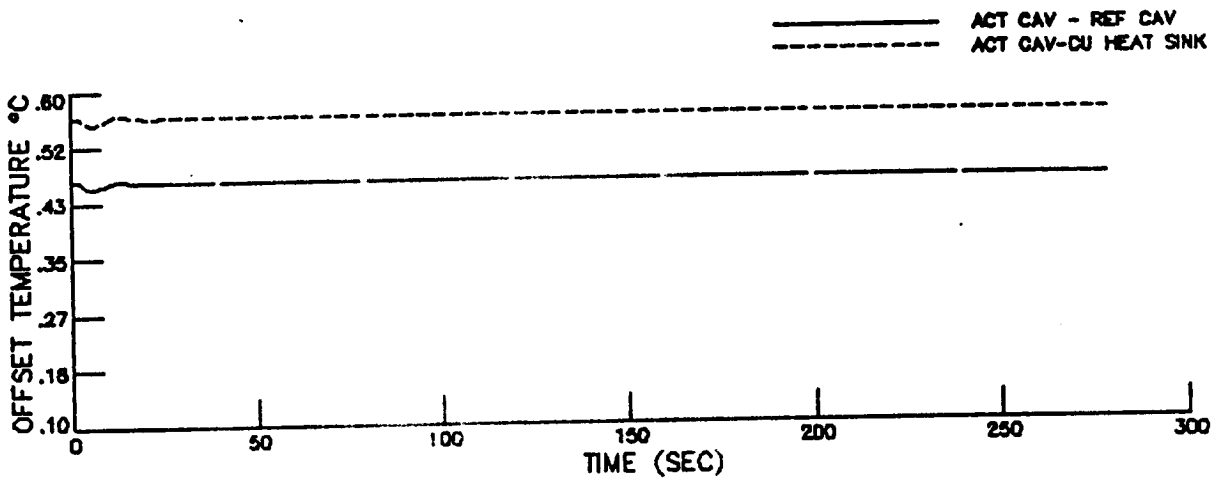

# SENSITIVITY ANALYSIS USING DYNAMIC MODEL

MFOV TOTAL SIMULATION

ACTIVE CAVITY SENSOR WIRE RESISTANCE CHANGED BY .5 Ω (NOMINAL 2319.1 Ω)

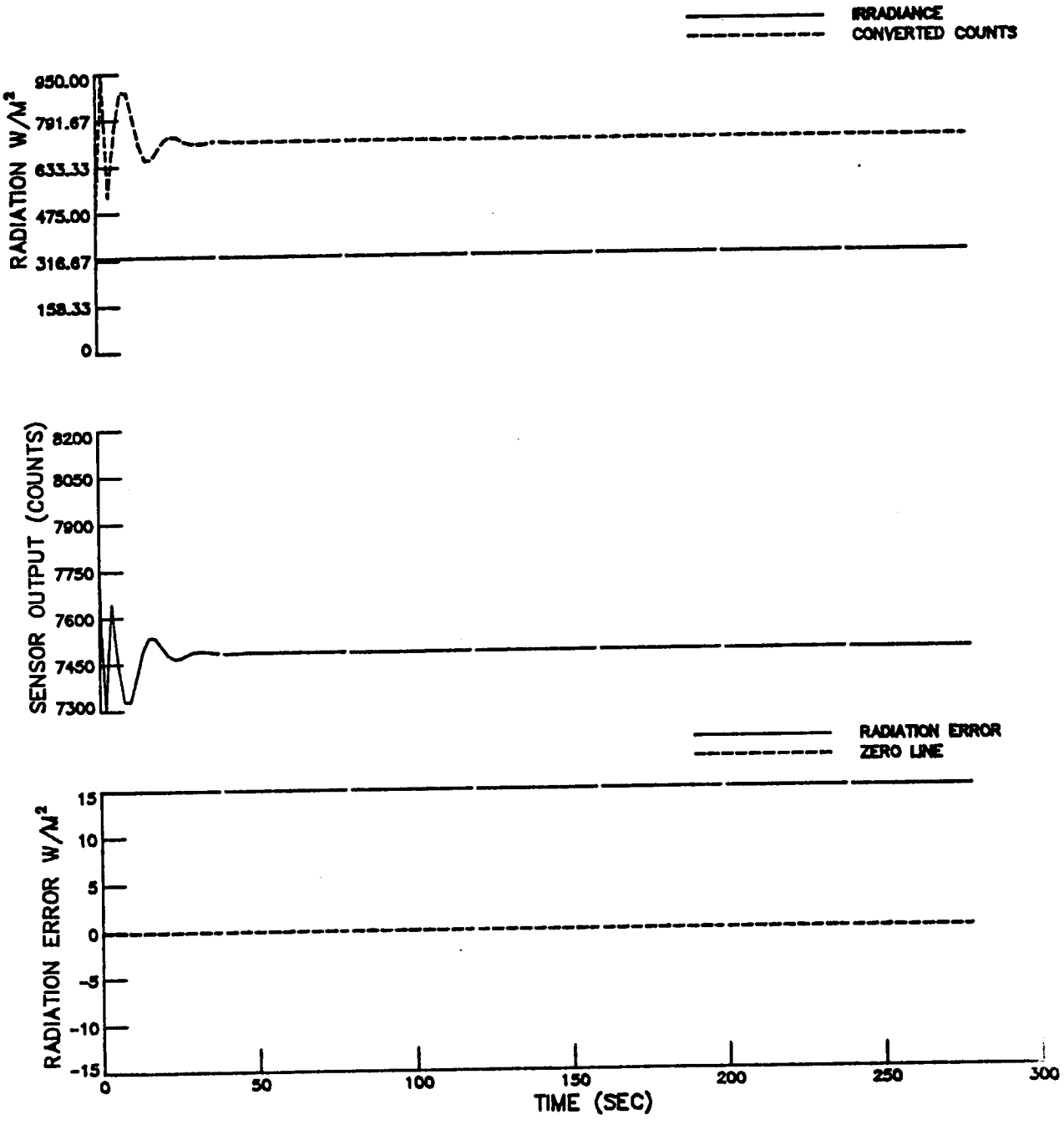

# SENSITIVITY ANALYSIS USING DYNAMIC MODEL

MFOV TOTAL SIMULATION

ACTIVE CAVITY SENSOR WIRE RESISTANCE CHANGED BY .5 Ω (NOMINAL 2319.1 Ω)

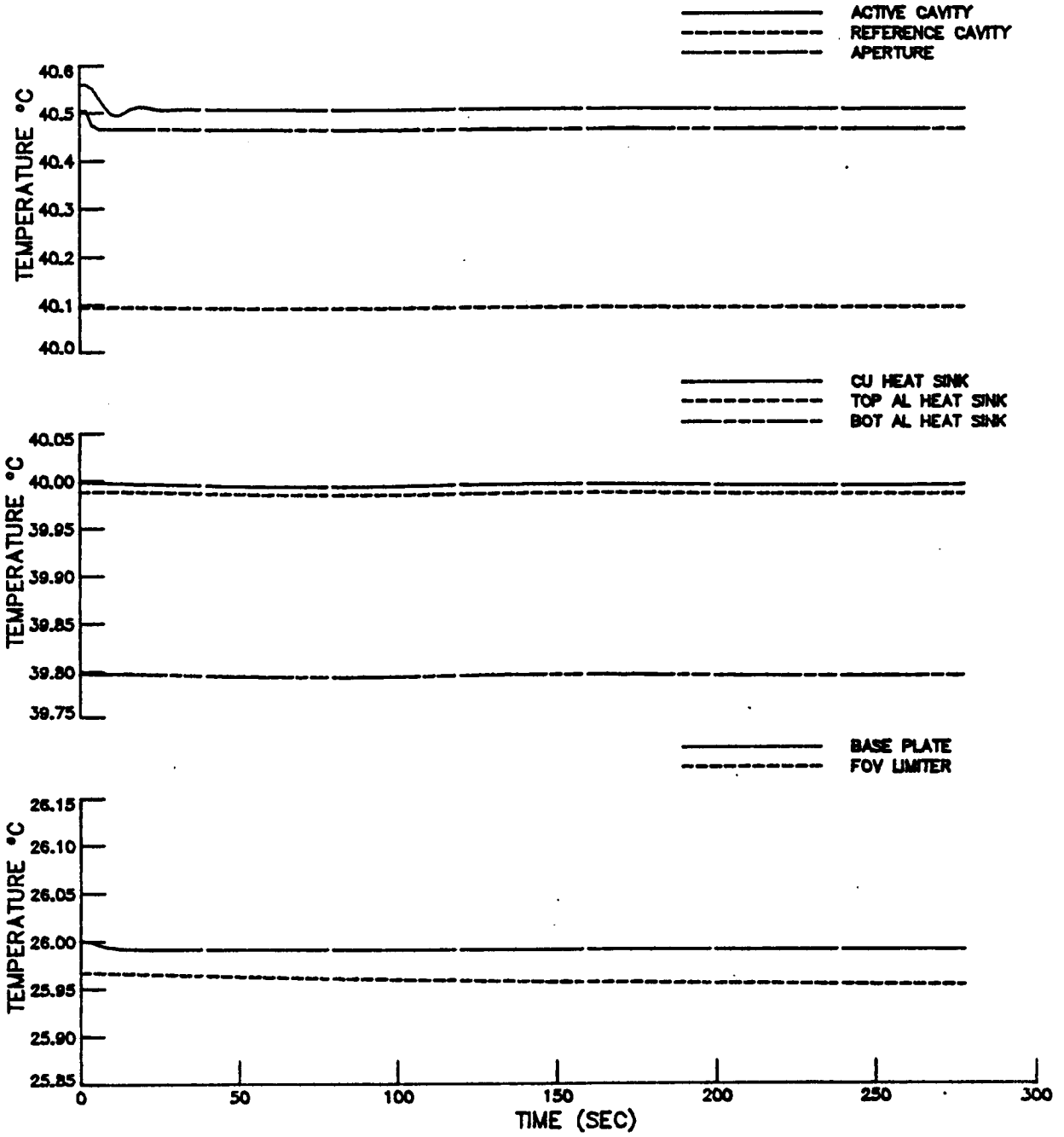

# SENSITIVITY ANALYSIS USING DYNAMIC MODEL

MFOV TOTAL SIMULATION

ACTIVE CAVITY SENSOR WIRE RESISTANCE CHANGED BY .5 Ω (NOMINAL 2319.1 Ω)

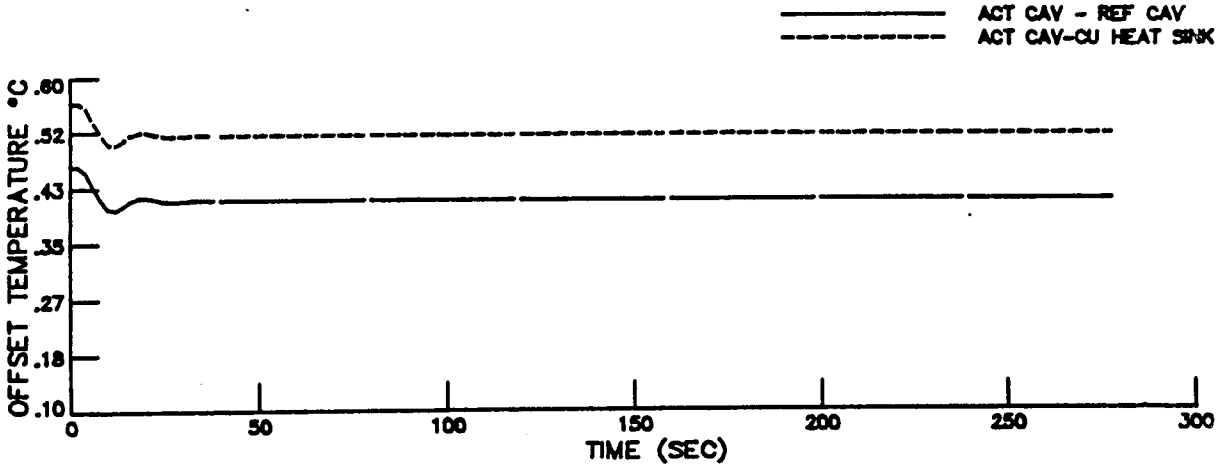

# SENSITIVITY ANALYSIS USING DYNAMIC MODEL

MFOV TOTAL SIMULATION

REDUCED CONDUCTANCE BETWEEN NODES 1 AND 2

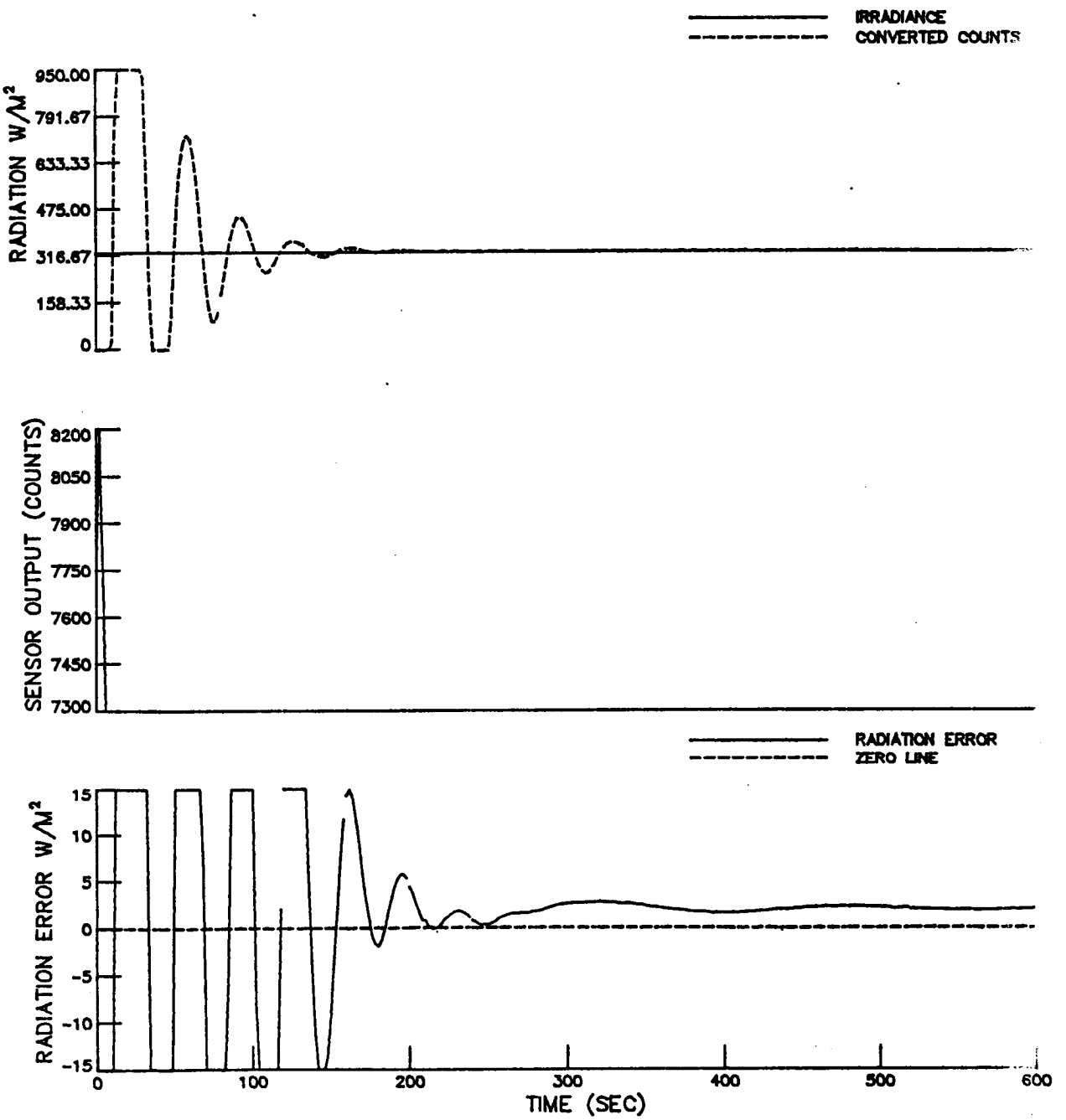

# SENSITIVITY ANALYSIS USING DYNAMIC MODEL

MFOV TOTAL SIMULATION

REDUCED CONDUCTANCE BETWEEN NODES 1 AND 2

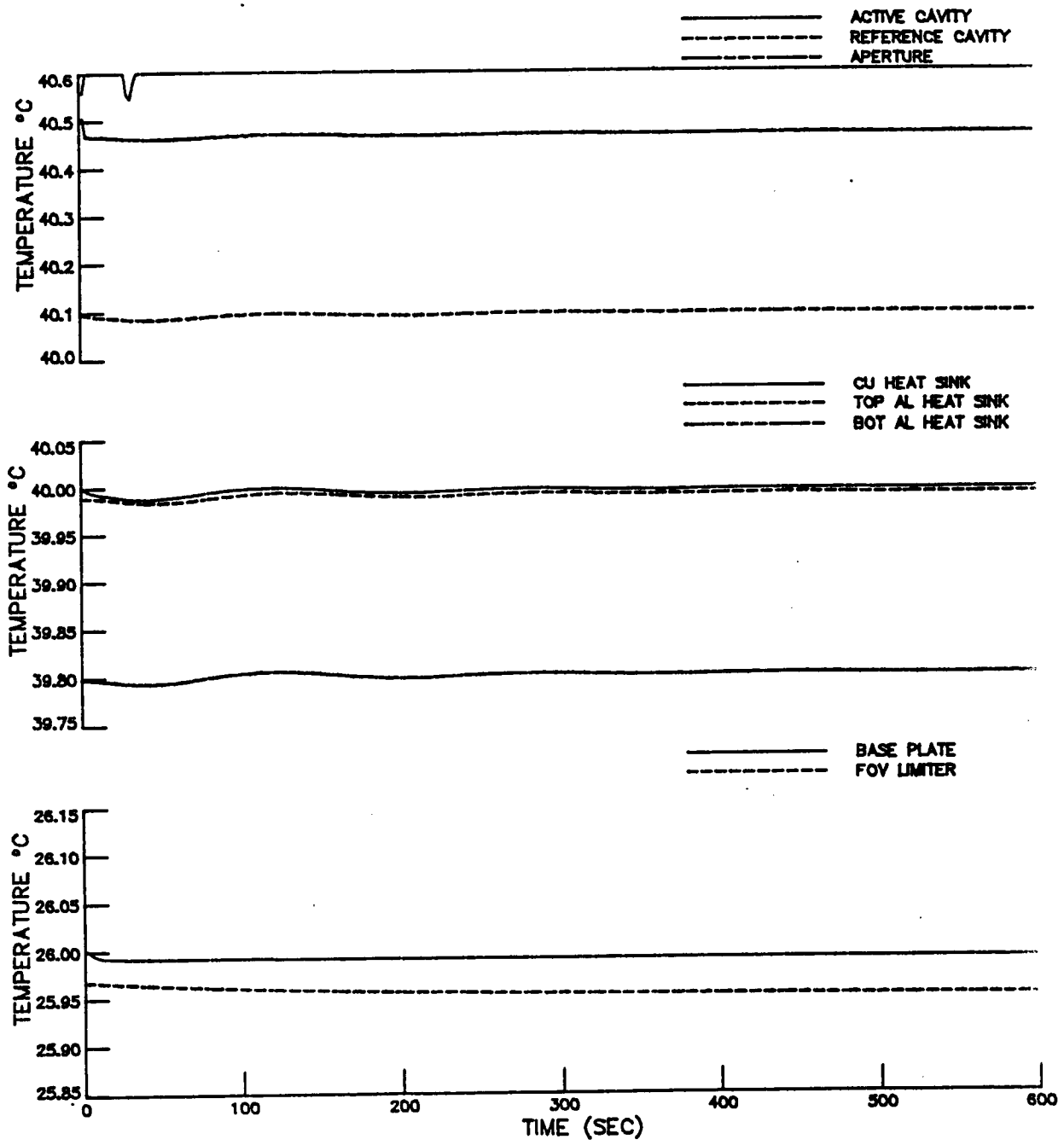

# SENSITIVITY ANALYSIS USING DYNAMIC MODEL

MFOV TOTAL SIMULATION

REDUCED CONDUCTANCE BETWEEN NODES 1 AND 2

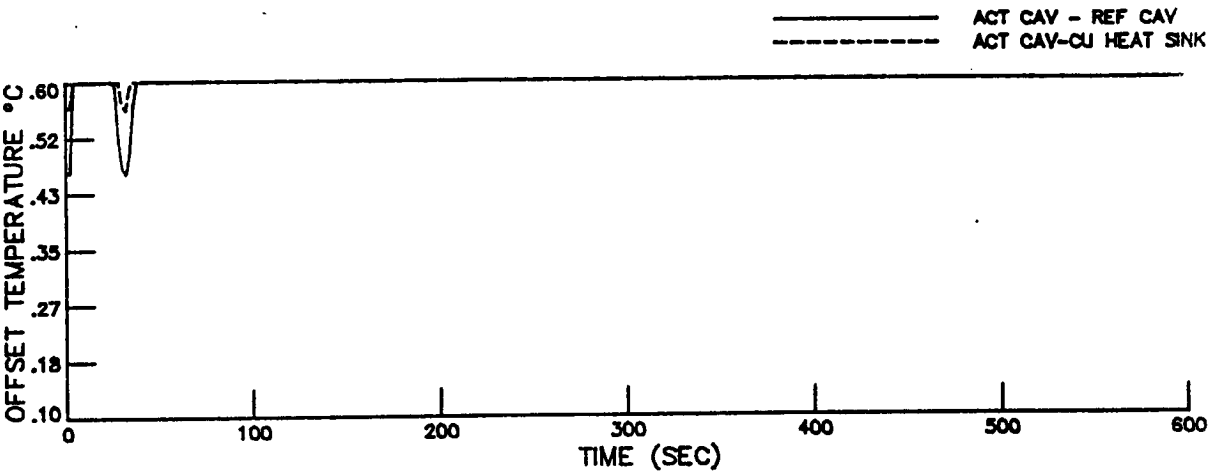

# SENSITIVITY ANALYSIS USING DYNAMIC MODEL

MFOV TOTAL SIMULATION

REDUCED CONDUCTANCE BETWEEN NODES 1 AND 2

ACTIVE CAVITY SENSOR WIRE RESISTANCE CHANGED BY .5 Ω (NOMINAL 2319.1 Ω)

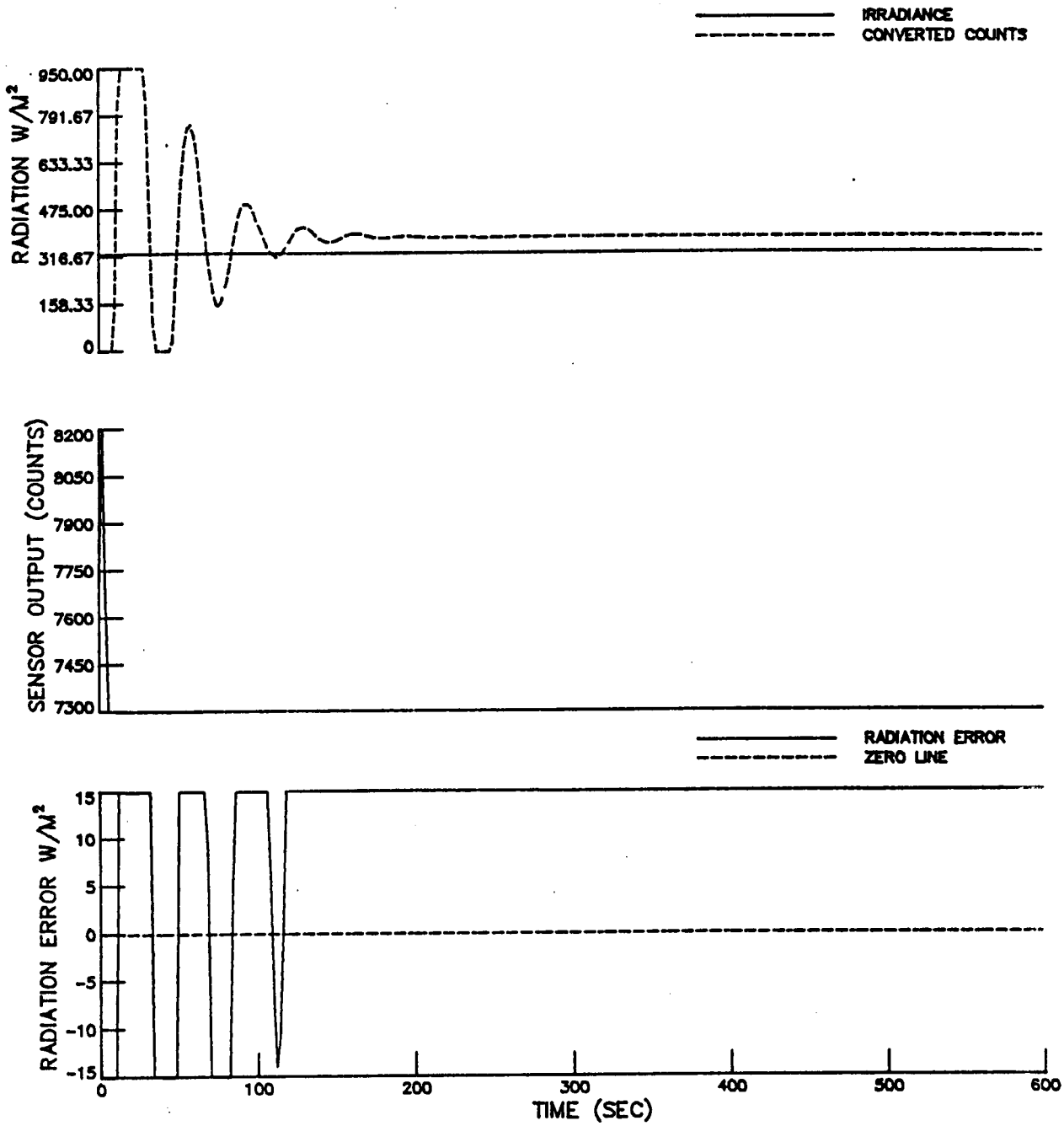

# SENSITIVITY ANALYSIS USING DYNAMIC MODEL

MFOV TOTAL SIMULATION

REDUCED CONDUCTANCE BETWEEN NODES 1 AND 2

ACTIVE CAVITY SENSOR WIRE RESISTANCE CHANGED BY .5 Ω (NOMINAL 2319.1 Ω)

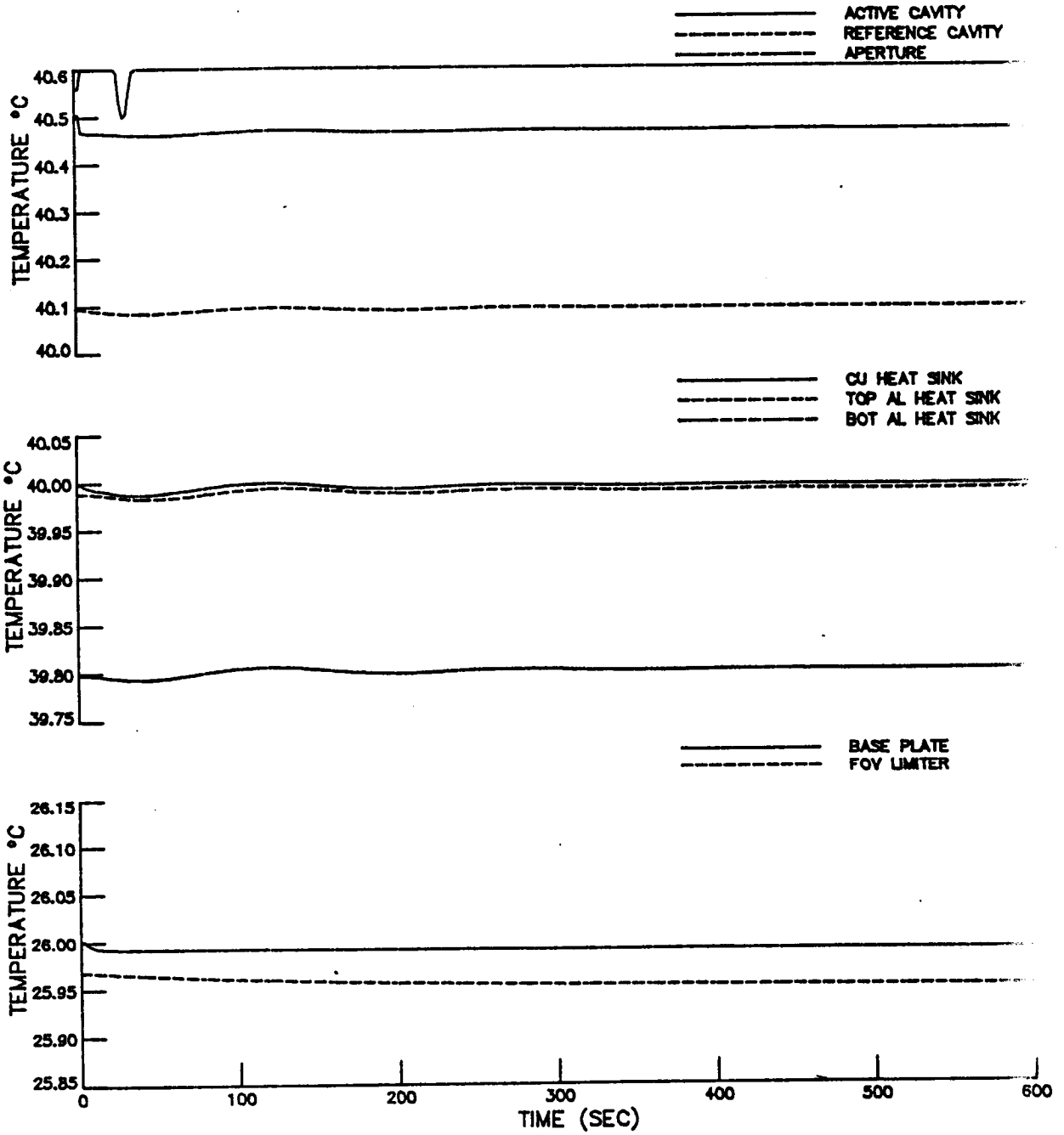

# SENSITIVITY ANALYSIS USING DYNAMIC MODEL

MFOV TOTAL SIMULATION

REDUCED CONDUCTANCE BETWEEN NODES 1 AND 2

ACTIVE CAVITY SENSOR WIRE RESISTANCE CHANGED BY .5 Ω (NOMINAL 2319.1 Ω)

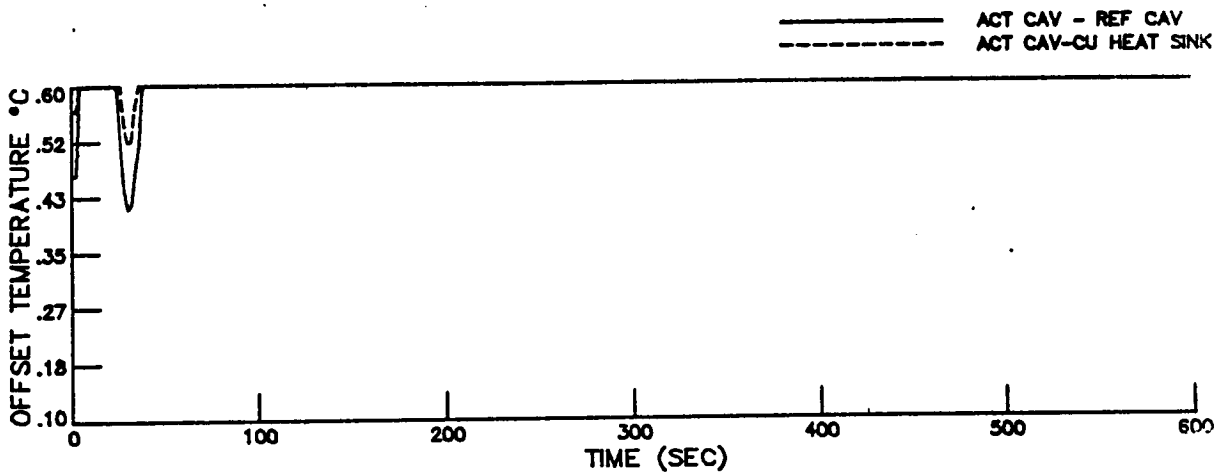

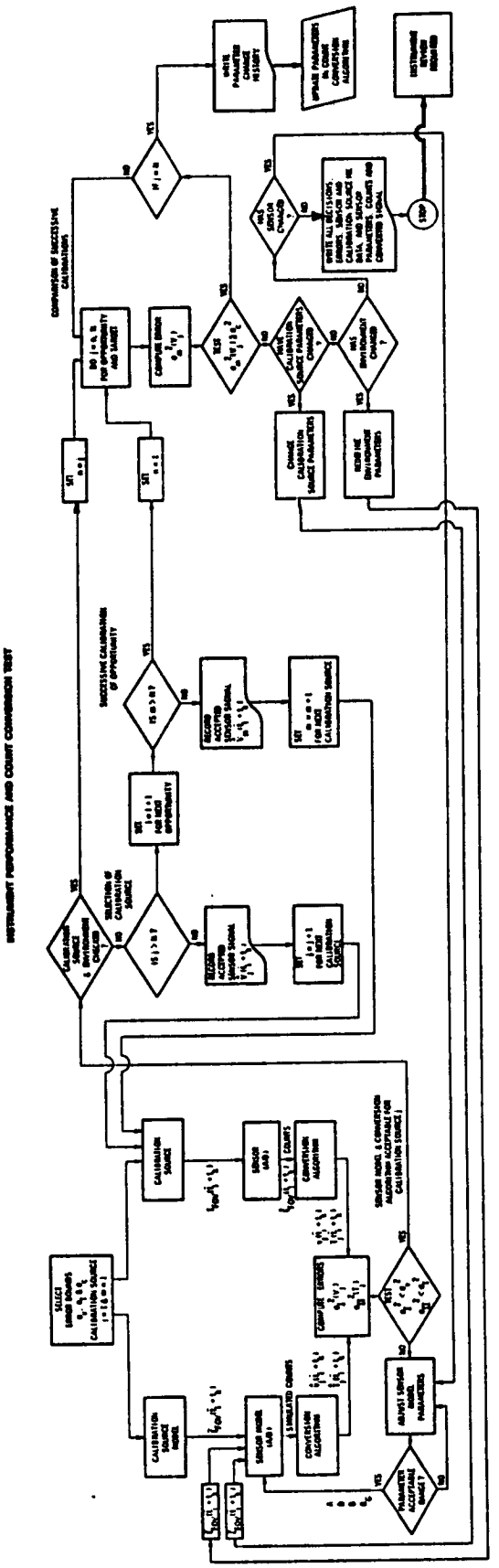

## CONCLUSIONS

- DYNAMIC MODELS HELP THE UNDERSTANDING OF THE ERBE INSTRUMENTS
- SIMPLE COUNT CONVERSION ALGORITHMS HAVE BEEN DEVELOPED
- STEADY STATE SIMULATION AND GROUND CALIBRATION RESULTS ARE IN GENERAL AGREEMENT
- THE ERRORS DUE TO COUNT CONVERSION ARE BEING ANALYZED BY SIMULATION
- INITIAL SENSITIVITY AND ERROR ANALYSES PROVIDE CONSTRUCTIVE RESULTS
- OVERALL APPROACH SEEMS WELL-SUITED TO ASSESS INSTRUMENT PERFORMANCE, ACCURACY AND VALIDATION

# APPENDIX B

# ERBE SCANNER SIMULATIONS

These graphical displays were produced during development of the simulation model. Please note that the plot of "OUTPUT (CNTS)" versus "TIME (SEC)" in the graph on pages 169, 173, 174, 177 and 180 does not display quantitatively absolute values for counts generated from the simulation model due to uncertain gain/offset parameters in the electronics.

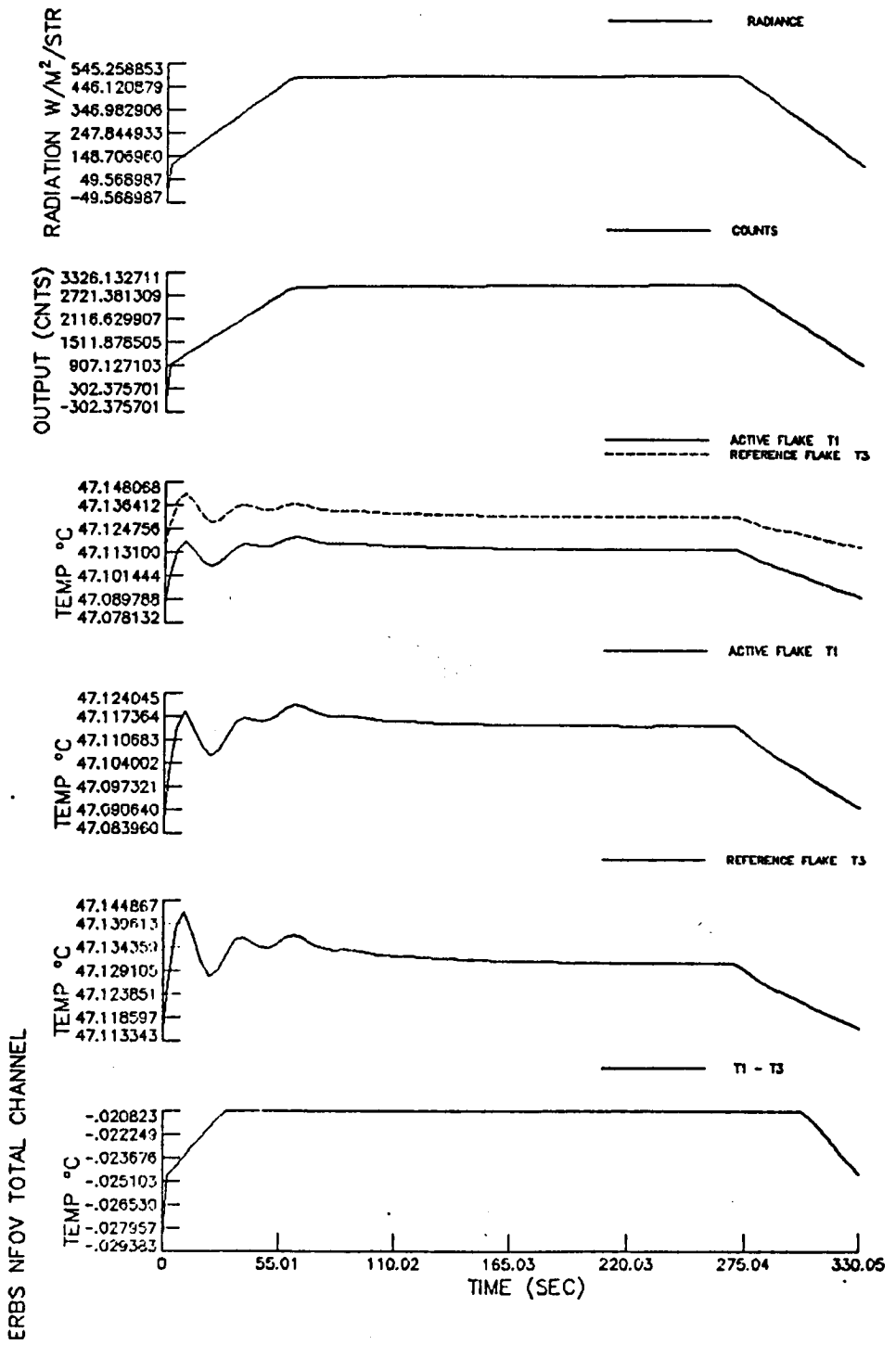
ERBS NFOV TOTAL CHANNEL
RADIANCE
RADIATION W/M²/STR
545.258853
446.120879
346.982906
247.844933
148.706960
49.568987
-49.568987
COUNTS
OUTPUT (CNTS)
3326.132711
2721.381309
2116.629907
1511.878505
907.127103
302.375701
-302.375701
ACTIVE FLAKE T1
REFERENCE FLAKE T3
TEMP °C
47.148068
47.136412
47.124756
47.113100
47.101444
47.089788
47.078132
ACTIVE FLAKE T1
TEMP °C
47.124045
47.117364
47.110683
47.104002
47.097321
47.090640
47.083960
REFERENCE FLAKE T3
TEMP °C
47.144867
47.139613
47.134359
47.129105
47.123851
47.118597
47.113343
T1 - T3
TEMP °C
-.020823
-.022249
-.023676
-.025103
-.026530
-.027957
-.029383
0
55.01
110.02
165.03
220.03
275.04
330.05
TIME (SEC)

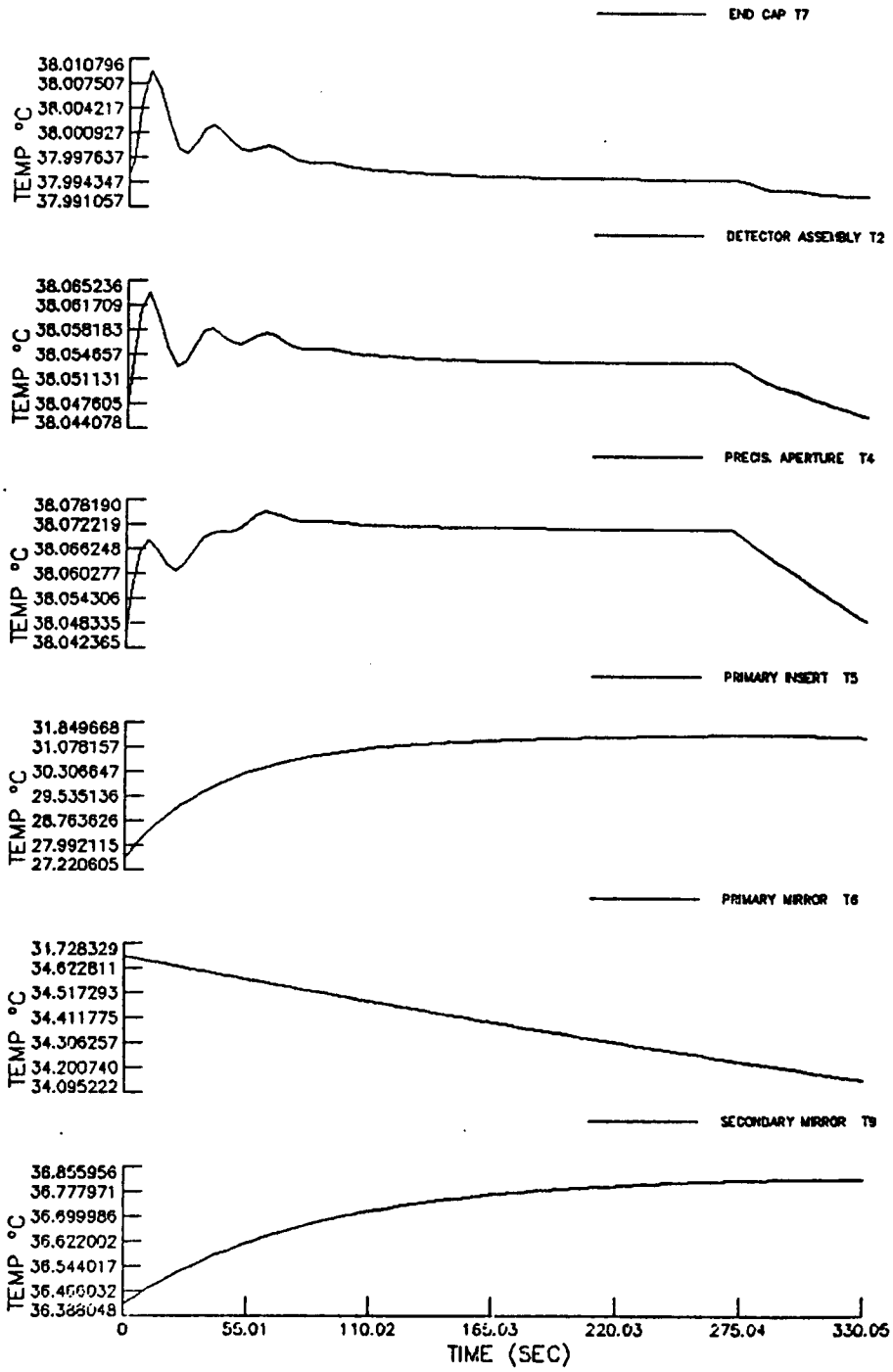
END CAP T7
38.010796
38.007507
38.004217
38.000927
37.997637
37.994347
37.991057
TEMP °C
DETECTOR ASSEMBLY T2
38.065236
38.061709
38.058183
38.054657
38.051131
38.047605
38.044078
TEMP °C
PRECIS. APERTURE T4
38.078190
38.072219
38.066248
38.060277
38.054306
38.048335
38.042365
TEMP °C
PRIMARY INSERT T5
31.849668
31.078157
30.306647
29.535136
28.763626
27.992115
27.220605
TEMP °C
PRIMARY MIRROR T6
34.728329
34.622811
34.517293
34.411775
34.306257
34.200740
34.095222
TEMP °C
SECONDARY MIRROR T9
36.855956
36.777971
36.699986
36.622002
36.544017
36.466032
36.388048
TEMP °C
0
55.01
110.02
165.03
220.03
275.04
330.05
TIME (SEC)

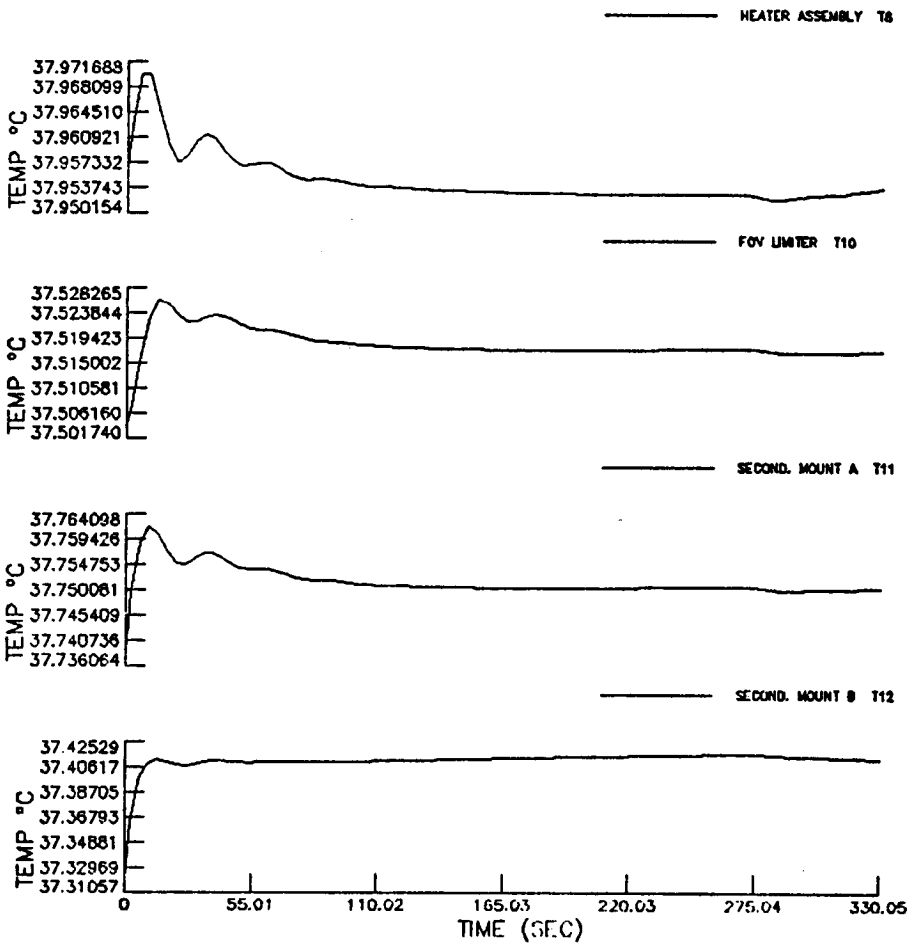
HEATER ASSEMBLY T8
37.971688
37.968099
37.964510
37.960921
37.957332
37.953743
37.950154
TEMP °C
FOV LIMITER T10
37.528265
37.523844
37.519423
37.515002
37.510581
37.506160
37.501740
TEMP °C
SECOND. MOUNT A T11
37.764098
37.759426
37.754753
37.750081
37.745409
37.740736
37.736064
TEMP °C
SECOND. MOUNT B T12
37.42529
37.40617
37.38705
37.36793
37.34881
37.32969
37.31057
TEMP °C
0
55.01
110.02
165.03
220.03
275.04
330.05
TIME (SEC)

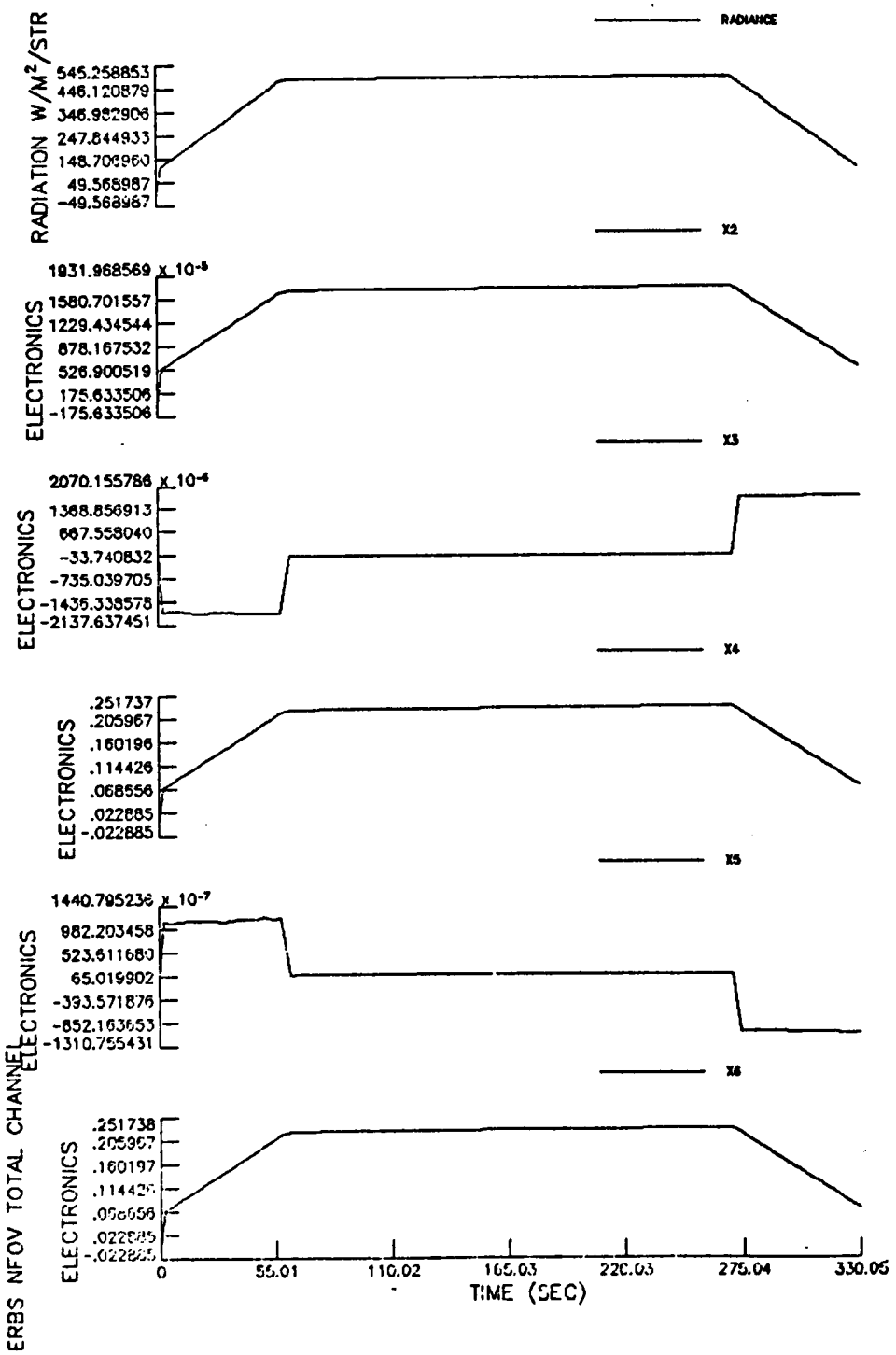
ERBS NFOV TOTAL CHANNEL
RADIANCE
RADIATION W/M²/STR
545.258853
446.120879
346.982906
247.844933
148.706960
49.568987
-49.568987
X2
ELECTRONICS
1931.968569 X 10⁻⁵
1580.701557
1229.434544
878.167532
526.900519
175.633506
-175.633506
X3
ELECTRONICS
2070.155786 X 10⁻⁴
1368.856913
667.558040
-33.740832
-735.039705
-1436.338578
-2137.637451
X4
ELECTRONICS
.251737
.205967
.160196
.114426
.068656
.022885
-.022885
X5
ELECTRONICS
1440.795236 X 10⁻⁷
982.203458
523.611680
65.019902
-393.571876
-852.163653
-1310.755431
X6
ELECTRONICS
.251738
.205967
.160197
.114426
.068656
.022885
-.022885
0
55.01
110.02
165.03
220.03
275.04
330.05
TIME (SEC)

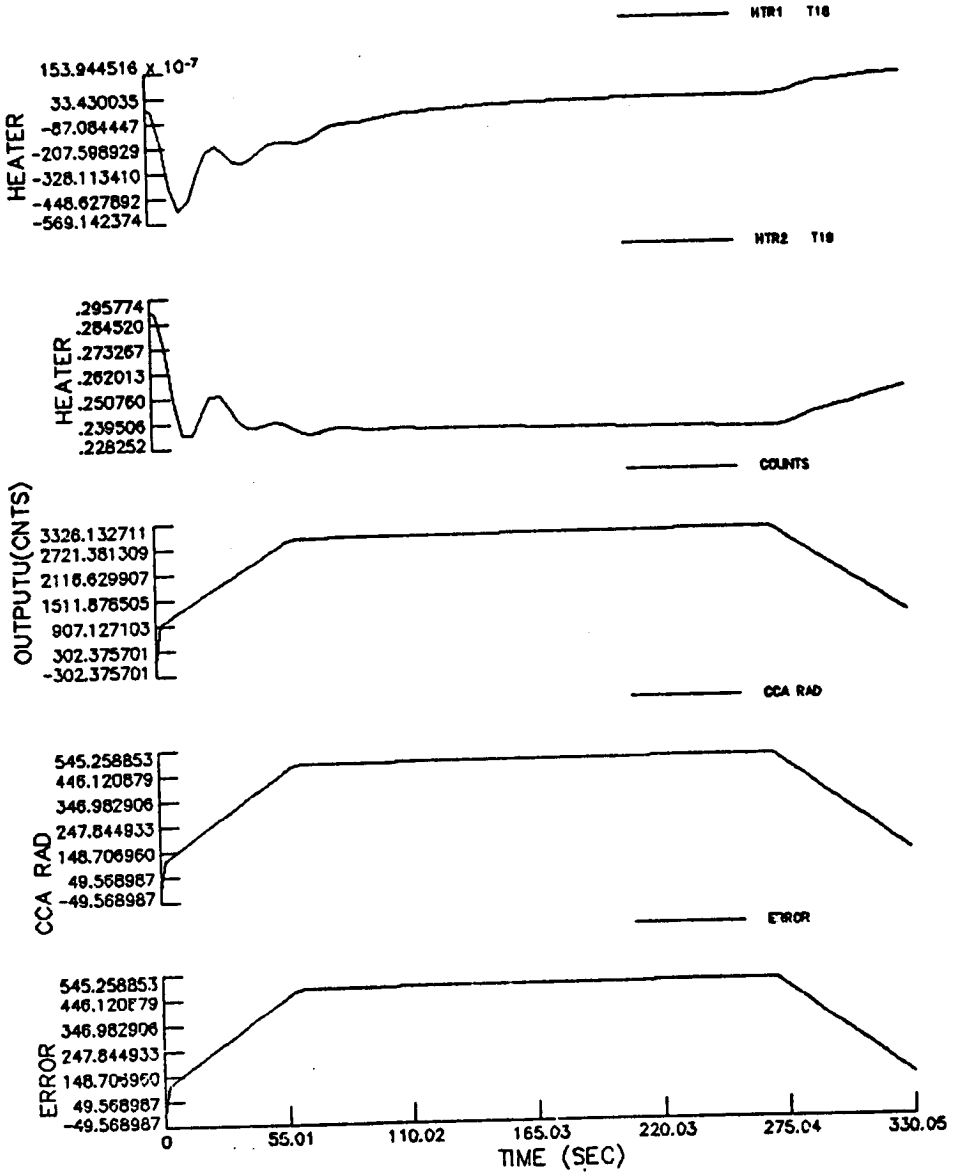
HTR1 T16
153.944516 x 10-7
33.430035
-87.084447
-207.598929
-328.113410
-448.627892
-569.142374
HEATER
HTR2 T19
.295774
.284520
.273267
.262013
.250760
.239506
.228252
HEATER
COUNTS
3326.132711
2721.381309
2116.629907
1511.878505
907.127103
302.375701
-302.375701
OUTPUTU(CNTS)
CCA RAD
545.258853
446.120879
346.982906
247.844933
148.706960
49.568987
-49.568987
CCA RAD
ERROR
545.258853
446.120879
346.982906
247.844933
148.706960
49.568987
-49.568987
ERROR
0
55.01
110.02
165.03
220.03
275.04
330.05
TIME (SEC)

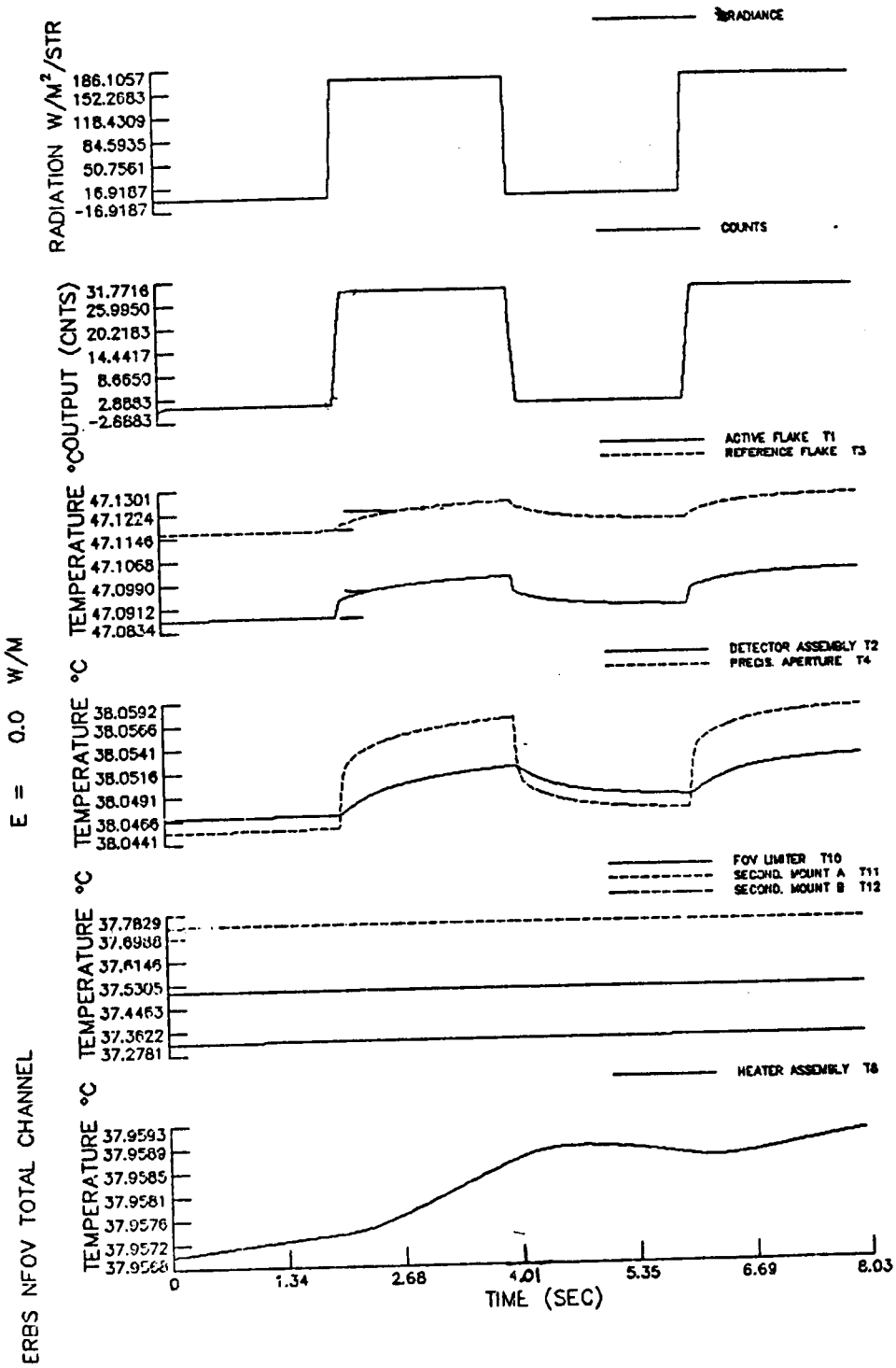
ERBS NFOV TOTAL CHANNEL
E = 0.0 W/M
RADIATION W/M²/STR
186.1057
152.2683
118.4309
84.5935
50.7561
16.9187
-16.9187
RADIANCE
COUNTS
°COUTPUT (CNTS)
31.7716
25.9950
20.2183
14.4417
8.6650
2.8883
-2.8883
ACTIVE FLAKE T1
REFERENCE FLAKE T3
TEMPERATURE °C
47.1301
47.1224
47.1146
47.1068
47.0990
47.0912
47.0834
DETECTOR ASSEMBLY T2
PRECIS. APERTURE T4
TEMPERATURE °C
38.0592
38.0566
38.0541
38.0516
38.0491
38.0466
38.0441
FOV LIMITER T10
SECOND. MOUNT A T11
SECOND. MOUNT B T12
TEMPERATURE °C
37.7829
37.6988
37.6146
37.5305
37.4463
37.3622
37.2781
HEATER ASSEMBLY T8
TEMPERATURE °C
37.9593
37.9589
37.9585
37.9581
37.9576
37.9572
37.9568
0
1.34
2.68
4.01
5.35
6.69
8.03
TIME (SEC)

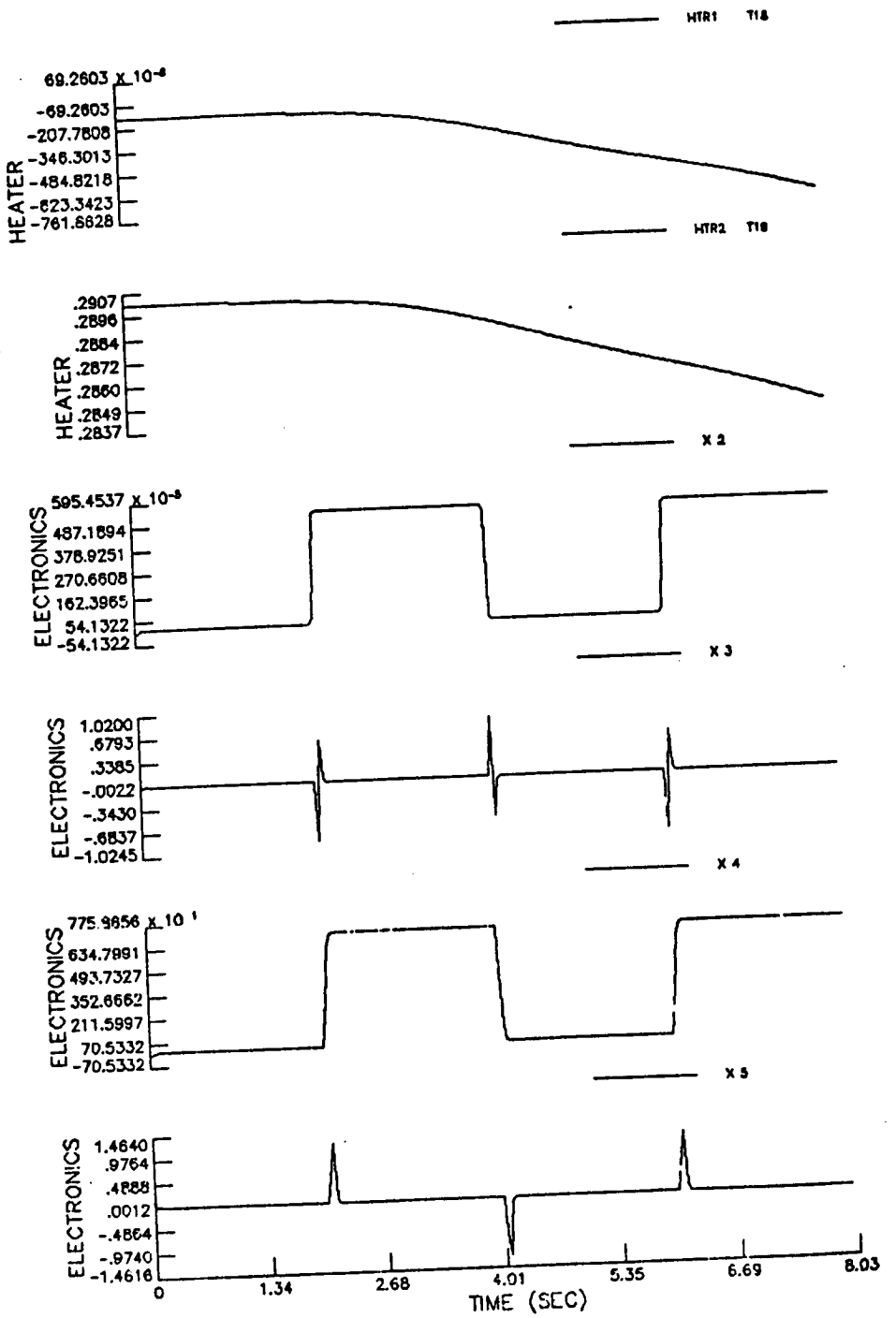
HTR1 T18
69.2603 X 10⁻⁶
-69.2603
-207.7808
-346.3013
-484.8218
-623.3423
-761.8628
HEATER
HTR2 T19
.2907
.2896
.2884
.2872
.2860
.2849
.2837
HEATER
X 2
595.4537 X 10⁻⁵
487.1694
378.9251
270.6608
162.3965
54.1322
-54.1322
ELECTRONICS
X 3
1.0200
.6793
.3385
-.0022
-.3430
-.6837
-1.0245
ELECTRONICS
X 4
775.9856 X 10⁻¹
634.7991
493.7327
352.6662
211.5997
70.5332
-70.5332
ELECTRONICS
X 5
1.4640
.9764
.4888
.0012
-.4864
-.9740
-1.4616
ELECTRONICS
0
1.34
2.68
4.01
5.35
6.69
8.03
TIME (SEC)

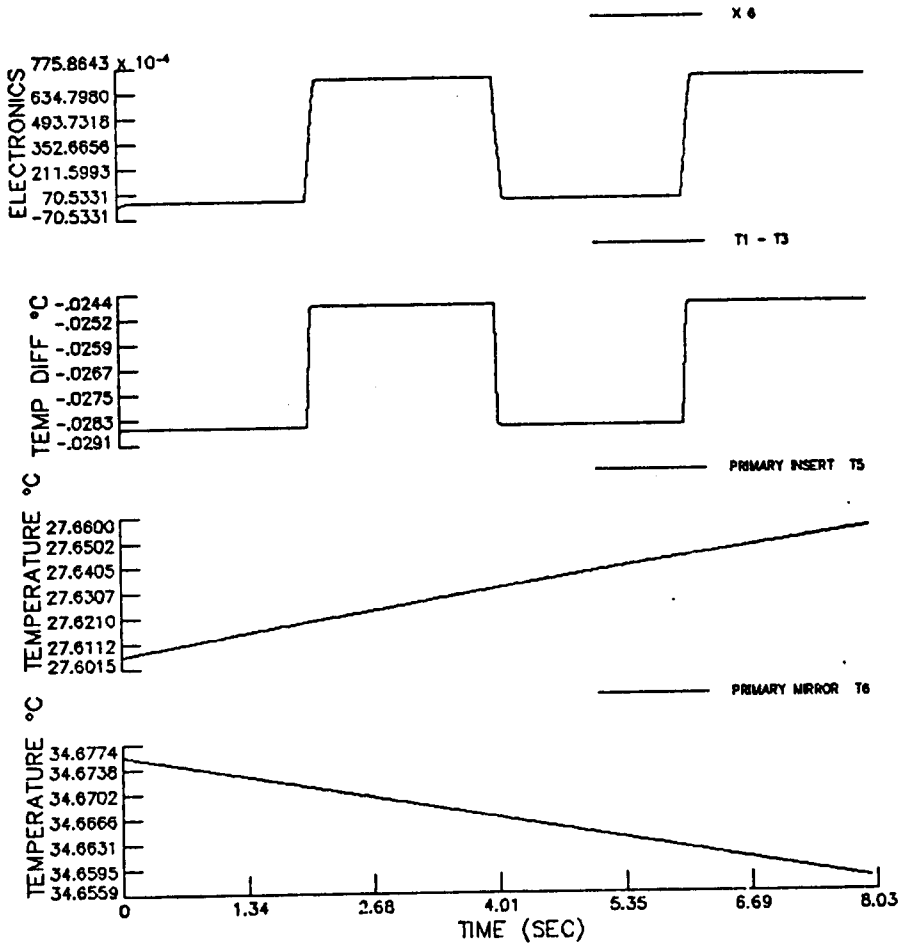
X 6
775.8643 X 10⁻⁴
634.7980
493.7318
352.6656
211.5993
70.5331
-70.5331
ELECTRONICS
T1 - T3
-.0244
-.0252
-.0259
-.0267
-.0275
-.0283
-.0291
TEMP DIFF °C
PRIMARY INSERT T5
27.6600
27.6502
27.6405
27.6307
27.6210
27.6112
27.6015
°C
TEMPERATURE
PRIMARY MIRROR T6
34.6774
34.6738
34.6702
34.6666
34.6631
34.6595
34.6559
°C
TEMPERATURE
0
1.34
2.68
4.01
5.35
6.69
8.03
TIME (SEC)

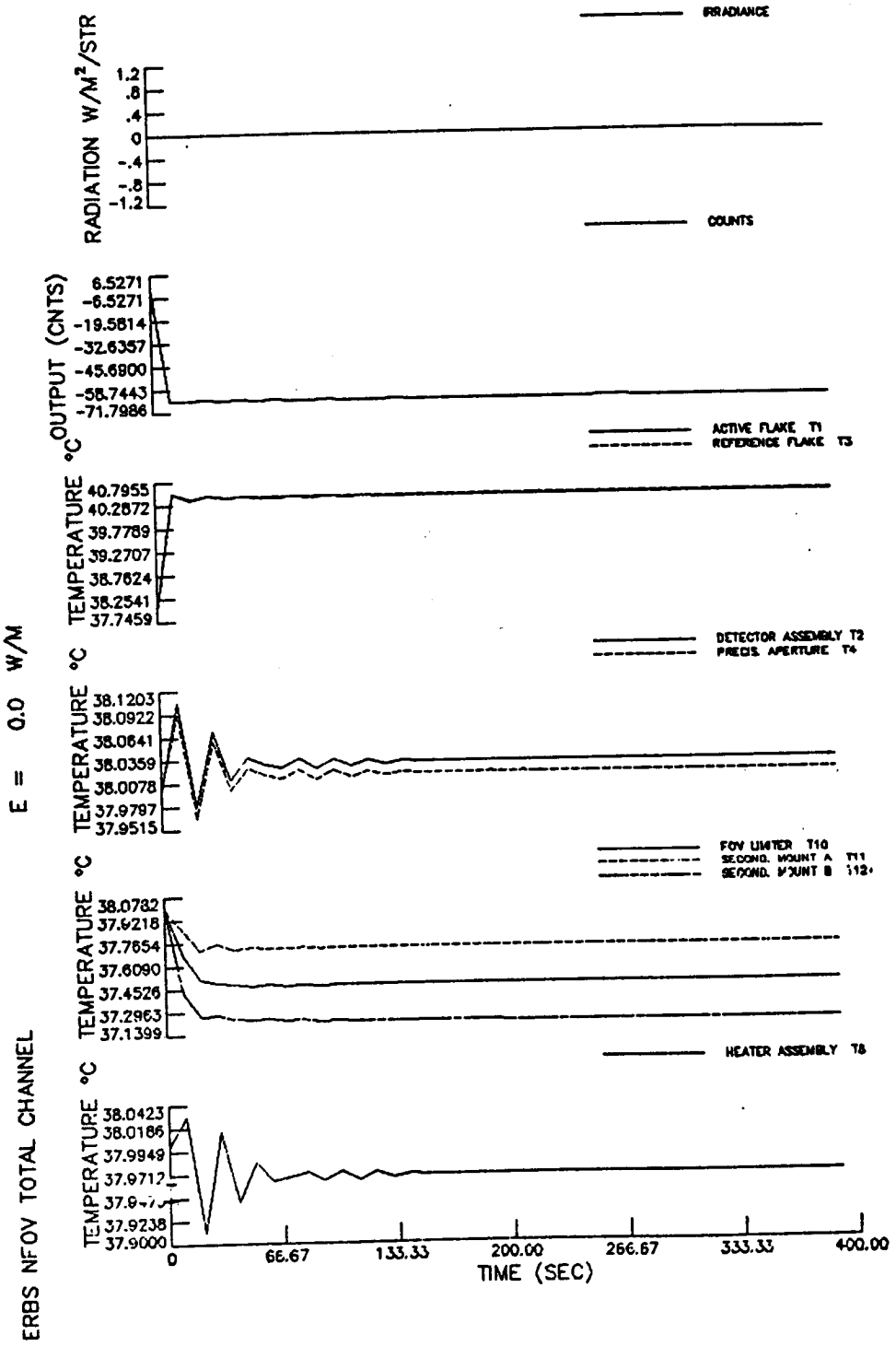
ERBS NFOV TOTAL CHANNEL
E = 0.0 W/M
IRRADIANCE
RADIATION W/M²/STR
1.2
.8
.4
0
-.4
-.8
-1.2
COUNTS
OUTPUT (CNTS)
6.5271
-6.5271
-19.5814
-32.6357
-45.6900
-58.7443
-71.7986
ACTIVE FLAKE T1
REFERENCE FLAKE T3
°C
TEMPERATURE
40.7955
40.2872
39.7789
39.2707
38.7624
38.2541
37.7459
DETECTOR ASSEMBLY T2
PRECIS. APERTURE T4
°C
TEMPERATURE
38.1203
38.0922
38.0641
38.0359
38.0078
37.9797
37.9515
FOV LIMITER T10
SECOND. MOUNT A T11
SECOND. MOUNT B T12
°C
TEMPERATURE
38.0782
37.9218
37.7654
37.6090
37.4526
37.2963
37.1399
HEATER ASSEMBLY T8
°C
TEMPERATURE
38.0423
38.0186
37.9949
37.9712
37.9238
37.9000
0
66.67
133.33
200.00
266.67
333.33
400.00
TIME (SEC)

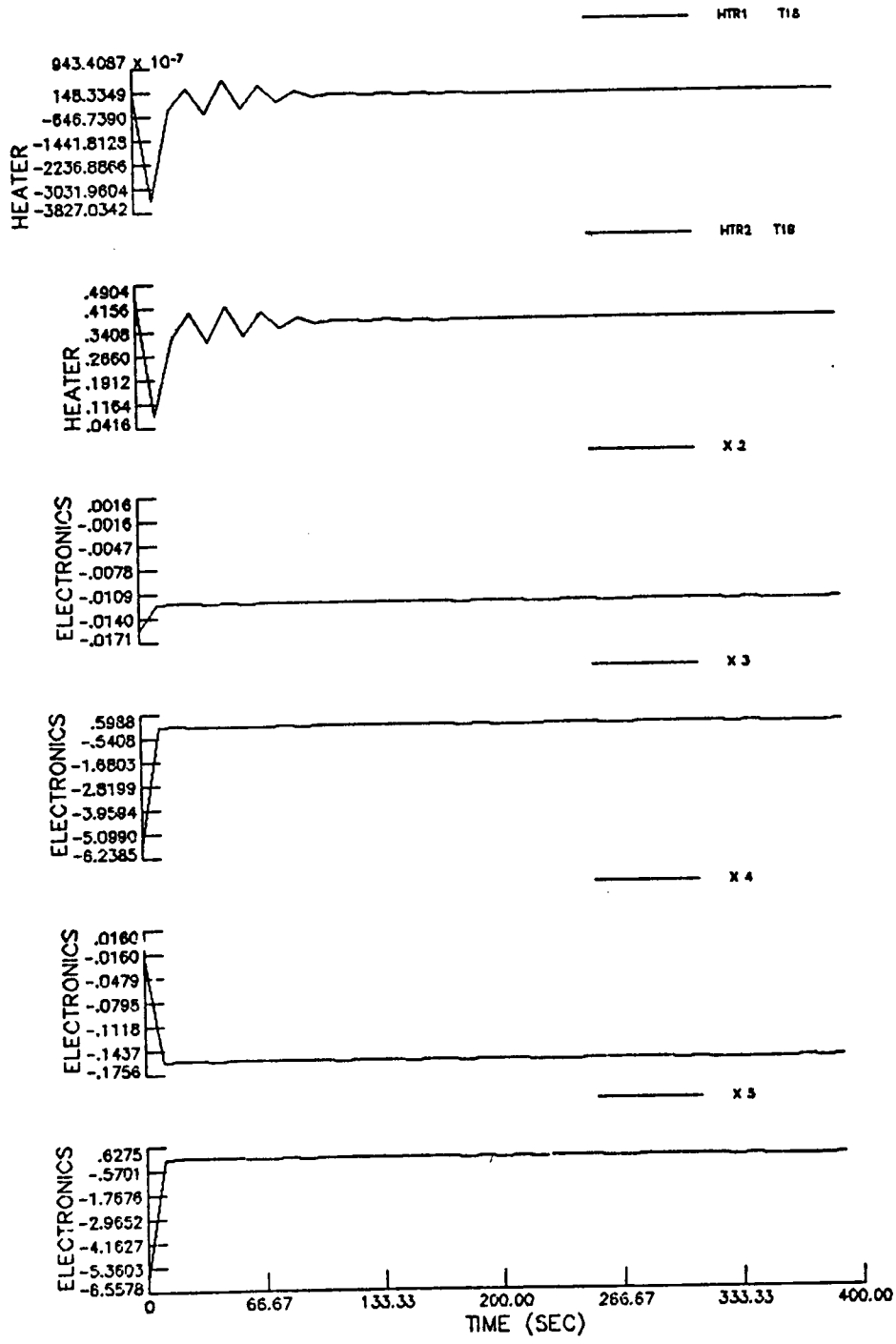
HTR1 T18
943.4087 X 10-7
148.3349
-646.7390
-1441.8128
-2236.8866
-3031.9604
-3827.0342
HEATER
HTR2 T18
.4904
.4156
.3408
.2660
.1912
.1164
.0416
HEATER
X 2
.0016
-.0016
-.0047
-.0078
-.0109
-.0140
-.0171
ELECTRONICS
X 3
.5988
-.5408
-1.6803
-2.8199
-3.9594
-5.0990
-6.2385
ELECTRONICS
X 4
.0160
-.0160
-.0479
-.0798
-.1118
-.1437
-.1756
ELECTRONICS
X 5
.6275
-.5701
-1.7676
-2.9652
-4.1627
-5.3603
-6.5578
ELECTRONICS
0
66.67
133.33
200.00
266.67
333.33
400.00
TIME (SEC)

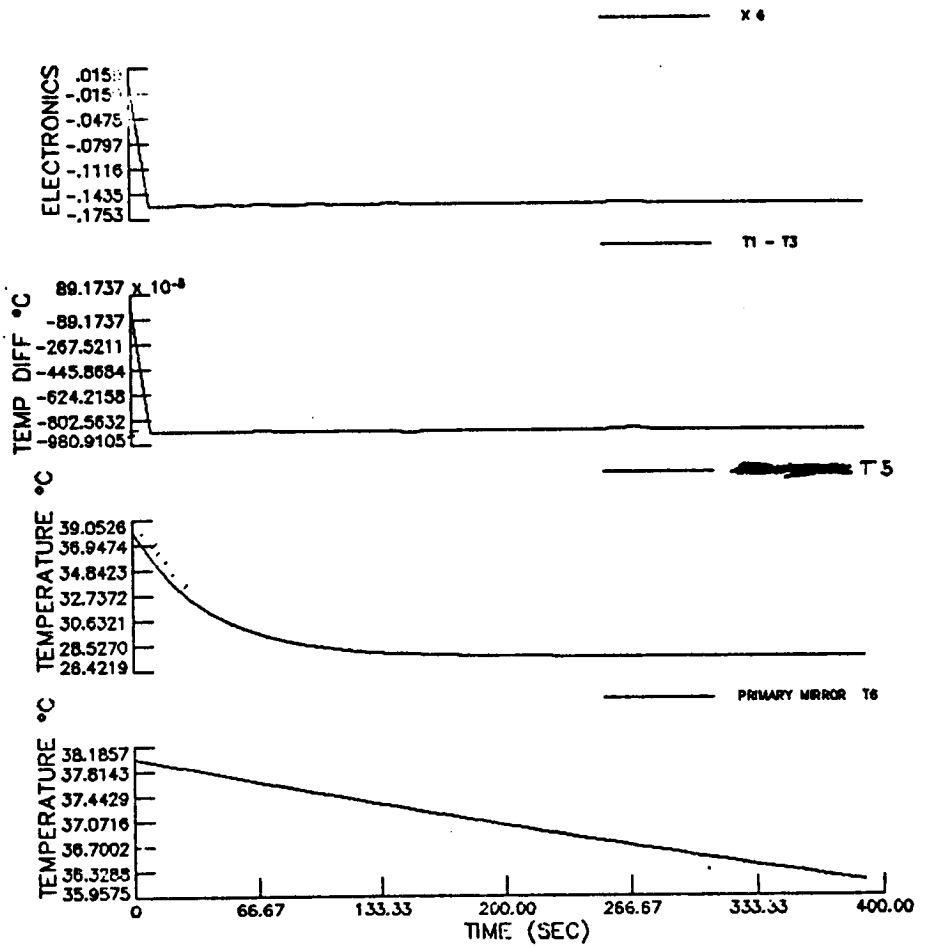
X 4
ELECTRONICS
.015
-.015
-.0475
-.0797
-.1116
-.1435
-.1753
T1 - T3
TEMP DIFF °C
89.1737 X 10⁻⁸
-89.1737
-267.5211
-445.8684
-624.2158
-802.5632
-980.9105
T 5
TEMPERATURE °C
39.0526
36.9474
34.8423
32.7372
30.6321
28.5270
26.4219
PRIMARY MIRROR T6
TEMPERATURE °C
38.1857
37.8143
37.4429
37.0716
36.7002
36.3288
35.9575
0
66.67
133.33
200.00
266.67
333.33
400.00
TIME (SEC)

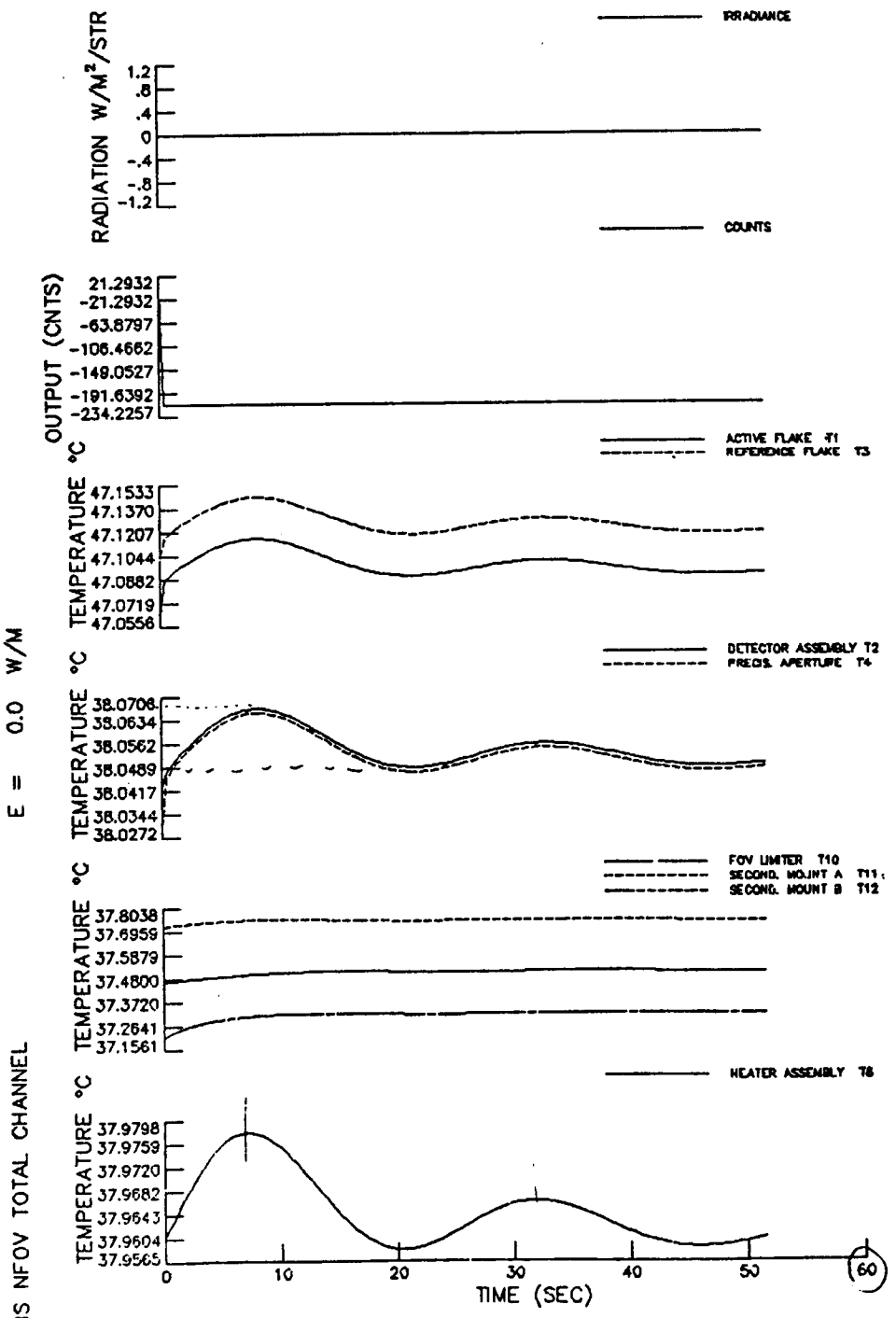
ERBS NFOV TOTAL CHANNEL
E = 0.0 W/M
RADIATION W/M²/STR
1.2
.8
.4
0
-.4
-.8
-1.2
IRRADIANCE
OUTPUT (CNTS)
21.2932
-21.2932
-63.8797
-106.4662
-149.0527
-191.6392
-234.2257
COUNTS
TEMPERATURE °C
47.1533
47.1370
47.1207
47.1044
47.0882
47.0719
47.0556
ACTIVE FLAKE T1
REFERENCE FLAKE T3
TEMPERATURE °C
38.0706
38.0634
38.0562
38.0489
38.0417
38.0344
38.0272
DETECTOR ASSEMBLY T2
PRECIS. APERTURE T4
TEMPERATURE °C
37.8038
37.6959
37.5879
37.4800
37.3720
37.2641
37.1561
FOV LIMITER T10
SECOND. MOUNT A T11
SECOND. MOUNT B T12
TEMPERATURE °C
37.9798
37.9759
37.9720
37.9682
37.9643
37.9604
37.9565
HEATER ASSEMBLY T8
0
10
20
30
40
50
60
TIME (SEC)

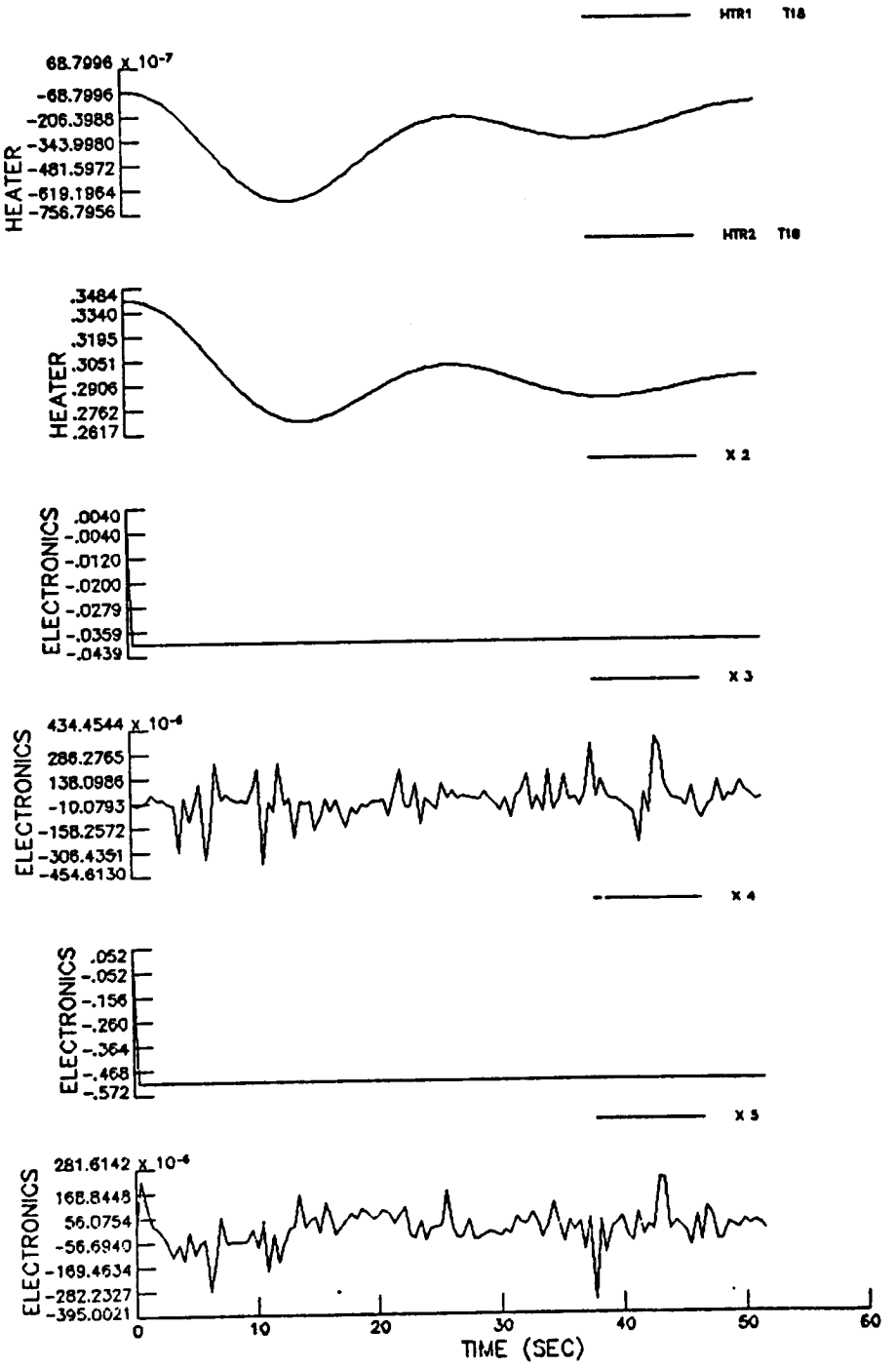
HTR1 T18
68.7996 X 10-7
-68.7996
-206.3988
-343.9980
-481.5972
-619.1964
-756.7956
HEATER
HTR2 T18
.3484
.3340
.3195
.3051
.2906
.2762
.2617
HEATER
X 2
.0040
-.0040
-.0120
-.0200
-.0279
-.0359
-.0439
ELECTRONICS
X 3
434.4544 X 10-6
286.2765
138.0986
-10.0793
-158.2572
-306.4351
-454.6130
ELECTRONICS
X 4
.052
-.052
-.156
-.260
-.364
-.468
-.572
ELECTRONICS
X 5
281.6142 X 10-6
168.8448
56.0754
-56.6940
-169.4634
-282.2327
-395.0021
ELECTRONICS
0
10
20
30
40
50
60
TIME (SEC)

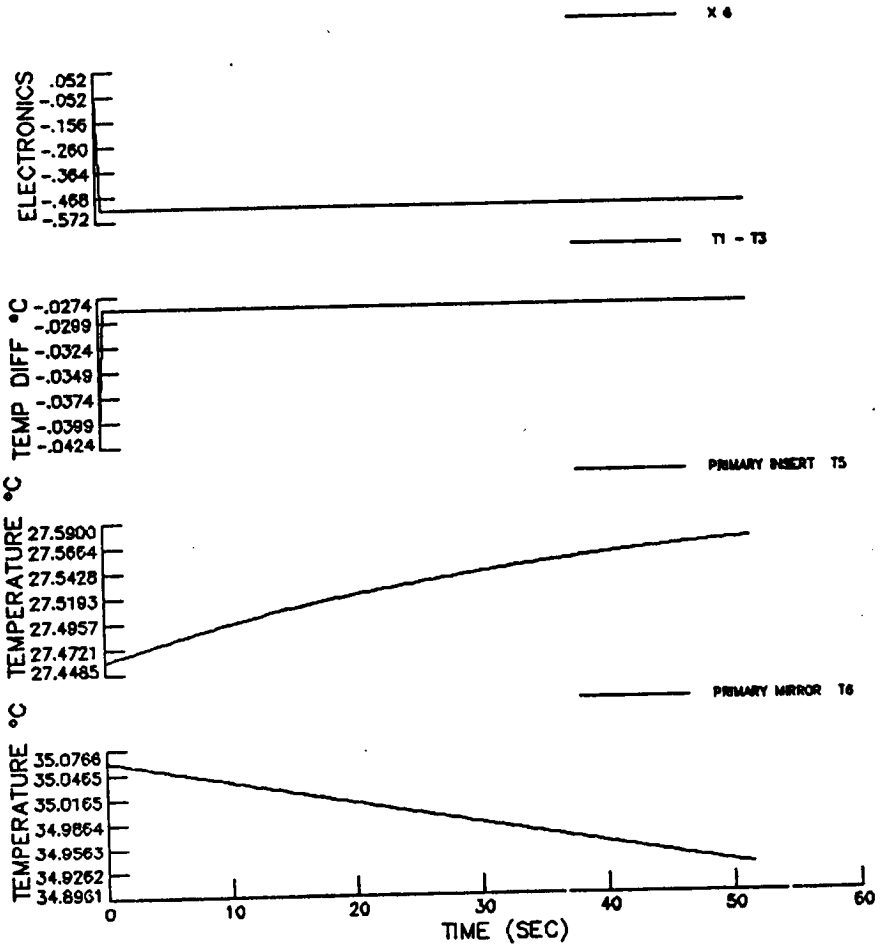


PRECEDING PAGE BLANK NOT FILMED

# APPENDIX C

# ERBE NON-SCANNER THERMAL MODEL

## NON-SCANNER MODEL

The energy balance equation

$$M_k \dot{T}_k = \sum_{j=1}^{n} \frac{T_j - T_k}{R_{kj}} + A_k \phi_k + \dot{Q}_{source} \tag{1}$$

The second term in the right-hand side of the above equation is the radiation interaction of the $k_{th}$ element to the other elements in an enclosure. This variables are defined by the following approach.

For the radiant interchange in an enclosure having both specular and diffuse surfaces, the surface properties are defined as the followings:

The reflectivity is

$$\rho_s = \rho_s^d + \rho_s^s$$

$$\rho_s = \rho_\ell^d + \rho_\ell^s$$

where subscripts, s and $\ell$, signify short and long waves and superscripts, d and s, denote diffuse and specular.

For diffuse and gray approximation, the following realtionships are obtained

$$\rho_s + \epsilon_s + \tau_s = 1$$

$$\rho_\ell \quad \epsilon_\ell \quad \tau_\ell = 1.$$

From now, the subscripts for short and longwaves are omitted for brevity.

The radiosoty at the $k_{th}$ surface is

$$M_k^d = \epsilon_k \sigma T_k^4 + \rho_k^d E_k + \tau_k \tilde{E}_k. \tag{2}$$

The incident radiant flux at the $k_{th}$ surface is

$$E_k = \sum_j \bar{F}_{k-j} M_j^d \tag{3}$$

Combining the above two equations yields

$$M_j^d = \sum_i (\delta_{ji} - \rho_j^d \bar{F}_{j-i})^{-1} \; (\epsilon_k \Omega_i + \tau_i \tilde{E}_i) \tag{4}$$

From (3) and (4),

$$E_k = \sum_i (\epsilon_i \Omega_i + \tau_i \tilde{E}_i) \sum_j \bar{F}_{k-j} \; P_{j-i} \tag{5}$$

where

$$P_{j-i} = (\delta_{ji} - \rho_j^d \bar{F}_{j-i})^{-1}$$

$$\Omega = \sigma T^4 .$$

The radiant engergy balance equation is the difference between the incident energy and the radiosoty. That is,

$$\begin{aligned} \phi_k &= E_k - M_k \\ &= E_k - \epsilon_k \Omega_k - \rho_k^d E_k - \rho_k^s E_k - \tau_k \tilde{E}_k \end{aligned} \tag{6}$$

Substituting (5) into (6) we have

$$\begin{aligned} \phi_k = &\sum_i [(1 - \rho_k) \epsilon_i \sum_j \bar{F}_{k-j} \; P_{j-i} - \epsilon_k \delta_{ki}] \; \Omega_i \\ &+ \sum_i [(1 - \rho_k) \tau_i \sum_j \bar{F}_{k-j} \; P_{j-i} - \tau_k \delta_{ki}] \; \tilde{E}_i \end{aligned} \tag{7}$$

Let $H_{k-i} = \sum_j \bar{F}_{k-j} \; P_{j-i}$

Then, for the cavity a, the equation (5) can be expanded as

$$\begin{aligned} E_{10} = &H_{10-1} \; \epsilon_1 \; \Omega_1 \\ &+ [H_{10-8} \; \epsilon_8 + H_{10-9} \; \epsilon_9] \; \Omega_8 \\ &+ H^a_{10-10} \; \epsilon_{10} \; \Omega_{10} \\ &+ H^a_{10-10} \; \tau_{10} \; \tilde{E}_{10} \end{aligned} \tag{A}$$

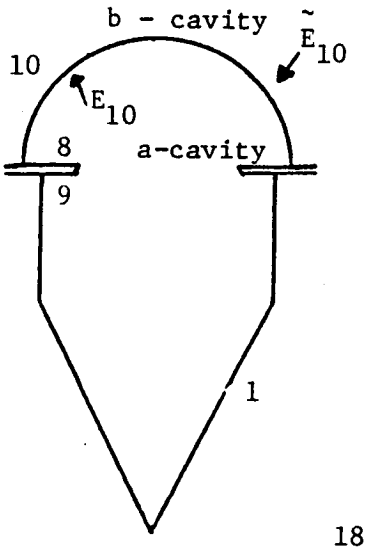

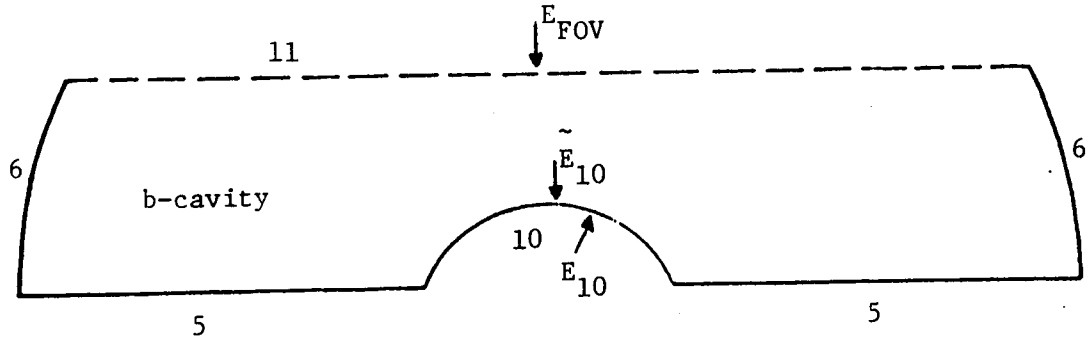


For the cavity, b

$$\tilde{E}_{10} = H_{10-5}\,\epsilon_5\,\Omega_5 + H_{10-6}\,\epsilon_6\,\Omega_6 + H^b_{10-10}\,\epsilon_{10}\,\Omega_{10} + H^b_{10-10}\,\tau_{10}\,E_{10} + H^b_{10-11}\,\tau_{11}\,E_{FOV} \qquad (B)$$

From (A) and (B),

$$E_{10} = G\,\epsilon_1\,H_{10-1}\,\Omega_1 + G\,\epsilon_5\,\tau_{10}\,H_{10-5}\,H^a_{10-10}\,\Omega_5 + G\,\epsilon_6\,\tau_{10}\,H_{10-6}\,H^a_{10-10}\,\Omega_6 + G[H_{10-8}\,\epsilon_8 + H_{10-9}\,\epsilon_9]\,\Omega_8 + G\,\epsilon_{10}[H^a_{10-10} + \tau_{10}\,H^a_{10-10}\,H^b_{10-10}]\,\Omega_{10} + G\,\tau_{10}\,\tau_{11}\,H^a_{10-10}\,H_{10-11}\,E_{FOV}$$

where $G = (1 - \tau^2_{10}\,H^a_{10-10}\,H^b_{10-10})^{-1}$.

$$\tilde{E}_{10} = G\,\epsilon_1\,\tau_{10}\,H^b_{10-10}\,H_{10-1}\,\Omega_1 + G\,\epsilon_5\,H_{10-5}\,\Omega_1 + G\,\epsilon_6\,H_{10-6}\,\Omega_6 + G\,\tau_{10}\,H^b_{10-10}[H_{10-8}\,\epsilon_8 + H_{10-9}\,\epsilon_9]\,\Omega_8 + G\,\epsilon_{10}\,H^b_{10-10}[1 + \tau_{10}\,H^a_{10-10}]\,\Omega_{10} + G\,\tau_{11}\,H^b_{10-11}\,E_{FOV}$$

$$\phi_i = \sum_j [(1 - \rho_i)\, H_{ij}\, \epsilon_j - \delta_{ij}\, \epsilon_j]\, \Omega_j + \sum_j [(1 - \rho_i)\, H_{ij}\, \tau_j - \delta_{ij}\, \tau_j] \tilde{E}_j$$

In cavity a:

$$\begin{aligned}
\phi_1^a = {} & \epsilon_1[(1 - \rho_1)H_{1-1} + (1 - \rho_1)\, \tau_{10}^2\, G\, H_{1-10}\, H_{10-10}^b\, H_{10-1} - 1]\, \Omega_1 \\
& + (1 - \rho_1)\, \epsilon_5\, \tau_{10}\, G\, H_{1-10}\, H_{10-5}\, \Omega_5 \\
& + (1 - \rho_1)\, \epsilon_6\, \tau_{10}\, G\, H_{1-10}\, H_{10-6}\, \Omega_6 \\
& + (1 - \rho_1)\, \{(\epsilon_8\, H_{1-8} + \epsilon_9\, H_{1-9}) + \tau_{10}^2\, G\, H_{1-10}\, H_{10-10}^b\, (\epsilon_8\, H_{10-8} \\
& \quad + H_{10-9} \epsilon_9)\}\, \Omega_8 \\
& + (1 - \rho_1)\, \epsilon_{10}\, H_{1-10}[1 + \tau_{10}\, G\, H_{10-10}^b (1 + \tau_{10}\, H_{10-10}^a)]\, \Omega_{10} \\
& + (1 - \rho_1)\, \tau_{10}\, \tau_{11}\, G\, H_{1-10}\, H_{10-11}\, E_{FOV}
\end{aligned}$$

$$\phi_8^a = \frac{A_8}{A_{(8+9)}}\, \phi_8 + \frac{A_9}{A_{(8+9)}}\, \phi_9$$

$$\begin{aligned}
\phi_8 = {} & (1 - \rho_8)[\epsilon_1\, H_{8-1} + \epsilon_1\, \tau_{10}^2\, G\, H_{8-10}\, H_{10-10}^b\, H_{10-1}]\, \Omega_1 \\
& + (1 - \rho_8)\, \epsilon_5\, \tau_{10}\, G\, H_{8-10}\, H_{10-5}\, \Omega_5 \\
& + (1 - \rho_8)\, \epsilon_6\, \tau_{10}\, G\, H_{8-10}\, H_{10-6}\, \Omega_6 \\
& + \{\epsilon_8[(1 - \rho_8)\, H_{8-8} - 1] + (1 - \rho_8)\, \tau_{10}^2\, G\, H_{8-10}\, H_{10-10}^b\, (H_{10-8}\, \epsilon_8 \\
& \quad + H_{10-9}\, \epsilon_9) + (1 - \quad_8)\, \epsilon_9\, H_{8-9}\}\, \Omega_8 \\
& + (1 - \rho_8)\, \epsilon_{10}\, H_{8-10}\, [1 + \tau_{10}\, G\, H_{10-10}^b\, (1 + \tau_{10}\, H_{10-10}^a)]\, \Omega_{10} \\
& + (1 - \quad \rho_8)\, \tau_{10}\, \tau_{11}\, G\, H_{8-10}\, H_{10-11}\, E_{FOV}
\end{aligned}$$

$$\phi_9 = (1 - \rho_9)\ \epsilon_1[H_{9-1} + \tau_{10}^2\ G\ H_{9-10}\ H^b_{10-10}\ H_{10-1}\ ]\ \Omega_1$$

$$+ (1 - \rho_9)\ \epsilon_5\ \tau_{10}\ G\ H_{9-10}\ H_{10-5}\ \Omega_5$$

$$+ (1 - \rho_9)\ \epsilon_6\ \tau_{10}\ G\ H_{9-10}\ H_{10-6}\ \Omega_6$$

$$+ \{(1 - \rho_9)\ \epsilon_9\ H_{9-8} + \epsilon_9[(1 - \rho_9)\ H_{9-9} - 1] + (1 - \rho_9)\ \tau_{10}^2\ G\ H_{9-10}\ H^b_{10-10}$$

$$(H_{10-8}\ \epsilon_8 + H_{10-9}\ \epsilon_9)\}\Omega_8$$

$$+ (1 - \rho_9)\ \epsilon_{10}\ H_{9-10}[1 + \tau_{10}\ G\ H^b_{10-10}\ (1 + \tau_{10}\ H^a_{10-10})]\ \Omega_{10}$$

$$+ (1 - \rho_9)\ \tau_{10}\ \tau_{11}\ G\ H_{9-10}\ H_{10-11}\ E_{FOV}$$

In Cavity b:

$$\phi^b_5 = (1 - \rho_5)\ \epsilon_1\ \tau_{10}\ G\ H_{5-10}\ H_{10-1}\ \Omega_1$$

$$+ \epsilon_5\ \{[(1 - \rho_5)\ H_{5-5} - 1] + (1 - \rho_5)\ \tau_{10}^2\ G\ H_{5-10}\ H_{10-5}\ H^a_{10-10}\}\ \Omega_5$$

$$+ (1 - \rho_5)\ \epsilon_6[H_{5-6} + \tau_{10}^2\ G\ H_{5-10}\ H_{10-6}\ H^a_{10-10}]\ \Omega_6$$

$$+ (1 - \rho_5)\ \tau_{10}\ G\ H_{5-10}\ (\epsilon_8\ H_{10-8} + \epsilon_9\ H_{10-9})\ \Omega_8$$

$$+ (1 - \rho_5)\ \epsilon_{10}\ H_{5-10}[1 + \tau_{10}\ G\ H^a_{10-10}\ (1 + \tau_{10}\ H^b_{10-10})]\ \Omega_{10}$$

$$+ (1 - \rho_5)\ \tau_{10}^2\ \tau_{11}\ G\ H_{5-10}\ H^a_{10-10}\ H_{10-11}\ E_{FOV}$$

$$\phi^b_6 = \epsilon_1(1 - \rho_6)\ \tau_{10}\ G\ H_{5-10}\ H_{10-1}\ \Omega_1$$

$$+ (1 - \rho_6)\ \epsilon_6[H_{6-5} + \tau_{10}^2\ G\ H_{6-10}\ H_{10-5}\ H^a_{10-10}]\ \Omega_5$$

$$+ \epsilon_6\{[(1 - \rho_6)\ H_{6-6} - 1] + (1 - \rho_6)\ \tau_{10}^2\ G\ H_{6-10}\ H_{10-5}\ H^a_{10-10}\}\ \Omega_6$$

$$+ (1 - \rho_6)\ \tau_{10}\ G\ H_{6-10}\ (\epsilon_8\ H_{10-8} + \epsilon_9\ H_{10-9})\ \Omega_8$$

$$+ (1 - \rho_6)\ \epsilon_{10}\ H_{5-10}\ [1 + \tau_{10}\ G\ H^a_{10-10}\ (1 + \tau_{10}\ H^b_{10-10})]\ \Omega_{10}$$

$$+ (1 - \rho_6)\ \tau_{10}^2\ \tau_{11}\ G\ H_{5-10}\ H^a_{10-10}\ H_{10-11}\ E_{FOV}$$

$$\phi_{10}^{b} = \epsilon_1 \tau_{10} G[(1 - \rho_{10}) H_{10-10}^{b} - 1] H_{10-1} \Omega_1$$
$$+ \epsilon_5 H_{10-5} \{(1 - \rho_{10}) + \tau_{10}^2 G[(1 - \rho_{10}) H_{10-10}^{b} - 1] H_{10-10}^{a}\} \Omega_5$$
$$+ \epsilon_6 H_{10-6} \{(1 - \rho_{10}) + \tau_{10}^2 G[(1 - \rho_{10}) H_{10-10}^{b} - 1] H_{10-10}^{a}\} \Omega_6$$
$$+ \tau_{10} G[(1 - \rho_{10}) H_{10-10}^{b} - 1] (\epsilon_8 H_{10-8} + \epsilon_9 H_{10-9}) \Omega_8$$
$$+ \epsilon_{10}[(1 - \rho_{10}) H_{10-10}^{b} - 1] \{1 + \tau_{10} G[H_{10-10}^{a} + \tau_{10} H_{10-10}^{a} H_{10-10}^{b}]\} \Omega_{10}$$
$$+ \tau_{10}^2 \tau_{11} G [(1 - \rho_{10}) H_{10-10}^{b} - 1] H_{10-10}^{a} H_{10-11} E_{FOV}$$

$$\phi_{10 \text{ filter}} = \frac{A_{10a}}{A_{10(a+b)}} \phi_{10}^{a} + \frac{A_{10b}}{A_{10(a+b)}} \phi_{10}^{b}$$

Cavity C:

$$\phi_1^{c} = \epsilon_1[(1 - \rho_1) H_{1-1} - 1] \Omega_1 + (1 - \rho_1) \epsilon_2 H_{1-2} \Omega_2$$
$$+ (1 - \rho_1) \epsilon_4 H_{1-4} \Omega_4$$

$$\phi_2^{c} = (1 - \rho_2) \epsilon_1 H_{2-1} \Omega_1 + \epsilon_2[(1 - \rho_2) H_{2-2} - 1] \Omega_2$$
$$+ (1 - \rho_2) \epsilon_4 H_{2-4} \Omega_4$$

$$\phi_4^{c} = (1 - \rho_4) \epsilon_1 H_{4-1} \Omega_1 + (1 - \rho_4) \epsilon_2 H_{4-2} \Omega_2$$
$$+ \epsilon_4[(1 - \rho_4) H_{4-4} - 1] \Omega_4$$

where $\epsilon$ and $\rho$ are $\epsilon^{c}$ and $\rho^{c}$.

Cavity d:

$$\phi_2^{d} = \epsilon_2[(1 - \rho_2) H_{2-2} - 1] \Omega_2 + (1 - \rho_2) \epsilon_3 H_{2-3} \Omega_3$$
$$+ (1 - \rho_2) \epsilon_7 H_{2-7} \Omega_7$$

$$\phi_3^d = (1 - \rho_3)\ \epsilon_2\ H_{3-2}\ \Omega_2 + \epsilon_3[(1 - \rho_3)\ H_{3-3} - 1]\ \Omega_3$$
$$+ (1 - \rho_3)\ \epsilon_7\ H_{3-7}\ \Omega_7$$

$$\phi_7^d = (1 - \rho_7)\ \epsilon_2\ H_{7-2}\ \Omega_2 + (1 - \rho_7)\ \epsilon_3\ H_{7-3}\ \Omega_3$$
$$+ \epsilon_7[(1 - \rho_7)\ H_{7-7} - 1]\ \Omega_7$$

Cavity e:

$$\phi_1^e = \epsilon_1[(1 - \rho_1)\ H_{1-1} - 1]\ \Omega_1 + (1 - \rho_1)\ \epsilon_2\ H_{1-2}\ \Omega_2$$
$$+ (1 - \rho_1)\ \epsilon_3\ H_{1-3}\ \Omega_3$$

$$\phi_2^e = (1 - \rho_2)\ \epsilon_1\ H_{2-1}\ \Omega_1 + \epsilon_2[(1 - \rho_2)\ H_{2-2} - 1]\ \Omega_2$$
$$+ (1 - \rho_2)\ \epsilon_3\ H_{2-3}\ \Omega_3$$

$$\phi_3^e = (1 - \rho_3)\ \epsilon_1\ H_{3-1}\ \Omega_1 + (1 - \rho_3)\ \epsilon_2\ H_{3-2}\ \Omega_2$$
$$+ \epsilon_3[(1 - \rho_3)\ H_{3-3} - 1]\ \Omega_3$$

Cavity f:

$$\phi_3^f = \epsilon_3[(1 - \rho_3)\ H_{3-3} - 1]\ \Omega_3 + (1 - \rho_3)\ \epsilon_7\ H_{3-7}\ \Omega_7$$

$$\phi_7^f = (1 - \rho_7)\ \epsilon_3\ H_{7-3}\ \Omega_3 + \epsilon_7[(1 - \rho_7)\ H_{7-7} - 1]\ \Omega_7$$

The energy balance equation (1) is written for each node as the followings:

$$\dot{T}_1 = \frac{1}{M_1}\left\{\frac{T_2 - T_1}{R_{1-2}} + A_1^c\ \phi_1^c + A_1^e\ \phi_1^e + A_1^a\ \phi_1^a + \dot{Q}_{H_1}\right\}$$

$$\dot{T}_2 = \frac{1}{M_2}\left\{\frac{T_1-T_2}{R_{2-1}} + \frac{T_4-T_2}{R_{2-4}} + \frac{T_3-T_2}{R_{2-3}} + \frac{T_7-T_2}{R_{2-7}} + A_2^e\ \phi_2^e + \dot{Q}_2\right\}$$

$$\dot{T}_3 = \frac{1}{M_3}\left\{\frac{T_2-T_3}{R_{3-2}} + A_3^e\ \phi_3^e + A_3^d\ \phi_3^d + A_3^f\ \phi_3^f + \dot{Q}_{H_3}\right\}$$

$$\dot{T}_4 = \frac{1}{M_4}\left\{\frac{T_2-T_4}{R_{4-2}} + \frac{T_5-T_4}{R_{4-5}} + \frac{T_8-T_4}{R_{4-8}} + A_4^c\ \phi_4^c + \dot{Q}_4\right\}$$

$$\dot{T}_5 = \frac{1}{M_5}\left\{\frac{T_4-T_5}{R_{5-4}} + \frac{T_6-T_5}{R_{5-6}} + \frac{T_{12}-T_5}{R_{5-12}} + A_5^b\ \phi_5^b\right\}$$

$$\dot{T}_6 = \frac{1}{M_6}\left\{\frac{T_5-T_6}{R_{6-5}} + A_6^b\ \phi_6^b\right\}$$

$$\dot{T}_7 = \frac{1}{M_7}\left\{\frac{T_2-T_7}{R_{2-7}} + A_7^d\ \phi_7^d + A_7^f\ \phi_7^f + \dot{Q}_7\right\}$$

$$\dot{T}_8 = \frac{1}{M_8}\left\{\frac{T_4-T_8}{R_{8-4}} + \frac{T_5-T_8}{R_{8-5}} + \frac{T_{10}-T_8}{R_{8-10}} + A_8^a\ \phi_8^a + A_9^a\ \phi_9^a\right\}$$

$$\dot{T}_{10} = \frac{1}{M_{10}}\left\{\frac{T_4-T_{10}}{R_{10-4}} + \frac{T_8-T_{10}}{R_{10-8}} + A_{10}^a\ \phi_{10}^a + A_{10}^b\ \phi_{10}^b\right\}$$

Where $M = V\ \gamma\ C$. In addition there are three more equations which were derived from the electronics model. These equations are already discussed in Section II.

In the above equations, the $\phi$s can be splitted as

$$\phi_k = (\phi_k)_{\text{shortwave}} + (\phi_k)_{\text{longwave}}.$$

Substituting $\phi_k$ into the above equations and rearranging the constants yeild a following type of equation

$$\dot{T}_k = \sum_j A_{kj}\ T_j + \sum_j D_{kj}\ T_j^4 + B_{Qk}\ \dot{Q}_k + B_k\ E_{FOV}$$

where

$A_{kj} = \frac{1}{M_k R_{k-j}}$

$D_{kj}$ = constants including all radiative parameters

$B_{Qk} = \frac{A_k}{M_k}$

$B_k$ = constants related with the irradiance at FOV limiter of radiometers.

The above constants are described in the following pages.

$$\{A_{1-1} = -\frac{1}{M_1 R_{1-2}}, \quad A_{1-2} = \frac{1}{M_1 R_{1-2}}$$

$$\begin{cases} A_{2-1} = \frac{1}{M_2 R_{2-1}}, & A_{2-2} = -\frac{1}{M_2}\left(\frac{1}{R_{2-1}} + \frac{1}{R_{2-4}} + \frac{1}{R_{2-3}} + \frac{1}{R_{-27}}\right) \\ A_{2-3} = \frac{1}{M_2 R_{2-3}}, & A_{2-4} = \frac{1}{M_2 R_{2-4}}, \quad A_{2-7} = \frac{1}{M_2 R_{2-7}} \end{cases}$$

$$\{A_{3-2} = \frac{1}{M_3 R_{3-2}}, \quad A_{3-3} = \frac{1}{M_3 R_{3-2}}$$

$$\begin{cases} A_{4-2} = \frac{1}{M_4 R_{4-2}}, & A_{4-4} = -\frac{1}{M_4}\left(\frac{1}{R_{4-2}} + \frac{1}{R_{4-5}} + \frac{1}{R_{4-8}}\right) \\ A_{4-5} = \frac{1}{M_4 R_{4-5}}, & A_{4-8} = \frac{1}{M_4 R_{4-8}} \end{cases}$$

$$\begin{cases} A_{5-4} = \frac{1}{M_5 R_{5-4}}, & A_{5-5} = -\frac{1}{M_5}\left(\frac{1}{R_{5-4}} + \frac{1}{R_{5-6}} + \frac{1}{R_{5-12}}\right) \\ A_{5-6} = \frac{1}{M_5 R_{5-6}}, & A_{5-12} = \frac{1}{M_5 R_{5-12}} \end{cases}$$

$$\{A_{6-5} = \frac{1}{M_6 R_{6-5}} \quad , \qquad A_{6-6} = -\frac{1}{M_6 R_{6-5}}$$

$$\{A_{7-2} = \frac{1}{M_7 R_{7-2}} \quad , \qquad A_{7-7} = -\frac{1}{M_7 R_{7-2}}$$

$$\begin{cases} A_{8-4} = \dfrac{1}{M_8 R_{8-4}} \\ A_{8-10} = \dfrac{1}{M_8 R_{8-10}} \end{cases} , \qquad A_{8-5} = \frac{1}{M_8 R_{8-5}} \quad , \quad A_{8-5} = -\frac{1}{M_8}\left(\frac{1}{R_{8-4}} + \frac{1}{R_{8-5}} + \frac{1}{R_{8-10}}\right)$$

$$\{A_{10-4} = \frac{1}{M_{10} R_{10-4}} \quad , \qquad A_{10-8} = \frac{1}{M_{10} R_{10-8}} \quad , \quad A_{10-10} = -\frac{1}{M_{10}}\left(\frac{1}{R_{10-4}} + \frac{1}{R_{10-8}}\right)$$

$$D_{1-1} = \frac{\sigma}{M_1}\{A_1^a \epsilon_1^a[(1 - \rho_1^a) H_{1-1}^a + (1 - \rho_1^a) \tau_{10}^2 G H_{1-10}^a H_{10-10}^b H_{10-1}^a - 1]$$

$$+ A_1^c \epsilon_1^c[(1 - \rho_1^c) H_{1-1}^c - 1] + A_1^e \epsilon_1^e[(1 - \rho_1^e) H_{1-1}^e - 1]\}$$

$$D_{1-2} = \frac{\sigma}{M_1}\{A_1^c (1 - \rho_1^c) \epsilon_2^c H_{1-2}^c + A_1^e (1 - \rho_1^e) \epsilon_2^e H_{1-2}^e\}$$

$$D_{1-3} = \frac{\sigma}{M_1} A_1^e (1 - \rho_1^e) \epsilon_3^e H_{1-3}^e$$

$$D_{1-5} = \frac{\sigma}{M_1}\{A_1^a(1 - \rho_1^a) \epsilon_5^a \tau_{10} G H_{1-10}^a H_{10-5}^b\}$$

$$D_{1-4} = \frac{\sigma}{M_1} A_1^c (1 - \rho_1^c) \epsilon_4^c H_{1-4}^c$$

$$D_{1-6} = \frac{\sigma}{M_1} A_1^a (1 - \rho_1^a) \epsilon_6^a \tau_{10} G H_{1-10}^a H_{10-6}^b$$

$$D_{1-8} = \frac{\sigma}{M_1} A_1^a (1 - \rho_1^a) \{(\epsilon_8^a H_{1-8}^a + \epsilon_9^a H_{1-9}^a) + \tau_{10}^2 G H_{1-10}^a H_{10-10}^b$$

$$(\epsilon_8^a H_{10-8}^a + \epsilon_9^a H_{10-9}^a)\}$$

$$D_{1-10} = \frac{\sigma}{M_1} A_1^a \epsilon_{10}^a H_{1-10}^a [1 + \tau_{10} G H_{10-10}^b (1 + \tau_{10} H_{10-10}^a)]$$

$$B_1 = \frac{1}{M_1} A_1^a (1 - \rho_1^a) \tau_{10} \tau_{11} G H_{1-10}^a H_{10-11}^b$$

$$D_{2-1} = \frac{\sigma}{M_2} [A_2^c (1 - \rho_2^c) \epsilon_1^c H_{2-1}^c + A_2^e (1 - \rho_2^e) \epsilon_1^e H_{2-1}^e]$$

$$D_{2-2} = \frac{\sigma}{M_2} \{A_2^c [(1 - \rho_2^c) H_{2-2}^c - 1] \epsilon_2^c + A_2^d \epsilon_2^d [(1 - \rho_2^d) H_{2-2}^d - 1]$$

$$+ A_2^e \epsilon_2^e [(1 - \rho_2^e) H_{2-2}^e - 1]\}$$

$$D_{2-3} = \frac{\sigma}{M_2} \{A_2^d (1 - \rho_2^d) \epsilon_3^d H_{2-3}^d + A_2^e (1 - \rho_2^e) \epsilon_3^e H_{2-3}^e\}$$

$$D_{2-4} = \frac{\sigma}{M_2} \{A_2^c (1 - \rho_2^c) \epsilon_4^c H_{2-4}\}$$

$$D_{2-7} = \frac{\sigma}{M_2} A_2^d (1 - \rho_2^d) \epsilon_7^d H_{2-7}^d$$

$$D_{3-1} = \frac{\sigma}{M_3} A_3^e (1 - \rho_3^e) \epsilon_1^e H_{3-1}^e$$

$$D_{3-2} = \frac{\sigma}{M_3} \{A_3^d (1 - \rho_3^d) \epsilon_2^d H_{3-2}^d + A_3^e (1 - \rho_3^e) \epsilon_2^e H_{3-2}^e\}$$

$$D_{3-3} = \frac{\sigma}{M_3} \{A_3^d \epsilon_3^d [(1 - \rho_3^d) H_{3-3}^d - 1] + A_3^e \epsilon_3^e [(1 - \rho_3^e) H_{3-3}^e - 1]$$

$$+ A_3^f \epsilon_3^f [(1 - \rho_3^f) H_{3-3}^f - 1]\}$$

$$D_{3-7} = \frac{\sigma}{M_3} \{A_3^d \epsilon_7^d (1 - \rho_3^d) H_{3-7}^d + A_3^f (1 - \rho_3^f) \epsilon_7^f H_{3-7}^f\}$$

$$D_{4-1} = \frac{\sigma}{M_4} A_4^c (1 - \rho_4^c) \epsilon_1^c H_{4-1}^c$$

$$D_{4-2} = \frac{\sigma}{M_4} A_4^c (1 - \rho_4^c) \epsilon_2^c H_{4-2}^c$$

$$D_{4-4} = \frac{\sigma}{M_4} A_4^c \epsilon_4^c [(1 - \rho_4^c) H_{4-4}^c - 1]$$

$$D_{5-1} = \frac{\sigma}{M_5} \{A_5^b (1 - \rho_5^b) \epsilon_1 \tau_{10} G H_{5-10}^b H_{10-1}^a\}$$

$$D_{5-5} = \frac{\sigma}{M_5} \{A_5^b [\epsilon_5^b [(1 - \rho_5^b) H^b{}_{5-5} - 1] + (1 - \rho_5^b) \tau_{10}^2 G H_{5-10}^b H_{10-5}^b H_{10-10}^a]\}$$

$$D_{5-6} = \frac{\sigma}{M_5} A_5^b (1 - \rho_5^b) \epsilon_5^b [H_{5-6}^b + \tau_{10}^2 G H_{5-10}^b H_{10-6}^b H^a{}_{10-10}]$$

$$D_{5-8} = \frac{\sigma}{M_5} A_5^b (1 - \rho_5^b) \tau_{10} G H_{5-10}^b (\epsilon_8^a H_{10-8}^a + \epsilon_9 H_{10-9})$$

$$D_{5-10} = \frac{\sigma}{M_5} A_5^b (1 - \rho_5^b) \epsilon_{10}^b H_{5-10}^b [1 + \tau_{10} G H_{10-10}^a (1 + \tau_{10} H_{10-10}^b)]$$

$$B_5 = \frac{1}{M_5} A_5^b (1 - \rho_5^b) \tau_{11} [\tau_{10}^2 G H_{5-10}^b H_{10-10}^a H_{10-11} + H_{5-11}]$$

$$D_{6-1} = \frac{\sigma}{M_6} A_6^b \epsilon_1^a (1 - \rho_6^b) \tau_{10} G H_{5-10}^b H_{10-1}^a$$

$$D_{6-5} = \frac{\sigma}{M_6} A_6^b (1 - \rho_6^b) \epsilon_6^b [H_{6-5}^b + \tau_{10}^2 G H_{6-10}^b H_{10-5}^b H_{10-10}^a]$$

$$D_{6-6} = \frac{\sigma}{M_6} A_6^b \epsilon_6^b \{[(1 - \rho_6^b) H_{6-6}^b - 1] + (1 - \rho_6^b) \tau_{10}^2 G H_{10-5}^b H_{10-10}^a\}$$

$$D_{6-8} = \frac{\sigma}{M_6} A_6^b (1 - \rho_6^b) \tau_{10} G H_{6-10}^b (\epsilon_8^a H_{10-8}^a + \epsilon_9 H_{10-9}^a)$$

$$D_{6-10} = \frac{\sigma}{M_6} A_6^b (1 - \rho_6^b) \epsilon_{10}^b H_{6-10}^b [1 + \tau_{10} G H_{10-10}^a (1 - \tau_{10} H_{10-10}^b)]$$

$$B_6 = \frac{1}{M_6} A_6^b (1 - \rho_6^b) \tau_{11} [H_{6-11} + \tau_{10}^2 G H_{6-10}^b H_{10-10}^a H_{10-10}]$$

$$D_{7-2} = \frac{\sigma}{M_7} A_7^d (1 - \rho_7^d) \epsilon_2^d H_{7-2}^d$$

$$D_{7-3} = \frac{\sigma}{M_7} \{A_7^d (1 - \rho_7^d) \epsilon_3^d H_{7-3}^d + A_7^f (1 - \rho_7^f) \epsilon_3^f H_{7-3}^f\}$$

$$D_{7-7} = \frac{\sigma}{M_7} \{A_7^d \epsilon_7^d [(1 - \rho_7^d) H_{7-7}^d - 1] + A_7^f \epsilon_7^f [(1 - \rho_7^f) H_{7-7}^f - 1]\}$$

$$D_{8-1} = \frac{\sigma}{M_8} \{\frac{A_8^a}{A_{(8+9)}^a} (1 - \rho_8^a) [\epsilon_1^a H_{8-1}^a + \epsilon_1^a \tau_{10}^2 G H_{8-10}^a H_{10-10}^b H_{10-1}^a]$$

$$+ \frac{A_9^a}{A_{(8+9)}^a} (1 - \rho_9^a) \epsilon_1^a [H_{9-1}^a + \tau_{10}^2 G H_{9-10}^a H_{10-10}^b H_{10-1}^a]\} A_{(8+9)}$$

$$D_{8-5} = \frac{\sigma}{M_8} \{A_8^a (1 - \rho_8^a) \epsilon_5^b \tau_{10} G H_{8-10}^a H_{10-5}^b + A_9^a (1 - \rho_9^a) \epsilon_5^b \tau_{10} G H_{9-10}^a H_{10-5}^b\}$$

$$D_{8-6} = \frac{\sigma}{M_8} \{A_8^a (1 - \rho_8^a) \epsilon_6^b \tau_{10} G H_{8-10}^a H_{10-6}^b + A_9^a (1 - \rho_9^a) \epsilon_6^b \tau_{10} H_{9-10}^a H_{10-6}^b\}$$

$$D_{8-8} = \frac{\sigma}{M_8} \{A_8^a [\epsilon_8^a ((1 - \rho_8^a) H_{8-8}^a - 1) + (1 - \rho_8^a) \tau_{10}^2 G H_{8-10}^a H_{10-10}^b (H_{10-8}^a$$

$$\epsilon_8^a + H_{10-9}^a \epsilon_9^a) + (1 - \rho_8^a) \epsilon_9 H_{8-9}^a] + A_9^a [(1 - \rho_9^a) \epsilon_9^a H_{9-8}^a + \epsilon_9^a$$

$$((1 - \rho_9) H_{9-9} - 1) + (1 - \rho_9) \tau_{10}^2 G H_{9-10} H_{10-10}^b (H_{10-8}^a \epsilon_8^a + H_{10-9}^a \epsilon_9^a)]\}$$

$$D_{8-10} = \frac{\sigma}{M_8} \{A_8 (1 - \rho_8^a) \epsilon_{10}^a H_{8-10}^a [1 + \tau_{10} G H_{10-10}^b (1 + \tau_{10} H_{10-10}^a)]$$

$$+ A_9 (1 - \rho_9^a) \epsilon_{10}^a H_{9-10}^a [1 + \tau_{10} G H_{10-10}^b (1 + \tau_{10} H_{10-10}^a)]\}$$

$$B_8 = \frac{1}{M_8} \{A_8 (1 - \rho_8^a) \tau_{10} \tau_{11} G H_{8-10}^a H_{10-11}^b + A_9 (1 - \rho_9^a) \tau_{10} \tau_{11} G H_{9-10}^a H_{10-11}^b\}$$

$$D_{10-1} = \frac{\sigma}{M_{10}} \{A_{10}^a \epsilon_1^a H_{10-1}^a [(1 - \rho_{10}^a) + \tau_{10}^2 G((1 - \rho_{10}^a) H_{10-10}^a - 1) H_{10-10}^b]$$

$$+ A_{10}^b \epsilon_1^a \tau_{10} G[(1 - \rho_{10}^b) H_{10-10}^b - 1] H_{10-1}^a\}$$

$$D_{10-5} = \frac{\sigma}{M_{10}} \{A_{10}^a \epsilon_5^b \tau_{10} G[(1 - \rho_{10}^a) H_{10-10}^a - 1 H_{10-5}^b$$

$$+ A_{10}^b \epsilon_5 H_{10-5}^b [(1 - \rho_{10}^b) + \tau_{10}^2 G (1 - \rho_{10}^b) H_{10-10}^b - 1) H_{10-10}^a]\}$$

$$D_{10-6} = \frac{\sigma}{M_{10}} \{A_{10}^a \epsilon_6^b \tau_{10} G[(1 - \rho_{10}^a) H_{10-10}^a - 1 H_{10-6}^b$$

$$+ A_{10}^b \epsilon_6^b H_{10-6}^b [(1 - \rho_{10}^b) + \tau_{10}^2 G((1 - \rho_{10}^b) H_{10-10}^b - 1 H_{10-10}^a]\}$$

$$D_{10-8} = \frac{\sigma}{M_{10}} \{A_{10}^a (\epsilon_8^a H_{10-8}^a + \epsilon_9^a H_{10-9}^a) [(1 - \rho_{10}^a) + \tau_{10}^2 G((1 - \rho_{10}^a) H_{10-10}^a - 1)$$

$$H_{10-10}^b] + A_{10}^b \tau_{10} G[(1 - \rho_{10}^b) H_{10-10}^b - 1](\epsilon_8^a H_{10-8}^a + \epsilon_9^a H_{10-9}^a)\}$$

$$D_{10-10} = \frac{\sigma}{M_{10}} \{A_{10}^a \epsilon_{10}[(1 - \rho_{10}^a) H_{10-10}^a - 1] [1 + \tau_{10} G H_{10-10}^b (1 + \tau_{10} H_{10-10}^a)]$$

$$+ A_{10}^b \epsilon_{10}^b [(1 - \rho_{10}^b) H_{10-10}^b - 1] [1 + \tau_{10} G H_{10-10}^a (1 + \tau_{10} H_{10-10}^b)]\}$$

$$B_{10} = \frac{1}{M_{10}} \{A^a_{10}\ \tau_{10}\ \tau_{11}\ G[(1 - \rho^a_{10})\ H^a_{10-10} - 1]\ H^b_{10-11}$$

$$+ A^b_{10}\ \tau_{10}\ \tau_{11}\ G[(1 - \rho_{10})\ H^b_{10-10} - 1]\ H^a_{10-10}\ H^b_{10-11}$$

$$+ A^b_{10}\ (1 - \rho^b_{10})\ \tau^b_{11}\ H^b_{10-11}\}$$

$$B_{10} = \frac{1}{M_{10}}\ \tau_1\ H^b_{10-11}\ \{A^a_{10}\ \tau_{10}\ G[(1 - \rho^a_{10})\ H^a_{10-10} - 1]$$

$$+ A^b_{10}\ (\tau^2_{10}\ G\ H^a_{10-10}\ [(1 - \rho^b_{10})\ H^b_{10-10} - 1] + 1 - \rho^b_{10})\}$$

# APPENDIX D

# ERBE SCANNER THERMAL MODEL EQUATIONS

## SCANNER MODEL

The scanner model was developed by the same methods which were used for the non-scanner model development. The Equations (1) through (7) in the Appendix C are used to generate the constants of the thermal model Equation (24) in the Section 2.1.3.

To define the coefficients in the themal model, the enclosure coupling technique was used as another alternative approach. The following pages contain those coefficients defined by using the enclosure coupling method.

The attached figure shows the scanner model which has node description and enclosure descriptions. The enclosure has the number which is circled around. The numbers describing enclosure surfaces are underlined. In the illustration of the coefficients, the word that explains the procedure of derivation was omitted because they were already shown in Appendix C.

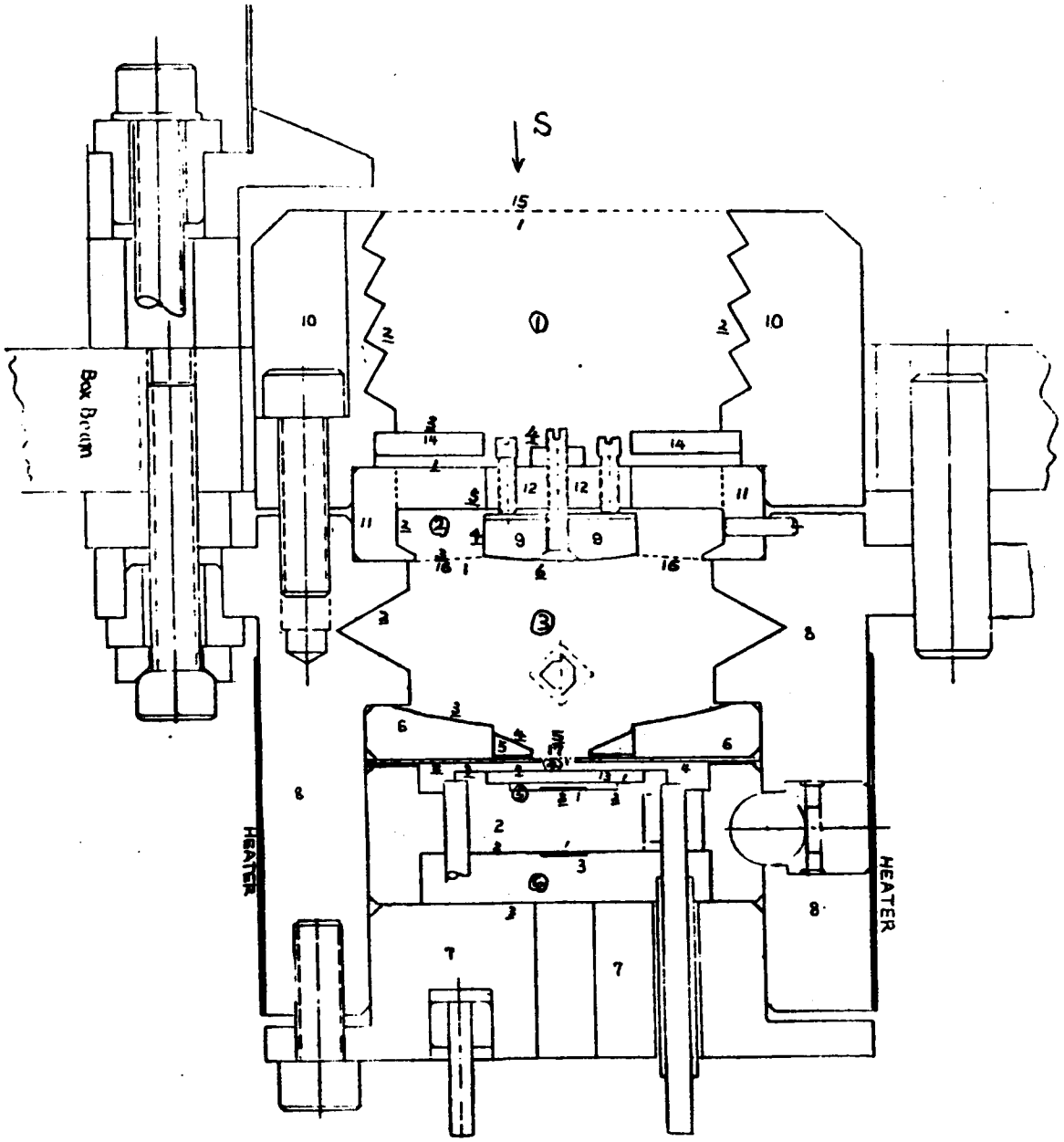


1. Active Flake
2. Heat Sink & Detector Assy.
3. Compensating Flake
4. Precision Aperture
5. Insert, Primary
6. Primary Mirror
7. Cap Assembly
8. Housing & Heater
9. Secondary Mirror
10. FOV Limiter
11. Mount, Secondary (A)
12. Mount, Secondary (B)
13. LW or SW Filter
14. SW Filter
15. Fictitious Surface at FOV
16. Fictitious Surface at Secondary
17. Fictitious Surface at Aperture

SCANNER MODEL

$$\begin{cases} A_{1,1} = -\dfrac{1}{M_1 R_{1-2}} \quad , \quad A_{1,2} = \dfrac{1}{M_1 R_{1-2}} \\ A_{1,3} = A_{1,4} = A_{1,5} = A_{1,6} = A_{1,7} = A_{1,8} = A_{1,9} = A_{1,10} = A_{1,11} = A_{1,12} = \\ \qquad A_{1,13} = A_{1,14} = 0 \end{cases}$$

$$\begin{cases} A_{2,1} = \dfrac{1}{M_1 R_{2-1}} \quad , \quad A_{2,2} = -\left(\dfrac{1}{M_2}\right)\left(\dfrac{1}{R_{2-1}} + \dfrac{1}{R_{2-3}} + \dfrac{1}{R_{2-4}} + \dfrac{1}{R_{2-7}} + \dfrac{1}{R_{2-8}} + \dfrac{1}{R_{2-13}}\right) \\ A_{2,3} = \dfrac{1}{M_2 R_{2-3}} \quad , \quad A_{2,4} = \dfrac{1}{M_2 R_{2-4}} \\ A_{2,5} = A_{2,6} = 0 \\ A_{2,7} = \dfrac{1}{M_2 R_{2-7}} \quad , \quad A_{2,8} = \dfrac{1}{M_2 R_{2-8}} \quad , \quad A_{2,13} = \dfrac{1}{M_2 R_{2-13}} \\ A_{2,9} = A_{2,10} = A_{2,11} = A_{2,12} = A_{2,14} = 0 \end{cases}$$

$$\begin{cases} A_{3,1} = 0 \quad , \quad A_{3,2} = +\dfrac{1}{M_3 R_{3-2}} \quad , \quad A_{3,3} = -\dfrac{1}{M_3 R_{3-2}} \\ A_{3,4} = A_{3,5} = A_{3,6} = A_{3,7} = A_{3,8} = A_{3,9} = A_{3,10} = A_{3,11} = A_{3,12} = A_{3,13} = A_{3,14} = 0 \end{cases}$$

$$\begin{cases} A_{4,1} = 0 \quad , \quad A_{4,2} = \dfrac{1}{M_4 R_{4-2}} \quad , \quad A_{4,3} = 0 \\ A_{4,4} = -\left(\dfrac{1}{M_4}\right)\left(\dfrac{1}{R_{4-2}} + \dfrac{1}{R_{4-6}} + \dfrac{1}{R_{4-8}}\right) \quad , \quad A_{4,5} = 0 \\ A_{4,6} = \dfrac{1}{M_4 R_{4-6}} \quad , \quad A_{4,7} = 0 \quad , \quad A_{4,8} = \dfrac{1}{M_4 R_{4-8}} \\ A_{4,9} = A_{4,10} = A_{4,11} = A_{4,12} = A_{4,13} = A_{4,14} = 0 \end{cases}$$

$$\begin{cases} A_{5,1} = A_{5,2} = A_{5,3} = A_{5,4} = 0 \\ A_{5,5} = -\dfrac{1}{M_5 R_{5-6}} \quad , \quad A_{5,6} = \dfrac{1}{M_5 R_{5-6}} \\ A_{5,7} = A_{5,8} = A_{5,9} = A_{5,10} = A_{5,11} = A_{5,12} = A_{5,13} = A_{5,14} = 0 \end{cases}$$

$$\begin{cases} A_{6,1} = A_{6,2} = A_{6,3} = 0 \\ A_{6,4} = \dfrac{1}{M_6 R_{6-4}} \quad , \quad A_{6,5} = \dfrac{1}{M_6 R_{6-5}} \\ A_{6,6} = -\left(\dfrac{1}{M_6}\right)\left(\dfrac{1}{R_{6-4}} + \dfrac{1}{R_{6-5}} + \dfrac{1}{R_{6-8}}\right) \\ A_{6,7} = 0 \quad , \quad A_{6,8} = \dfrac{1}{M_6 R_{6-8}} \\ A_{6,9} = A_{6,10} = A_{6,11} = A_{6,12} = A_{6,13} = A_{6,14} = 0 \end{cases}$$

$$\begin{cases} A_{7,1} = 0 \quad , \quad A_{7,2} = \dfrac{1}{M_7 R_{7-2}} \\ A_{7,3} = A_{7,4} = A_{7,5} = A_{7,6} = 0 \\ A_{7,7} = -\left(\dfrac{1}{M_7}\right)\left(\dfrac{1}{R_{7-2}} + \dfrac{1}{R_{7-8}}\right) \quad , \quad A_{7,8} = \dfrac{1}{M_7 R_{7-8}} \\ A_{7,9} = A_{7,10} = A_{7,11} = A_{7,12} = A_{7,13} = A_{7,14} = 0 \end{cases}$$

$$\begin{cases} A_{8,1} = 0 \ , \quad A_{8,2} = \dfrac{1}{M_8 R_{8-2}} \ , \quad A_{8,3} = 0 \ , \quad A_{8,4} = \dfrac{1}{M_8 R_{8-4}} \\ A_{8,5} = 0 \ , \quad A_{8,6} = \dfrac{1}{M_8 R_{8-6}} \ , \quad A_{8,7} = \dfrac{1}{M_8 R_{8-7}} \\ A_{8,8} = -\left(\dfrac{1}{M_8}\right)\left(\dfrac{1}{R_{8-2}} + \dfrac{1}{R_{8-4}} + \dfrac{1}{R_{8-6}} + \dfrac{1}{R_{8-7}} + \dfrac{1}{R_{8-10}} + \dfrac{1}{R_{8-11}}\right) \\ A_{8,9} = 0 \ , \quad A_{8,10} = \dfrac{1}{M_8 R_{8-10}} \ , \quad A_{8,11} = \dfrac{1}{M_8 R_{8-11}} \\ A_{8,12} = A_{8,13} = A_{8,14} = 0 \end{cases}$$

$$\begin{cases} A_{9,1} = A_{9,2} = A_{9,3} = A_{9,4} = A_{9,5} = A_{9,6} = A_{9,7} = A_{9,8} = 0 \\ A_{9,9} = -\dfrac{1}{M_9 R_{9-12}} \ , \quad A_{9,10} = 0 \ , \quad A_{9,11} = 0 \ , \quad A_{9,12} = \dfrac{1}{M_9 R_{9-12}} \\ A_{9,13} = A_{9,14} = 0 \end{cases}$$

$$\begin{cases} A_{10,1} = A_{10,2} = A_{10,3} = A_{10,4} = A_{10,5} = A_{10,6} = A_{10,7} = 0 \\ A_{10,8} = \dfrac{1}{M_{10} R_{10-8}} \ , \quad A_{10-9} = 0 \ , \\ A_{10-10} = -\left(\dfrac{1}{M_{10}}\right)\left(\dfrac{1}{R_{10-8}} + \dfrac{1}{R_{10-11}} + \dfrac{1}{R_{10-14}}\right) \\ A_{10-11} = \dfrac{1}{M_{10} R_{10-11}} \ , \quad A_{10-12} = 0 \ , \quad A_{10,13} = 0 \ , \quad A_{10,14} = \dfrac{1}{M_{10} R_{10-14}} \end{cases}$$

$$\begin{cases} A_{11,1} = A_{11,2} = A_{11,3} = A_{11,4} = A_{11,5} = A_{11,6} = A_{11,7} = 0 \\ A_{11,8} = \dfrac{1}{M_{11}R_{11-8}} \ , \quad A_{11,9} = 0 \ , \quad A_{11,10} = \dfrac{1}{M_{11}R_{11-10}} \ , \quad A_{11,12} = 0 \\ A_{11,13} = A_{11,14} = 0 \ , \quad A_{11,11} = -\left(\dfrac{1}{M_{11}}\right)\left(\dfrac{1}{R_{11-8}} + \dfrac{1}{R_{11-10}}\right) \end{cases}$$

$$\begin{cases} A_{12,1} = A_{12,2} = A_{12,3} = A_{12,4} = A_{12,5} = A_{12,6} = A_{12,7} = A_{12,8} = 0 \\ A_{12,9} = \dfrac{1}{M_{12}R_{12-9}} \ , \quad A_{12,10} = A_{12,11} = 0 \ , \quad A_{12,12} = -\dfrac{1}{M_{12}R_{12-9}} \\ A_{12,13} = 0 \ , \quad A_{12,14} = 0 \end{cases}$$

$$\begin{cases} A_{13,1} = 0 \ , \quad A_{13,2} = \dfrac{1}{M_{13}R_{13-2}} \ , \quad A_{13,3} = A_{13,4} = A_{13,5} = A_{13,6} = 0 \\ A_{13,7} = A_{13,8} = A_{13,9} = A_{13,10} = A_{13,11} = A_{13,12} = 0 \\ A_{13,13} = -\dfrac{1}{M_{13}R_{13-2}} \ , \quad A_{13,14} = 0 \end{cases}$$

$$\begin{cases} A_{14-1} = A_{14,2} = A_{14,3} = A_{14,4} = A_{14,5} = A_{14,6} = A_{14,7} = A_{14,8} = A_{14,9} = 0 \\ A_{14,10} = \dfrac{1}{M_{14}R_{14-10}} \ , \quad A_{14,11} = 0 \ , \quad A_{14,12} = 0 \ , \quad A_{14,13} = 0 \\ A_{14m14} = -\dfrac{1}{M_{14}R_{14-10}} \end{cases}$$

For the total channel, the filter glasses are removed. Accordingly, the $(\frac{1}{R_{i-j}})$ related with node number of filters have to set zero.

$$B_Q = [0, 0, 0, 0, 0, 0, 0, \frac{1}{M_8}, 0, 0, 0, 0, 0, 0]$$

Scanner:

Let

$$(H_{kji})_A = (\sum_j{}_{k-j} P_{j-i})_A ,$$

where subscript A denotes the enclosure A.

Then let

$$G_1 = [1 - \tau_{13}^2 (H_{13j13})_D (H_{13m13})_F]^{-1}$$

$$S_1 = (H_{17m17})_F + \tau_{13}^2 G_1 (H_{17m13})_F (H_{13j13})_D (H_{13m17})_F$$

$$G_2 = [1 - \tau_{17}^2 S_1 (H_{17j17})_C]^{-1}$$

$$S_2 = (H_{16j16})_C + \tau_{17}^2 S_1 G_2 (H_{17j16})_C (H_{16j17})_C$$

$$G_3 = [1 - \tau_{16}^2 S_2 (H_{16m16})_B]^{-1}$$

$$S_3 = (H_{14m14})_B + \tau_{16}^2 S_2 G_3 (H_{14m16})_B (H_{16m14})_B$$

$$G_4 = [1 - \tau_{14}^2 S_3 (H_{14j14})_A]^{-1}$$

$$X_1 = F_{1,1}\Omega_1 + F_{1,2}\Omega_2 + F_{1,4}\Omega_4 + F_{1,5}\Omega_5 + F_{1,6}\Omega_6 + F_{1,8}\Omega_8 + F_{1,9}\Omega_9$$

$$+ F_{1,13}\Omega_{13}$$

where

$$F_{1,1} = \tau_{13}\,\epsilon_1\,G_1\,G_2(H_{17m13})_F\,(H_{13j1})_D$$

$$F_{1,2} = \epsilon_2\,G_2\,\{(H_{17m2})_F + \tau_{13}\,G_1(H_{17m13})_F\,(H_{13j2})_D + \tau_{13}^2\,G_1(H_{17m13})_F$$

$$(H_{13j13})_D\,(H_{13m2})_F\}$$

$$F_{1,4} = \epsilon_4\,G_2\,\{(H_{17m4})_F + \tau_{13}^2\,G_1(H_{17m13})_F\,(H_{13m13})_D\,(H_{13m4})_F\}$$

$$F_{1,5} = \tau_{17}\,\epsilon_5\,S_1\,G_2(H_{17j5})_C$$

$$F_{1,6} = \tau_{17}\,\epsilon_6\,S_1\,G_2(H_{17j6})_C$$

$$F_{1,8} = \tau_{17}\,\epsilon_8\,S_1\,G_2(H_{17j8})_C$$

$$F_{1,9} = \tau_{17}\,\epsilon_9\,S_1\,G_2(H_{17j9})_C$$

$$F_{1,13} = \epsilon_{13}\,G_2\,\{(H_{17m13})F + \tau_{13}\,G_1(H_{17m13})_F\,(H_{13j13})_D + \tau_{13}^2\,G_1\,(H_{17m13})_F$$

$$(H_{13j13})_D\,(H_{13m13})_F\}$$

$$X_2 = F_{2,1}\Omega_1 + F_{2,2}\Omega_2 + F_{2,4}\Omega_4 + F_{2,5}\Omega_5 + F_{2,6}\Omega_6 + F_{2,8}\Omega_8 + F_{2,9}\Omega_9 + F_{2,11}\Omega_{11}$$

$$+ F_{2,12}\Omega_{12} + F_{2,13}\Omega_{13} + F_{2,14}\Omega_{14}$$

where

$$F_{2,1} = \tau_{13}\ \tau_{17}\ G_1\ G_2\ G_3 (H_{16j17})_C\ (H_{17m13})_F\ (H_{13j1})_D$$

$$F_{2,2} = \tau_{17}\ \epsilon_2\ G_2\ G_3 (H_{16j17})_C \{(H_{17m2})_F + \tau_{13}\ G_1 (H_{17m13})_F\ (H_{13j2})_D + \tau_{13}^2\ G_1 (H_{17m13})_F\ (H_{13j13})_D\ (H_{13m2})_F\}$$

$$F_{2,4} = \tau_{17}\ \epsilon_4\ G_2\ G_3 (H_{16j17})_C \{(H_{17m4})_F + \tau_{13}^2\ G_1 (H_{17m13})_F\ (H_{13m13})_D\ (H_{13m4})_F\}$$

$$F_{2,5} = \epsilon_5\ G_3 \{(H_{16j5})_C + \tau_{17}^2\ S_1\ G_2 (H_{16j17})_C\ (H_{17j5})_C\}$$

$$F_{2,6} = \epsilon_6\ G_3 \{(H_{16j6})_C + \tau_{17}^2\ S_1\ G_2 (H_{16j17})_C\ (H_{17j6})_C\}$$

$$F_{2,8} = \epsilon_8\ G_3 \{(H_{16j8})_C + \tau_{17}^2\ S_1\ G_2 (H_{16j17})_C\ (H_{17j8})_C\}$$

$$F_{2,9} = \epsilon_9\ G_3 \{(H_{16j9})_C + \tau_{16}\ S_2 (H_{16m9})_B + \tau_{17}^2\ S_1\ G_2 (H_{16j17})_C\ (H_{17j9})_C\}$$

$$F_{2,11} = \tau_{16}\ \epsilon_{11}\ S_2\ G_3 (H_{16m11})_B$$

$$F_{2,12} = \tau_{16}\ \epsilon_{12}\ S_2\ G_3 (H_{16m12})_B$$

$$F_{2,13} = \tau_{17}\ \epsilon_{13}\ G_2\ G_3 (H_{16j17})_C\ (H_{17m13})_F \{1 + \tau_{13}\ G_1 (H_{13j13})_D + \tau_{13}^2\ G_1 (H_{13j13})_D\ (H_{13m13})_F\}$$

$$F_{2,14} = \tau_{16}\ \epsilon_{14}\ S_2\ G_3 (H_{16m14})_B$$

$$\check{E}_{14} = U_{1,1}\Omega_1 + U_{1,2}\Omega_2 + U_{1,4}\Omega_3 + U_{1,5}\Omega_5 + U_{1,6}\Omega_6 + U_{1,8}\Omega_8 + U_{1,9}\Omega_9 + U_{1,10}\Omega_{10}$$

$$+ U_{1,11}\Omega_{11} + U_{1,12}\Omega_{12} + U_{1,13}\Omega_{13} + U_{1,14}\Omega_{14} + U_{1,15}E$$

$$U_{1,1} = \tau_{16}\, G_4 (H_{14m16})_B\, F_{2,1}$$

$$U_{1,2} = \tau_{16}\, G_4 (H_{14m16})_B\, F_{2,2}$$

$$U_{1,4} = \tau_{16}\, G_4 (H_{14m16})_B\, F_{2,4}$$

$$U_{1,5} = \tau_{16}\, G_4 (H_{14m16})_B\, F_{2,5}$$

$$U_{1,6} = \tau_{16}\, G_4\, (H_{14m16})_B\, F_{2,6}$$

$$U_{1,8} = \tau_{16}\, G_4 (H_{14m16})_B\, F_{2,8}$$

$$U_{1,9} = G_4\{\tau_{16}(H_{14m16})_B\, F_{2,9} + \epsilon_9 (H_{14m9})_B\}$$

$$U_{1,10} = \tau_{10}\, S_3\, G_4\, \epsilon_{10} (H_{14j10})_A$$

$$U_{1,11} = G_4\, \{\epsilon_{11}(H_{14m11})_B + \tau_{16}(H_{14m16})_B\, F_{2,11}\}$$

$$U_{1,12} = G_4\, \{\epsilon_{12}(H_{14m12})_B + \tau_{14}\, \epsilon_{12}\, S_3 (H_{14j12})_A + \tau_{16}(H_{14m16})_B\, F_{2,12}\}$$

$$U_{1,13} = \tau_{16}\, G_4 (H_{14m16})_B\, F_{2,13}$$

$$U_{1,14} = G_4\, \{\epsilon_{14}(H_{14m14})_B + \tau_{14}\, \epsilon_{14}\, S_3 (H_{14j14})_A + \tau_{16}(H_{14m16})_B\, F_{2,14}\}$$

$$U_{1,15} = \tau_{15}\, G_4 (H_{14j15})_A$$

$$\tilde{E}_{14} = U_{2,1}\Omega_1 + U_{2,2}\Omega_2 + U_{2,4}\Omega_4 + U_{2,5}\Omega_5 + U_{2,6}\Omega_6 + U_{2,8}\Omega_8 + U_{2,9}\Omega_9 + U_{2,10}\Omega_{10}$$

$$+ U_{2,11}\Omega_{11} + U_{2,12}\Omega_{12} + U_{2,13}\Omega_{13} + U_{2,14}\Omega_{14} + U_{2,15}E$$

$$U_{2,1} = \tau_{14}\,\tau_{16}\,G_4(H_{14j14})_A\,(H_{14m16})_B\,F_{2,1}$$

$$U_{2,2} = \tau_{14}\,\tau_{16}\,G_4(H_{14h14})_A\,(H_{14m16})_B\,F_{2,2}$$

$$U_{2,4} = \tau_{14}\,\tau_{16}\,G_4(H_{14j14})_A\,(H_{14m16})_B\,F_{2,4}$$

$$U_{2,5} = \tau_{14}\,\tau_{16}\,G_4(H_{14j14})_A\,(H_{14m16})_B\,F_{2,5}$$

$$U_{2,6} = \tau_{14}\,\tau_{16}\,G_4(H_{14j14})_A\,(H_{14m16})_B\,F_{2,6}$$

$$U_{2,8} = \tau_{14}\,\tau_{16}\,G_4(H_{14j14})_A\,(H_{14m16})_B\,F_{2,8}$$

$$U_{2,9} = G_4(H_{14j14})_A\,\{\tau_{14}\,\tau_{16}(H_{14m16})_B\,F_{2,9} + \tau_{14}\,\epsilon_9(H_{14m9})_B\}$$

$$U_{2,10} = \epsilon_{10}(H_{14j10})_A\,\{1 + \tau_{14}^2\,S_3\,G_4(H_{14j14})_A\}$$

$$U_{2,11} = G_4(H_{14j14})_A\,\{\tau_{14}\,\tau_{16}(H_{14m16})_B\,F_{2,11} + \tau_{14}\,\epsilon_{11}(H_{14m11})_B\}$$

$$U_{2,12} = \tau_{14}\,\tau_{16}\,G_4(H_{14j14})_A\,(H_{14m16})_B\,F_{2,12} + \epsilon_{12}(H_{14j12})_A[1 + \tau_{14}^2\,S_3\,G_4$$

$$(H_{14j14})_A] + \tau_{14}\,\epsilon_{12}\,G_4(H_{14j14})_A\,(H_{14m12})_B$$

$$U_{2,13} = \tau_{14}\,\tau_{16}\,G_4(H_{14j14})_A\,(H_{14m16})_B\,F_{2,13}$$

$$U_{2,14} = (H_{14j14})_A \{\tau_{14}\ \epsilon_{14}\ G_4(H_{14ml4})_B + \tau_{14}\ \tau_{16}\ G_4(H_{14ml6})_B\ F_{2,14} + \epsilon_{14}$$

$$[1 + \tau_{14}^2\ S_3\ G_4(H_{14j14})_A]\}$$

$$U_{2,15} = \tau_{15}(H_{14j15})_A \{1 + \tau_{14}\ G_4(H_{14j14})_A\}$$

$$\hat{E}_{16} = U_{3,1}\Omega_1 + U_{3,2}\Omega_2 + U_{3,4}\Omega_4 + U_{3,5}\Omega_5 + U_{3,6}\Omega_6 + U_{3,8}\Omega_8 + U_{3,9}\Omega_9 + U_{3,10}\Omega_{10}$$

$$+ U_{3,11}\Omega_{11} + U_{3,12}\Omega_{12} + U_{3,13}\Omega_{13} + U_{3,14}\Omega_{14} + U_{3,15}E$$

$$U_{3,1} = \tau_{14}\ \tau_{16}\ S_2\ G_3(H_{16ml4})_B\ U_{2,1} + \tau_{13}\ \tau_{17}\ G_1\ G_2\ G_3\ \epsilon_1(H_{16j17})_C\ (H_{17ml3})_F$$

$$(H_{13j1})_D$$

$$U_{3,2} = \tau_{14}\ \tau_{16}\ S_2\ G_3(H_{16ml4})_B\ U_{2,2} + \tau_{13}\ \tau_{17}\ \epsilon_2\ G_1\ G_2\ G_3(H_{16j17})_C\ (H_{17ml3})_F$$

$$(H_{13j13})_D + \tau_{17}\ \epsilon_2\ G_2\ G_3(H_{16j17})_C\ (H_{17m2})_F + \tau_{13}^2\ \tau_{17}\ \epsilon_2\ G_1\ G_2\ G_3$$

$$(H_{16j17})_C\ (H_{17ml3})_F\ (H_{13j13})_D\ *\ (H_{13m2})_F$$

$$U_{3,4} = \tau_{14}\ \tau_{16}\ S_2\ G_3(H_{16ml4})_B\ U_{2,4} + \tau_{17}\ \epsilon_4\ G_2\ G_3(H_{16j17})_C\ (H_{17m4})_F$$

$$+ \tau_{13}^2\ \tau_{17}\ \epsilon_4\ G_1\ G_2\ G_3(H_{16j17})_C\ (H_{17n13})_F\ (H_{13j13})_D\ (H_{13m4})_F$$

$$U_{3,5} = \tau_{14}\ \tau_{16}\ S_2\ G_3(H_{16ml4})_B\ U_{2,5} + G_3\ \epsilon_5(H_{16j5})_C + \tau_{17}^2\ \epsilon_5\ S_1\ G_2(H_{16j17})_C$$

$$(H_{17j5})_C$$

$$U_{3,6} = \tau_{14}\ \tau_{16}\ G_3(H_{16ml4})_B\ U_{2,6} + \epsilon_6\ G_3(H_{16j6})_C + \tau_{17}^2\ \epsilon_6\ S_1\ G_2\ G_3\ (H_{16j17})_C$$

$$(H_{17j6})_C$$

$$U_{3,8} = \tau_{14}\,\tau_{16}\,S_2\,G_3(H_{16m14})_B\,U_{2,8} + \epsilon_8\,G_3(H_{16j8})_C + \tau_{17}^2\,\epsilon_8\,S_1\,G_2\,G_3(H_{16j17})_C$$
$$(H_{17j8})_C$$

$$U_{3,9} = \tau_{14}\,\tau_{16}\,S_2\,G_3(H_{16m14})_B\,U_{2,9} + \epsilon_9\,G_3(H_{16j9})_C + \tau_{17}^2\,\epsilon_8\,S_1\,G_2\,G_3(H_{16j17})_C$$
$$(H_{17j9})_C + \tau_{16}\,\epsilon_9\,S_2\,G_3(H_{17j9})_C$$

$$U_{3,10} = \tau_{14}\,\tau_{10}\,S_2\,G_3(H_{16m14})_B\,U_{2,10}$$

$$U_{3,11} = \tau_{14}\,\tau_{16}\,S_2\,G_3(H_{16m14})_B\,U_{2,11} + \tau_{16}\,\epsilon_{11}\,S_2\,G_3(H_{17j11})_C$$

$$U_{3,12} = \tau_{14}\,\tau_{16}\,S_2\,G_3(H_{16m14})_B\,U_{2,12} + \tau_{16}\,\epsilon_{12}\,S_2\,G_3(H_{17j12})_C$$

$$U_{3,13} = \tau_{14}\,\tau_{16}\,S_2\,G_3(H_{16m14})_B\,U_{2,13} + \tau_{17}\,\epsilon_{13}\,G_3(H_{16j17})_C\,(H_{17m13})_F$$
$$+ \tau_{13}\,\tau_{17}\,\epsilon_{13}\,G_1\,G_2\,G_3(H_{16j17})_C\,(H_{13j13})_D\,(H_{17m13})_F[1 + \tau_{13}(H_{13m13})_F]$$

$$U_{3,14} = \tau_{14}\,\tau_{16}\,S_2\,G_3(H_{16m14})_B\,U_{2,14} + \tau_{16}\,\epsilon_{14}\,S_2\,G_3(H_{17j14})_C$$

$$U_{3,15} = \tau_{14}\,\tau_{16}\,S_2\,G_3(H_{16m14})_B\,U_{2,15}$$

$$\check{E}_{16} = U_{4,1}\Omega_1 + U_{4,2}\Omega_2 + U_{4,4}\Omega_4 + U_{4,5}\Omega_5 + U_{4,6}\Omega_6 + U_{4,8}\Omega_8 + U_{4,9}\Omega_9 + U_{4,10}\Omega_{10}$$
$$+ U_{4,11}\Omega_{11} + U_{4,12}\Omega_{12} + U_{4,13}\Omega_{13} + U_{4,14}\Omega_{14} + U_{4,15}E$$

$$U_{4,1} = \tau_{14}(H_{16m14})_B[1 + \tau_{16}^2\,S_2\,G_3(H_{16m16})_B]\,U_{2,1} + \tau_{16}\,\tau_{17}\,G_3(H_{16m16})_B$$
$$(H_{16j17})_C\,F_{1,1}$$

$$U_{4,2} = \tau_{14}(H_{16m14})_B[1 + \tau_{16}^2\ S_2\ G_3(H_{16m16})_B]\ U_{2,2} + \tau_{16}\ \tau_{17}\ G_3(H_{16m16})_B$$

$$(H_{16j17})_C\ F_{1,2}$$

$$U_{4,4} = \tau_{14}(H_{16m14})_B[1 + \tau_{16}^2\ S_2\ G_3(H_{16m16})_B]\ U_{2,4} + \tau_{16}\ \tau_{17}\ G_3(H_{16m16})_B$$

$$(H_{16j17})_C\ F_{1,4}$$

$$U_{4,5} = \tau_{14}(H_{16m14})_B[1 + \tau_{16}^2\ S_2\ G_3(H_{16m16})_B]\ U_{2,5} + \tau_{16}\ \tau_{17}\ G_3(H_{16m16})_B$$

$$(H_{16j17})_C\ F_{1,5} + \tau_{16}\ \epsilon_5\ G_3(H_{16m16})_B\ (H_{16j5})_C$$

$$U_{4,8} = \tau_{14}(H_{16m14})_B[1 + \tau_{16}^2\ S_2\ G_3(H_{16m16})_B]\ U_{2,8} + \tau_{16}\ \tau_{17}\ G_3(H_{16m16})_B$$

$$(H_{16j17})_C\ F_{1,8} + \tau_{16}\ \epsilon_8\ G_3(H_{16m16})_B\ (H_{16j8})_C$$

$$U_{4,9} = \tau_{14}(H_{16m14})_B[1 + \tau_{16}^2\ S_2\ G_3(H_{16m16})_B]\ U_{2,9} + \tau_{16}\ \tau_{17}\ G_3(H_{16m16})_B$$

$$(H_{16j17})_C\ F_{1,9} + \epsilon_9(H_{16m9})_B + \tau_{16}\ \epsilon_9\ G_3(H_{16m16})_B\ (H_{16j9})_C$$

$$+ \tau_{16}^2\ \epsilon_9\ S_2\ G_3(H_{16m16})_B\ (H_{16m9})_B$$

$$U_{4,10} = \tau_{14}(H_{16m14})_B[1 + \tau_{16}^2\ S_2\ G_3(H_{16m16})_B]\ U_{2,10}$$

$$U_{4,11} = \tau_{14}(H_{16m14})_B[1 + \tau_{16}^2\ S_2\ G_3(H_{16m16})_B]\ U_{2,11} + \epsilon_{11}(H_{16m11})_B$$

$$+ \tau_{16}^2\ \epsilon_{11}\ S_2\ G_3(H_{16m16})_B\ (H_{16m11})_B$$

$$U_{4,12} = \tau_{14}(H_{16m14})_B[1 + \tau_{16}^2\ S_2\ G_3(H_{16m16})_B]\ U_{2,12} + \epsilon_{12}(H_{16m12})_B$$

$$+ \tau_{16}^2\ \epsilon_{12}\ S_2\ G_3(H_{16m16})_B\ (H_{16m12})_B$$

$$U_{4,13} = \tau_{14}(H_{16m14})_B[1 + \tau_{16}^2 S_2 G_3(H_{16m16})_B] U_{2,13} + \tau_{16} \tau_{17} G_3(H_{16m16})_B (H_{16j17})_C F_{1,13}$$

$$U_{4,14} = \tau_{14}(H_{16m14})_B[1 + \tau_{16}^2 S_2 G_3(H_{16m16})_B] U_{2,14} + \tau_{16}^2 \epsilon_{14} S_2 G_3 (H_{16m16})_B (H_{16m14})_B + \epsilon_{14}(H_{16m14})_B$$

$$U_{4,15} = \tau_{14}(H_{16m14})_B[1 + \tau_{16}^2 S_2 G_3(H_{16m16})_B] U_{2,15}$$

$$\bar{E}_{17} = U_{5,1}\Omega_1 + U_{5,2}\Omega_2 + U_{5,4}\Omega_4 + U_{5,5}\Omega_5 + U_{5,6}\Omega_6 + U_{5,8}\Omega_8 + U_{5,9}\Omega_9 + U_{5,10}\Omega_{10} + U_{5,11}\Omega_{11} U_{5,12}\Omega_{12} + U_{5,13}\Omega_{13} + U_{5,14}\Omega_{14} + U_{5,15}E$$

$$U_{5,1} = \epsilon_1 \tau_{13} G_1 G_2(H_{17m13})_F (H_{13j1})_D + \tau_{16} \tau_{17} S_1 G_2(H_{17j16})_C U_{4,1}$$

$$U_{5,2} = \epsilon_2 G_2(H_{17m2})_F + \epsilon_2 \tau_{13} G_1 G_2(H_{17m13})_F[(H_{13j2})_D + (H_{13j13})_D (H_{13m2})_F \tau_{13}] + \tau_{16} \tau_{17} S_1 G_2(H_{17j16})_C U_{4,2}$$

$$U_{5,4} = \epsilon_4 G_2(H_{17m4})_F + \epsilon_4 \tau_{13}^2 G_1 G_2(H_{17m13})_F (H_{13j13})_D (H_{13m4})_F + \tau_{16} \tau_{17} S_1 G_2(H_{17j16})_C U_{4,4}$$

$$U_{5,5} = \epsilon_5 \tau_{17} S_1 G_2(H_{17j5})_C + \tau_{16} \tau_{17} S_1 G_2(H_{17j16})_C U_{4,5}$$

$$U_{5,6} = \epsilon_6 \tau_{17} S_1 G_2(H_{17j6})_C + \tau_{16} \tau_{17} S_1 G_2(H_{17j16})_C U_{4,6}$$

$$U_{5,8} = \epsilon_8 \tau_{17} S_1 G_2(H_{17j8})_C + \tau_{16} \tau_{17} S_1 G_2(H_{17j16})_C U_{4,8}$$

$$U_{5,9} = \epsilon_9 \tau_{17} S_1 G_2(H_{17j9})_C + \tau_{16} \tau_{17} S_1 G_2(H_{17j16})_C U_{4,9}$$

$$U_{5,10} = \tau_{16} \tau_{17} S_1 G_2(H_{17j16})_C U_{4,10}$$

$$U_{5,11} = \tau_{16} \tau_{17} S_1 G_2(H_{17j16})_C U_{4,11}$$

$$U_{5,12} = \tau_{16} \tau_{17} S_1 G_2(H_{17j16})_C U_{4,12}$$

$$U_{5,13} = \epsilon_{13} G_2(H_{17m13})_F + \epsilon_{13} \tau_{13} G_1 G_2(H_{17m13})_F (H_{13j13})_D[1 + \tau_{13}(H_{13m13})_F]$$
$$+ \tau_{16} \tau_{17} S_1 G_2(H_{17j16})_C U_{4,13}$$

$$U_{5,14} = \tau_{16} \tau_{17} S_1 G_2(H_{17j16})_C U_{4,14}$$

$$U_{5,15} = \tau_{16} \tau_{17} S_1 G_2(H_{17j16})_C U_{4,15}$$

$$\hat{E}_{17} = U_{6,1}\Omega_1 + U_{6,2}\Omega_2 + U_{6,4}\Omega_4 + U_{6,5}\Omega_5 + U_{6,6}\Omega_6 + U_{6,8}\Omega_8 + U_{6,9}\Omega_9 + U_{6,10}\Omega_{10}$$
$$+ U_{6,11}\Omega_{11} + U_{6,12}\Omega_{12} + U_{6,13}\Omega_{13} + U_{6,14}\Omega_{14} + U_{6,15}E$$

$$U_{6,1} = \epsilon_1 \tau_{13} \tau_{17} G_1 G_2(H_{17j17})_C (H_{17m13})_F (H_{13j1})_D + \tau_{16} G_2(H_{17j16})_C U_{4,1}$$

$$U_{6,2} = \epsilon_2 \tau_{17} G_2(H_{17j17})_C (H_{17m2})_F + \epsilon_2 \tau_{13} \tau_{17} G_1 G_2(H_{17j17})_C (H_{17m13})_F$$
$$[(H_{13j2})_D + \tau_{13}(H_{13j13})_D (H_{13m2})_F] + \tau_{16} G_2(H_{17j16})_C U_{4,2}$$

$$U_{6,4} = \epsilon_4 \tau_{17} G_2(H_{17j17})_C (H_{17m4}(_F + \epsilon_4 \tau_{13}^2 \tau_{17} G_1 G_2(H_{17j17})_C (H_{17m13})_F$$
$$(H_{13j13})_D (H_{13m4})_F + \tau_{16} G_2(H_{17j16})_C U_{4,4}$$

$$U_{6,5} = \epsilon_5\, G_2(H_{17j5})_C + \tau_{16}\, G_2(H_{17j16})_C\, U_{4,5}$$

$$U_{6,6} = \epsilon_6\, G_2(H_{17j6})_C + \tau_{16}\, G_2(H_{17j16})_C\, U_{4,6}$$

$$U_{6,8} = \epsilon_8\, G_2(H_{17j8})_C + \tau_{16}\, G_2(H_{17j16})_C\, U_{4,8}$$

$$U_{6,9} = \epsilon_9\, G_2(H_{17j9})_C + \tau_{16}\, G_2(H_{17j16})_C\, U_{4,9}$$

$$U_{6,10} = \tau_{16}\, G_2(H_{17j16})_C\, U_{4,10}$$

$$U_{6,11} = \tau_{16}\, G_2(H_{17j16})_C\, U_{4,11}$$

$$U_{6,12} = \tau_{16}\, G_2(H_{17j16})_C\, U_{4,12}$$

$$U_{6,13} = \epsilon_{13}\, \tau_{13}\, \tau_{17}\, G_1\, G_2(H_{17j17})_C\, (H_{17m13})_F\, (H_{13j13})_D[1 + \tau_{13}(H_{13m13})_F]$$

$$+ \epsilon_{13}\, \tau_{17}\, G_2(H_{17j17})_C\, (H_{17n13})_F + \tau_{16}\, G_2(H_{17j16})_C\, U_{4,13}$$

$$U_{6,14} = \tau_{16}\, G_2(H_{17j16})_C\, U_{4,14}$$

$$U_{6,15} = \tau_{16}\, G_2(H_{17j16})_C\, U_{4,15}$$

$$E_{13} = U_{7,1}\Omega_1 + U_{7,2}\Omega_2 + U_{7,4}\Omega_4 + U_{7.5}\Omega_5 + U_{7,6}\Omega_6 + U_{7,8}\Omega_8 + U_{7,9}\Omega_9 + U_{7,10}\Omega_{10}$$

$$+ U_{7,11}\Omega_{11} + U_{7,12}\Omega_{12} + U_{7,13}\Omega_{13} + U_{7,14}\Omega_{14} + U_{7,15}E$$

$$U_{7,1} = \epsilon_1\, G_1(H_{13j1})_D + \tau_{13}\, \tau_{17}\, G_1(H_{13j13})_D\, (H_{13m17})_F\, U_{6,1}$$

$$U_{7,2} = \epsilon_2 G_1(H_{13j2})_D + \epsilon_2 \tau_{13} G_1(H_{13j13})_D (H_{13m2})_F + \tau_{13} \tau_{17} G_1(H_{13j13})_D (H_{13m17})_F U_{6,2}$$

$$U_{7,4} = \epsilon_4 \tau_{13} G_1(H_{13j13})_D (H_{13m4})_F + \tau_{13} \tau_{17} G_1(H_{13j13})_D (H_{13m17})_F U_{6,4}$$

$$U_{7,5} = \tau_{13} \tau_{17} G_1(H_{13j13})_D (H_{13m17})_F U_{6,5}$$

$$U_{7,6} = \tau_{13} \tau_{17} G_1(H_{13j13})_D (H_{13m17})_F U_{6,6}$$

$$U_{7,8} = \tau_{13} \tau_{17} G_1(H_{13j13})_D (H_{13m17})_F U_{6,8}$$

$$U_{7,9} = \tau_{13} \tau_{17} G_1 (H_{13j13})_D (H_{13m17})_F U_{6,9}$$

$$U_{7,10} = \tau_{13} \tau_{17} G_1(H_{13j13})_D (H_{13m17})_F U_{6,10}$$

$$U_{7,11} = \tau_{13} \tau_{17} G_1(H_{13j13})_D (H_{k3m17})_F U_{6,11}$$

$$U_{7,12} = \tau_{13} \tau_{17} G_1(H_{13j13})_D (H_{13m17})_F U_{6,12}$$

$$U_{7,13} = \epsilon_{13} G_1(H_{13j13})_D + \epsilon_{13} \tau_{13} G_1(H_{13j13})_D (H_{13m13})_F + \tau_{13} \tau_{17} G_1 (H_{13j13})_D (H_{13m17})_F U_{6,13}$$

$$U_{7,14} = \tau_{13} \tau_{17} G_1(H_{13j13})_D (H_{13m17})_F U_{6,14}$$

$$U_{7,15} = \tau_{13} \tau_{17} G_1(H_{13j13})_D (H_{13m17})_F U_{6,15}$$

$$\bar{E}_{13} = U_{8,1}\Omega_1 + U_{8,2}\Omega_2 + U_{8,4}\Omega_4 + U_{8,5}\Omega_5 + U_{8,6}\Omega_6 + U_{8,8}\Omega_8 + U_{8,9}\Omega_9 + U_{8,10}\Omega_{10}$$

$$+ U_{8,11}\Omega_{11} + U_{8,12}\Omega_{12} + U_{8,13}\Omega_{13} + U_{8,\Omega_{14}\ 14} + U_{8,15}E$$

$$U_{8,1} = \epsilon_1\ \tau_{13}\ G_1(H_{13m13})_F\ (H_{13j1})_D + \tau_{17}\ G_1(H_{13m17})_F\ U_{6,1}$$

$$U_{8,2} = \epsilon_2\ \tau_{13}\ G_1(H_{13m13})_F\ (H_{13i2})_D + \epsilon_2\ G_2(H_{13m2})_F + \tau_{17}\ G_1(H_{13m17})_F\ U_{6,2}$$

$$U_{8,4} = \epsilon_4\ G_1(H_{13m4})_F + \tau_{17}\ G_1(H_{13m17})_F\ U_{6,4}$$

$$U_{8,5} = \tau_{17}\ G_1(H_{13m17})_F\ U_{6,5}$$

$$U_{8,6} = \tau_{17}\ G_1(H_{13m17})_F\ U_{6,6}$$

$$U_{8,8} = \tau_{17}\ G_1(H_{13m17})_F\ U_{6,8}$$

$$U_{8,9} = \tau_{17}\ G_1(H_{13m17})_F\ U_{6,9}$$

$$U_{8,10} = \tau_{17}\ G_1(H_{13m17})_F\ U_{6,10}$$

$$U_{8,11} = \tau_{17}\ G_1(H_{13m17})_F\ U_{6,11}$$

$$U_{8,12} = \tau_{17}\ G_1(H_{13m17})_F\ U_{6,12}$$

$$U_{8,13} = \epsilon_{13}\ \tau_{13}\ G_1(H_{13m13}(_F\ (H_{13j13})_D + \epsilon_{13}\ G_1(H_{13m13})_F + \tau_{17}\ G_1(H_{13m17})_F\ U_{6,13}$$

$$U_{8,14} = \tau_{17}\ G_1(H_{13m17})_F\ U_{6,14}$$

$$U_{8,15} = \tau_{17}\ G_1(H_{13m17})_F\ U_{6,15}$$

$$D_{1,1} = \left(\frac{\sigma A_1}{M_1}\right)[(1-\rho_1)\ \epsilon_1\ (H_{1j1})_D - \epsilon_1 + (1-\rho_1)\ \tau_{13}\ (H_{1j13})_D\ U_{8,1}]_{S,L}$$

$$D_{1,2} = \left(\frac{\sigma A_1}{M_1}\right)[(1-\rho_1)\ \epsilon_2 (H_{1j2})_D + (1-\rho_1)\ \tau_{13} (H_{1j13})_D\ U_{8,2}]_{S,L}$$

$$D_{1,3} = 0$$

$$D_{1,4} = \left(\frac{\sigma A_1}{M_1}\right)[(1-\rho_1)\ \tau_{13} (H_{1j13})_D\ U_{8,4}]_{S,L}$$

$$D_{1,5} = \left(\frac{\sigma A_1}{M_1}\right)[(1-\rho_1)\ \tau_{13} (H_{1j13})_D\ U_{8,5}]_{S,L}$$

$$D_{1,6} = \left(\frac{\sigma A_1}{M_1}\right)[(1-\rho_1)\ \tau_{13} (H_{1j13})_D\ U_{8,6}]_{S,L}$$

$$D_{1,7} = 0$$

$$D_{1,8} = \left(\frac{\sigma A_1}{M_1}\right)[(1-\rho_1)\ \tau_{13} (H_{1j13})_D\ U_{8,8}]_{S,L}$$

$$D_{1,9} = \left(\frac{\sigma A_1}{M_1}\right)[(1-\rho_1)\ \tau_{13} (H_{1j13})_D\ U_{8,9}]_{S,L}$$

$$D_{1,10} = \left(\frac{\sigma A_1}{M_1}\right)[(1-\rho_1)\ \tau_{13} (H_{1j13})_D\ U_{8,10}]_{S,L}$$

$$D_{1,11} = \left(\frac{\sigma A_1}{M_1}\right)[(1-\rho_1)\ \tau_{13} (H_{1j13})_D\ U_{8,11}]_{S,L}$$

$$D_{1,12} = \left(\frac{\sigma A_1}{M_1}\right)[(1-\rho_1)\ \tau_{13} (H_{1j13})_D\ U_{8,12}]_{S,L}$$

$$D_{1,13} = \left(\frac{\sigma A_1}{M_1}\right)[(1-\rho_1)\ \tau_{13} (H_{1j13})_D\ U_{1,13} + (1-\rho_1)\ \epsilon_{13} (H_{1j13})_D]_{S,L}$$

$$D_{1,14} = \left(\frac{\sigma A_1}{M_1}\right)[(1-\rho_1)\ \tau_{13} (H_{1j1\tilde{3}})_D\ U_{8,14}]_{S,L}$$

$$D_{2,1} = \left(\frac{\sigma}{M_2}\right) \{A_{2D}(1-\rho_2)[\epsilon_1(H_{2j1})_D + \tau_{13}(H_{2j13})_D\ U_{8,1}] + A_{2F}(1-\rho_2)[\tau_{13}$$
$$(H_{2m13})_F\ U_{7,1} + \tau_{17}(H_{2m17})_F\ U_{6,1}]\}_{S,L}$$

$$D_{2,2} = \left(\frac{\sigma}{M_2}\right) \{A_{2E}[(1-\rho_2)\ \epsilon_2(H_{2j2})_E - \epsilon_2] + A_{2D}[(1-\rho_2)\ \epsilon_2(H_{2j2}) - \epsilon_2$$
$$+ (1-\rho_2)\ \tau_{13}(H_{2j13})_D\ U_{8,2}] + A_{2F}[(1-\rho_2)\ \epsilon_2(H_{2m2})_F - \epsilon_2 + (1-\rho_2)$$
$$+ (1-\rho_2)\ \tau_{13}\ {}^*(H_{2m13})_F\ U_{7,2} + (1-\rho_2)\ \tau_{17}(H_{2m17})_F\ U_{6,2}]\}_{S,L}$$

$$D_{2,3} = \left(\frac{\sigma}{M_2}\right)[A_{2E}(1-\rho_2)\ \epsilon_3(H_{2j3})_E]_{S,L}$$

$$D_{2,4} = \left(\frac{\sigma}{M_2}\right) \{A_{2D}(j-\rho_2)\ \tau_{13}(H_{2j13})_D\ U_{8,4} + A_{2F}[(1-\rho_2)\ \epsilon_4\ (H_{2m4})_F + (1-\rho_2)\ \tau_{13}$$
$$(H_{2m13})_F\ U_{7,4} + (1-\rho_2)\ \tau_{17}(H_{2m17})_F\ U_{6,4}]\}_{S,L}$$

$$D_{2,5} = \left(\frac{\sigma}{M_2}\right) \{A_{2D}(1-\rho_2)\ \tau_{13}(H_{2j13})_D\ U_{8,5} + A_{2F}(1-\rho_2)[\tau_{13}(H_{2m13})_F\ U_{7,5} + \tau_{17}$$
$$(H_{2m17})_F\ U_{6,5}]\}_{S,L}$$

$$D_{2,6} = \left(\frac{\sigma}{M_2}\right) \{A_{2D}(1-\rho_2)\ \tau_{13}(H_{2j13})_D\ U_{8,6} + A_{2F}(1-\rho_2)[\tau_{13}(H_{2m13})_F\ U_{7,6} + \tau_{17}$$
$$(H_{2m17})_F\ U_{6,6}]\}_{S,L}$$

$$D_{2,7} = \left(\frac{\sigma}{M_2}\right)[A_{2E}(1-\rho_2)\ \epsilon_7(H_{2j7})_E]_{S,L}$$

$$D_{2,8} = \left(\frac{\sigma}{M_2}\right) \{A_{2D}(1-\rho_2)\ \tau_{13}(H_{2j13})_D\ U_{8,8} + A_{2F}(1-\rho_2)[\tau_{13}(H_{2m13})_F\ U_{7,8} + \tau_{17}$$
$$(H_{2m17})_F\ U_{6,8}]\}_{S,L}$$

$$D_{2,9} = \left(\frac{\sigma}{M_2}\right) \{A_{2D}(1-\rho_2)\ \tau_{13}(H_{2j13})_D\ U_{8,9} + A_{2F}(1-\rho_2)[\tau_{13}(H_{2m13})_F\ U_{7,9} + \tau_{17}(H_{2m17})_F\ U_{6,9}]\}_{S,L}$$

$$D_{2,10} = \left(\frac{\sigma}{M_2}\right) \{A_{2D}(1-\rho_2)\ \tau_{13}(H_{2j13})_D\ U_{8,10} + A_{2F}(1-\rho_2)[\tau_{13}(H_{2m13})_F\ U_{7,10} + \tau_{17}(H_{2m17})_F\ U_{6,10}]\}_{S,L}$$

$$D_{2,11} = \left(\frac{\sigma}{M_2}\right) \{A_{2D}(1-\rho_2)\ \tau_{13}(H_{2j13})_D\ U_{8,11} + A_{2F}(1-\rho_2)[\tau_{13}(H_{2m13})_F\ U_{7,11} + \tau_{17}(H_{2m17})_F\ U_{6,11}]\}_{S,L}$$

$$D_{2,12} = \left(\frac{\sigma}{M_2}\right) \{A_{2D}(1-\rho_2)\ \tau_{13}(H_{2j13})_D\ U_{8,12} + A_{2F}(1-\rho_2)[\tau_{13}(H_{2m13})_F\ U_{7,12} + \tau_{17}(H_{2m17})_F\ U_{6,12}]\}_{S,L}$$

$$D_{2,13} = \left(\frac{\sigma}{M_2}\right) \{A_{2D}(1-\rho_2)[\epsilon_{13}(H_{2j13})_D + \tau_{13}(H_{2j13})_D\ U_{8,13}] + A_{2F}(1-\rho_2)[\epsilon_{13}(H_{2m13})_F + \tau_{13}(H_{2m13})_F\ U_{7,13} + {}_{17}(H_{2m17})_F\ U_{6,13}]\}_{S,L}$$

$$D_{2,14} = \left(\frac{\sigma}{M_2}\right) \{A_{2D}(1-\rho_2)\ \tau_{13}(H_{2j13})_D\ U_{8,14} + A_{2F}(1-\rho_2)[\tau_{13}(H_{2m13})_F\ U_{7,14} + \tau_{17}(H_{2m17})_F\ U_{6,14}]\}_{S,L}$$

$$D_{3,1} = 0$$

$$D_{3,2} = \left(\frac{\sigma}{M_3}\right) A_3[(1-\rho_3)\ \epsilon_2(H_{3j2})_E]_{S,L}$$

$$D_{3,3} = \left(\frac{\sigma}{M_3}\right) A_3[(1-\rho_3)\ \epsilon_3(H_{3j3})_E - \epsilon_3]_{S,L}$$

$$D_{3,4} = D_{3,5} = D_{3,6} = 0$$

$$D_{3,7} = \left(\frac{\sigma}{M_3}\right) A_3[(1-\rho_3)\ \epsilon_7(H_{3j7})_E]_{S,L}$$

$$D_{3,8} = D_{3,9} = D_{3,10} = D_{3,11} = D_{3,12} = D_{3,13} = D_{3,14} = 0$$

$$D_{4,1} = \left(\frac{\sigma A_4}{M_4}\right) \{(1-\rho_4)[\tau_{13}(H_{4m13})_F\ U_{7,1} + \tau_{17}(H_{4m17})_F\ U_{6,1}]\}_{S,L}$$

$$D_{4,2} = \left(\frac{\sigma A_4}{M_4}\right) \{(1-\rho_4)[\epsilon_2(H_{4m2})_F + \tau_{13}(H_{4m13})_F\ U_{7,2} + \tau_{17}(H_{4m17})_F\ U_{6,2}]\}_{S,L}$$

$$D_{4,3} = 0$$

$$D_{4,4} = \left(\frac{\sigma A_4}{M_4}\right) \{(1-\rho_4)\ \epsilon_4(H_{4m4})_F - \epsilon_4 + (1-\rho_4)\ \tau_{13}(H_{4m13})_F\ U_{7,4} + (1-\rho_4)\ \tau_{17}(H_{4m17})_F\ U_{6,4}\}_{S,L}$$

$$D_{4,5} = \left(\frac{\sigma A_4}{M_4}\right) \{(1-\rho_4)[\tau_{13}(H_{4m13})_F\ U_{7,5} + \tau_{17}(H_{4m17})_F\ U_{6,5}]\}_{S,L}$$

$$D_{4,6} = \left(\frac{\sigma A_4}{M_4}\right) \{(1-\rho_4)[\tau_{13}(H_{4m13})_F\ U_{7,6} + \tau_{17}(H_{4m17})_F\ U_{6,6}]\}_{S,L}$$

$$D_{4,7} = 0$$

$$D_{4,8} = \left(\frac{\sigma A_4}{M_4}\right) \{(1-\rho_4)[\tau_{13}(H_{4m13})_F\ U_{7,8} + \tau_{17}(H_{4,17})_F\ U_{6,8}]\}_{S,L}$$

$$D_{4,9} = \left(\frac{\sigma A_4}{M_4}\right)\{(1-\rho_4)[\tau_{13}(H_{4ml3})_F\ U_{7,9} + \tau_{17}(H_{4ml7})_F\ U_{6,9}]\}_{S,L}$$

$$D_{4,10} = \left(\frac{\sigma A_4}{M_4}\right)\{(1-\rho_4)[\tau_{13}(H_{4ml3})_F\ U_{7,10} + \tau_{17}(H_{4ml7})_F\ U_{6,10}]\}_{S,L}$$

$$D_{4,11} = \left(\frac{\sigma A_4}{M_4}\right)\{(1-\rho_4)[\tau_{13}(H_{4ml3})_F\ U_{7,11} + \tau_{17}(H_{4ml7})_F\ U_{6,11}]\}_{S,L}$$

$$D_{4,12} = \left(\frac{\sigma A_4}{M_4}\right)\{(1-\rho_4)[\tau_{13}(H_{4ml3})_F\ U_{7,12} + \tau_{17}(H_{4ml7})_F\ U_{6,12}]\}_{S,L}$$

$$D_{4,13} = \left(\frac{\sigma A_4}{M_4}\right)\{[\epsilon_{13}(H_{4ml3})_F + \tau_{13}(H_{4ml3})_F\ U_{7,13} + \tau_{17}(H_{4ml7})_F\ U_{6,13}](1-\rho_4)\}_{S,L}$$

$$D_{4,14} = \left(\frac{\sigma A_4}{M_4}\right)\{(1-\rho_4)[\tau_{13}(H_{4ml3})_F\ U_{7,14} + \tau_{17}(H_{4ml7})_F\ U_{6,14}]\}_{S,L}$$

$$D_{5,1} = \left(\frac{\sigma A_5}{M_5}\right)\{(1-\rho_5)[\tau_{16}(H_{5j16})_c\ U_{4,1} = \tau_{17}(H_{5j17})_c\ U_{5,1}]\}_{S,L}$$

$$D_{5,2} = \left(\frac{\sigma A_5}{M_5}\right)\{(1-\rho_5)[\tau_{16}(H_{5j16})_c\ U_{4,2} + \tau_{17}(H_{5j17})_c\ U_{5,2}]\}_{S,L}$$

$$D_{5,3} = 0$$

$$D_{5,4} = \left(\frac{\sigma A_5}{M_5}\right)\{(1-\rho_5)[\tau_{16}(H_{5j16})_c\ U_{4,4} + \tau_{17}(H_{5j17})_c\ U_{5,4}]\}_{S,L}$$

$$D_{5,5} = \left(\frac{\sigma A_5}{M_5}\right)\{(1-\rho_5)[\tau_{16}(H_{5j16})_c\ U_{4,5} + \tau_{17}(H_{5j17})_c\ U_{5,5}] + [(1-\rho_5)\ \epsilon_5\ (H_{5j5})_c - \epsilon_5]\}_{S,L}$$

$$D_{5,6} = \left(\frac{\sigma A_5}{M_5}\right)\{(1-\rho_5)[\epsilon_6(H_{5j6})_c + \tau_{16}(H_{5j16})_c\ U_{4,6} + \tau_{17}(H_{5j17})_c\ U_{5,6}]\}_{S,L}$$

$$D_{5,7} = 0$$

$$D_{5,8} = \left(\frac{\sigma A_5}{M_5}\right)\{(1-\rho_5)[\epsilon_8(H_{5j8})_c + \tau_{16}(H_{5j16})_c\, U_{4,8} + \tau_{17}(H_{5j17})_c\, U_{5,8}]\}_{S,L}$$

$$D_{5,9} = \left(\frac{\sigma A_5}{M_5}\right)\{(1-\rho_5)[\epsilon_9(H_{5j9})_c + \tau_{16}(H_{5j16})_c\, U_{4,9} + \tau_{17}(H_{5j17})_c\, U_{5,9}]\}_{S,L}$$

$$D_{5,10} = \left(\frac{\sigma A_5}{M_5}\right)\{(1-\rho_5)[\tau_{16}(H_{5j16})_c\, U_{4,10} + \tau_{17}(H_{5j17})_c\, U_{5,10}]\}_{S,L}$$

$$D_{5,11} = \left(\frac{\sigma A_5}{M_5}\right)\{(1-\rho_5)[\tau_{16}(H_{5j16})_c\, U_{4,11} + \tau_{17}(H_{5j17})_c\, U_{5,11}]\}_{S,L}$$

$$D_{5,12} = \left(\frac{\sigma A_5}{M_5}\right)\{(1-\rho_5)[\tau_{16}(H_{5j16})_c\, U_{4,12} + \tau_{17}(H_{5j17})_c\, U_{5,12}]\}_{S,L}$$

$$D_{5,13} = \left(\frac{\sigma A_5}{M_5}\right)\{(1-\rho_5)[\tau_{16}(H_{5j16})_c\, U_{4,13} + \tau_{17}(H_{5j17})_c\, U_{5,13}]\}_{S,L}$$

$$D_{5,14} = \left(\frac{\sigma A_5}{M_5}\right)\{(1-\rho_5)[\tau_{16}(H_{5j16})_c\, U_{4,14} + \tau_{17}(H_{5j17})_c\, U_{5,14}]\}_{S,L}$$

$$D_{6,1} = \left(\frac{\sigma A_6}{M_6}\right)\{(1-\rho_6)[\tau_{16}(H_{6j16})_c\, U_{4,1} + \tau_{17}(H_{6j17})_c\, U_{5,1}]\}_{S,L}$$

$$S_{6,2} = \left(\frac{\sigma A_6}{M_6}\right)\{(1-\rho_6)[\tau_{16}(H_{6j16})_c\, U_{4,2} + \tau_{17}(H_{6j16})_c\, U_{5,2}]\}_{S,L}$$

$$D_{6,3} = 0$$

$$D_{6,4} = \left(\frac{\sigma A_6}{M_6}\right)\{(1-\rho_6)[\tau_{16}(H_{6j16})_c\, U_{4,4} + \tau_{17}(H_{6j17})_c\, U_{5,4}]\}_{S,L}$$

$$D_{6,5} = \left(\frac{\sigma A_6}{M_6}\right)\{(1-\rho_6)[\epsilon_5(H_{6j5})_c + \tau_{16}(H_{6j16})_c\, U_{4,5} + \tau_{17}(H_{6j17})_c\, U_{5,5}]\}_{S,L}$$

$$D_{6,6} = \left(\frac{\sigma A_6}{M_6}\right)\{(1-\rho_6)[\epsilon_6(H_{6j6})_c + \tau_{16}(H_{6j16})_c\, U_{4,6} + \tau_{17}(H_{6j17})_c\, U_{5,6} - \epsilon_6\}_{S,L}$$

$$D_{6,7} = 0$$

$$D_{6,8} = \left(\frac{\sigma A_6}{M_6}\right)\{(1-\rho_6)[\epsilon_8(H_{6j8})_c + \tau_{16}(H_{6j16})_c\, U_{4,8} + \tau_{17}(H_{6j17})\, U_{5,8}]\}_{S,L}$$

$$D_{6,9} = \left(\frac{\sigma A_6}{M_6}\right)\{(1-\rho_6)[\epsilon_9(H_{6j9})_c + \tau_{16}(H_{6j16})_c\, U_{4,9} + \tau_{17}(H_{6j17})_c\, U_{5,9}]\}_{S,L}$$

$$D_{6,10} = \left(\frac{\sigma A_6}{M_6}\right)\{(1-\rho_6)[\tau_{16}(H_{6h16})_c\, U_{4,10} + \tau_{17}(H_{6j17})_c\, U_{5,10}]\}_{S,L}$$

$$D_{6,11} = \left(\frac{\sigma A_6}{M_6}\right)\{(1-\rho_6)[\tau_{16}(H_{6j16})_c\, U_{4,11} + \tau_{17}(H_{6j17})_c\, U_{5,11}]\}_{S,L}$$

$$D_{6,12} = \left(\frac{\sigma A_6}{M_6}\right)\{(1-\rho_6)[\tau_{16}(H_{6j16})_c\, U_{4,12} + \tau_{17}(H_{6j17})_c\, U_{5,12}]\}_{S,L}$$

$$D_{6,13} = \left(\frac{\sigma A_6}{M_6}\right)\{(1-\rho_6)[\tau_{16}(H_{6j16})_c\, U_{4,13} + \tau_{17}(H_{6j17})_c\, U_{5,13}]\}_{S,L}$$

$$D_{6,14} = \left(\frac{\sigma A_6}{M_6}\right)\{(1-\rho_6)[\tau_{16}(H_{6j16})_c\, U_{4,14} + \tau_{17}(H_{6j17})_c\, U_{5,15}]\}_{S,L}$$

$$D_{7,1} = 0$$

$$D_{7,2} = \left(\frac{\sigma A_7}{M_7\, E}\right)\{(1-\rho_7)\, \epsilon_2(H_{7j2})_E\}_{S,L}$$

$$D_{7,3} = \left(\frac{\sigma A_7}{M_7}\right)_E \{(1-\rho_7)\ \epsilon_3 (H_{7j3})_E\}_{S,L}$$

$$D_{7,4} = D_{7,5} = D_{7,6} = 0$$

$$D_{7,7} = \left(\frac{\sigma A_7}{M_7}\right)_E \{(1-\rho_7)\ \epsilon_7 (H_{7j7})_E - \epsilon_7\}_{S,L}$$

$$D_{7,8} = D_{7,9} = D_{7,10} = D_{7,11} = D_{7,12} = D_{7,13} = D_{7,14} = 0$$

$$D_{8,1} = \left(\frac{\sigma A_8}{M_8}\right)\{(1-\rho_8)[\tau_{16}(H_{8j16})_c\ U_{4,1} + \tau_{17}(H_{8j17})_c\ U_{5,1}]\}_{S,L}$$

$$D_{8,2} = \left(\frac{\sigma A_8}{M_8}\right)\{(1-\rho_8)[\tau_{16}(H_{8j16})_c\ U_{4,2} + \tau_{17}(H_{8j17})_c\ U_{5,2}]\}_{S,L}$$

$$D_{8,3} = 0$$

$$D_{8,4} = \left(\frac{\sigma A_8}{M_8}\right)\{(1-\rho_8)[\tau_{16}(H_{8j16})_c\ U_{4,4} + \tau_{17}(H_{8j17})_c\ U_{5,4}]\}_{S,L}$$

$$D_{8,5} = \left(\frac{\sigma A_8}{M_8}\right)\{(1-\rho_8)[\epsilon_5(H_{8j5})_c + \tau_{16}(H_{8j16})_c\ U_{4,5} + \tau_{17}(H_{8j17})_c\ U_{5,5}]\}_{S,L}$$

$$D_{8,6} = \left(\frac{\sigma A_8}{M_8}\right)\{(1-\rho_8)[\epsilon_6(H_{8j6})_c + \tau_{16}(H_{8j16})_c\ U_{4,6} + \tau_{17}(H_{8j17})_c\ U_{5,6}]\}_{S,L}$$

$$D_{8,7} = 0$$

$$D_{8,8} = \left(\frac{\sigma A_8}{M_8}\right)\{(1-\rho_8)[\epsilon_8(H_{8j8})_c + \tau_{16}(H_{8j16})_c\ U_{4,8} + \tau_{17}(H_{8j17})_c\ U_{5,8}] - \epsilon_8\}_{S,L}$$

$$D_{8,9} = \left(\frac{\sigma A_8}{M_8}\right) \{(1-\rho_8)[e_9(H_{8j9})_c + \tau_{16}(H_{8j16})_c U_{4,9} + \tau_{17}(H_{8j17})_c U_{5,9}]\}_{S,L}$$

$$D_{8,10} = \left(\frac{\sigma A_8}{M_8}\right)\{(1-\rho_8)[\tau_{16}(H_{8j16})_c U_{4,10} + \tau_{17}(H_{8j17})_c U_{5,10}]\}_{S,L}$$

$$D_{8,11} = \left(\frac{\sigma A_8}{M_8}\right)\{(1-\rho_8)[\tau_{16}(H_{8j16})_c U_{4,11} + \tau_{17}(H_{8j17})_c U_{5,11}]\}_{S,L}$$

$$D_{8,12} - \left(\frac{\sigma A_8}{M_8}\right)\{(1-\rho_8)[\tau_{16}(H_{8j16})_c U_{4,12} + \tau_{17}(H_{8j17})_c U_{5,12}]\}_{S,L}$$

$$D_{8,13} = \left(\frac{\sigma A_8}{M_8}\right)\{(1-\rho_8)[\tau_{16}(H_{8j16})_c U_{4,13} + \tau_{17}(H_{8j17})_c U_{5,13}]\}_{S,L}$$

$$D_{8,14} = \left(\frac{\sigma A_8}{M_8}\right)\{(1-\rho_8)[\tau_{16}(H_{8j16})_c U_{4,14} + \tau_{17}(H_{8j17})_c U_{5,14}]\}_{S,L}$$

$$D_{9,1} = \left(\frac{\sigma}{M_9}\right)\{A_{9B}(1-\rho_9)_B[\tau_{14}(H_{9m14})_B U_{2,1} + \tau_{16}(H_{9m16})_B U_{3,1}] + A_{9c}(1-\rho_9)_c$$

$$[\tau_{16}(H_{9j16})_c U_{4,1} + \tau_{17}(H_{9j17})_c U_{5,1}]\}_{S,L}$$

$$D_{9,2} = \left(\frac{\sigma}{M_9}\right)\{A_{9B}(1-\rho_9)_B[\tau_{14}(H_{9m14})_B U_{2,2} + \tau_{16}(H_{9m16})_B U_{3,2}] + A_{9c}(1-\rho_9)_c$$

$$[\tau_{16}(H_{9j16})_c U_{4,2} + \tau_{17}(H_{9j17})_c U_{5,2}]\}_{S,L}$$

$$D_{9,3} = 0$$

$$D_{9,4} = \left(\frac{\sigma}{M_9}\right)\{A_{9B}(1-\rho_9 B[\tau_{14}(H_{9m14})_B U_{2,4} + \tau_{16}(H_{9m16})_B U_{3,4}] + A_{9c}(1-\rho_9)_c$$

$$[\tau_{16}(H_{9j16})_c U_{4,4} + \tau_{17}(H_{9j17})_c U_{5,4}]\}_{S,L}$$

$$D_{9,5} = (\frac{\sigma}{M_9})\{A_{9B}(1-\rho_9)_B[\tau_{14}(H_{9m14})_B\ U_{2,5} + \tau_{16}(H_{9m16})_B\ U_{3,5}] + A_{9c}\ (1-\rho_9)_c$$

$$[\epsilon_5(H_{9j5})_c + \tau_{16}(H_{9j16})_c\ U_{4,5} + \tau_{17}(H_{9j17})_c\ U_{5,5}]\}_{S,L}$$

$$D_{9,6} = (\frac{\sigma}{M_9})\{A_{9B}(1-\rho_9)_B[\tau_{14}(H_{9m14})_B\ U_{2,6} + \tau_{16}(H_{9m16})_B\ U_{3,6}] + A_{9c}(1-\rho_9)_c$$

$$[\epsilon_6(H_{9j6})_c + \tau_{16}(H_{9j16})_c\ U_{4,6} + \tau_{17}(H_{9j17})_c\ U_{5,6}]\}_{S,L}$$

$$D_{9,7} = 0$$

$$D_{9,8} = (\frac{\sigma}{M_9})\{A_{9B}(1-\rho_9)_B[\tau_{14}(H_{9m14})_B\ U_{2,8} + \tau_{16}(H_{9m16})_B\ U_{3,8}] + A_{9c}(1-\rho_9)_c$$

$$[\epsilon_8(H_{9j6})_c + \tau_{16}(H_{9j16})_c\ U_{4,8} + \tau_{17}(H_{9j17})_c\ U_{5,8}]\}_{S,L}$$

$$D_{9,9} = (\frac{\sigma}{M_9})\{A_{9B}(1-\rho_9)_B[\epsilon_9(H_{9m9})_B + \tau_{14}(H_{9m14})_B\ U_{4,9} + \tau_{16}(H_{9j16})_c\ U_{5,9}] - A_{9B}\ \epsilon_9$$

$$+ A_{9c}(1-\rho_9)_c[\epsilon_9(H_{9j9})_c + \tau_{16}(H_{9j16})_c\ U_{4,9} + \tau_{17}(H_{9j17})_c\ U_{5,9}] - A_{9c}\ \epsilon_9\}_{S,L}$$

$$D_{9,10} = (\frac{\sigma}{M_9})\{A_{9B}(1-\rho_9)_B[\tau_{14}(H_{9m14})_B\ U_{2,10} + \tau_{16}(H_{9m16})_B\ U_{3,10}] + A_{9c}[\tau_{16}$$

$$(H_{9j16})_c\ U_{4,10} + \tau_{17}(H_{9j17})_c\ U_{5,10}]\}_{S,L}$$

$$D_{9,11} = (\frac{\sigma}{M_9})\{A_{9B}(1-\rho_9)_B[\epsilon_{11}(H_{9m11})_B = \tau_{14}(H_{9m14})_B\ U_{2,11} + \tau_{16}(H_{9m16})_B\ U_{3,11}]$$

$$+ A_{9c}(1-\rho_9)_c[\tau_{16}(H_{9j16})_c\ U_{4,11} + \tau_{17}(H_{9j17})_c\ U_{5,11}]\}_{S,L}$$

$$D_{9,12} = (\frac{\sigma}{M_9})\{A_{9B}(1-\rho_9)_B[\epsilon_{12}(H_{9m12})_B + \tau_{14}(H_{9m14})_B\ U_{2,12} + \tau_{16}(H_{9m16})_B\ U_{3,12}]$$

$$+ A_{9c}(1-\rho_9)_c[\tau_{16}(H_{9j16})_c\ U_{4,12} + \tau_{17}(H_{9j17})_c\ U_{5,12}]\}_{S,L}$$

$$D_{9,13} = \left(\frac{\sigma}{M_9}\right)\{A_{9B}(1-\rho_9)_B[\tau_{14}(H_{9ml4})_B\ U_{2,3} + \tau_{16}(H_{9ml6})_m\ U_{3,13}] + A_{9c}(1-\rho_9)_c$$

$$[\tau_{16}(H_{9jl6})_c\ U_{4,13} + \tau_{17}(H_{9jl7})_c\ U_{5,13}]\}_{S,L}$$

$$D_{9,14} = \left(\frac{\sigma}{M_9}\right)\{A_{9B}(1-\rho_9)_B[\epsilon_{14}(H_{9ml4})_B + \tau_{14}(H_{9ml4})_B\ U_{2,14} + \tau_{16}(H_{9ml6})_B\ U_{3,14}]$$

$$+ A_{9c}(1-\rho_9)_c[\tau_{16}(H_{9jl6})_c\ U_{4,14} + \tau_{17}(H_{9jl7})_c\ U_{5,14}]\}_{S,L}$$

$$D_{10,1} = \left(\frac{\sigma A_{10}}{M_{10}}\right)\{(1-\rho_{10})\ \tau_{14}(H_{10jl4})_A\ U_{1,1}\}_{S,L}$$

$$D_{10,2} = \left(\frac{\sigma A_{10}}{M_{10}}\right)\{(1-\rho_{10})\ \tau_{14}(H_{10jl4})_A\ U_{1,2}\}_{S,L}$$

$$D_{10,3} = 0$$

$$D_{10,4} = \left(\frac{\sigma A_{10}}{M_{10}}\right)\{(1-\rho_{10})\ \tau_{14}(H_{10jl4})_A\ U_{1,4}\}_{S,L}$$

$$D_{10,5} = \left(\frac{\sigma A_{10}}{M_{10}}\right)\{(1-\rho_{10})\ \tau_{14}(H_{10jl4})_A\ U_{1,5}\}_{S,L}$$

$$D_{10,6} = \left(\frac{\sigma A_{10}}{M_{10}}\right)\{(1-\rho_{10})\ \tau_{14}(H_{10jl4})_A\ U_{1,6}\}_{S,L}$$

$$D_{10,7} = 0$$

$$D_{10,8} = \left(\frac{\sigma A_{10}}{M_{10}}\right)\{(1-\rho_{10})\ \tau_{14}(H_{10jl4})_A\ U_{1,8}\}_{S,L}$$

$$D_{10,9} = \left(\frac{\sigma A_{10}}{M_{10}}\right)\{(1-\rho_{10})\ \tau_{14}(H_{10jl4})_A\ U_{1,9}\}_{S,L}$$

$$D_{10,10} = \left(\frac{\sigma A_{10}}{M_{10}}\right)\{(1-\rho_{10})\ \epsilon_{10}(H_{10j10})_A - \epsilon_{10} + (1-\rho_{10})\ \tau_{14}(H_{10j14})_A\ U_{1,10}\}_{S,L}$$

$$D_{10,11} = \left(\frac{\sigma A_{10}}{M_{10}}\right)\{(1-\rho_{10})\ \tau_{14}(H_{10j14})_A\ U_{1,11}\}$$

$$D_{10,12} = \left(\frac{\sigma A_{10}}{M_{10}}\right)\{(1-\rho_{10})[\epsilon_{12}(H_{10j12})_A + \tau_{14}(H_{10j14})_A\ U_{1,12}]\}_{S,L}$$

$$D_{10,13} = \left(\frac{\sigma A_{10}}{M_{10}}\right)\{(1-\rho_{10})\ \tau_{14}(H_{10j14})_A\ U_{1,13}\}_{S,L}$$

$$D_{10,14} = \left(\frac{\sigma A_{10}}{M_{10}}\right)\{\epsilon_{14}(H_{10j14})_A + \tau_{14}(H_{10j14})_A\ U_{1,14}\}$$

$$D_{11,1} = \left(\frac{\sigma A_{11}}{M_{11}}\right)\{(1-\rho_{11})[\tau_{14}(H_{11m14})_B\ U_{2,1} + \tau_{16}(H_{11m16})_B\ U_{3,1}]\}_{S,L}$$

$$D_{11,2} = \left(\frac{\sigma A_{11}}{M_{11}}\right)\{(1-\rho_{11})[\tau_{14}(H_{11m14})_B\ U_{2,2} + \tau_{16}(H_{11m16})_B\ U_{3,2}]\}_{S,L}$$

$$D_{11,3} = 0$$

$$D_{11,4} = \left(\frac{\sigma A_{11}}{M_{11}}\right)\{(1-\rho_{11})[\tau_{14}(H_{11m14})_B\ U_{2,4} + \tau_{16}(H_{11m16})_B\ U_{3,4}]\}_{S,L}$$

$$D_{11,5} = \left(\frac{\sigma A_{11}}{M_{11}}\right)\{(1-\rho_{11})[\tau_{14}(H_{11m14})_B\ U_{2,5} + \tau_{16}(H_{11m16})_B\ U_{3,5}]\}_{S,L}$$

$$D_{11,6} = \left(\frac{\sigma A_{11}}{M_{11}}\right)\{(1-\rho_{11})[\tau_{14}(H_{11m14})_B\ U_{2,6} + \tau_{16}(H_{11m16})_B\ U_{3,6}]\}_{S,L}$$

$$D_{11,7} = 0$$

$$D_{11,8} = \left(\frac{\sigma A_{11}}{M_{11}}\right)\{(1-\rho_{11})[\tau_{14}(H_{11m14})_B\ U_{2,8} + \tau_{16}(H_{11m16})_B\ U_{3,8}]\}_{S,L}$$

$$D_{11,9} = \left(\frac{\sigma A_{11}}{M_{11}}\right)\{\epsilon_9 (H_{11m9})_B + \tau_{14}(H_{11m14})_B\, U_{2,9} + \tau_{16}(H_{11m16})_B\, U_{3,9}]\}_{S,L}$$

$$D_{11,10} = \left(\frac{\sigma A_{11}}{M_{11}}\right)\{\tau_{14}(H_{11m14})_B\, U_{2,10} + \tau_{16}(H_{11m16})_B\, U_{3,10}]\}_{S,L}$$

$$D_{11,11} = \left(\frac{\sigma A_{11}}{M_{11}}\right)\{(1-\rho_{11})\,\epsilon_{11}(H_{11m11})_B - \epsilon_{11} + \tau_{14}(H_{11m14})_B\, U_{2,11}$$

$$+ \tau_{16}(H_{11m16})_B\, U_{3,11}\}_{S,L}$$

$$D_{11,12} = \left(\frac{\sigma A_{11}}{M_{11}}\right)\{(1-\rho_{11})[\epsilon_{12}(H_{11m12})_B + \tau_{14}(H_{11m14})_B\, U_{2,12}$$

$$+ \tau_{16}(H_{11m16})_B\, U_{3,12}]\}_{S,L}$$

$$D_{11,13} = \left(\frac{\sigma A_{11}}{M_{11}}\right)\{(1-\rho_{11})[\tau_{14}(H_{11m14})_B\, U_{2,13} + \tau_{16}(H_{11m16})_B\, U_{3,13}]\}_{S,L}$$

$$D_{11,14} = \left(\frac{\sigma A_{11}}{M_{11}}\right)\{(1-\rho_{11})[\epsilon_{14}(H_{11m14})_B + \tau_{14}(H_{11m14})_B\, U_{2,14}$$

$$+ \tau_{16}(H_{11m16})_B\, U_{3,14}]\}_{S,L}$$

$$D_{12,1} = \left(\frac{\sigma}{M_{12}}\right)\{A_{12A}(1-\rho_{12})_A\, \tau_{14}(H_{12j14})_A\, U_{1,1} + A_{12B}(1-\rho_{12})_B[\tau_{14}(H_{12m14})_B\, U_{2,1}$$

$$+ \tau_{16}(H_{12m16})_B\, U_{3,1}]\}_{S,L}$$

$$D_{12,2} = \left(\frac{\sigma}{M_{12}}\right)\{A_{12A}(1-\rho_{12})_A\, \tau_{14}\, (H_{12j14})_A\, U_{1,2} + A_{12B}(1-\rho_{12})_B[\tau_{14}(H_{12m14})_B\, U_{2,2}$$

$$+ \tau_{16}(H_{12m16})_B\, U_{3,2}]\}_{S,L}$$

$$D_{12,3} = 0$$

$$D_{12,4} = \left(\frac{\sigma}{M_{12}}\right)\{A_{12A}(1-\rho_{12})_A\ \tau_{14}(H_{12j14})_A\ U_{1,4} + A_{12B}(1-\rho_{12})_B[\tau_{14}(H_{12m14})_B\ U_{2,4} + \tau_{16}(H_{12m16})_B\ U_{3,4}]\}_{S,L}$$

$$D_{12,5} = \left(\frac{\sigma}{M_{12}}\right)\ A_{12A}(1-\rho_{12})_A\ \tau_{14}(H_{12j14})_A\ U_{1,5} + A_{12B}(1-\rho_{12})_B[\tau_{14}(H_{12m14})_B\ U_{2,5} + \tau_{16}(H_{12m16})_B\ U_{3,5}]\}_{S,L}$$

$$D_{12,6} = \left(\frac{\sigma}{M_{12}}\right)\{A_{12A}(1-\rho_{12})_A\ \tau_{14}(H_{12j14})_A\ U_{1,6} + A_{12B}(1-\rho_{12})_B[\tau_{14}(H_{12m14})_B\ U_{2,6} + \tau_{16}(H_{12m16})_B\ U_{3,6}]\}_{S,L}$$

$$D_{12,7} = 0$$

$$D_{12,8} = \left(\frac{\sigma}{M_{12}}\right)\{A_{12A}(1-\rho_{12})_A\ \tau_{14}(H_{12j14})_A\ U_{1,8} + A_{12B}(1-\rho_{12})_B[\tau_{14}(H_{12m14})_B\ U_{2,8} + \tau_{16}(H_{12m16})_B\ U_{3,8}]\}_{S,L}$$

$$D_{12,9} = \left(\frac{\sigma}{M_{12}}\right)\{A_{12A}(1-\rho_{12})_A\ \tau_{14}(H_{12j14})_A\ U_{1,9} + A_{12B}(1-\rho_{12})_B[\epsilon_9(H_{12m9})_B + \tau_{14}(H_{12m14})_B\ U_{2,9} + \tau_{16}(H_{12m16})_B\ U_{3,9}]\}_{S,L}$$

$$D_{12,10} = \left(\frac{\sigma}{M_{12}}\right)\{A_{12A}(1-\rho_{12})_A[\epsilon_{10}(H_{12j10})_A + \tau_{12}(H_{12j14})_A\ U_{1,10}] + A_{12B}(1-\rho_{12})_B [\tau_{14}(H_{12m14})_B\ U_{2,10} + \tau_{16}(H_{12m16})_B\ U_{3,10}]\}_{S,L}$$

$$D_{12,11} = \left(\frac{\sigma}{M_{12}}\right)\{A_{12A}(1-\rho_{12})_A\ \tau_{14}(H_{12j14})_A\ U_{1,11} + A_{12B}(1-\rho_{12})_B[\epsilon_{11}(H_{12m11})_B + \tau_{14}(H_{12m14})_B\ U_{2,11} + \tau_{16}(H_{12m16})_B\ U_{3,11}]\}_{S,L}$$

$$D_{12,12} = \left(\frac{\sigma}{M_{12}}\right)\{A_{12A}(1-\rho_{12})_A[\epsilon_{12}(H_{12j12})_A + \tau_{14}(H_{12j14})_A\, U_{1,12}] - A_{12A}\,\epsilon_{12}$$
$$+ A_{12B}(1-\rho_{12})_B[\epsilon_{12}(H_{12m12})_B + \tau_{14}(H_{12j14})_B\, U_{2,12} + \tau_{16}(H_{12m16}{}^B$$
$$U_{3,12}] - A_{12B}\,\epsilon_{12}\}_{S,L}$$

$$D_{12,13} = \left(\frac{\sigma}{M_{12}}\right)\{A_{12A}(1-\rho_{12})_A\,\tau_{14}(H_{12j14})_A\, U_{1,13} + A_{12B}(1-\rho_{12})_B[\tau_{14}(H_{12m14})_B\, U_{2,13}$$
$$+ \tau_{16}(H_{12m16})_B\, U_{3,13}]\}_{S,L}$$

$$D_{12,14} = \left(\frac{\sigma}{M_{12}}\right)\{A_{12A}(1-\rho_{12})[\epsilon_{12}(H_{12j14})_A + \tau_{14}(H_{12j14})_A\, U_{1,14} + A_{12B}(1-\rho_{12})_B$$
$$[\epsilon_{14}(H_{12m14})_B + \tau_{14}(H_{12m14})_B\, U_{2,4} + \tau_{16}(H_{12m16})_B\, U_{3,14}]\}_{S,L}$$

$$D_{13,1} = \left(\frac{\sigma}{M_{13}}\right)\{A_{13F}(1-\rho_{13})_F[\tau_{17}(H_{13m17})_F\, U_{6,1} + \tau_{13}(H_{13m13})_F\, U_{7,1}] - A_{13F}\, U_{7,1}$$
$$+ A_{13D}(1-\rho_{13})_D[\epsilon_1(H_{13j1})_D + \tau_{13}(H_{13j13})_D\, U_{8,1}] - A_{13D}\,\tau_{13}\, U_{8,1}\}_{S,L}$$

$$D_{13,2} = \left(\frac{\sigma}{M_{13}}\right)\{A_{13F}(1-\rho_{13})_F[\tau_{17}(H_{13m17})_F\, U_{6,2} + \tau_{13}(H_{13m13})_F\, U_{7,2}$$
$$+ \epsilon_2(H_{13m2})_F] - A_{13F}\,\tau_{13}\, U_{7,2} + A_{13D}(1-\rho_{13})_D[\epsilon_2(H_{13j2})_D$$
$$+ \tau_{13}(H_{13j13})_D\, U_{8,2}] - A_{13D}\,\tau_{13}\, U_{8,2}\}_{S,L}$$

$$D_{13,3} = 0$$

$$D_{14,4} = \left(\frac{\sigma}{M_{13}}\right)\{A_{13F}(1-\rho_{13})_F[\tau_{17}(H_{13m17})_F\, U_{6,4} + \tau_{13}(H_{13m13})_F + \epsilon_4(H_{13m4})_F] - A_{13F}$$
$$\tau_{13}\, U_{7,4} + A_{13D}[(1-\rho_{13})_D\,\tau_{13}(H_{13j13})_D - \tau_{13}]\, U_{8,4}\}_{S,L}$$

$$D_{13,5} = \left(\frac{\sigma}{M_{13}}\right)\{A_{13F}(1-\rho_{13})_F[\tau_{17}(H_{13m17})_F\ U_{6,5} + \tau_{13}(H_{13m13})_F\ U_{7,5}] - A_{13F}$$

$$\tau_{13}\ U_{7,5} + A_{13D}[(1-\rho_{13})_D\ \tau_{13}(H_{13j13})_D - \tau_{13}]\ U_{8,5}\}_{S,L}$$

$$D_{13,6} = \left(\frac{\sigma}{M_{13}}\right)\{A_{13F}(1-\rho_{13})_F[\tau_{17}(H_{13m17})_F\ U_{6,6} + \tau_{13}(H_{13m13})_F\ U_{7,6}] - A_{13F}$$

$$\tau_{13}\ U_{7,6} + A_{13D}[(1-\rho_{13})_D\ \tau_{13}(H_{13j13})_D - \tau_{13}]\ U_{8,6}\}_{S,L}$$

$$D_{13,7} = 0$$

$$D_{13,8} = \left(\frac{\sigma}{M_{13}}\right)\{A_{13F}(1-\rho_{13})_F[\tau_{17}(H_{13m17})_F\ U_{6,8} + \tau_{13}(H_{13m13})_F\ U_{7,8}] - A_{13F}$$

$$\tau_{13}\ U_{7,8} + A_{13D}[(1-\rho_{13})_D\ \tau_{13}(H_{13j13})_D - \tau_{13}]\ U_{8,8}\}_{S,L}$$

$$D_{13,9} = \left(\frac{\sigma}{M_{13}}\right)\{A_{13F}(1-\rho_{13})_F[\tau_{17}(H_{13m17})_F\ U_{6,9} + \tau_{13}(H_{13m13})_F\ U_{7,9}] - A_{13F}$$

$$\tau_{13}\ U_{7,9} + A_{13D}[(1-\rho_{13})_D\ \tau_{13}(H_{13j13})_D - \tau_{13}]\ U_{8,9}\}_{S,L}$$

$$D_{13,10} = \left(\frac{\sigma}{M_{13}}\right)\{A_{13F}(1-\rho_{13})_F[\tau_{17}(H_{13m17})_F\ U_{6,10} + \tau_{13}(H_{13m13})_F\ U_{7,10}] - A_{13F}$$

$$\tau_{13}\ U_{7,10} + A_{13D}[(1-\rho_{13})_D\ \tau_{13}(H_{13j13})_D - \tau_{13}]\ U_{8,10}\}_{S,L}$$

$$D_{13,11} = \left(\frac{\sigma}{M_{13}}\right)\{A_{13F}(1-\rho_{13})_F[\tau_{17}(H_{13m17})_F\ U_{6,11} + \tau_{13}(H_{13m13})_F\ U_{7,11}] - A_{13F}$$

$$\tau_{13}\ U_{7,11} + A_{13D}[(1-\rho_{13})_D\ \tau_{13}(H_{13j13})_D - \tau_{13}]\ U_{8,11}\}_{S,L}$$

$$D_{13,12} = \left(\frac{\sigma}{M_{13}}\right)\{A_{13F}(1-\rho_{13})_F[\tau_{17}(H_{13m17})_F\ U_{6,12} + \tau_{13}(H_{13m13})_F\ U_{7,12}] - A_{13F}$$

$$\tau_{13}\ U_{7,12} + A_{13D}[(1-\rho_{13})_D\ \tau_{13}(H_{13j13})_D - \tau_{13}]\ U_{8,12}\}_{S,L}$$

$$D_{13,13} = \left(\frac{\sigma}{M_{13}}\right)\{A_{13F}(1-\rho_{13})_F[\tau_{17}(H_{13m17})_F\ U_{6,13} + \tau_{13}(H_{13m13})_F\ U_{7,13} + \epsilon_{13}$$

$$(H_{13m13})_F] - A_{13F}(e_{13} + \tau_{13}\ U_{7,13}) + A_{13D}(1-\rho_{13})_D[\epsilon_{13}(H_{13j13})_D$$

$$+ \tau_{13}(H_{13j13})_D\ U_{8,13}] - A_{13D}\ (\epsilon_{13} + \tau_{13}\ U_{8,13})\}_{S,L}$$

$$D_{13,14} = \left(\frac{\sigma}{M_{13}}\right)\{A_{13F}(1-\rho_{13})_F[\tau_{17}(H_{13m17})_F\ U_{6,14} + \tau_{13}(H_{13m13})_F\ U_{7,14}] - A_{13F}$$

$$\tau_{13}\ U_{7,14} + A_{13D}[(1-\rho_{13})_D\ \ 13(H_{13j13})_D - \tau_{13}]\ U_{8,14}\}_{S,L}$$

$$D_{14,1} = \left(\frac{\sigma}{M_{14}}\right)\{A_{14A}\ \tau_{14}[(1-\rho_{14})(H_{14j14})_A - 1]\ U_{1,1} + A_{14B}[(1-\rho_{14})\ \tau_{14}$$

$$(H_{14m14})_B - \tau_{14}]\ U_{2,1} + A_{14B}\ \tau_{16}(1-\rho_{14})(H_{14m16})_B\ U_{3,1}\}_{S,L}$$

$$D_{14,2} = \left(\frac{\sigma}{M_{14}}\right)\{A_{14A}\ \tau_{14}[(1-\rho_{14})(H_{14j14})_A - 1]\ U_{1,2} + A_{14B}[(1-\rho_{14})\ \tau_{14}$$

$$(H_{14m14})_B - \tau_{14}]\ U_{2,2} + A_{14B}\ \tau_{16}(1-\rho_{14})(H_{14m16})_B\ U_{3,2}\}_{S,L}$$

$$D_{14,3} = 0$$

$$D_{14,4} = \left(\frac{\sigma}{M_{14}}\right)\{A_{14A}\ \tau_{14}[(1-\rho_{14})(H_{14j14})_A - 1]\ U_{1,4} + A_{14B}\ \tau_{14}[(1-\rho_{14})$$

$$(H_{14m14})_B - 1]\ U_{2,4} + A_{14B}\ \tau_{16}(1-\rho_{14})(H_{14m16})_B\ U_{3,4}\}_{S,L}$$

$$D_{14,5} = \left(\frac{\sigma}{M_{14}}\right)\{A_{14A}\ \tau_{14}[(1-\rho_{14})(H_{14j14})_A - 1]\ U_{1,5} + A_{14B}\ \tau_{14}[(1-\rho_{14})$$

$$(H_{14m14})_B - 1]\ U_{2,5} + A_{14B}\ \tau_{16}(1-\rho_{14})(H_{14m16})_B\ U_{3,5}\}_{S,L}$$

$$D_{14,6} = \left(\frac{\sigma}{M_{14}}\right)\{A_{14A}\,\tau_{14}[(1-\rho_{14})(H_{14j14})_A - 1]\,U_{1,6} + A_{14B}\,\tau_{14}[(1-\rho_{14})(H_{14m14})_B - 1]\,U_{2,6} + A_{14B}\,\tau_{16}(1-\rho_{14})(H_{14m16})_B\,U_{3,6}\}_{S,L}$$

$$D_{14,7} = 0$$

$$D_{14,8} = \left(\frac{\sigma}{M_{14}}\right)\{A_{14A}\,\tau_{14}[(1-\rho_{14})(H_{14h14})_A - 1]\,U_{1,8} + A_{14B}\,\tau_{14}[(1-\rho_{14})(H_{14m14})_B - 1]\,U_{2,8} + A_{14B}\,\tau_{16}(1-\rho_{14})(H_{14m16})_B\,U_{3,8}\}_{S,L}$$

$$D_{14,9} = \left(\frac{\sigma}{M_{14}}\right)\{A_{14A}\,\tau_{14}[(1-\rho_{14})(H_{14j14})_A - 1]\,U_{1,9} + A_{14B}(1-\rho_{14})_B[\epsilon_9(H_{14m9})_B + \tau_{14}(H_{14m14})_B\,U_{2,9} + \tau_{16}(H_{14m16})_B\,U_{3,9}] - A_{14B}\,\tau_{14}\,U_{2,9}\}_{S,L}$$

$$D_{14,10} = \left(\frac{\sigma}{M_{14}}\right)\{A_{14A}(1-\rho_{14})[\epsilon_{10}(H_{14j10})_A + \tau_{14}(H_{14j14})_A\,U_{1,10}] - A_{14A}\,\tau_{14}\,U_{1,10} + A_{14B}(1-\rho_{14})[\tau_{14}(H_{14m14})_B\,U_{2,10} + \tau_{16}(H_{14m16})_B\,U_{3,10}] - A_{14B}\,\tau_{14}\,U_{2,10}\}_{S,L}$$

$$D_{14,11} = \left(\frac{\sigma}{M_{14}}\right)\{A_{14A}\,\tau_{14}[(1-\rho_{14})(H_{14j14})_A - 1]\,U_{1,11} + A_{14B}(1-\rho_{14})[\epsilon_{11}(H_{14m11})_B + \tau_{14}(H_{14m14})_B\,U_{2,11} + \tau_{16}(H_{14m16})_B\,U_{3,11}] - A_{14B}\,\tau_{14}\,U_{2,11}\}_{S,L}$$

$$D_{14,12} = \left(\frac{\sigma}{M_{14}}\right)\{A_{14A}(1-\rho_{14})[\epsilon_{12}(H_{14j12})_A + \tau_{14}(H_{14j14})_A\,U_{1,12}] - A_{14A}\,\tau_{14}\,U_{1,2} + A_{14B}(1-\rho_{14})[\epsilon_{12}(H_{14m12})_B + \tau_{14}(H_{14m14})_B\,U_{2,12} + \tau_{16}(H_{14m16})_B\,U_{3,12}] - A_{14B}\,\tau_{14}\,U_{2,12}\}_{S,L}$$

$$D_{14,13} = \left(\frac{\sigma}{M_{14}}\right)\{A_{14A}\,\tau_{14}[(1-\rho_{14})(H_{14j14})_A - 1]\,U_{1,13} + A_{14B}(1-\rho_{14})[\tau_{14}(H_{14m14})_B\,U_{2,13} - \tau_{16}(H_{14m16})_B\,U_{3,13}] - A_{14B}\,\tau_{14}\,U_{2,13}\}_{S,L}$$

$$D_{14,14} = \left(\frac{\sigma}{M_{14}}\right)\{A_{14A}[(1-\rho_{14})(H_{14j14})_A - 1](\epsilon_{14} + \tau_{14}\, U_{1,14}) + A_{14B}(1-\rho_{14})$$

$$[\epsilon_{14}(H_{14m14})_B + \tau_{14}(H_{14m14})_B\, U_{2,14} + \tau_{16}(H_{14m16})_B\, U_{3,14}] - A_{14B}$$

$$(\epsilon_{14} + \tau_{14}\, U_{2,14})\}_{S,L}$$

$$(B_1)_{S,L} = \left(\frac{1}{M_1}\right)[A_1(1-\rho_1)\ \tau_{13}(H_{1j13})_D\, U_{8,15}]_{S,L}$$

$$(B_2)_{S,L} = \left(\frac{1}{M_2}\right)[A_{2D}(1-\rho_2)\ \tau_{13}(H_{2j13})_D\, U_{8,15} + A_{2F}(1-\rho_2)\{\tau_{13}(H_{2m13})_F\, U_{7,15}$$

$$+ \tau_{17}(H_{2m17})_F\, U_{6,15}\}]_{S,L}$$

$$(B_4)_{S,L} = \left(\frac{1}{M_4}\right)[A_4(1-\rho_4)\{\tau_{13}(H_{4m13})_F\, U_{7,15} + \tau_{17}(H_{4m17})_F\, U_{6,15}\}]_{S,L}$$

$$(B_5)_{S,L} = \left(\frac{1}{M_5}\right)[A_5(1-\rho_5)\ \{\tau_{16}(H_{5j16})_c\, U_{4,15} + \tau_{17}(H_{5j17})_c\, U_{5,15}\}]_{S,L}$$

$$(B_6)_{S,L} = \left(\frac{1}{M_6}\right)[A_6(1-\rho_6)\{\tau_{16}(H_{6j16})_c\, U_{4,15} + \tau_{17}(H_{6j17})_c\, U_{5,15}\}]_{S,L}$$

$$(B_8)_{S,L} = \left(\frac{1}{M_8}\right)[A_8(1-\rho_8)\{\tau_{16}(H_{8j16})_c\, U_{4,15} + \tau_{17}(H_{8j17})_c\, U_{5,15}\}]_{S,L}$$

$$(B_9)_{S,L} = \left(\frac{1}{M_9}\right)[A_{9B}(1-\rho_9)\{\tau_{14}(H_{9m14})_B\, U_{2,15} + \tau_{16}(H_{9m16})_B\, U_{3,15}\} + A_{9c}(1-\rho_9)$$

$$\{\tau_{16}(H_{9j16})_c\, U_{4,15} + \tau_{17}(H_{9j17})_c\, U_{5,15}\}]_{S,L}$$

$$(B_{10})_{S,L} = \left(\frac{1}{M_{10}}\right)[A_{10}(1-\rho_{10})\{\tau_{14}(H_{10j14})_A\, U_{1,15} + \tau_{15}(H_{10j15})_A\}]_{S,L}$$

$$(B_{11})_{S,L} = \left(\frac{1}{M_{11}}\right)[A_{11}(1-\rho_{11})\{\tau_{14}(H_{11m14})_B\, U_{2,15} + \tau_{16}(H_{11m16})_B\, U_{3,15}\}]_{S,L}$$

$$(B_{12})_{S,L} = \left(\frac{1}{M_{12}}\right)[A_{12A}(1-\rho_{12})\{\tau_{14}(H_{12j14})_A\ U_{1,15} + \tau_{15}(H_{12j15})_A\} + A_{12B}(1-\rho_{12})$$

$$\{\tau_{14}(H_{12m14})_B\ U_{2,15} + \tau_{16}(H_{12m16})_B\ U_{3,15}\}]_{S,L}$$

$$(B_{13})_{S,L} = \left(\frac{1}{M_{13}}\right)[A_{13D}\ \tau_{13}\ \{(1-\rho_{13})(H_{13j13})_D - 1\}U_{8,15} + A_{13F}\ \tau_{13}\{(1-\rho_{13})$$

$$(H_{13m13})_F - 1\}U_{7,15} + A_{13F}(1-\rho_{13})\ \tau_{17}(H_{13m17})_F\ U_{6,15}]_{S,L}$$

$$(B_{14})_{S,L} = \left(\frac{1}{M_{14}}\right)[A_{14A}\ \tau_{14}\{(1-\rho_{14})(H_{14j14})_A - 1\}U_{1,5} + A_{14A}(1-\rho_{14})\ \tau_{15}$$

$$(H_{14j15})_A + A_{14B}\ \tau_{14}\{(1-\rho_{14})(H_{14m14})_B - 1\}U_{2,15} + A_{14B}\ \tau_{16}$$

$$(1-\rho_{14})(H_{14m16})_B\ U_{3,15}]_{S,L}$$

For the total channel,

$$(B_i)_{S,L} \qquad B_i$$

$$\tau_{13} = \tau_{14} = 1\ ,$$

$$\epsilon_{13} = \epsilon_{14} = 0\ .$$

Scanner Model Equations

Total Channel

$$\dot{T}_i = A_{ij}T_j + D_{ij}T_j^4 + B_{Qi}\dot{Q} + B_iE + b + e$$

SW/LW Channels

$$\dot{T}_i = A_{ij}T_j + D_{ij}T_j^4 + B_{Qi}\dot{Q} + (B_i)_S E_S + (B_i)_L E_L + b + e$$

Scanner (using Enclosure Coupling Method)

$$E = \begin{bmatrix} E^1 \\ E^2 \\ E^3 \\ E^4 \\ E^5 \\ E^6 \end{bmatrix} \qquad \text{where } m = 6$$

For each cavity (or enclosure in the scanner model)

$$E^1 = \begin{bmatrix} E_1^1 \\ E_2^1 \\ E_3^1 \\ E_4^1 \end{bmatrix} \quad E^2 = \begin{bmatrix} E_1^2 \\ E_2^2 \\ E_3^2 \\ E_4^2 \\ E_5^2 \end{bmatrix} \quad E^3 = \begin{bmatrix} E_1^3 \\ E_2^3 \\ E_3^3 \\ E_4^3 \\ E_5^3 \\ E_6^3 \end{bmatrix} \quad E^4 = \begin{bmatrix} E_1^4 \\ E_2^4 \\ E_3^4 \\ E_4^4 \end{bmatrix} \quad E^5 = \begin{bmatrix} E_1^5 \\ E_2^5 \\ E_3^5 \end{bmatrix} \quad E^6 = \begin{bmatrix} E_1^6 \\ E_2^6 \\ E_3^6 \end{bmatrix}$$

where $E_1^1 = E_{15}^1$ , $E_2^1 = E_{10}^1$ , $E_3^1 = E_{14}^1$ , $E_4^1 = E_{12}^1$

$E_1^2 = E_{14}^2$ , $E_2^2 = E_{11}^2$ , $E_3^2 = E_{k6}^2$ , $E_4^2 = E_9^2$ , $E_5^2 = E_{12}^2$

$E_1^3 = E_{10}^3$ , $E_2^3 = E_8^3$ , $E_3^3 = E_6^3$ , $E_4^3 = E_5^3$ , $E_5^3 = E_{17}^3$ , $E_6^3 = E_9^3$

$E_1^4 = E_{17}^4$ , $E_2^4 = E_4^4$ , $E_3^4 = E_2^4$ , $E_4^4 = E_{13}^4$

$E_1^5 = E_{13}^5$ , $E_2^5 = E_2^5$ , $E_3^5 = E_1^5$

$E_1^6 = E_3^6$ , $E_2^6 = E_2^6$ , $E_3^6 = E_7^6$

$$\tilde{E}^1 = \begin{bmatrix} 0 & 0 & 0 & 0 & 0 \\ 0 & 0 & 0 & 0 & 0 \\ 1 & 0 & 0 & 0 & 0 \\ 0 & 0 & 0 & 0 & 0 \end{bmatrix} E^2$$

$$\tilde{E}^2 = \begin{bmatrix} 0 & 0 & 1 & 0 \\ 0 & 0 & 0 & 0 \\ 0 & 0 & 0 & 0 \\ 0 & 0 & 0 & 0 \\ 0 & 0 & 0 & 0 \end{bmatrix} E^1 + \begin{bmatrix} 0 & 0 & 0 & 0 & 0 & 0 \\ 0 & 0 & 0 & 0 & 0 & 0 \\ 1 & 0 & 0 & 0 & 0 & 0 \\ 0 & 0 & 0 & 0 & 0 & 0 \\ 0 & 0 & 0 & 0 & 0 & 0 \end{bmatrix} E^3$$

$$\tilde{E}^3 = \begin{bmatrix} 0 & 0 & 1 & 0 & 0 \\ 0 & 0 & 0 & 0 & 0 \\ 0 & 0 & 0 & 0 & 0 \\ 0 & 0 & 0 & 0 & 0 \\ 0 & 0 & 0 & 0 & 0 \\ 0 & 0 & 0 & 0 & 0 \end{bmatrix} E^2 + \begin{bmatrix} 0 & 0 & 0 & 0 \\ 0 & 0 & 0 & 0 \\ 0 & 0 & 0 & 0 \\ 0 & 0 & 0 & 0 \\ 1 & 0 & 0 & 0 \\ 0 & 0 & 0 & 0 \end{bmatrix} E^4$$

$$\tilde{E}^4 = \begin{bmatrix} 0 & 0 & 0 & 0 & 1 & 0 \\ 0 & 0 & 0 & 0 & 0 & 0 \\ 0 & 0 & 0 & 0 & 0 & 0 \\ 0 & 0 & 0 & 0 & 0 & 0 \end{bmatrix} E^3 + \begin{bmatrix} 0 & 0 & 0 \\ 0 & 0 & 0 \\ 0 & 0 & 0 \\ 1 & 0 & 0 \end{bmatrix} E^5$$

$$\tilde{E}^5 = \begin{bmatrix} 0 & 0 & 0 & 1 \\ 0 & 0 & 0 & 0 \\ 0 & 0 & 0 & 0 \end{bmatrix} E^4 \quad , \quad \tilde{E}^6 = 0$$

Thus D matrix is formed by the above $\tilde{E}$s.

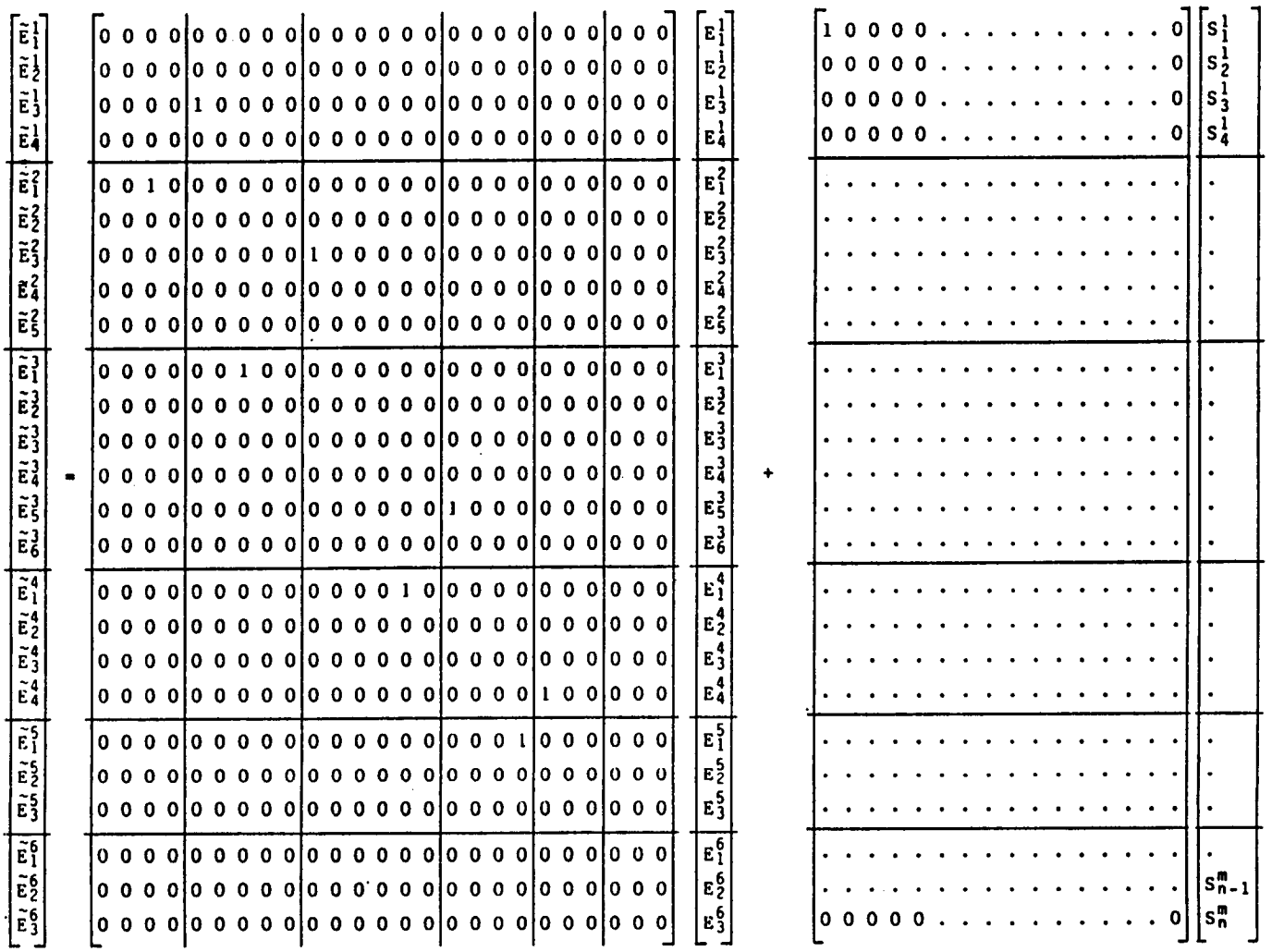

$$\tau = \begin{bmatrix} 0 & & & & & & & & & & & & & & & & & & & & & & & \\ & \tau_{14} & & & & & & & & & & & & & & & & & & & & & & \\ & & 0 & & & & & & & & & & & & & & & & & & & & & \\ & & & \tau_{14} & & & & & & & & & & & & & & & & & & & & \\ & & & & 0 & & & & & & & & & & & & & & & & & & & \\ & & & & & 1 & & & & & & & & & & & & & & & & & & \\ & & & & & & 0 & & & & & & & & & & & & & & & & & \\ & & & & & & & 0 & & & & & & & & & & & & & & & & \\ & & & & & & & & 1 & & & & & & & & & & & & & & & \\ & & & & & & & & & 0 & & & & & & & & & & & & & & \\ & & & & & & & & & & 0 & & & & & & & & & & & & & \\ & & & & & & & & & & & 1 & & & & & & & & & & & & \\ & & & & & & & & & & & & 0 & & & & & & & & & & & \\ & & & & & & & & & & & & & 0 & & & & & & & & & & \\ & & & & & & & & & & & & & & \tau_{13} & & & & & & & & & \\ & & & & & & & & & & & & & & & \tau_{13} & & & & & & & & \\ & & & & & & & & & & & & & & & & 0 & & & & & & & \\ & & & & & & & & & & & & & & & & & 0 & & & & & & \\ & & & & & & & & & & & & & & & & & & 0 & & & & & \\ & & & & & & & & & & & & & & & & & & & 0 & & & & \\ & & & & & & & & & & & & & & & & & & & & 0 & & & \end{bmatrix}.$$

$$
\tau D = \left[\begin{array}{cccc|ccccc|cccccc|cccc|cc|ccc}
0&0&0&0&0&0&0&0&0&0&0&0&0&0&0&0&0&0&0&0&0&0&0\\
0&0&0&0&0&0&0&0&0&0&0&0&0&0&0&0&0&0&0&0&0&0&0\\
0&0&0&0&\tau_{14}&0&0&0&0&0&0&0&0&0&0&0&0&0&0&0&0&0&0\\
0&0&0&0&0&0&0&0&0&0&0&0&0&0&0&0&0&0&0&0&0&0&0\\
\hline
0&0&\tau_{14}&0&0&0&0&0&0&0&0&0&0&0&0&0&0&0&0&0&0&0&0\\
0&0&0&0&0&0&0&0&0&0&0&0&0&0&0&0&0&0&0&0&0&0&0\\
0&0&0&0&0&0&0&0&0&1&0&0&0&0&0&0&0&0&0&0&0&0&0\\
0&0&0&0&0&0&0&0&0&0&0&0&0&0&0&0&0&0&0&0&0&0&0\\
0&0&0&0&0&0&0&0&0&0&0&0&0&0&0&0&0&0&0&0&0&0&0\\
\hline
0&0&0&0&0&0&1&0&0&0&0&0&0&0&0&0&0&0&0&0&0&0&0\\
0&0&0&0&0&0&0&0&0&0&0&0&0&0&0&0&0&0&0&0&0&0&0\\
0&0&0&0&0&0&0&0&0&0&0&0&0&0&0&0&0&0&0&0&0&0&0\\
0&0&0&0&0&0&0&0&0&0&0&0&0&0&0&0&0&0&0&0&0&0&0\\
0&0&0&0&0&0&0&0&0&0&0&0&0&0&1&0&0&0&0&0&0&0&0\\
0&0&0&0&0&0&0&0&0&0&0&0&0&0&0&0&0&0&0&0&0&0&0\\
\hline
0&0&0&0&0&0&0&0&0&0&0&0&1&0&0&0&0&0&0&0&0&0&0\\
0&0&0&0&0&0&0&0&0&0&0&0&0&0&0&0&0&0&0&0&0&0&0\\
0&0&0&0&0&0&0&0&0&0&0&0&0&0&0&0&0&0&0&0&0&0&0\\
0&0&0&0&0&0&0&0&0&0&0&0&0&0&0&0&\tau_{13}&0&0&0&0&0&0\\
\hline
0&0&0&0&0&0&0&0&0&0&0&0&0&0&0&\tau_{13}&0&0&0&0&0&0&0\\
0&0&0&0&0&0&0&0&0&0&0&0&0&0&0&0&0&0&0&0&0&0&0\\
0&0&0&0&0&0&0&0&0&0&0&0&0&0&0&0&0&0&0&0&0&0&0\\
\hline
0&0&0&0&0&0&0&0&0&0&0&0&0&0&0&0&0&0&0&0&0&0&0\\
0&0&0&0&0&0&0&0&0&0&0&0&0&0&0&0&0&0&0&0&0&0&0\\
0&0&0&0&0&0&0&0&0&0&0&0&0&0&0&0&0&0&0&0&0&0&0
\end{array}\right]
$$

$$
A = \begin{array}{|c|c|c|c|c|c|}
\hline
\begin{matrix} A_{11} & A_{12} & A_{13} & A_{14} \\ A_{21} & A_{22} & A_{23} & A_{24} \\ A_{31} & A_{32} & A_{33} & A_{34} \\ A_{41} & A_{42} & A_{43} & A_{44} \end{matrix} & & & & & \\
\hline
 & \begin{matrix} A_{11} & A_{12} & A_{13} & A_{14} & A_{15} \\ A_{21} & A_{22} & A_{23} & A_{24} & A_{25} \\ A_{31} & A_{32} & A_{33} & A_{34} & A_{35} \\ A_{41} & A_{42} & A_{43} & A_{44} & A_{45} \\ A_{51} & A_{52} & A_{53} & A_{54} & A_{55} \end{matrix} & & & & \\
\hline
 & & \begin{matrix} A_{11} & A_{12} & A_{13} & A_{14} & A_{15} & A_{16} \\ A_{21} & A_{22} & A_{23} & A_{24} & A_{25} & A_{26} \\ A_{31} & A_{32} & A_{33} & A_{34} & A_{35} & A_{36} \\ A_{41} & A_{42} & A_{43} & A_{44} & A_{45} & A_{46} \\ A_{51} & A_{52} & A_{53} & A_{54} & A_{55} & A_{56} \\ A_{61} & A_{62} & A_{63} & A_{64} & A_{65} & A_{66} \end{matrix} & & & \\
\hline
 & & & \begin{matrix} A_{11} & A_{12} & A_{13} & A_{14} \\ A_{21} & A_{22} & A_{23} & A_{24} \\ A_{31} & A_{32} & A_{33} & A_{34} \\ A_{41} & A_{42} & A_{43} & A_{44} \end{matrix} & & \\
\hline
 & & & & \begin{matrix} A_{11} & A_{12} & A_{13} \\ A_{21} & A_{22} & A_{23} \\ A_{31} & A_{32} & A_{33} \end{matrix} & \\
\hline
 & & & & & \begin{matrix} A_{11} & A_{12} & A_{13} \\ A_{21} & A_{22} & A_{23} \\ A_{31} & A_{32} & A_{33} \end{matrix} \\
\hline
\end{array}
$$

$$A = (I - {}^{d}E)^{-1} E \epsilon$$

PRECEDING PAGE BLANK NOT FILMED

# APPENDIX E

# ERBE SOLAR MONITOR THERMAL MODEL

## SOLAR MONITOR MODEL

As described in the non-scanner and scanner modeling efforts, the same notations are used for constants and variables in developing the energy balance equation of the solar monitor.

To avoid the burden to write the same equations as used in developing the other models, the same variable name in the equation such as $R_{ij}$ is here simply used.

A general form of the equation for the solar monitor which is divided into 19 nodes is presented here as

$$\dot{T} = AT + DT^4 + B_Q\dot{Q} + BE + b.$$

Now the computational algorithm for the constants of the above equation has been developed by using the enclosure coupling technique. It is available and can be used for all 8 non-scanner, scanner and solar monitor models.

The following constants, $A_{ij}$, represent the coefficients of themal conduction terms in the energy balance equations.

$$A_{11} = -1/(R_{13}M_1)$$

$$A_{12} = 0$$

$$A_{13} = 1/(R_{13}M_1)$$

$$A_{21} = 0$$

$$A_{22} = -1/(R_{23}M_2)$$

$$A_{23} = 1/(R_{23}M_2)$$

$$
C = \begin{array}{c}
\begin{array}{cccccc} 1 & 2 & 3 & 4 & 5 & 6 \end{array} \\
\left[\begin{array}{cccccc}
\begin{array}{cccc} c_{11} & c_{12} & c_{13} & c_{14} \\ c_{21} & c_{22} & c_{23} & c_{24} \\ c_{31} & c_{32} & c_{33} & c_{34} \\ c_{41} & c_{42} & c_{43} & c_{44} \end{array} & & & & & \\
& \begin{array}{ccccc} c_{11} & c_{12} & c_{13} & c_{14} & c_{15} \\ c_{21} & c_{22} & c_{23} & c_{24} & c_{25} \\ c_{31} & c_{32} & c_{33} & c_{34} & c_{35} \\ c_{41} & c_{42} & c_{43} & c_{44} & c_{45} \\ c_{51} & c_{52} & c_{53} & c_{54} & c_{55} \end{array} & & & & \\
& & \begin{array}{cccccc} c_{11} & c_{12} & c_{13} & c_{14} & c_{15} & c_{16} \\ c_{21} & c_{22} & c_{23} & c_{24} & c_{25} & c_{26} \\ c_{31} & c_{32} & c_{33} & c_{34} & c_{35} & c_{36} \\ c_{41} & c_{42} & c_{43} & c_{44} & c_{45} & c_{46} \\ c_{51} & c_{52} & c_{53} & c_{54} & c_{55} & c_{56} \\ c_{61} & c_{62} & c_{63} & c_{64} & c_{65} & c_{66} \end{array} & & & \\
& & & \begin{array}{cccc} c_{11} & c_{12} & c_{13} & c_{14} \\ c_{21} & c_{22} & c_{23} & c_{24} \\ c_{31} & c_{32} & c_{33} & c_{34} \\ c_{41} & c_{42} & c_{43} & c_{44} \end{array} & & \\
& & & & \begin{array}{ccc} c_{11} & c_{12} & c_{13} \\ c_{21} & c_{22} & c_{23} \\ c_{31} & c_{32} & c_{33} \end{array} & \\
& & & & & \begin{array}{ccc} c_{11} & c_{12} & c_{13} \\ c_{21} & c_{22} & c_{23} \\ c_{31} & c_{32} & c_{33} \end{array}
\end{array}\right]
\end{array}
$$

$$C = (I - \rho^{d}E)^{-1} \; E \; \tau \cdot$$

$$\Phi = [(I - \rho - \tau D)(I - CD)^{1-} \; A - \epsilon]\Omega + [(1 - \rho - \tau D)(I - CD)^{1-}C - \tau] \; F \; S$$

$$A_{31} = 1/(R_{31}M_3)$$

$$A_{32} = 1/(R_{32}M_3)$$

$$A_{33} = -(\frac{1}{R_{31}} + \frac{1}{R_{32}} + \frac{1}{R_{34}})/M_3$$

$$A_{34} = 1/(R_{34}M_3)$$

$$A_{43} = 1/(R_{43}M_4)$$

$$A_{44} = -(\frac{1}{R_{43}} + \frac{1}{R_{45}} + \frac{1}{R_{47}} + \frac{1}{R_{4-19}})/M_4$$

$$A_{45} = 1/(R_{45}M_4)$$

$$A_{47} = 1/(R_{47}M_4)$$

$$A_{4-19} = 1/(R_{4-19}M_4)$$

$$A_{54} = 1/(R_{54}M_5)$$

$$A_{55} = -(\frac{1}{R_{54}} + \frac{1}{R_{56}})/M_5$$

$$A_{56} = 1/(R_{56}M_5)$$

$$A_{65} = 1/(R_{65}M_6)$$

$$A_{66} = -(\frac{1}{R_{65}} + \frac{1}{R_{67}})/M_6$$

$$A_{67} = 1/(R_{67}M_6)$$

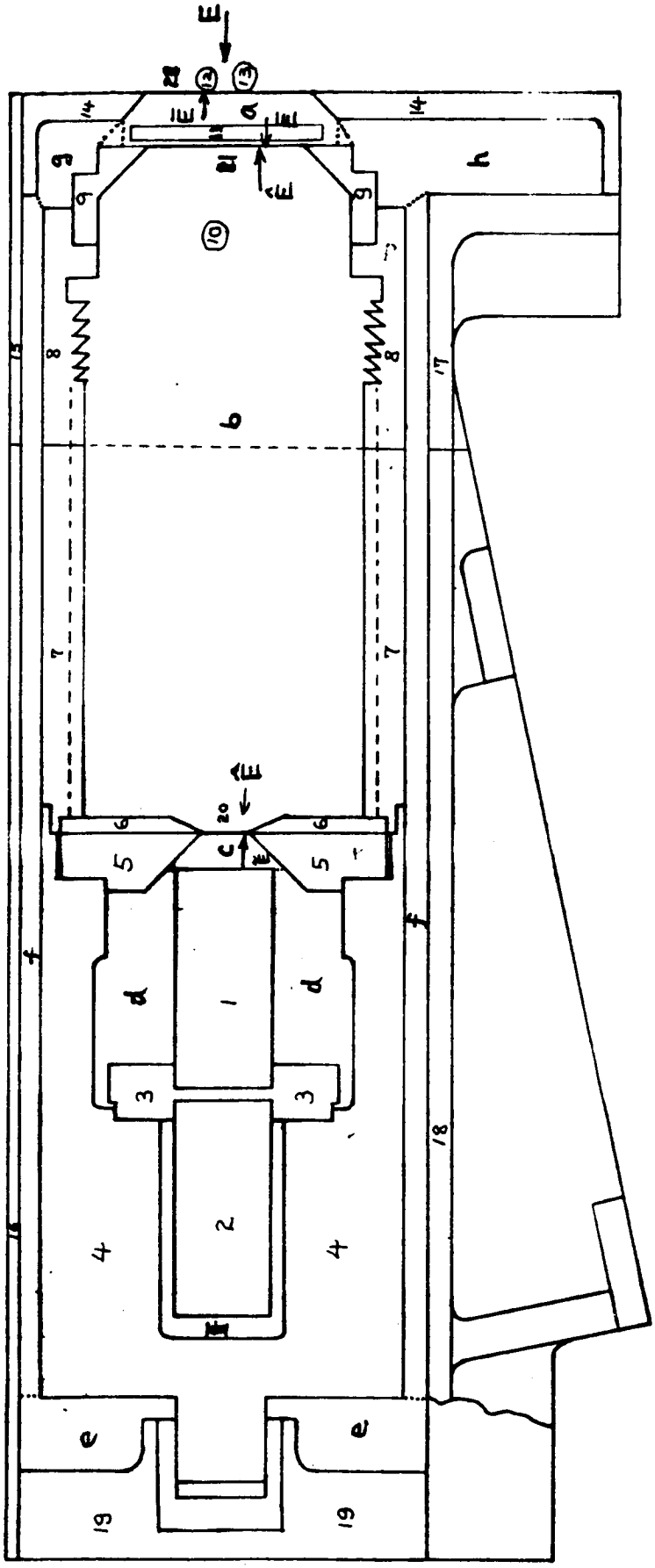

SOLAR MONITOR MODEL

1. Active Cavity
2. Reference Cavity
3. Button, Duplex Cone Cavities
4. Heat Sink
5. Aperture, Primary
6. Shield, Aperture
7. Body (Rear Barrel)
8. Body (Front Barrel)
9. Aperture, Secondary (or FOV Limiter)
10. Motor Housing
11. Chopper Blade
12. Chopper Pendulum
13. Motor, Chopper
14. FOV Limiter
15. Front Top Housing Cover
16. Rear Top Housing Cover
17. Front Housing
18. Rear Housing
19. Holder, Heat Sink
20. Fictitious Surface

p. Temperature Probe

$E$. Total Incident Radiation

$\bar{E}$. Irradiance in enclosure a

$\hat{E}$. Irradiance in enclosure b

$\tilde{E}$. Rate of Incident Radiation From a Neighboring Surface

a-h. Cavities Within The Sensor, i.e., Enclosures or Spaces Between Sensor Nodes

$$A_{74} = 1/(R_{74}M_7)$$

$$A_{76} = 1/(R_{76}M_7)$$

$$A_{77} = -(\frac{1}{R_{74}} + \frac{1}{R_{76}} + \frac{1}{R_{78}})/M_7$$

$$A_{78} = 1/(R_{78}M_7)$$

$$A_{87} = 1/(R_{87}M_8)$$

$$A_{88} = 1(\frac{1}{R_{87}} + \frac{1}{R_{89}} + \frac{1}{R_{8-10}})/M_8$$

$$A_{89} = 1/(R_{87}M_8)$$

$$A_{8-10} = 1/(R_{8-10}M_8)$$

$$A_{9-8} = 1/(R_{9-8}M_9)$$

$$A_{9-9} = -\frac{1}{R_{9-8}M_9}$$

$$A_{10-8} = 1/(R_{10-8}M_{10})$$

$$A_{10-10} = -1/(R_{10-8}M_{10}) - 1/(R_{10-12}M_{10}) - 1/(R_{10-13}M_{10})$$

$$A_{10-12} = 1/(R_{10-12}M_{10})$$

$$A_{10-13} \; 1 \; 1/(R_{10-13}M_{10})$$

$$A_{11-12} = 1/(R_{11-12}M_{11})$$

$$A_{11-11} = -1/(R_{11-12}M_{11})$$

$$A_{12-11} = 1/(R_{12-11}M_{12})$$

$$A_{12-12} = -(1/R_{12-11} + 1/R_{12-13})/M_{12}$$

$$A_{12-13} = 1/(R_{12-11}M_{12})$$

$$A_{13-12} = 1/(R_{13-12}M_{12})$$

$$A_{13-13} = -(1/R_{13-12} + 1/R_{13-10})/M_{12}$$

$$A_{13-10} = 1/(R_{13-10}M_{13})$$

$$A_{14-14} = -(1/R_{14-15} + 1/R_{14-17})/M_{14}$$

$$A_{14-15} = 1/(R_{14-15}M_{14})$$

$$A_{14-17} = 1/(R_{14-17}M_{14})$$

$$A_{15-15} = -1/(R_{15-16}M_{15}) - 1/(R_{15-14}R_{15})$$

$$A_{15-16} = 1/(R_{15-16}M_{15})$$

$$A_{15-14} = 1/(R_{15-14}M_{15})$$

$$A_{16-15} = 1/(R_{16-15}M_{16})$$

$$A_{16-16} = -(1/R_{16-15} + 1/R_{16-19})/M_{16}$$

$$A_{16-19} = 1/(R_{16-19}M_{16})$$

$$A_{17-14} = 1/(R_{17-14}M_{17})$$

$$A_{17-17} = -(1/R_{17-14} + 1/R_{17-18})/M_{17}$$

$$A_{17-18} = 1/(R_{17-18}M_{17})$$

$$A_{18-17} = 1/(R_{18-17}M_{18})$$

$$A_{18-18} = -(1/R_{18-17} + 1/R_{18-19})/M_{18}$$

$$A_{18-19} = 1/(R_{18-19}M_{18})$$

$$A_{19-4} = 1/(R_{19-4}M_{19})$$

$$A_{19-16} = 1/(_{19-16}M_{19})$$

$$A_{19-18} = 1/(R_{19-18}M_{19})$$

$$A_{19-19} = -(1/R_{19-4} + 1/R_{19-16} + 1/R_{19-18})/M_{19}$$

For the radiative interaction term, considering the specular reflection,

$$\rho = \rho^d + \rho^s \tag{1}$$

$$\epsilon + \rho + \tau = 1 \tag{2}$$

$$M_k^d = \epsilon_k \sigma T_k^4 + \rho_k^d E_k + \tau_k \bar{E}_k \tag{3}$$

$$E_k = \sum_j E_{k-j} M_j^d \tag{4}$$

The energy balance equation is now

$$\phi_k = E_k = M_k \tag{5}$$

where

$$M_k = {}^{s}E_k + M_k^d \quad .$$

Thus

$$\kappa_k = E_k = \epsilon_k \Omega_k - \rho_k^d E_k - \rho_k^s E_k - \tau_k \bar{E}_k \tag{6}$$

where

$$\Omega_k = \sigma T_k^4 \quad .$$

From (3) and (4),

$$M_j^d = \sum_{i=1}^{n} (\delta_{ij} - \rho_j^d E_{j-1})^{-1} (\epsilon_i \Omega_i + \tau_i \bar{E}_i) \tag{7}$$

From (7) through (4)

$$\begin{aligned} E_k &= \sum_j E_{k-j} \sum_i P_{j-i} (\epsilon_i \Omega_i + \tau_i \bar{E}_i) \\ &= \sum_i (\epsilon_i \Omega_i + \tau_i \bar{E}_i) \sum_{j=1}^{n} E_{k-j} P_{j-i} \end{aligned} \tag{8}$$

Equation (6) becomes

$$\begin{aligned} \phi_k &= (1 - \rho_k) E_k - \epsilon_k \Omega_k - \tau_k \bar{E}_k \\ &= \sum_i [(1 - \rho_k) \epsilon_i \sum_j E_{k-j} P_{j-i} - \epsilon_k \delta_{ki}] \Omega_i \\ &+ \sum_i [(1 - \rho_k) \tau_i \sum_j E_{k-j} P_{j-i} - \tau_k \delta_{ki}] \bar{E}_i \end{aligned} \tag{9}$$

Let

$$H_{kji} = \sum_j E_{k-j} P_{j-i}$$

$$H_{nm\ell} = \sum_m E_{n-m} P_{m-\ell}$$

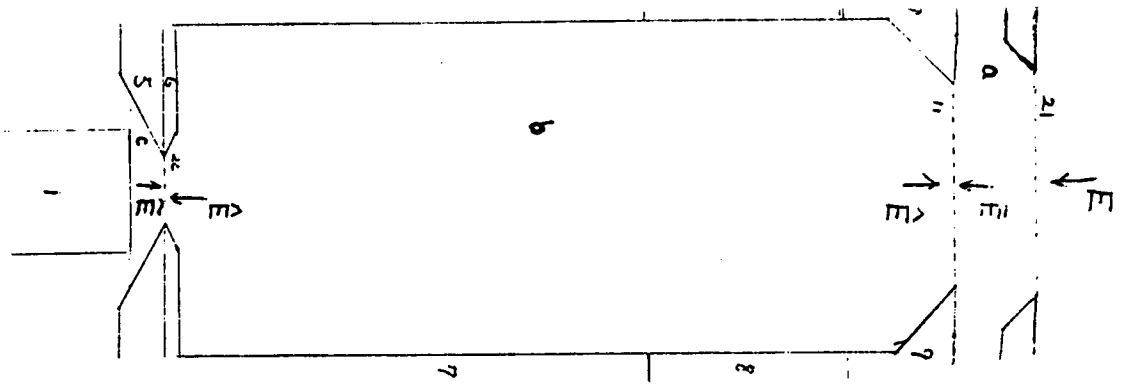

From the above drawing, the enclosures, a, b and c, are found. For each enclosure, the incoming radiance to a certain surface can be described by Equation (8).

Choose the enclosure b and c and couple them together, then one can define the transmitted radiance through the filtering surface.

First,

| | | Index |
|---|---|---|
| enclosure b - | elements 6,7,8,9,11,20 | i,j,k |
| enclosure c - | elements 1,5,20 | ℓ,m,n |

From Equation (8)

$$E_k = \sum_i \epsilon_i \Omega_i \sum_j E_{k-j} P_{j-i} + \sum_i \tau_i \bar{E}_i \sum_j E_{k-j} P_{j-i}$$

where in this equation i, j and k are dummy index

or

$$E_k = \sum_i \epsilon_i \Omega_i H_{kji} + \sum_i \tau_i \bar{E}_i H_{kji}$$

For the enclosure c, Equation (8) becomes

$$\tilde{E}_{20} = \left(\sum_\ell \epsilon_\ell \Omega_\ell H_{20m\ell}\right)_c + \tau_{20} \hat{E}_{20} (H_{20m20})_c \qquad (10)$$

where ℓ, m and n = 1, 5 and 20.

Likewise, for the enclosure b,

$$\hat{E}_{20} = \left(\sum_i \epsilon_i \Omega_i H_{20ji}\right)_b + \tau_{20} \tilde{E}_{20} (H_{20j20})_b + \tau_{11} \bar{E}_{11} (H_{20j11})_b \tag{11}$$

where i and j = 6, 7, 8, 9, 11 and 20.

Combining (10) and (11) to obtain $\tilde{E}_{20}$ and $\hat{E}_{20}$ as a function of $\bar{E}_{11}$, we have

$$\tilde{E}_{20} = G_1 \left[ \left(\sum_\ell \epsilon_\ell \Omega_\ell H_{20m\ell}\right)_c + \tau_{20} (H_{20m20})_c \left(\sum_i \epsilon_i \Omega_i H_{20ji}\right)_b \right.$$
$$\left. + \tau_{11} \tau_{20} (H_{20m20})_c (H_{20j11})_b \bar{E}_{11} \right] \tag{12}$$

and

$$\hat{E}_{20} = G_1 \left[ \left(\sum_i \epsilon_i \Omega_i H_{20ji}\right)_n + \tau_{20} (H_{20j20})_b \left(\sum_\ell \epsilon_\ell \Omega_\ell H_{20m\ell}\right)_c \right.$$
$$\left. + \tau_{11} (H_{20j11})_b \bar{E}_{11} \right] \tag{13}$$

where

$$G_1 = \left[1 - \tau_{20}^2 (H_{20j20})_b (H_{20m20})_c\right]^{-1} .$$

The radiation energy balances in the enclosures b and c are

$$\phi_k\Big|_b = \sum_i \left[(1 - \rho_k) \epsilon_i H_{kji} - \epsilon_k \delta_{ki}\right] \Omega_i$$
$$+ \sum_i \left[(1 - \rho_k) \tau_i H_{kji} - \tau_k \delta_{ki}\right] (\tilde{E}_{i=20} \text{ or } \bar{E}_{i=11}) \tag{14}$$

and

$$\phi_n\Big|_b = \sum_\ell [(1 - \rho_n)\, e_\ell H_{nm\ell} - e_n \delta_{n\ell}]\, \Omega_\ell$$

$$+ \sum_\ell [(1 - \rho_n)\, \tau_\ell H_{nm\ell} - \tau_n \delta_{n\ell}]\, \hat{E}_\ell \qquad (15)$$

Second,

| | | | Index |
|---|---|---|---|
| enclosure d | - | elements 11,14,21 | $\ell$,m,n |
| enclosure b | - | elements 6,7,8,9,11,20 | i,j,k |

From Equation (8)

$$\hat{E}_{11} = (\sum_i \epsilon_i \Omega_i H_{11ji})_b + \tau_{11}(H_{11j11})_b \bar{E}_{11} + \tau_{20}(H_{11j20})_b \tilde{E}_{20} \qquad (16)$$

and

$$\bar{E}_{11} = (\sum_\ell \epsilon_\ell \Omega_\ell H_{11m\ell})_a + \tau_{11}(H_{11m11})_a\, \hat{E}_{11} + \tau_{21}(H_{11m21})_a\, E \qquad (17)$$

Substituting (12) into (16), Equation (16) becomes

$$\hat{E}_{11} = (\sum_i \epsilon_i \Omega_i H_{11ji})_b + \tau_{20}\, G_1 (H_{11j20})_b\, (\sum_\ell \epsilon_\ell \Omega_\ell H_{20m\ell})_c$$

$$+ \tau_{20}^2\, G_1 (H_{11j20})_b\, (H_{20m20})_c\, (\sum_i \epsilon_i \Omega_i H_{20ji})_b$$

$$+ [\tau_{11}(H_{11j11})_b + \tau_{11}\, \tau_{20}^2\, G_1 (H_{11j20})_b\, (H_{20m20})_c\, (H_{2-j11})_b]\, \bar{E}_{11} \qquad (18)$$

Substituting (18) into (17)

$$\bar{E}_{11} = G_2 [(\sum_\ell \epsilon_\ell \Omega_\ell\, H_{nm\ell})_a + \tau_{21}(H_{11m21})_a E + \tau_{11}(H_{11m11})_a\, (\sum_i \epsilon_i \Omega_i H_{11ji})_b$$

$$+ \tau_{11}\, \tau_{20}\, G_1 (H_{11m11})_a\, (H_{11j20})_b\, (\sum_\ell \epsilon_\ell \Omega_\ell\, H_{20m\ell})_c$$

$$+ \tau_{11}\, \tau_{20}^2\, G_1 (H_{11m11})_a\, (H_{11j20})_b\, (H_{20m20})_c\, (\sum_i \epsilon_i \Omega_i H_{20ji})_b] \qquad (19)$$

where

$$G_2 = [1 - \tau_{11}^2 \; S_1 (H_{11m11})_a]^{-1}$$

$$S_1 = (H_{11j11})_b + \tau_{20}^2 \; G_1 (H_{11j20})_b \; (H_{20m20})_c \; (H_{20j11})_b \quad .$$

On the other hand, substitution (17) into (18)

$$\begin{aligned} \hat{E}_{11} = G_2 [ & (\sum_i \epsilon_i \Omega_i H_{11ji})_b + \tau_{20} \; G_1 (H_{11j20})_b \; (\sum_\ell \epsilon_\ell \Omega_\ell \; H_{20m\ell})_c \\ & + \tau_{20}^2 \; G_1 (H_{11j20})_b \; (H_{20m20})_c \; (\sum_i \epsilon_i \Omega_i H_{20ji})_b \\ & + \tau_{11} \; S_1 (\sum_\ell \epsilon_\ell \Omega_\ell \; H_{11m\ell})_a + \tau_{11} \tau_{21} \; S_1 (H_{11m21})_a \; E ] \end{aligned} \tag{20}$$

For the enclosure a: nodes: 11,14,21

$$\begin{aligned} \phi_{11}\Big|_a = & [(1 - \rho_{11}) \; \epsilon_{11} (H_{11m11})_a - \epsilon_{11}] \Omega_{11} + (1 - \rho_{14}) \; \epsilon_{14} (H_{11m14})_a \; \Omega_{14} \\ & + [1 - \rho_{11}) \; \tau_{21} (H_{11m21})_a \; E + [(1 - \rho_{11}) \; \tau_{11} (H_{11m11})_a - \tau_{11}] \hat{E}_{11} \end{aligned}$$

(0 for open position; 0 for closed position)

$$\begin{aligned} \phi_{14}\Big|_a = & (1 - \rho_{14}) \; \epsilon_{11} (H_{14m11})_a \; \Omega_{11} + [(1 - \rho_{14}) \; G_{14} (H_{14m14})_a - \epsilon_{14}] \; \Omega_{14} \\ & + (1 - \rho_{14}) \; \tau_{11} (H_{14m11})_a \; \hat{E}_{11} + (1 - \rho_{14}) \; \tau_{21} (H_{14m21})_a \; E \end{aligned}$$

(0 for open position)

For the enclosure b: nodes: 6,7,8,9,11,20

$$\phi_6\Big|_b = [(1-\rho_6)\,\epsilon_6(H_{6j6})_b - \epsilon_6]\,\Omega_6 + (1-\rho_6)\,\epsilon_7(H_{6j7})_b\,\Omega_7$$

$$+ (1-\rho_6)\,\epsilon_8(H_{6j8})_b\,\Omega_8 + (1-\rho_6)\,\epsilon_9(H_{6j9})_b\,\Omega_9 + (1-\rho_6)\,\epsilon_{11}(H_{6j11})_b\,\Omega_{11}$$

($\epsilon_{11}$: 0 for open position)

$$+ (1-\rho_6)\,\epsilon_{11}(H_{6j11})_b\,\bar{E}_{11} + (1-\rho_6)\,\tau_{20}(H_{6j20})_b\,\tilde{E}_{20}$$

($\epsilon_{11}$: 0 for closed position)

$$\phi_7\Big|_b = (1-\rho_7)\,\epsilon_6(H_{7j6})_b\,\Omega_6 + [(1-\rho_7)\,\epsilon_7(H_{7j7})_b - \epsilon_7]\,\Omega_7$$

$$+ (1-\rho_7)\,\epsilon_8(H_{7j8})_b\,\Omega_8 + (L-\rho_7)\,\epsilon_9(H_{7j9})_b\,\Omega_9 + (1-\rho_7)\,\epsilon_{11}(H_{7j11})_b\,\Omega_{11}$$

($\epsilon_{11}$: 0 for open position)

$$+ (1-\rho_7)\,\epsilon_{11}(H_{7j11})_b\,\bar{E}_{11} + (1-\rho_7)\,\tau_{20}(H_{7j20})_b\,\tilde{E}_{20}$$

($\epsilon_{11}$: 0 for closed position)

$$\phi_8\Big|_b = (1-\rho_8)\,\epsilon_6(H_{8j6})_b\,\Omega_6 + (1-\rho_8)\,\epsilon_7(H_{8j7})_b\,\Omega_7 + [(1-\rho_8)\,\epsilon_8$$

$$(H_{8j8})_b - \epsilon_8]\,\Omega_8$$

$$+ (1-\rho_8)\,\epsilon_9(H_{8j9})_b\,\Omega_9 + (1-\rho_8)\,\epsilon_{11}(H_{8j11})_b\,\Omega_{11}$$

($\epsilon_{11}$: 0 for open position)

$$+ (1-\rho_8)\,\epsilon_{11}(H_{8j11})_b\,\bar{E}_{11} + (1-\rho_8)\,\tau_{20}(H_{7j20})_b\,\tilde{E}_{20}$$

($\epsilon_{11}$: 0 for closed position)

$$\phi_9\Big|_b = (1-\rho_9)\,\epsilon_6(H_{9j6})_b\,\Omega_6 + (1-\rho_9)\,\epsilon_7(H_{9j7})_b\,\Omega_7 + (L-\rho_9)\,\epsilon_8(H_{9j8})_b\,\Omega_8$$

$$+ [(1-\rho_9)\,\epsilon_9(H_{9j9})_b - \epsilon_9]\,\Omega_9 + (1-\rho_9)\,\not{\epsilon}_{11}(H_{9j11})_b\,\Omega_{11}$$

(0 for open position)

$$+ (1-\rho_9)\,\not{\tau}_{11}(H_{9j11})_b\,\bar{E}_{11} + (1-\rho_9)\,\tau_{20}(H_{9j20})_b\,\tilde{E}_{20}$$

(0 for closed position)

$$\phi_{11}\Big|_b = (1-\rho_{11})\,\epsilon_6(H_{11j6})_b\,\Omega_6 + (1-\rho_{11})\,\epsilon_7\,(H_{11j7})_b\,\Omega_7 + (1-\rho_{11})\,\epsilon_8$$

$$(H_{11j8})_b\,\Omega_8$$

$$+(1-\rho_{11})\,\epsilon_9(H_{11j9})_b\,\Omega_9 + [(1-\rho_{11})\,\not{\epsilon}_{11}(H_{11j11})_b - \epsilon_{11}]\,\Omega_{11}$$

(0 for open position)

$$+ (L-\rho_{11})\,\tau_{20}(H_{11j20})_b\,\tilde{E}_{20} + [(1-\rho_{11})\,\not{\tau}_{11}(H_{11j11})_b - \tau_{11}]\,\bar{E}_{11}$$

(0 for closed position)

$$\phi_{20}\Big|_b = (1-\rho_{20})\,\epsilon_6(H_{20j6})_b\,\Omega_6 + (1-\rho_{20})\,\epsilon_7(H_{20j7})_b\,\Omega_7$$

(0 for open position)

$$+ (1-\rho_{20})\,\epsilon_8(H_{20j8})_b\,\Omega_8 + (1-\rho_{20})\,\epsilon_9(H_{20j9})_b\,\Omega_9 + (1-\rho_{20})\,\not{\epsilon}_{11}$$

$$(H_{20j11})_b\,\Omega_{11}$$

$$+ (1-\rho_{20})\,\tau_{11}(H_{20j11})_b\,\bar{E}_{11} + [(1-\rho_{20})\,\tau_{20}(H_{20j20})_b - \tau_{20}]\,\tilde{E}_{20}$$

Enclosure c: Nodes: 1,5,20

$$\phi_1\Big|_c = [(1-\rho_1)\,\epsilon_1(H_{1j1})_c - \epsilon_1]\,\Omega_1 + (L-\rho_1)\,\epsilon_5(H_{1j5})_c\,\Omega_5$$
$$(1-\rho_1)\,\tau_{20}(H_{1j20})_c\,\hat{E}_{20}$$

$$\phi_5\Big|_c = (1-\rho_5)\,\epsilon_1(H_{5j1})_c\,\Omega_1 + [(1-\rho_5)\,\epsilon_5(H_{5h5})_c - \epsilon_5]\,\Omega_5$$
$$+ (1-\rho_5)\,\tau_{20}(H_{5j20})_c\,\hat{E}_{20}$$

$$\phi_{20}\Big|_c = (1-\rho_{20})\,\epsilon_1(H_{20j1})_c\,\Omega_1 + (1-\rho_{20})\,\epsilon_5(H_{20h5})_c\,\Omega_5$$
$$+ [(1-\rho_{20})\,\tau_{20}(H_{20j20}) - \tau_{20}]\,\hat{E}_{20}$$

For the enclosure d: Nodes: i,j,k = 1,3,4,5

$$\phi_1\Big|_d = [(1-\rho_1)\,\epsilon_1(H_{1j1})_d - \epsilon_1]\,\Omega_1 + (1-\rho_1)\,\epsilon_3(H_{1j3})_d\,\Omega_3$$
$$+ (1-\rho_1)\,\epsilon_4(H_{1j4})_d\,\Omega_4 + (1-\rho_1)\,\epsilon_5(H_{ij5})_d\,\Omega_5$$

$$\phi_3\Big|_d = (1-\rho_3)\,\epsilon_1(H_{3j1})_d\,\Omega_1 + [(1-\rho_3)\,\epsilon_3(H_{3j3})_d - \epsilon_3]\,\Omega_3$$
$$+ (1-\rho_3)\,\epsilon_4(H_{3j4})_d\,\Omega_4 + (1-\rho_3)\,\epsilon_3(H_{3j5})_d\,\Omega_5$$

$$\phi_4\Big|_d = (1-\rho_4)\,\epsilon_1(H_{4j1})_d\,\Omega_1 + (1-\rho_4)\,\epsilon_3(H_{4j3})_d\,\Omega_3$$
$$+ [(1-\rho_4)\,\epsilon_4(H_{4j4})_d - \epsilon_4]\,\Omega_4 + (1-\rho_4)\,\epsilon_5(H_{4j5})_d\,\Omega_5$$

$$\phi_5\Big|_d = (1-\rho_5)\,\epsilon_1(H_{5j1})_d\,\Omega_1 + (1-\rho_5)\,\epsilon_3\,(H_{5j3})_d\,\Omega_3$$

$$+ (1-\rho_5)\,\epsilon_4\,(H_{5j4})_d\,\Omega_4 + [(1-\rho_5)\,\epsilon_5\,(H_{5j5})_d - \epsilon_5]\,\Omega_5$$

For the enclosure e: Nodes: 4,16,18,19

$$\phi_4\Big|_e = [(1-\rho_4)\,\epsilon_4\,(H_{4j4})_e - \epsilon_4]\,\Omega_4 + (1-\rho_4)\,\epsilon_{16}\,(H_{4j16})_e\,\Omega_{16}$$

$$+ (1-\rho_4)\,\epsilon_{18}\,(H_{4j18})_e\,\Omega_{18} + (1-\rho_4)\,\epsilon_{19}\,(H_{4j19})_e\,\Omega_{19}$$

$$\phi_{16}\Big|_e = (1-\rho_{16})\,\epsilon_4\,(H_{16j4})_e\,\Omega_4 + [(1-\rho_{16})\,\epsilon_{16}\,(H_{16j16})_e - \epsilon_{16}]\,\Omega_{16}$$

$$+ (1-\rho_{16})\,\epsilon_{18}\,(H_{16j18})_e\,\Omega_{18} + (1-\rho_{16})\,\epsilon_{19}\,(H_{16j19})_e\,\Omega_{19}$$

$$\phi_{18}\Big|_e = (1-\rho_{18})\,\epsilon_4\,(H_{18j4})_e\,\Omega_4 + (1-\rho_{18})\,\epsilon_{16}\,(H_{18j16})_e\,\Omega_{16}$$

$$+ [(1-\rho_{18})\,\epsilon_{18}\,(H_{18j18})_e - \epsilon_{18}]\,\Omega_{18} + (1-\rho_{18})\,\epsilon_{19}\,(H_{18j19})_e\,\Omega_{19}$$

$$\phi_{19}\Big|_e = (1-\rho_{19})\,\epsilon_4\,(H_{19j4})_e\,\Omega_4 + (1-\rho_{19})\,\epsilon_{16}\,(H_{19j16})_e\,\Omega_{16}$$

$$+ (1-\rho_{19})\,\epsilon_{18}\,(H_{19j18})_e\,\Omega_{18} + [(1-\rho_{19})\,\epsilon_{19}\,(H_{19j19})_e - \epsilon_{19}]\,\Omega_{19}$$

For the enclosure f: Nodes: 4,7,8,14,15,16,17,18

$$\phi_4\Big|_f = [(1-\rho_4)\,\epsilon_4\,(H_{4j4})_f - \epsilon_4]\,\Omega_4 + (1-\rho_4)\,\epsilon_7\,(H_{4j7})_f\,\Omega_7$$

$$+ (1-\rho_4)\,\epsilon_8\,(H_{4j8})_f\,\Omega_8 + (1-\rho_4)\,\epsilon_{14}\,(H_{4j14})_f\,\Omega_{14} + (1-\rho_4)\,\epsilon_{15}\,(H_{4j15})_f\,\Omega_{15}$$

$$+ (1-\rho_4)\,\epsilon_{16}\,(H_{4j16})_f\,\Omega_{16} + (1-\rho_4)\,\epsilon_{17}\,(H_{4j17})_f\,\Omega_{17} + (1-\rho_4)\,\epsilon_{18}\,(H_{4j18})_f\,\Omega_{18}$$

$$\phi_7\Big|_f = (1-\rho_7)\ \epsilon_4 (H_{7j4})_f\ \Omega_4 + [(1-\rho_7)\ \epsilon_7\ (H_{7j7})_f - \epsilon_7]\ \Omega_7 + (1-\rho_7)\ \epsilon_8$$

$$(H_{7j8})_j\ \Omega_8$$

$$+ (1-\rho_7)\ \epsilon_{14}\ (H_{7j14})_f\ \Omega_{14} + (1-\rho_7)\ \epsilon_{15}\ (H_{7j15})_f\ \Omega_{15} + (1-\rho_7)\ \epsilon_{16}$$

$$(H_{7j16})_f\ \Omega_{16}$$

$$+ (1-\rho_7)\ \epsilon_{17}\ (H_{7j17})_f\ \Omega_{17} + (1-\rho_7)\ \epsilon_{18}\ (H_{7j18})_f\ \Omega_{18}$$

$$\phi_8\Big|_f = (1-\rho_8)\ \epsilon_4\ (H_{8j4})_f\ \Omega_4 + (1-\rho_8)\ \epsilon_7\ (H_{8j7})_f\ \Omega_7 + [(1-\rho_8)\ \epsilon_8$$

$$(H_{8j8})_f - \epsilon_8]\ \Omega_8$$

$$+ (1-\rho_8)\ \epsilon_{14}\ (H_{8j14})_f\ \Omega_{14} + (1-\rho_8)\ \epsilon_{15}\ (H_{8j15})_f\ \Omega_{15} + (1-\rho_8)\ \epsilon_{16}$$

$$(H_{8j16})_f\ \Omega_{16}$$

$$+ (1-\rho_8)\ \epsilon_{17}\ (H_{8j17})_f\ \Omega_{17} + (1-\rho_8)\ \epsilon_{18}\ (H_{8j18})_f\ \Omega_{18}$$

$$\phi_{14}\Big|_f = (1-\rho_{14})\ \epsilon_4\ (H_{14j14})_f\ \Omega_4 + (1-\rho_{14})\ \epsilon_7\ (H_{14j7})_f\ \Omega_7 + (1-\rho_{14})\ \epsilon_8$$

$$(H_{14j8})_f\ \Omega_8$$

$$+ [(1-\rho_{14})\ \epsilon_{14}\ (H_{14j14})_f - \epsilon_{14}]\ \Omega_{14} + (1-\rho_{14})\ \epsilon_{15}\ (H_{14j15})_f\ \Omega_{15} +$$

$$(1-\rho_{14})\ \epsilon_{16}\ (H_{14j16})_f\ \Omega_{16}$$

$$+ (1-\rho_{14})\ \epsilon_{17}\ (H_{14j17})_f\ \Omega_{17} + (1-\rho_{14})\ \epsilon_{18}\ (H_{14j18})_f\ \Omega_{18}$$

$$\phi_{15}\Big|_f = (1-\rho_{15})\,\epsilon_4\,(H_{15j4})_f\,\Omega_4 + (1-\rho_{15})\,\epsilon_7\,(H_{15j7})_f\,\Omega_7 + (1-\rho_{15})\,\epsilon_8\,(H_{15j8})_f\,\Omega_8$$

$$+ (1-\rho_{15})\,\epsilon_{14}\,(H_{15j14})_f\,\Omega_{14} + [(1-\rho_{15})\,\epsilon_{15}\,(H_{15j15})_f - \epsilon_{15}]\,\Omega_{15} + (1-\rho_{15})\,\epsilon_{16}\,(H_{15j16})_f\,\Omega_{16}$$

$$+ (1-\rho_{15})\,\epsilon_{17}\,(H_{15j17})_f\,\Omega_{17} + (1-\rho_{15})\,\epsilon_{18}\,(H_{15j18})_f\,\Omega_{18}$$

$$\phi_{16}\Big|_f = (1-\rho_{16})\,\epsilon_4\,(H_{16j4})_f\,\Omega_4 + (1-\rho_{16})\,\epsilon_7\,(H_{16j7})_f\,\Omega_7 + (1-\rho_{16})\,\epsilon_8\,(H_{16j8})_f\,\Omega_8$$

$$+ (1-\rho_{16})\,\epsilon_{14}\,(H_{16j14})_f\,\Omega_{14} + (1-\rho_{16})\,\epsilon_{15}\,(H_{16j15})_f\,\Omega_{15} + [(1-\rho_{16})\,\epsilon_{16}\,(H_{16j16})_f - \epsilon_{16}]\,\Omega_{16}$$

$$+ (1-\rho_{16})\,\epsilon_{17}\,(H_{16j17})_f\,\Omega_{17} + (1-\rho_{17})\,\epsilon_{18}\,(H_{16j18})_f\,\Omega_{18}$$

$$\phi_{17}\Big|_f = (1-\rho_{17})\,\epsilon_4\,(H_{17j4})_f\,\Omega_4 + (1-\rho_{17})\,\epsilon_7\,(H_{17j7})_f\,\Omega_7 + (1-\rho_{17})\,\epsilon_8\,(H_{17j8})_f\,\Omega_8$$

$$+ (1-\rho_{17})\,\epsilon_{14}\,(H_{17j14})_f\,\Omega_{14} + (1-\rho_{17})\,\epsilon_{15}\,(H_{17j15})_f\,\Omega_{15} + (1-\rho_{17})\,\epsilon_{16}\,(H_{17j16})_f\,\Omega_{16}$$

$$+ [(1-\rho_{17})\,\epsilon_{17}\,(H_{17j17})_f - \epsilon_{17}]\,\Omega_{17} + (1-\rho_{17})\,\epsilon_{18}\,(H_{17j18})_f\,\Omega_{18}$$

$$\phi_{18}\Big|_f = (1-\rho_{18})\ \epsilon_4\ (H_{18j4})_f\ \Omega_f + (1-\rho_{18})\ \epsilon_7\ (H_{18j7})_f\ \Omega_7 + (1-\rho_{18})\ \epsilon_8$$

$$(H_{18j18})_f\ \Omega_8$$

$$+ (1-\rho_{i8})\ \epsilon_{14}\ (H_{18j14})_f\ \Omega_{14} + (1-\rho_{18})\ \epsilon_{15}\ (H_{18j15})_f\ \Omega_{15} + (1-\rho_{18})$$

$$\epsilon_{16}\ (H_{18j16})_f\ \Omega_{16}$$

$$+ (1-\rho_{18})\ \epsilon_{17}\ (H_{18j17})_f\ \Omega_{17} + [(1-\rho_{18})\ \epsilon_{18}\ (H_{18j18})_f - \epsilon_{18}]\ \Omega_{18}$$

For the enclosure g: Nodes: 8,9,14

$$\phi_8\Big|_g = [(1-\rho_8)\ \epsilon_8\ (H_{8j8})_g - \epsilon_8]\ \Omega_8 + (1-\rho_8)\ \epsilon_9\ (H_{8j9})_f\ \Omega_9$$

$$+ (1-\rho_8)\ \epsilon_{14}\ (H_{8j14})_g\ \Omega_{14}$$

$$\phi_9\Big|_g = (1-\rho_9)\ \epsilon_8\ (H_{9j8})_g\ \Omega_8 + [(1-\rho_9)\ \epsilon_9\ (H_{9j9})_g - \epsilon_9]\ \Omega_9$$

$$+ (1-\rho_9)\ \epsilon_{14}\ (H_{9j14})_g\ \Omega_{14}$$

$$\phi_{14}\Big|_g = (1-\rho_{14})\ \epsilon_8\ (H_{14j8})_g\ \Omega_8 + (1-\rho_{14})\ \epsilon_9\ (H_{14j9})_g\ \Omega_9$$

$$+ [(1-\rho_{14})\ \epsilon_{14}\ (H_{14j14})_g - \epsilon_{14}]\ \Omega_{14}$$

For the enclosure h: Nodes: 8,9,14,17 - i,j,k

$$\phi_8\Big|_h = [(1-\rho_8)\ \epsilon_8\ (H_{8j8})_h - \epsilon_8]\ \Omega_8 + (1-\rho_8)\ \epsilon_9\ (H_{8j9})_h\ \Omega_9$$

$$+ (1-\rho_8)\ \epsilon_{14}\ (H_{8j14})_h\ \Omega_{14} + (1-\rho_8)\ \epsilon_{17}\ (H_{8j17})_h\ \Omega_{17}$$

$$\phi_9\Big|_h = (1-\rho_9)\,\epsilon_8\,(H_{9j8})_h\,\Omega_8 + [(1-\rho_9)\,\epsilon_9\,(H_{9j9})_h - \epsilon_9]\,\Omega_9$$
$$+ (1-\rho_9)\,\epsilon_{14}\,(H_{9j14})_h\,\Omega_{14} + (1-\rho_9)\,\epsilon_{17}\,(H_{9j17})_h\,\Omega_{17}$$

$$\phi_{14}\Big|_h = (1-\rho_{14})\,\epsilon_8\,(H_{14j8})_h\,\Omega_8 + (1-\rho_{14})\,\epsilon_9\,(H_{14j9})_h\,\Omega_9$$
$$+ [(1-\rho_{14})\,\epsilon_{14}\,(H_{14j14})_h - \epsilon_{14}]\,\Omega_{14} + (1-\rho_{14})\,\epsilon_{17}\,(H_{14j17})_h\,\Omega_{17}$$

$$\phi_{17}\Big|_h = (1-\rho_{17})\,\epsilon_8\,(H_{17j8})_g\,\Omega_8 + (1-\rho_{17})\,\epsilon_9\,(H_{17j9})_h\,\Omega_9$$
$$+ (1-\rho_{17})\,\epsilon_{14}\,(H_{17j14})_h\,\Omega_{14} + [(1-\rho_{17})\,\epsilon_{17}\,(H_{17j17})_h - \epsilon_{17}]\,\Omega_{17}$$

For the enclosure I: Nodes: 2,3,4 - i,j,k

$$\phi_2\Big|_i = [(1-\rho_2)\,\epsilon_2\,(H_{2j2})_i - \epsilon_2]\,\Omega_2 + (1-\rho_2)\,\epsilon_3\,(H_{2j3})_i\,\Omega_3$$
$$+ (1-\rho_2)\,\epsilon_4\,(H_{2j4})_i\,\Omega_4$$

$$\phi_3\Big|_i = (1-\rho_3)\,\epsilon_2\,(H_{3j2})_i\,\Omega_2 + [(1-\rho_3)\,\epsilon_3\,(H_{3j3}) - \epsilon_3]\,\Omega_3$$
$$+ (1-\rho_3)\,\epsilon_4\,(H_{3j4})_i\,\Omega_4$$

$$\phi_4\Big|_i = (1-\rho_4)\,\epsilon_2\,(H_{4j2})_i\,\Omega_2 + (1-\rho_4)\,\epsilon_3\,(H_{4j3})_i\,\Omega_3$$
$$+ [(1-\rho_4)\,\epsilon_4\,(H_{4j4})_i - \epsilon_4]\,\Omega_4$$

The following are the constants for the radiation transfer terms in the energy balance equation.

$$G_1 = [1 - \tau_{20}^2 \, (H_{20j20})_b \, (H_{20m20})_c]^{-1}$$

$$S_1 = (H_{11j11})_b + \tau_{20}^2 \, G_1 \, (H_{11j20})_b \, (H_{20m20})_c \, (H_{20j11})_b$$

$$G_2 = [1 - \tau_{11}^2 \, S_1 \, (H_{11m11})_a]^{-1}$$

$$U_k = G_2 \, \epsilon_k \, [(H_{11hk})_b + \tau_{20}^2 \, G_1 \, (H_{11j20})_b \, (H_{20m20})_c \, (H_{20jk})_b]$$

$$V_k = G_1 \, \epsilon_k \, \tau_{20} \, [(H_{20j20})_b \, (H_{20mk})_c + \tau_{11}^2 \, G_1 \, G_2 \, (H_{20j11})_b \, (H_{11m11})_a \, (H_{11j20})_b \, (H_{20mk})_c]$$

$$Y_k = G_1 \, \epsilon_k \, [(H_{20mk})_c + \tau_{11}^2 \, \tau_{20}^2 \, G_1 \, G_2 \, (H_{20m20})_c \, (H_{20j11})_b \, (H_{11m11})_a \, (H_{11j20})_b \, (H_{20mk})_c]$$

$$W_k = G_1 \, [(H_{20jk})_b \, \epsilon_k + \tau_{11}^2 \, (H_{11m11})_a \, (H_{20j11})_b \, U_k]$$

$$D_{11} = \left(\frac{\sigma}{M_1}\right) \{A_{1c}[(1-\rho_1) \, \epsilon_1 \, (H_{1j1})_c - \epsilon_1] + A_{1c} \, (1-\rho_1) \, \tau_{20} \, (H_{1j20})_c \, V_1 + A_{1d}[(1-\rho_1) \, \epsilon_1 \, (H_{1j1})_d - e_1]\}$$

$$D_{12} = 0$$

$$D_{13} = \left(\frac{\sigma}{M_1}\right) A_{id} \, (1-\rho_1) \, \epsilon_3 \, (H_{1j3})_d$$

$$D_{14} = \left(\frac{\sigma}{M_1}\right) A_{1d} \, (1-\rho_1) \, \epsilon_4 \, (H_{1j4})_d$$

$$D_{15} = \left(\frac{\sigma}{M_1}\right) \{A_{1c}[(1-\rho_1)\ \epsilon_5\ (H_{1j5})_c + (1-\rho_1)\ \tau_{20}\ (H_{1j20})_c\ V_5] + A_{1d}\ (1-\rho_1)\ \epsilon_5\ (H_{1j5})_d\}$$

$$D_{16} = \left(\frac{\sigma}{M_1}\right) A_{1c}\ (1-\rho_1)\ \tau_{20}\ (H_{1j20})_c\ W_6$$

$$D_{17} = \left(\frac{\sigma}{M_1}\right) A_{1c}\ (1-\rho_1)\ \tau_{20}\ (H_{1j20})_c\ W_7$$

$$D_{18} = \left(\frac{\sigma}{M_1}\right) A_{1c}\ (1-\rho_1)\ \tau_{20}\ (H_{1j20})_c\ W_8$$

$$D_{19} = \left(\frac{\sigma}{M_1}\right) A_{1c}\ (1-\rho_1)\ \tau_{20}\ (H_{1j20})_c\ W_9$$

$$D_{1-10} = 0$$

$$D_{1-11} = \left(\frac{\sigma}{M_1}\right) A_{1c}\ (1-\rho_1)\ \tau_{20}\ (H_{1j20})_c\ [W_{11} + G_1\ G_2\ \tau_{11}\ \epsilon_{11}\ (H_{20j11})_b\ (H_{11m11})_a]$$

$$D_{1-12} = D_{1-13} = 0$$

$$D_{1-14} = \left(\frac{\sigma}{M_1}\right) A_{1c}\ (1-\rho_1)\ \tau_{20}\ (H_{1j20})_c\ \tau_{11}\ \epsilon_{14}\ G_1\ G_2\ (H_{20j11})_b\ (H_{11m14})_c$$

$$D_{1-15} = D_{1-16} = D_{1-17} = D_{1-18} = D_{1-19} = 0$$

$$B_1 = \left(\frac{A_{1c}}{M_1}\right) \tau_{11}\ \tau_{20}\ \tau_{21}\ (1-\rho_1)\ G_1\ G_2\ (H_{1j20})_c\ (H_{20j11})_b\ (H_{11m21})_a$$

$$D_{2-1} = 0$$

$$D_{2-2} = \left(\frac{\sigma}{M_2}\right) A_{2i}[(1-\rho_2)\ \epsilon_2\ (H_{2j2})_i - \epsilon_2]$$

$$D_{2-3} = \left(\frac{\sigma}{M_1}\right) A_{2i} (1-\rho_2) \epsilon_3 (H_{2j3})_i$$

$$D_{2-4} = \left(\frac{\sigma}{M_2}\right) A_{2i} (1-\rho_2) \epsilon_4 (H_{2j4})_i$$

$$D_{2-5} = D_{2-6} = D_{2-7} = D_{2-8} = D_{2-9} = D_{2-10} = D_{2-11} = D_{2-12} = D_{2-13} = D_{2-14}$$
$$= D_{2-15} = D_{2-16} = D_{2-17} = D_{2-18} = D_{2-19} = 0$$

$$D_{3-1} = \left(\frac{\sigma}{M_3}\right) A_{3d} (1-\rho_3) \epsilon_1 (H_{3j1})_d$$

$$D_{3-2} = \left(\frac{\sigma}{M_3}\right) A_{3d} (1-\rho_3) \epsilon_2 (H_{3j2})_i$$

$$D_{3-3} = \left(\frac{\sigma}{M_3}\right) \{A_{3d}[(1-\rho_3) \epsilon_3 (H_{3j3})_d - \epsilon_3] + A_{3i}[(1-\rho_3) \epsilon_3 (H_{3j3})_i - \epsilon_3]\}$$

$$D_{3-4} = \left(\frac{\sigma}{M_3}\right) \{A_{3d} (1-\rho_3) \epsilon_4 (H_{3j4})_d + A_{3i} (1-\rho_3) \epsilon_4 (H_{3j4})_i\}$$

$$D_{3-5} = \left(\frac{\sigma}{M_3}\right) A_{3d} (1-\rho_3) \epsilon_5 (H_{3j5})_d$$

$$D_{3-6} = D_{3-7} = D_{3-8} = D_{3-9} = D_{3-10} = D_{3-11} = D_{3-12} = D_{3-13} = D_{3-14} = D_{3-15}$$
$$= D_{3-16} = D_{3-17} = D_{3-18} = D_{3-19} = 0$$

$$D_{4-1} = \left(\frac{\sigma}{M_4}\right) A_{4d} (1-\rho_4) \epsilon_1 (H_{4j1})_d$$

$$D_{4-2} = \left(\frac{\sigma}{M_4}\right) A_{4i} (1-\rho_4) \epsilon_2 (H_{4j2})_i$$

$$D_{4-3} = \left(\frac{\sigma}{M_4}\right) \{A_{4d} (1-\rho_4) \epsilon_3 (H_{4j3})_d + A_{4i} (1-\rho_4) \epsilon_3 (H_{4h3})_i\}$$

$$D_{4-4} = \left(\frac{\sigma}{M_4}\right) \{A_{4d}[(1-\rho_4)\ \epsilon_4\ (H_{4j4})_d - \epsilon_4] + A_{4e}[(1-\rho_4)\ \epsilon_4\ (H_{4j4})_e - \epsilon_4]$$
$$+ A_{4f}[(1-\rho_4)\ \epsilon_4\ (H_{4j4})_f - \epsilon_4] + A_{4i}[(1-\rho_4)\ \epsilon_4\ (H_{4j4})_i - \epsilon_4]\}$$

$$D_{4-5} = \left(\frac{\sigma}{M_4}\right) \{A_{4d}\ (1-\rho_4)\ \epsilon_5\ (H_{4j5})_d\}$$

$$D_{4-6} = 0$$

$$D_{4-7} = \left(\frac{\sigma}{M_4}\right) A_{4f}\ (1-\rho_4)\ \epsilon_7\ (H_{4j7})_f$$

$$D_{4-8} = \left(\frac{\sigma}{M_4}\right) A_{4f}\ (1-\rho_4)\ \epsilon_8\ (H_{4h8})_f$$

$$D_{4-9} = D_{4-10} = D_{4=11} = D_{4-12} = D_{4-13} = 0$$

$$D_{4-14} = \left(\frac{\sigma}{M_4}\right) A_{4f}\ (1-\rho_4)\ \epsilon_{14}\ (H_{4j14})_f$$

$$D_{4-15} = \left(\frac{\sigma}{M_4}\right) A_{4f}\ (1-\rho_4)\ \epsilon_{15}\ (H_{4j15})_f$$

$$D_{4-16} = \left(\frac{\sigma}{M_4}\right) \{A_{4e}\ (1-\rho_4)\ \epsilon_{16}\ (H4j16) + A_{4f}\ (1-\rho_4)\ \epsilon_{16}\ (H_{4j16})_f\}$$

$$D_{4-17} = \left(\frac{\sigma}{M_4}\right) A_{4f}\ (1-\rho_4)\ \epsilon_{17}\ (H_{4j17})_f$$

$$D_{4-18} = \left(\frac{\sigma}{M_4}\right) \{A_{4e}\ (1-\rho_4)\ \epsilon_{18}\ (H_{4j18})_e + A_{4f}\ (1-\rho_4)\ \epsilon_{18}\ (H_{4j18})_f\}$$

$$D_{4-19} = \left(\frac{\sigma}{M_4}\right) A_{4e}\ (1-\rho_4)\ \epsilon_{19}\ (H_{4j19})_e$$

$$D_{5-1} = \left(\frac{\sigma}{M_5}\right) \{A_{5c}\ (1-\rho_5)[\epsilon_1\ (H_{5j1})_c + \tau_{20}\ (H_{5j20})_c\ V_1] + A_{5d}\ (1-\rho_5)\ \epsilon_1$$
$$(H_{5j1})_d\}$$

$$D_{5-2} = 0$$

$$D_{5-3} = \left(\frac{\sigma}{M_5}\right) A_{5d} (1-\rho_5) \epsilon_3 (H_{5j3})_d$$

$$D_{5-4} = \left(\frac{\sigma}{M_5}\right) A_{5d} (1-\rho_5) \epsilon_4 (H_{5j4})_d$$

$$D_{5-5} = \left(\frac{\sigma}{M_5}\right) \{A_{5d}[(1-\rho_5) \epsilon_5 (H_{5h5})_c - \epsilon_5 + (1-\rho_5) \tau_{20} (H_{5j20})_c V_5]$$
$$+ A_{5d}[(1-\rho_5) \epsilon_5 (H_{5j5})_d - \epsilon_5]_d\}$$

$$D_{5-6} = \left(\frac{\sigma}{M_5}\right) A_{5c} (1-\rho_5) \tau_{20} (H_{5j20})_c W_6$$

$$D_{5-7} = \left(\frac{\sigma}{M_5}\right) A_{5c} (1-\rho_5) \tau_{20} (H_{5j20})_c W_7$$

$$D_{5-8} = \left(\frac{\sigma}{M_5}\right) A_{5c} (1-\rho_5) \tau_{20} (H_{5j20})_c W_8$$

$$D_{5-9} = \left(\frac{\sigma}{M_5}\right) A_{5c} (1-\rho_5) \tau_{20} (H_{5j20})_c W_9$$

$$D_{5-10} = 0$$

$$D_{5-11} = \left(\frac{\sigma}{M_5}\right) A_{5c} (1-\rho_5) \tau_{20} (H_{5j20})_c [W_{11} + G_1 G_2 \tau_{11} \epsilon_{11} (H_{20j11})_b$$
$$(H_{11m11})_a \epsilon_{14}]$$

$$D_{5-12} = D_{5-13} = 0$$

$$D_{5-14} = \left(\frac{\sigma}{M_5}\right) A_{5c} \tau_{11} \tau_{20} G_1 G_2 (1-\rho_5)(H_{5j20})_c (H_{20j11})_b (H_{11m14})_a \epsilon_{14}$$

$$D_{5-15} = D_{5-16} = D_{5-17} = D_{5-18} = D_{5-19} = 0$$

$$B_5 = \left(\frac{A_{5c}}{M_5}\right) (1-\rho_5)\ \tau_{11}\ \tau_{20}\ \tau_{21}\ G_1\ G_2\ (H_{5j20})_c\ (H_{20j11})_b\ (H_{11m21})_a$$

$$D_{6-1} = \left(\frac{\sigma}{M_6}\right) A_{6b}\ (1-\rho_6)[\tau_{11}^2\ \tau_{20}\ \epsilon_1\ G_1\ G_2\ (H_{6j11})_b\ (H_{11m11})_a\ (H_{11j20})_b$$

$$(H_{20m1})_c + \tau_{20}\ (H_{gj20})_b\ Y_1]$$

$$D_{6-2} = 0\ ,\quad D_{6-3} = 0\ ,\quad D_{6-4} = 0$$

$$D_{6-5} = \left(\frac{\sigma}{M_6}\right) A_{6b}\ (1-\rho_6)[\tau_{11}^2\ \tau_{20}\ \epsilon_5\ G_1\ G_2\ (H_{6j11})_b\ (H_{11m11})_a\ (H_{11j20})_c$$

$$+ \tau_{20}\ (H_{6j20})_b\ Y_5]$$

$$D_{6-6} = \left(\frac{\sigma}{M_6}\right)\ A_{6b}\{(1-\rho_6)\ \epsilon_6\ (H_{6j6})_b - \epsilon_6 + (1-\rho_6)[\tau_{11}^2\ (H_{6j11})_b\ (H_{11m11})_a\ U_6$$

$$+ \tau_{20}^2\ (H_{6j20})_b\ (H_{20m20})_c\ W_6]\}$$

$$D_{6-7} = \left(\frac{\sigma}{M_6}\right) A_{6b}\ (1-\rho_6)\ \{\epsilon_7\ (H_{6j7})_b + \tau_{11}^2\ (H_{6j11})_b\ (H_{11m11})_a\ U_7$$

$$+ \tau_{20}^2\ (H_{6j20})_b\ (H_{20m20})_c\ W_7\}$$

$$D_{6-8} = \left(\frac{\sigma}{M_6}\right) A_{6b}\ (1-\rho_6)\ \{\epsilon_8\ (H_{6j8})_b + \tau_{11}^2\ (H_{6j11})_b\ (H_{11m11})_a\ U_8$$

$$+ \tau_{20}^2\ (H_{6j20})_b\ (H_{20m20})_c\ W_8\}$$

$$D_{6-9} = \left(\frac{\sigma}{M_6}\right) A_{6b}\ (1-\rho_6)\ \{\epsilon_9\ (H_{6j9})_b + \tau_{11}^2\ (H_{6j11})_b\ (H_{11m11})_a\ U_9$$

$$+ \tau_{20}^2\ (H_{6j20})_b\ (H_{20m20})_c\ W_9\}$$

$$D_{6-10} = 0$$

$$D_{6-11} = \left(\frac{\sigma}{M_6}\right) A_{6b} (1-\rho_6) \{\epsilon_{11} (H_{6j11})_b + \tau_{11} (H_{6j11})_b (H_{11m11})_a$$

$$(\tau_{11} U_{11} + \epsilon_{11} G_2) + \tau_{20}^2 (H_{6j20})_b (H_{20m20})_c [W_{11} + G_1 G_2 \epsilon_{11} \tau_{11}$$

$$(H_{20j11})_b (H_{11m11})_a\}$$

$$D_{6-12} = D_{6-13} = 0$$

$$D_{6-14} = \left(\frac{\sigma}{M_6}\right) A_{6b} (1-\rho_6)[\tau_{11} \epsilon_{14} G_2 (H_{6j11})_b (H_{11m14}) + \tau_{11} \tau_{20}^2 G_1 G_2 \epsilon_{14}$$

$$(H_{6j20})_b (H_{20m20})_c (H_{20j11})_b (H_{11m11})_a]$$

$$D_{5-15} = D_{6-16} = D_{6-17} = D_{6-18} = D_{6-19} = 0$$

$$B_6 = \left(\frac{A_{6b}}{M_6}\right) (1-\rho_6) \tau_{11} \tau_{21} G_2[(H_{6j11})_b (H_{11m21})_a + G_1 \tau_{20}^2 (H_{6j20})_b (H_{20m20})_c$$

$$(H_{20j11})_b (H_{11m21})_a]$$

$$D_{7-1} = \left(\frac{\sigma}{M_7}\right) A_{7b} (1-\rho_7)\{\tau_{11}^2 \tau_{20} G_1 G_2 (H_{7j11})_b (H_{11m11})_a (H_{11j20})_b (H_{20m1})_c \epsilon_1$$

$$+ \tau_{20} (H_{7j20})_b Y_1\}$$

$$D_{7-2} = D_{7-3} = 0$$

$$D_{7-4} = \left(\frac{\sigma}{M_1}\right) A_{7f} (1-\rho_7) \epsilon_4 (H_{7j4})_f$$

$$D_{7-5} = \left(\frac{\sigma}{M_7}\right) A_{7b} (1-\rho_7) \tau_{20} \{\tau_{11}^2 \epsilon_5 G_1 G_2 (H_{7j11})_b (H_{11m11})_a (H_{11j20})_b$$

$$(H_{20m5})_c + (H_{7j20})_b Y_5\}$$

$$D_{7-6} = \left(\frac{\sigma}{M_7}\right) A_{7b} (1-\rho_7) \{\epsilon_6 (H_{7j6})_b + \tau_{11}^2 (H_{7j11})_b (H_{11m11})_a U_6 + \tau_{20}^2$$

$$(H_{7j20})_b (H_{20m20})_c W_6\}$$

$$D_{7-7} = \left(\frac{\sigma}{M_7}\right) \{A_{7b}[(1-\rho_7)\ \epsilon_7\ (H_{7j7})_b - \epsilon_7 + (1-\rho_7)[\tau_{11}^2\ (H_{7j11})_b\ (H_{11m11})_a\ U_7$$

$$+ \tau_{20}^2\ (H_{7j20})_b\ (H_{20m20})_c\ W_7]] + A_{7f}[(1-\rho_7)\ \epsilon_7\ (H_{7j7})_f - \epsilon_7]\}$$

$$D_{7-8} = \left(\frac{\sigma}{M_7}\right) \{A_{7b}\ (1-\rho_7)[\epsilon_8\ (H_{7j8})_b + \tau_{11}^2\ (H_{7j11})_b\ (H_{11m11})_a\ U_8$$

$$+ \tau_{20}^2\ (H_{7j20})_b\ (H_{20m20})_c\ W_8] + A_{7f}\ (1-\rho_7)\ \epsilon_8\ (H_{7j8})_f\}$$

$$D_{7-9} = \left(\frac{\sigma}{M_7}\right) \{A_{7b}\ (1-\rho_7)[\epsilon_9\ (H_{7j9})_b + \tau_{11}^2\ (H_{7j11})_b\ (H_{11m11})_a\ U_9$$

$$+ \tau_{20}^2\ (H_{7j20})_b\ (H_{20m20})_c\ W_9]\}$$

$$D_{7-10} = 0$$

$$D_{7-11} = \left(\frac{\sigma}{M_7}\right) A_{7b}\ (1-\rho_7)\ \{\epsilon_{11}\ (H_{7j11})_b + \tau_{11}\ (H_{7j11})_b\ (\tau_{11}\ U_{11} + \epsilon_{11}\ G_2)$$

$$(H_{1-m11})_a + \tau_{20}^2\ (H_{7j20})_b\ (H_{20m20})_c[W_{11} + G_1\ G_2\ \epsilon_{11}\ \tau_{11}\ (H_{20j11})_b$$

$$(H_{11m11})_a]\}$$

$$D_{7-12} = D_{7-13} = 0$$

$$D_{7-14} = \left(\frac{\sigma}{M_7}\right) \{A_{7b}\ (1-\rho_7)\ \tau_{11}\ G_2\ \epsilon_{14}[(H_{7j11})_b\ (H_{11m14})_a + \tau_{20}^2\ G_1\ (H_{7j20})_b$$

$$(H_{20m20})_c\ (H_{20j11})_b\ (H_{11m14})_a] + A_{7f}\ (1-\rho_7)\ \epsilon_{14}\ (H_{7j14})_f\}$$

$$D_{7-15} = \left(\frac{\sigma}{M_7}\right) A_{7f}\ (1-\rho_7)\ \epsilon_{15}\ (H_{7j15})_f$$

$$D_{7-16} = \left(\frac{\sigma}{M_7}\right) A_{7f}\ (1-\rho_7)\ \epsilon_{16}\ (H_{7j16})_f$$

$$D_{7-17} = \left(\frac{\sigma}{M_7}\right) A_{7f} (1-\rho_7) \epsilon_{17} (H_{7j17})_f$$

$$D_{7-18} = \left(\frac{\sigma}{M_7}\right) A_{7f} (1-\rho_7) \epsilon_{18} (H_{7j18})_f$$

$$D_{7-19} = 0$$

$$B_7 = \left(\frac{A_{7b}}{M_7}\right) (1-\rho_7) \tau_{11} G_2 \{\tau_{21} (H_{7j11})_b (H_{11m21})_a + \tau_{20}^2 \tau_{21} G_1 (H_{7j20})_b$$
$$(H_{20m20})_c (H_{20j11})_b (H_{11m21})_a\}$$

$$D_{8-1} = \left(\frac{\sigma}{M_8}\right) A_{8b} (1-\rho_8)\{\tau_{11}^2 \tau_{20} \epsilon_1 G_1 G_2 (H_{8j11})_b (H_{11m11})_a (H_{11j20})_b (H_{20m1})_c$$
$$+ \tau_{20} (H_{8j20})_b Y_1\}$$

$$D_{8-2} = D_{8-3} = 0$$

$$D_{8-4} = \left(\frac{\sigma}{M_8}\right) A_{8f} (1-\rho_8) \epsilon_4 (H_{8j4})_f$$

$$D_{8-5} = \left(\frac{\sigma}{M_8}\right) A_{8b} (1-\rho_8)\{\tau_{11}^2 \tau_{20} \epsilon_5 G_1 G_2 (H_{8j11})_b (H_{11m11})_a (H_{11j20})_b$$
$$(H_{20m5})_c + \tau_{20} (H_{8j20})_b Y_5\}$$

$$D_{8-6} = \left(\frac{\sigma}{M_8}\right) A_{8b} (1-\rho_8) \{\epsilon_6 (H_{8j6})_b + \tau_{11}^2 (H_{8j11})_b (H_{11m11})_a U_6$$
$$+ \tau_{20}^2 (H_{8j20})_b (H_{20m20})_c W_6\}$$

$$D_{8-7} = \left(\frac{\sigma}{M_8}\right) \{A_{8b} (1-\rho_8)[\epsilon_7 (H_{8j7})_b + \tau_{11}^2 (H_{8j11})_b (H_{11m11})_a U_7 + \tau_{20}^2$$
$$(H_{8j20})_b (H_{20m20}) W_7] + A_{8f} (1-\rho_8) \epsilon_7 (H_{8j7})_f\}$$

$$D_{8-8} = \left(\frac{\sigma}{M_8}\right) \{A_{8b}[(1-\rho_8)\ \epsilon_8\ (H_{8j8})_b - \epsilon_8 + (1-\rho_8)[\tau_{11}^2\ (H_{8j11})_b\ (H_{11m11})_a\ U_8 + \tau_{20}^2\ (H_{8j20})_b\ (H_{20m20})_c\ W_8]] + A_{8f}[(1-\rho_8)\ \epsilon_8\ (H_{8j8})_f - \epsilon_8] + A_{8g}[(1-\rho_8)\ \epsilon_8\ (H_{8j8})_g - \epsilon_8] + A_{8h}[(1-\rho_8)\ \epsilon_8\ (H_{8j8})_h - \epsilon_8]\}$$

$$D_{8-9} = \left(\frac{\sigma}{M_8}\right) \{A_{8b}\ (1-\rho_8)[\epsilon_9\ (H_{8j9})_b + \tau_{11}^2\ (H_{8j11})_b\ (H_{11m11})_a\ U_9 + \tau_{20}^2\ (H_{8j20})_b\ (H_{20m20})_c\ W_9] + A_{8g}\ (1-\rho_8)\ \epsilon_9\ (H_{8j9})_g + A_{8h}\ (1-\rho_8)\ \epsilon_9\ (H_{8j9})_h\}$$

$$D_{8-10} = \left(\frac{\sigma}{M_8}\right) \times 0 = 0$$

$$D_{8-11} = \left(\frac{\sigma}{M_8}\right) A_{8b}\ (1-\rho_8)\ \{\epsilon_{11}\ (H_{8j11})_b + \tau_{11}\ (H_{8j11})_b\ (H_{11m11})_a\ (\tau_{11}\ U_{11} + \epsilon_{11}\ G_2) + \tau_{20}^2\ (H_{8j20})_b\ (H_{20m20})_c[W_{11} + \tau_{11}\ \epsilon_{11}\ G_1\ G_2\ (H_{20j11})_b\ (H_{11m11})_a]\}$$

$$D_{8-12} = D_{8-13} = 0$$

$$D_{8-14} = \left(\frac{\sigma}{M_8}\right) \{A_{8b}\ (1-\rho_8)\ \tau_{11}\ \epsilon_{14}\ G_2[(H_{8j11})_b\ (H_{11m14})_a - \tau_{20}^2\ G_1\ (H_{8j20})_b\ (H_{20m20})_c\ (H_{20j11})_b\ (H_{11m14})_a] + A_{8f}\ (1-\rho_8)\ \epsilon_{14}\ (H_{8j14})_f + A_{8g}\ (1-\rho_8)\ \epsilon_{14}\ (H_{8j14})_g + A_{8h}\ (1-\rho_8)\ \epsilon_{14}\ (H_{8j14})_h\}$$

$$D_{8-15} = \left(\frac{\sigma}{M_8}\right) A_{8f}\ (1-\rho_8)\ \epsilon_{15}\ (H_{8j15})_f$$

$$D_{8-16} = \left(\frac{\sigma}{M_8}\right) A_{8f}\ (1-\ 8)\ \epsilon_{16}\ (H_{8j16})_f$$

$$D_{8-17} = \left(\frac{\sigma}{M_8}\right)[A_{8f}\ (1-\rho_8)\ \epsilon_{17}\ (H_{8j17})_f + A_{8h}\ (1-\rho_8)\ \epsilon_{17}\ (H_{9j17})_h]$$

$$D_{8-19} = 0$$

$$B_8 = \left(\frac{A_{8b}}{M_8}\right)\ (1-\rho_8)\ \tau_{11}\ \tau_{21}\ G_2\ \{(H_{11m21})_a + \tau_{20}^2\ G_1\ (H_{8j20})_b\ (H_{20m20})_b\ (H_{11m21})_a\}$$

$$D_{9-1} = \left(\frac{\sigma}{M_9}\right)\ A_{9b}\ (1-\rho_9)\ \tau_{20}\{\tau_{11}^2\ G_1\ G_2\ (H_{9j11})_b\ (H_{11m11})_a\ (H_{11j20})_b\ (H_{20m1})$$

$$\epsilon_1 + (H_{9j20})_b\ Y_1\}$$

$$D_{9-2} = 0\ ,\quad D_{9-3} = 0\ ,\quad D_{9-4} = 0$$

$$D_{9-5} = \left(\frac{\sigma}{M_9}\right)\ A_{9b}\ (1-\rho_9)\ \tau_{20}\{\tau_{11}^2\ \epsilon_5\ G_1\ G_2\ (H_{9j11})_b\ (H_{11m11})_a\ (H_{11j20})_b$$

$$(H_{20m5})_c + (H_{9j20})_b\ Y_5\}$$

$$D_{9-6} = \left(\frac{\sigma}{M_9}\right)\ A_{9b}\ (1-\rho_9)\ \{\epsilon_6\ (H_{9j6})_b + \tau_{11}^2\ (H_{9j11})_b\ (H_{11m11})_a\ U_6 + \tau_{20}^2$$

$$(H_{9j20})_b\ (H_{20m20})_c\ W_6\}$$

$$D_{9-7} = \left(\frac{\sigma}{M_9}\right)\ A_{9b}\ (1-\rho_9)\ \{\epsilon_7\ (H_{9j7})_b + \tau_{11}^2\ (H_{9j11})_b\ (H_{11m11})_a\ U_7 + \tau_{20}^2$$

$$(H_{9j20})_b\ (H_{20m20})_c\ W_7\}$$

$$D_{9-8} = \left(\frac{\sigma}{M_9}\right)\ \{A_{9b}\ (1-\rho_9)[\epsilon_8\ (H_{9j8})_b + \tau_{11}^2\ (H_{9j11})_b\ (H_{11m11})_a\ U_8 + \tau_{20}^2$$

$$(H_{9j20})_b\ (H_{20m20})_c\ W_8 + A_{9g}\ (1-\rho_9)\ \epsilon_8\ (H_{9j8})_g + A_{9h}\ (1-\rho_9)\ \epsilon_8$$

$$(H_{9j8})_h\}$$

$$D_{9-9} = \left(\frac{\sigma}{M_9}\right) \{A_{9b}[(1-\rho_9)\ \epsilon_9\ (H_{9j9})_b - \epsilon_9 + (1-\rho_9)[\tau_{11}^2\ (H_{9j11})_b\ (H_{11m11})_a\ U_9 + \tau_{20}^2\ (H_{9j20})_b\ (H_{20m20})_c\ W_9]] + A_{9g}[(1-\rho_9)\ \epsilon_9\ (H_{9j9})_g - \epsilon_9] + A_{9h}[(1-\rho_9)\ \epsilon_9\ (H_{9j9})_h - \epsilon_9]\}$$

$$D_{9-10} = 0$$

$$D_{9-11} = \left(\frac{\sigma}{M_9}\right) A_{9b}\ (1-\rho_9) \{\epsilon_{11}\ (H_{9j11})_b + \tau_{11}\ (H_{9j11})_b\ (H_{11m11})_a\ (\tau_{11}\ U_{11} + \epsilon_{11}\ G_2) + \tau_{20}^2\ (H_{9j20})_b\ (H_{20m20})_c [W_{11} + \epsilon_{11}\ \tau_{11}\ G_1\ G_2\ (H_{20j11})_b\ (H_{11m11})_a]\}$$

$$D_{9-12} = D_{9-13} = 0$$

$$D_{9-14} = \left(\frac{\sigma}{M_9}\right) \{A_{9b}\ \tau_{11}\ \epsilon_{14}\ G_2[(H_{9j11})_b\ (H_{11m14})_a + \tau_{20}^2\ G_1\ (H_{9j20})_b\ (H_{20m20})_c\ (H_{20j11})_b\ (H_{11m14})_a] + A_{9g}\ (1-\rho_9)\ \epsilon_{14}\ (H_{9j14})_g + A_{9h}\ (1-\rho_9)\ \epsilon_{14}\ (H_{9j14})_h\}$$

$$D_{9-15} = D_{9-16} = 0$$

$$D_{9-17} = \left(\frac{\sigma}{M_9}\right) A_{9h}\ (1-\rho_9)\ \epsilon_{17}\ (H_{9j19})_h$$

$$D_{9-18} = D_{9-19} = 0$$

$$B_9 = \left(\frac{A_{8b}}{M_9}\right) (1-\rho_9)\ \tau_{11}\ \tau_{21}\ G_2\{(H_{9j11})_b\ (H_{11m21})_a + \tau_{20}^2\ G_1\ (H_{9j20})_b\ (H_{20m20})_c\ (H_{20j11})_b\ (H_{11m21})_a\}$$

$$D_{10-1} = D_{10-2} = D_{10-3} = D_{10-4} = D_{10-5} = D_{10-6} = D_{10-7} = D_{10-8} = D_{10-9} =$$

$$D_{10-10} = D_{10-11} = D_{10-12} = D_{10-13} = D_{10-14} = D_{10-15} = D_{10-16} =$$

$$D_{10-17} = D_{10-18} = D_{10-19} = 0$$

$$D_{11-1} = \left(\frac{\sigma}{M_{11}}\right)[A_{11b}\{\tau_{11}^2\ \tau_{20}\ G_1\ G_2\ \epsilon_1[(1-\rho_{11})\ (H_{11j11})_b - 1]\ (H_{11m11})_a\ (H_{11j20})$$

$$(H_{20m1})_c + (1-\rho_{11})\ \tau_{20}\ (H_{11j20})_b\ Y_1\} + A_{11a}\ \tau_{11}\ \tau_{20}\ \epsilon_1\ G_1\ G_2[(1-\rho_{11})$$

$$(H_{11m11})_a - 1]\ (H_{11j20})_a\ (H_{20m1})_c]$$

$$D_{11-2} = D_{11-3} = D_{11-4} = 0$$

$$D_{11-5} = \left(\frac{\sigma}{M_{11}}\right)[A_{11b}\{\tau_{11}^2\ \tau_{20}\ G_1\ G_2\ \epsilon_5[(1-\rho_{11})\ (H_{11j11})_n - 1](H_{11m11})_a\ (H_{11j20})_b$$

$$(H_{20m5})_c + (1-\rho_{11})\ \tau_{20}\ (H_{11j20})_b\ Y_5\} + A_{11a}\ \tau_{11}\ \tau_{20}\ \epsilon_5\ G_1\ G_5$$

$$[(1-\rho_{11})(H_{11m11})_a - 1](H_{11j20})_b\ (H_{20m5})_c]$$

$$D_{11-6} = \left(\frac{\sigma}{M_{11}}\right)[A_{11b}\ \{(1-\rho_{11})\ \epsilon_6\ (H_{11j6})_b + \tau_{11}^2[(1-\rho_{11})\ (H_{11j11})_b - 1]$$

$$(H_{11m11})_a\ U_6 + \tau_{20}^2\ (1-\rho_{11})\ (H_{11j20})_b\ (H_{20m20})_c\ W_6\} + A_{11a}\ \tau_{11}$$

$$[(1-\rho_{11})\ (H_{11m11})_a - 1]\ U_6]$$

$$D_{11-7} = \left(\frac{\sigma}{M_{11}}\right)[A_{11b}\ \{(1-\rho_{11})\ \epsilon_7\ (H_{11j7})_b + \tau_{11}^2[(1-\rho_{11})\ (H_{11j11})_b - 1]\ U_7$$

$$+ \tau_{20}^2\ (1-\rho_{11})\ (H_{11j20})_b\ (H_{20m20})_c\ W_9\} + A_{11a}\ \tau_{11}[(1-\rho_{11})$$

$$(H_{11m11})_a - 1]\ U_7]$$

$$D_{11-8} = \left(\frac{\sigma}{M_{11}}\right)[A_{11b}\{(1-\rho_{11})\,\epsilon_8\,(H_{11j8})_b + \tau_{11}^2[(1-\rho_{11})\,(H_{11j11})_b - 1]$$
$$(H_{11m11})_a\,U_8 + \tau_{20}^2\,(1-\rho_{11})\,(H_{11j20})_b\,(H_{20m20})_c\,W_8\} + A_{11a}\,\tau_{11}$$
$$[(1-\rho_{11})\,(H_{11m11})_a - 1]\,U_8]$$

$$D_{11-9} = \left(\frac{\sigma}{M_{11}}\right)[A_{11b}\{(1-\rho_{11})\,\epsilon_9\,(H_{11j9})_b + \tau_{11}^2[(1-\rho_{11})\,(H_{11j11})_b - 1]$$
$$(H_{11m11})_a\,U_9 + \tau_{20}^2\,(1-\rho_{11})\,(H_{11j20})_b\,(H_{20m20})_c\,W_9\} + A_{11a}\,\tau_{11}$$
$$[(1-\rho_{11})\,(H_{11m11})_a - 1]\,U_9]$$

$$D_{11-10} = 0$$

$$D_{11-11} = \left(\frac{\sigma}{M_{11}}\right)[A_{11b}\{(1-\rho_{11})\,\epsilon_{11}\,(H_{11j11})_b - \epsilon_{11} + \tau_{11}[(1-\rho_{11})\,(H_{11j11})_b - 1]$$
$$(H_{11m11})_a\,(\tau_{11}\,U_{11} + e_{11}\,G_2) + \tau_{20}^2\,(1-\rho_{i1})\,(H_{11j20})_b\,(H_{1120m20})_c$$
$$[W_{11} + \epsilon_{11}\,\tau_{11}\,G_1\,G_2\,(H_{20j11})_b\,(H_{11m11})_a]\} + A_{11a}\{(1-\rho_{11})\,\epsilon_{11}$$
$$(H_{11m11})_a - \epsilon_{11} + \tau_{11}[(1-\rho_{11})\,(H_{11m11})_a - 1][U_{11} + \tau_{11}\,\epsilon_{11}\,G_2$$
$$S_1\,(H_{11m11})_a]\}]$$

$$D_{11-12} = D_{11-13} = 0$$

$$D_{11-14} = \left(\frac{\sigma}{M_{11}}\right)[A_{11b}\{\tau_{11}\,\epsilon_{14}[(1-\rho_{11})\,(H_{11j11})_b - 1]G_2\,(H_{11m14})_a + (1-\rho_{11})\,\tau_{11}$$
$$\tau_{20}^2\,\epsilon_{14}\,G_1\,G_2\,(H_{11j20})_b\,(H_{20m20})_c(H_{20j11})_b\,(H_{11m14})_a\} + A_{11a}\,(1-\rho_{11})$$
$$\epsilon_{14}\,S_1\,G_2[(1-\rho_{11})\,(H_{11m11})_a\}]$$

$$D_{11-15} = D_{11-16} = D_{11-17} = D_{11-18}\ D_{11-19} = 0$$

$$B_{11} = \left(\frac{1}{M_{11}}\right)[A_{11b}\{\tau_{11}\ \tau_{21}\ G_2[(1-\rho_{11})\ (H_{11j11})_b - 1]\ (H_{11m21})_a + (1-\rho_{11})\ \tau_{11}$$
$$\tau_{20}^2\ \tau_{21}\ G_1\ G_2\ (H_{11j20})_b\ (H_{20m20})_c\ (H_{20j11})_b\ (H_{11m2k})\} + A_{11a}\{(1-\rho_{11})$$
$$\tau_{21}\ (H_{11m21})_a + \tau_{11}^2\ \tau_{21}\ S_1\ G_2[(1-\rho_{11})\ (H_{11m11})_a - 1]\ (H_{11m21})_a\}]$$

$$D_{12-1} = D_{12-2} = D_{12-3} = D_{12-4} = D_{12-5} = D_{12-6} = D_{12-7} = D_{12-8} = D_{12-9} =$$
$$D_{12-10} = D_{12-11} = D_{12-12} = D_{12-13} = D_{12-14} = D_{12-15} = D_{12-16} =$$
$$D_{12-17} = D_{12-18} = D_{12-19} = 0$$

$$D_{13-1} = D_{13-2} = D_{13-3} = D_{13-4} = D_{13-5} = D_{13-6} = D_{13-7} = D_{13-8} = D_{13-9} =$$
$$D_{13-10} = D_{13-11} = D_{13-12} = D_{13-13} = D_{13-14} = D_{13-15} = D_{13-16} =$$
$$D_{13-17} = D_{13-18} = D_{13-19} = 0$$

$$D_{14-1} = D_{14-2} = D_{14-3} = D_{14-4} = D_{14-5} = D_{14-6} = D_{14-7} = 0$$

$$D_{14-8} = \left(\frac{\sigma}{M_{14}}\right)[A_{14g}\ (1-\rho_{14})\ \epsilon_8\ (H_{14j8})_g + A_{14h}\ (1-\rho_{14})\ \epsilon_8\ (H_{14j8})_h]$$

$$D_{14-9} = \left(\frac{\sigma}{M_{14}}\right)\ [A_{14g}\ (1-\rho_{14})\ \epsilon_9\ (H_{14j9})_g + A_{14h}\ (1-\rho_{14})\ \epsilon_9\ (H_{14j9})_h]$$

$$D_{14-10} = D_{14-11} = D_{14-12} = D_{14-13} = 0$$

$$D_{14-14} = \left(\frac{\sigma}{M_{14}}\right)\ \{A_{14g}\ \epsilon_{14}[(1-\rho_{14})\ (H_{14j14})_g - 1] + A_{14h}\ \epsilon_{14}[(1-\rho_{14})\ (H_{14j14})_h - 1]\}$$

$$D_{14-15} = D_{14-16} = 0$$

$$D_{14-17} = \left(\frac{\sigma}{M_{14}}\right) A_{14h} (1-\rho_{14}) \epsilon_{17} (H_{14j17})_h$$

$$D_{14-18} = D_{14-19} = 0$$

$$D_{15-1} = D_{15-2} = D_{15-3} = 0$$

$$D_{14-4} = \left(\frac{\sigma}{M_{15}}\right) A_{15f} (1-\rho_{15}) \epsilon_4 (H_{15j4})_f$$

$$D_{15-5} = D_{15-6} = 0$$

$$D_{15-7} = \left(\frac{\sigma}{M_{15}}\right) A_{15f} (1-\rho_{15}) \epsilon_7 (H_{15j7})_f$$

$$D_{15-8} = \left(\frac{\sigma}{M_{15}}\right) A_{15f} (1-\rho_{15}) \epsilon_8 (H_{15j8})_f$$

$$D_{15-9} = D_{15-10} = D_{15-11} = D_{15-12} = D_{15-13} = 0$$

$$D_{15-14} = \left(\frac{\sigma}{M_{15}}\right) A_{15f} (1-\rho_{15}) \epsilon_{14} (H_{15j14})_f$$

$$D_{15-15} = \left(\frac{\sigma}{M_{15}}\right) A_{15f}[(1-\rho_{15}) \epsilon_{15} (H_{15j15})_f - \epsilon_{15}]$$

$$D_{15-16} = \left(\frac{\sigma}{M_{15}}\right) A_{15f} (1-\rho_{15}) \epsilon_{16} (H_{15j16})_f$$

$$D_{15-17} = \left(\frac{\sigma}{M_{15}}\right) A_{15f} (1-\rho_{15}) \epsilon_{17} (H_{15j17})_f$$

$$D_{15-18} = \left(\frac{\sigma}{M_{15}}\right) A_{15f} (1-\rho_{15}) \epsilon_{18} (H_{15j18})_f$$

$$D_{15-19} = 0$$

$$D_{16-1} = D_{16-2} = D_{16-3} = 0$$

$$D_{16-4} = \left(\frac{\sigma}{M_{16}}\right) \{A_{16e}(1-\rho_{16})\ \epsilon_4\ (H_{16j4})_e + A_{16f}(1-\rho_{16})\ \epsilon_4\ (H_{16j4})_f\}$$

$$D_{16-5} = D_{16-6} = 0$$

$$D_{16-7} = \left(\frac{\sigma}{M_{16}}\right) A_{16f}(1-\rho_{16})\ \epsilon_7\ (H_{16j7})_f$$

$$D_{16-8} = \left(\frac{\sigma}{M_{16}}\right) A_{16f}(1-\rho_{16})\ \epsilon_8\ (H_{16j8})_f$$

$$D_{16-9} = D_{16-10} = D_{16-11} = D_{16-12} = D_{16-13} = 0$$

$$D_{16-14} = \left(\frac{\sigma}{M_{16}}\right) A_{16f}(1-\rho_{16})\ \epsilon_{14}\ (H_{16j14})_f$$

$$D_{16-15} = \left(\frac{\sigma}{M_{16}}\right) A_{16f}(1-\rho_{16})\ \epsilon_{15}\ (H_{16j15})_f$$

$$D_{16-16} = \left(\frac{\sigma}{M_{16}}\right) \{A_{16e}[(1-\rho_{16})(H_{16j16})_e - 1] + A_{16f}\ \epsilon_{16}[(1-\rho_{16})(H_{16j16})_f - 1]\}$$

$$D_{16-17} = \left(\frac{\sigma}{M_{16}}\right) A_{16f}(1-\rho_{16})\ \epsilon_{17}\ (H_{16j17})_f$$

$$D_{16-18} = \left(\frac{\sigma}{M_{16}}\right) \{A_{16e}(1-\rho_{16})\ \epsilon_{18}\ (H_{16j18}) + A_{16f}(1-\rho_{16})\ \epsilon_{18}\ (H_{16j18})_f\}$$

$$D_{16-19} = \left(\frac{\sigma}{M_{16}}\right) A_{16f}(1-\rho_{16})\ \epsilon_{19}\ (H_{16j19})_e$$

$$D_{17-1} = D_{17-2} = D_{17-3} = 0$$

$$D_{17-4} = \left(\frac{\sigma}{M_{17}}\right) A_{17f}(1-\rho_{17})\ \epsilon_4\ (H_{17j4})_f$$

$$D_{17-5} = D_{17-6} = 0$$

$$D_{17-7} = \left(\frac{\sigma}{M_{17}}\right) A_{17f}(1-\rho_{17})\ \epsilon_7\ (H_{17j7})_f$$

$$D_{17-8} = \left(\frac{\sigma}{M_{17}}\right) \{A_{17f}(1-\rho_{17})\ \epsilon_8\ (H_{17j8})_f + A_{17h}(1-\rho_{17})\ \epsilon_8\ (H_{17j8})_h\}$$

$$D_{17-9} = \left(\frac{\sigma}{M_{17}}\right) A_{17h}(1-\rho_{17})\ \epsilon_9\ (H_{17j9})_h$$

$$D_{17-10} = D_{17-11} = D_{17-12} = D_{17=13} = 0$$

$$D_{17-14} = \left(\frac{\sigma}{M_{17}}\right) \{A_{17f}(1-\rho_{17})\ \epsilon_{14}\ (H_{17j14})_f + A_{17h}(1-\rho_{17})\ \epsilon_{14}\ (H_{17j14})_h\}$$

$$D_{17-15} = \left(\frac{\sigma}{M_{17}}\right) A_{17f}(1-\rho_{17})\ \epsilon_{15}\ (H_{17j15})_f$$

$$D_{17-16} = \left(\frac{\sigma}{M_{17}}\right) A_{17f}(1-\rho_{17})\ \epsilon_{16}\ (H_{17j16})_f$$

$$D_{17-17} = \left(\frac{\sigma}{M_{17}}\right) \{A_{17f}\ \epsilon_{17}[(1-\rho_{17})(H_{17j17})_f - 1] + A_{17h}\ \epsilon_{17}[(1-\rho_{17})(H_{17j17})_h - 1]\}$$

$$D_{17-18} = D_{17-19} = 0$$

$$D_{18-1} = D_{18-2} = D_{18-3} = 0$$

$$D_{18-4} = \left(\frac{\sigma}{M_{18}}\right) \{A_{18e}(1-\rho_{18})\ \epsilon_4\ (H_{18j4})_e + A_{18f}(1-\rho_{18})\ \epsilon_4\ (H_{18j4})_h\}$$

$$D_{18-5} = D_{18-6} = 0$$

$$D_{18-7} = \left(\frac{\sigma}{M_{18}}\right) A_{18f}(1-\rho_{18})\ \epsilon_7\ (H_{18j7})_f$$

$$D_{18-8} = \left(\frac{\sigma}{M_{18}}\right) A_{18f}(1-\rho_{18})\ \epsilon_8\ (H_{18j8})_f$$

$$D_{18-9} = D_{18-10} = D_{18-11} = D_{18-12} = D_{18-13} = 0$$

$$D_{18-14} = \left(\frac{\sigma}{M_{18}}\right) A_{18f}(1-\rho_{18})\ \epsilon_{14}\ (H_{18j14})_f$$

$$D_{18-15} = \left(\frac{\sigma}{M_{18}}\right) A_{18f}(1-\rho_{18})\ \epsilon_{15}\ (H_{18j15})_f$$

$$D_{18-16} = \left(\frac{\sigma}{M_{18}}\right) \{A_{18e}(1-\rho_{18})\ \epsilon_{16}\ (H_{18j16}) + A_{18f}(1-\rho_{18})\ \epsilon_{16}\ (H_{18j16})_f\}$$

$$D_{18-17} = \left(\frac{\sigma}{M_{18}}\right) A_{18f}(1-\rho_{18})\ \epsilon_{17}\ (H_{18j17})_f$$

$$D_{18-18} = \left(\frac{\sigma}{M_{18}}\right) \{A_{18e}\ \epsilon_{18}[(1-\rho_{18})(H_{18j18})_e - 1] + A_{18f}\ \epsilon_{18}[(1-\rho_{18})(H_{18j18})_f - 1]\}$$

$$D_{18-19} = \left(\frac{\sigma}{M_{18}}\right) A_{18e}(1-\rho_{18})\ \epsilon_{19}\ (H_{18j19})_e$$

$$D_{19-1} = D_{19-2} = D_{19-3} = 0$$

$$D_{19-4} = \left(\frac{\sigma}{M_{19}}\right) A_{19e}(1-\rho_{19})\ \epsilon_{4}\ (H_{19j4})_e$$

$$D_{19-5} = D_{19-6} = D_{19-7} = D_{19-8} = D_{19-9} = D_{19-10} = D_{19-11} = D_{19-12} = D_{19-13} =$$

$$D_{19-14} = D_{19-15} = 0$$

$$D_{19-16} - \left(\frac{\sigma}{M_{19}}\right) A_{19e}(1-\rho_{19})\ \epsilon_{16}\ (H_{19j16})_e$$

$$D_{19-17} = 0$$

$$D_{19-18} = \left(\frac{\sigma}{M_{18}}\right) A_{19e}(1-\rho_{19})\ \epsilon_{18}\ (H_{19j18})_e$$

$$D_{19-19} = \left(\frac{\sigma}{M_{18}}\right) A_{19e}\ \epsilon_{19}[(1-\rho_{19})(H_{19j19})_e - 1]$$

Standard Bibliographic Page

| 1. Report No. | 2. Government Accession No. | 3. Recipient's Catalog No. |
|---|---|---|
| NASA CR-178292 | | |

| 4. Title and Subtitle | 5. Report Date |
|---|---|
| Development of Response Models for the Earth Radiation Budget Experiment (ERBE) Sensors: PartI - Dynamic Models and Computer Simulations for the ERBE Nonscanner, Scanner and Solar Monitor Sensors | March 20, 1987 |
| | 6. Performing Organization Code |
| 7. Author(s) Nesim Halyo, Sang H. Choi, Dan A. Chrisman, Jr., Richard W. Samms | 8. Performing Organization Report No. FR 687103 |
| 9. Performing Organization Name and Address Information & Control Systems, Incorporated 28 Research Drive Hampton, VA 23666 | 10. Work Unit No. 665-45-30-01 |
| | 11. Contract or Grant No. NAS1-16130 |
| 12. Sponsoring Agency Name and Address National Aeronautics and Space Administration Langley Research Center Hampton, VA 23665 | 13. Type of Report and Period Covered Contractor Report |
| | 14. Sponsoring Agency Code |

15. Supplementary Notes

Langley Technical Monitor: Robert J. Keynton

Final Report

16. Abstract

Dynamic models and computer simulations were developed for the radiometric sensors utilized in the Earth Radiation Budget Experiment (ERBE). The models were developed to understand sensor performance, improve measurement accuracy by updating model parameters and provide the constants needed for the count conversion algorithms. Model simulations were compared with the sensor's actual responses demonstrated in the ground and inflight calibrations. The models consider thermal and radiative exchange effects, surface specularity, spectral dependence of a filter, radiative interactions among an enclosure's nodes, partial specular and diffuse enclosure surface characteristics and steady-state and transient sensor responses. Relatively few sensor nodes were chosen for the models since there is an accuracy tradeoff between increasing the number of nodes and approximating parameters such as the sensor's size, material properties, geometry, enclosure surface characteristics, etc. Given that the temperature gradients within a node and between nodes are small enough, approximating with only a few nodes does not jeopardize the accuracy required to perform the parameter estimates and error analyses.

| 17. Key Words (Suggested by Authors(s)) | 18. Distribution Statement |
|---|---|
| Dynamic Models, Computer Simulations, Radiometric Sensors, Count Conversion Algorithms, Ground and Inflight Calibrations, Thermal and Radiative Exchange Effects, Surface Specularity, Spectral Dependence, Enclosure Nodes | Unclassified - Unlimited<br>Subject Category 35 |

| 19. Security Classif.(of this report) | 20. Security Classif.(of this page) | 21. No. of Pages | 22. Price |
|---|---|---|---|
| Unclassified | Unclassified | 305 | A14 |

For sale by the National Technical Information Service, Springfield, Virginia 22161